Collagen and Gelatin from Golden Carp Skin and Squalene from Fish Liver Extracted with the Aid of Ultrasound: Properties and Applications

Ali Muhammed Moula Ali

A Thesis Submitted in Fulfillment of the Requirements for the Degree of Doctor of Philosophy in Food Science and Technology

Prince of Songkla University

2019

Collagen and Gelatin from Golden Carp Skin and Squalene from Fish Liver Extracted with the Aid of Ultrasound: Properties and Applications

Ali Muhammed Moula Ali

A Thesis Submitted in Fulfillment of the Requirements for the Degree of Doctor of Philosophy in Food Science and Technology

Prince of Songkla University

2019

Thesis Title	Collagen and Gelatin from Golden Carp Skin and Squalene from Fish Liver Extracted with the Aid of Ultrasound: Properties and Applications.
Author	Mr. Ali Muhammed Moula Ali
Major Program	Food Science and Technology

Major Advisor

…….…….....
(Prof. Dr. Soottawat Benjakul)

Co-Advisor

……
(Asst. Prof. Dr. Thummanoon Prodpran)

Examining Committee:

…….……..….....Chairperson
(Asst. Prof. Dr. Phanat Kittiphattanabawon)

…….…...…....Committee
(Prof. Dr. Soottawat Benjakul)

…….…….....Committee
(Asst. Prof. Dr. Thummanoon Prodpran)

…….……...Committee
(Asst. Prof. Dr. Saowakon Wattanachant)

…….……...Committee
(Asst. Prof. Dr. Supachai Pisuchpen)

The Graduate School, Prince of Songkla University, has approved this thesis as fulfillment of the requirements for the Doctor of Philosophy Degree in Food Science and Technology.

…..……..…….…….....
(Prof. Dr. Damrongsak Faroongsarng)
Dean of Graduate School

This is to certify that the work here submitted is the result of the candidate's own investigations. Due acknowledgement has been made of any assistance received.

…….…….Signature
(Prof. Dr. Soottawat Benjakul)
Major Advisor

…….…….Signature
(Mr. Ali Muhammed Moula Ali)
Candidate

I hereby certify that this work has not been accepted in substance for any degree, and is not being currently submitted in candidature for any degree.

…….…….Signature

(Mr. Ali Muhammed Moula Ali)

Candidate

Thesis Title	Collagen and Gelatin from Golden Carp Skin and Squalene from Fish Liver Extracted with the Aid of Ultrasound: Properties and Applications
Author	Mr. Ali Muhammed Moula Ali
Major Program	Food Science and Technology
Academic Year	2018

ABSTRACT

Acid solubilized collagen (ASC) and pepsin solubilized collagen (PSC) were isolated from the skin and scales of golden carp (*Probarbus jullieni*). Yield of ASC and PSC from skin was 21.16 and 39.05%, respectively, while the scales had a yield of 0.42 and 1.16%, respectively (based on the dry weight basis). Both ASC and PSC from skin and scales were composed of α_1 and α_2 chains and were characterized as type I collagen. Imino acid contents of ASC and PSC from skin were 197 and 199 residues/1000 residues, respectively, scales had 197 and 202 residues per 1000 residues, respectively. Fourier transform infrared (FTIR) and Circular dichroism (CD) spectra of both the samples were almost similar between ASC and PSC. Specifically, ASC and PSC from skin showed T_{max} of 36.28 °C and 37.87 °C, respectively, which were higher than those of most temperate and cold-water fish collagens. The maximum solubility for both collagens was found at acidic pH (1–3). When ultrasonication was implemented as the extraction aid, yield of ASC and PSC increased as ultrasonication (20 kHz) time and amplitude increased ($p < 0.05$). ASC and PSC with ultrasound aided process, named as UASC and UPSC, had the yields of 81.53 and 94.88%, while ASC and PSC prepared with typical method showed the yields of 51.90 and 79.27%, respectively. Amino acid compositions of all the collagens were similar. Overall, ultrasound treatment under appropriate condition effectively improved the extraction efficiency of ASC and PSC without affecting their physiochemical properties.

Gelatins from golden carp skin pretreated using different acids (acetic acid and sulfuric acid + acetic acid), with and without prior-ultrasonication, extracted at 55 ºC for 3 and 6 h, were characterized. Prior-ultrasonication (20 kHz) with amplitude

of 80% and time 30 min increased the yield of gelatins by 110.9% and 174.8%, respectively compared with the corresponding controls (without prior-ultrasonication), when extracted for 6 h. Nevertheless, gelatin extracted from skin with prior-ultrasonication showed slightly higher content of imino acids, regardless of acid pretreatments with coincidentally higher gelling and melting temperature along with finer gel network than those produced by conventional method. Thus, appropriate acid pretreatment in combination with prior-ultrasonication effectively improved the extraction efficiency and gelling properties of gelatin from golden carp skin.

Squalene from livers of four fish species including, *L. calcarifer*, *K. pelamis, C. sorrah* and *C. griseum* were extracted using ultrasound-assisted direct in-situ saponification (U-DS) process, in comparison with the conventional process. Based on Box-Behnken experimental design (BBD), optimal condition involved mass/methanol ratio (1:6, w/v), 50% KOH volume (6.5 ml) and sonication time (15 min). Higher yield was achieved with U-DS from 0.13±0.03 to 6.86±0.05 g $(100\ g)^{-1}$ depending on the fish species. After extraction, squalene was further concentrated up to ≥ 60% of purity from all the fish species via fractional crystallization (yield of squalene concentrate ranged from 48.35-74.49%) and purified using a silica gel column with a maximum recovery up to 98%. Entire extraction processes yielded squalene with a purity of ≥ 94%. Fourier transform infrared (FTIR) analysis confirmed the native structure of squalene with six nonconjugated bonds, suggesting no degradation of squalene taken place during U-DS process.

Golden carp skin gelatin films incorporated with squalene rich fraction from shark liver (SRF) at various levels (5-25%, w/w) were characterized in comparison with palm oil (PO) incorporated film and control film (CON) (without oil addition). SRF films added with 25% SRF showed higher EAB as well as TS, compared to both CON and PO films ($p < 0.05$). SRF films showed significantly lower water vapor permeability (WVP) and lower lightness (L^*) value than CON and PO films ($p < 0.05$). SEM images showed that CON and SRF films exhibited relatively smoother surface, compared to PO film. Both SRF and PO films demonstrated lower degradation (T_d), glass transition (T_g) and melting transition (T_{max}) temperatures than CON film.

SRF could render stronger films and enhanced flexibility with improved moisture barrier property of gelatin films.

When gelatin films prepared by using glycerol (GLY) and squalene (SQ) at different ratios (10:0, 7:3, 5:5, 3:7 and 0:10; w/w) as plasticizer were characterized, incorporation of SQ reduced the moisture content of the gelatin film ($p < 0.05$). Films plasticized with GLY/SQ at a ratio of 5:5 (w/w) had highest tensile strength (TS), which was 61.7% higher than that using GLY as plasticizer (GLY). Nevertheless, continuous decrease in EAB were attained with increasing SQ ratios ($p < 0.05$). SQ films had a decrease in WVP and oxygen permeability (OP), compared to GLY film ($p < 0.05$). Based on FTIR and DSC spectra, SQ decreased gelatin-gelatin interactions associated with disordered structure. In addition, SQ film demonstrated lower T_{max}, and enthalpy (ΔH), but a slightly increased T_g. Thermal degradation behavior of films showed that GLY film possessed a greater number of gelatin-gelatin interaction than that incorporated with SQ. Thus, SQ could replace GLY up to 50% to render stronger films with improved WVP as well as OP of gelatin films.

The influence of bags from fish skin gelatin film prepared by substituting glycerol (GLY) with squalene (SQ) at 50% (GLY/SQ) was evaluated on the quality characteristics of fried fish crackers (FFC) stored for 30 days at 28 ± 0.5 °C and 70 ± 5 % RH, in comparison with bags from control (CON) gelatin film and nylon/LLDPE film. After 30 days, GLY/SQ and nylon/LLDPE stored FFC had lower PV and TBARS than others. In addition, GLY/SQ and nylon/LLDPE stored FFC had less volatile compounds, especially those formed from autoxidation and non-enzymatic browning reaction. GLY/SQ bag lowered the oxidation and loss of polyunsaturated fatty acids, mainly n-3 and n-6 when compared to other bags. Nevertheless, FFC stored in nylon/LLDPE and GLY/SQ bags exhibited negligible changes in color and texture. GLY/SQ bag had an excellent oxygen barrier property and could lower water vapor permeability (WVP), thus lowering migration of reactants and oxidizing radicals. The prepared GLY/SQ bag could therefore improve oxidative stability of FFC.

Therefore, value-added products from fish processing by-products could be potentially recovered with the aid of ultrasound and further uses of those products can be maximized via appropriate optimization.

ACKNOWLEDGEMENT

I would like to express my deepest appreciation and sincere gratitude to my advisor, Prof. Dr. Soottawat Benjakul of the Department of Food Technology, Faculty of Agro-Industry, Prince of Songkla University for his able guidance, perpetual support, kindness and constructive criticism during my study. His strong encouragement to work, enthusiasm, invaluable inputs and faith in me throughout has been extremely helpful. He was always available to me for his kind help through his immeasurable knowledge and I truly appreciate for giving generously of his time. His patience to correct my writings and assistance to improve my skills are profoundly appreciated. His energy level, intellectual dimension, workaholic nature, confidence, guidance style and numerous publications have always motivated and inspired me to gear up my carrier path. I am sincerely grateful for his dedication for creating an excellent work ambiance and facilities. I truly thank him for accepting me to work under him and I realized this is one of the greatest blessings of my life for studying under his supervision.

It is my great pleasure to express my heartfelt and profound gratitude to my co-advisors, Asst. Prof. Dr. Thummanoon Prodpran of the Department of Material Product Technology, Faculty of Agro-Industry, Prince of Songkla University for his invaluable comments, suggestions and timely help. I would like to especially thank him for his kind help to work at his lab and to improve the quality of my work and writing.

I am using this opportunity to convey my deepest thanks and regards to the chairperson and members of my examining committee. Asst. Prof. Dr. Phanat Kittiphattanabawon of the Department of Food Science and Technology, Faculty of Agro- and Bio-Industry, Thaksin University, Phatthalung, Thailand, Asst. Prof. Dr. Saowakon Wattanachant of the Department of Food Technology, Faculty of Agro-Industry, Prince of Songkla University and Asst. Prof. Dr. Supachai Pisuchpen of the Department of Material Product Technology, Faculty of Agro-Industry, Prince of Songkla University for the valuable time devoted to my thesis and their kindness, comments and helpful suggestion.

I would like to express my sincere thanks and best wishes to Dr. Tanaji G. Kudre for introducing me to Prof. Dr. Soottawat Benjakul. My deep gratitude is also dedicated to my dear friends and colleagues of Fish Chemistry and Biochemistry lab (2205) members who shared their work experiences and acquired time in helping hands with me in their busy schedule. It was a great experience with all of you during my study.

Above all, I am grateful to my Father Mahaboob Pasha, Mother Athiya Bee, my sister Noor Jahan and brothers Noor and Sufi for their encouragement, emotional and financial support throughout my study. A special thanks to my beloved wife Dr. Bindu for all her kind support and encouragement during my work. I always knew that you all believed in me and wanted the best for me.

I also would like to thank all the faculty members of Agro-Industry and staff, students for their kind co-operation during my study period. Thailand's Education Hub for Southern Region of ASEAN Countries (TEH-AC, 2015) scholarship from Graduate School of Prince of Songkla University, Hat Yai, Thailand also acknowledged for the financial support.

Finally, many thanks to all the Thai and International friends who have supported me directly or indirectly to complete the research work.

Ali Muhammed Moula Ali

CONTENTS

CONTENTS (Continued)

Chapter **Page**

CONTENTS (Continued)

CONTENTS (Continued)

CONTENTS (Continued)

Chapter **Page**

CONTENTS (Continued)

CONTENTS (Continued)

CONTENTS (Continued)

CONTENTS (Continued)

LIST OF FIGURES

LIST OF FIGURES (Continued)

LIST OF FIGURES (Continued)

LIST OF FIGURES (Continued)

LIST OF FIGURES (Continued)

LIST OF TABLES

LIST OF TABLES (Continued)

LIST OF TABLES (Continued)

CHAPTER 1

INTRODUCTION AND REVIEW OF LITERATURE

1.1. Introduction

Golden carp is a freshwater fish, typically found in Southeast Asian river basins and is aquacultured mainly in Thailand and Lao. Based on the FAO statistics, golden carp aquaculture production has an annual rate of 3.86% owing to the increasing demand for freshwater fish consumption (FAO, 2016). Fish processing industry generates a considerable amount of by-products (60-70%) which are utilized as a feedstock or discarded as waste. Golden carp skin and scales constitute around 8-10% of body weight. Owing to the abundance availability, its skin can be used for extraction of value-added products such as collagen and gelatin.

Generally, collagen is the chief structural protein present in the connective tissues of vertebrates. As a fibrous protein, it plays an exceptional role in skins, tendons, bones and cartilages (Jongjareonrak *et al.*, 2005). Several collagens including Type I–XXVIII from animal origin have been reported (Zunying *et al.*, 2009). Collagen has been widely used in food, cosmetic, pharmaceutical and biomedical industries. Amongst all, type I collagen is commonly found in fish and mammals. Type I collagen is in the form of triple helical structure consisting of 2 α_1 and 1 α_2 chains. Those chains are stabilized by interchain hydrogen bonding between amide group and glycine of protein chains (Shoulders and Raines, 2009).

Gelatin, a functional biopolymer with a high molecular weight (MW), is generated by thermal denaturation of collagen (Kaewruang *et al.*, 2013). Most commonly gelatin is used in the food industry as a thickening agent, texturizer in confectionaries and stabilizer, gelling agent, salad dressing, as well as employed as food foams (Badii and Howell, 2006; Saha and Bhattacharya, 2010). Additionally, gelatin has plentiful and emerging applications in pharmaceuticals, cosmetics, biomedical and biomaterial-based packaging industries (Gennadios *et al.*, 1997; Ishida *et al.*, 2007; Yakimets *et al.*, 2005). Nevertheless, the annual usage of gelatin is increasing worldwide. The estimated usage in the food industry alone stands about 200,000 metric

tons per year, which is predominantly from mammalian origins (Badii and Howell, 2006).

Commercial production of collagen and gelatin are from porcine as well as bovine skin and bones (Kaewruang *et al.*, 2013; Khiari *et al.*, 2017). Despite a wide range of applications, a strong concern of collagen and gelatin still exists among the consumers, principally due to the religious restrictions or health matters (Benjakul *et al.*, 2010). As a consequence, the increasing attention and attempts have been given to the alternative sources, mainly from seafood processing by-products. Conventional methods have been employed for extraction of both collagen and gelatin. However, a low yield for both collagen and gelatin is a drawback, indicating that an effective recovery of collagenous material is not successfully performed (Chuaychan *et al.*, 2015; Kittiphattanabawon *et al.*, 2016).

In past decade, high-intensity ultrasound (20 kHz) has been extensively employed to accelerate the mass transfer, in which drying, mixing, homogenization and extraction can be improved (Pingret *et al.*, 2013). The mechanism of ultrasound in a liquid system is mainly due to the cavitation effect (Schmidt *et al.*, 2016). When the waves generate regions of high and low pressure, this leads to formation and collapse of cavitation bubbles (Pingret *et al.*, 2013). Moreover, ultrasound has been used to enhance the functional properties of proteins from eggs, poultry, soy, and milk (Soria and Villamiel, 2010). Ultrasound-assisted extraction (UAE) has been introduced for recovery of biomolecules from different sources (Marić *et al.*, 2018; Vilkhu *et al.*, 2008). Sonication has been effectively used to improve the extraction yield of phenolic compounds, oils and some organic acids from various plant sources (Hashemi *et al.*, 2017a; Pingret *et al.*, 2013; Shirsath *et al.*, 2012). The use of ultrasound under the appropriate conditions can be a potential approach to increase the yield while maintaining the molecular property of either collagen or gelatin from the fish skin of golden carp.

Nowadays, gelatin has gained increasing attention for the production of an edible/biodegradable film, which can maintain the quality of food products and reduce waste disposal problems (Nagarajan *et al.*, 2014). Due to the highly hydrophilic nature of gelatin, it tends to swell or be dissolved when putting in contact with the

surface of foodstuffs with high moisture content. Some crosslinkers have been added, while hydrophilic plasticizers are reduced in amount to improve the water vapor barrier property of gelatin films (Ramos *et al.*, 2016). Additionally, a hydrophobic substance such as lipid, wax, etc. have been employed to decrease the water vapor migration through the film. Squalene is a highly hydrophobic lipid with the formula $C_{30}H_{50}$ (Fox, 2009). Squalene is widely found in marine animal oils as a trace component and has been used in drug delivery, anti-cancer, anti-obesity, immune-modulatory functions, etc. (Fox, 2009; Kelly, 1999; Rizk and Mostafa, 2016). Since it has been well known that the liver oil of some varieties of shark, especially those inhabiting the deep sea, is rich in squalene. It has been mostly fractionated from shark liver oil (Kohno *et al.*, 1995b). In humans, squalene is one of the significant components of skin surface lipids, where it is not very susceptible to peroxidation and appears to function in the skin as a quencher of singlet oxygen in UV related skin damage and other sources of ionizing radiation (Kelly, 1999). The incorporation of squalene extracted from shark liver inhabiting in the sea of Thailand could be a promising means to improve the properties of edible gelatin film with promising health benefit. The developed squalene incorporated gelatin film can be used for packaging dry food for extending their shelf-life. The data gained regarding the collagen or gelatin extracted with the aid of ultrasound as well as the development of gelatin-based film incorporated with squalene can be a benefit for fish processing industry as well as food or packaging industries.

1.2. Literature Reviews

1.2.1. Golden carp (Probarbus jullieni)

Probarbus jullieni is commonly called as *Jullien's* golden carp, seven-striped barb, Pla Isok (Thai), Trey Trawsak (Khmer), and Pa Eun Ta Deng (Lao). It is identified by a dorsal fin with one spine and nine-branched rays; five-branched anal rays; five longitudinal stripes above the lateral line. Golden carp is one of the largest carps in the Mekong River Basin. Each reaches a maximum weight of about 70 kg (Baird, 2006). The natural habitats of golden carp include the Chao Phraya and Mae Klong river basins in Thailand; the Mekong basin in the Lao PDR, Thailand, Vietnam and Cambodia; and the Pahang and Perak basins in peninsular Malaysia (Baird, 2006). Golden carp has

attracted considerable interest from fisheries scientists and conservationists, owing to its large size, prized taste as a food fish and alleged migratory behavior (Roberts, 1993). Poulsen *et al.* (2004) reported that it is one of the most esteemed species in the Mekong, and it has been considerable potential as a 'flagship species.'

Reproduction: In the Mekong River Basin, golden carp spawn during the dry season between November and February. Artificial breeding for aquaculture occurs in Laos and Thailand using wild stock (Baird, 2006; Hogan *et al.*, 2009).

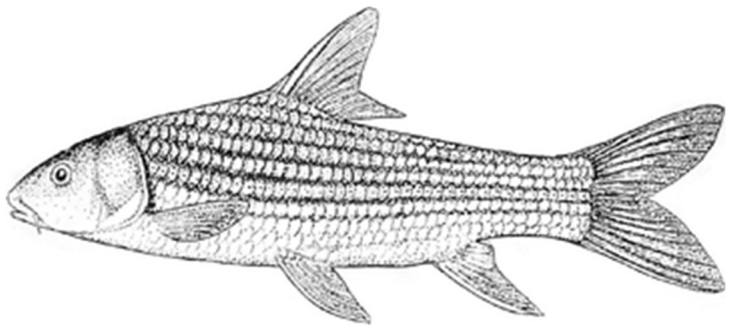

Golden carp (*Probarbus jullieni*)

1.2.2. Fish skin and scales

The primary function of fish skin is to act as a barrier. It protects against physical damage and assists with the maintenance of homeostasis by minimizing the exchange between the animal and the environment. However, in some fish, the skin may play a more active physiological role in chemical and physical protection, communication, sensory perception, movement, respiration excretion and thermal regulation (Glover *et al.*, 2013). The skin of fish is made up of two distinct layers, viz. an outermost layer, the epidermis and an inner layer dermis or corium.

Table 1: Chemical composition of the selected fish skin

	Composition (%)			
	Moisture	**Protein**	**Lipid**	**Ash**
Alaskan pollock	78.2	25.0	0.4	0.7
Pacific cod	78.1	24.5	0.3	2.0
Giant catfish	53.8	43.0	1.6	0.35
Cobia	61.0	28.9	7.4	2.6
Croaker	66.3	27.7	3.9	1.9

Sources: Bechtel (2003); Sai-Ut *et al.* (2012); Silva *et al.* (2014).

During processing, e.g. deskinning, a considerable volume of skin is generated. However, due to environmental and legislative issues regarding the disposal of fish processing by-products including skin, various means of utilization have been researched and developed. Among them, the conversion of these low market valued materials into value-added functional materials is a promising approach. Fish skin is rich in protein (Table 1). Sai-Ut *et al.* (2012) documented that giant catfish skin contained 43.0% of protein, which was higher than other fish species such as Pacific cod and Alaska pollock. The variation in the chemical composition of fish skins may depend on the species, sex, age, season and feeding (Silva *et al.*, 2014).

In nature, fish scales play a significant role in external protection. The enormous diversity of fish species also results in scales with varying size, shape, structure and composition. Nevertheless, the structure of the fish scale generally consists of two layers: a thin well-calcified external layer called the bony layer, and a thick partially calcified internal layer referred to as the basal plate, which consists of mainly type 1 collagen fibrils (Bigi *et al.*, 2001). Erts *et al.* (1994) reported that collagen fibrils act as a template for the deposition of the mineral phase. The first crystal from inside the gap region of the collagen staggers the structure. Subsequently, calcification proceeds; the crystals penetrate the overlap zone and compress the triple-helical collagen molecules.

1.2.3. Fish collagen

The main component of extracellular matrices in fish is type I collagen, a protein that gives strength and resistance to biological tissues. Collagen monomers are assembled in typical cross-striated fibrils, in which the triple helices are aligned parallel to the long axis of the structure with an apparent hexagonal lateral packing (Hulmes *et al.*, 1995). Fibrils are further assembled into extracellular domains in specific and ordered arrays, classically described in bone, cornea, dermis and tendon (Giraud-Guille *et al.*, 2000). Type I collagen is the most widely occurring collagen in connective tissue. Collagen is derived from tropocollagen, which consists of three polypeptide chains intertwined to from rod-shaped triple helical structure This particular structure is mainly stabilized by hydrogen bonding among the functional groups including –CO and –NH group (Benjakul *et al.*, 2012c). Each α-chain is the product of an almost continuous repeating of the Gly-X-Y- sequence, where X is mostly proline and Y is mostly hydroxyproline (Johnston-Banks, 1990). Only the very short N- and C-terminal regions, called telopeptides (15–26 amino acid residues), do not form triple helical structures as they are primarily made up of lysine and hydroxylysine (Hyl) residues, as well as their aldehyde derivatives, in both intra- and inter-molecular covalent cross-links (Bateman *et al.*, 1996).

1.2.3.1. Extraction of collagen

The extraction of collagen from fish has been carried out in several species using different byproducts, such as sea bass skin (Sinthusamran *et al.*, 2013), skin of clown featherback and brownbanded bamboo shark (Kittiphattanabawon *et al.*, 2016; Kittiphattanabawon *et al.*, 2010a), skin and bone from Japanese seerfish (Li *et al.*, 2013), bladder of yellowfin tuna (Kaewdang *et al.*, 2014), cartilage from Japanese sturgeon (Liang *et al.*, 2014), the fins, scales, skins, swim bladders and bones from bighead carp (Liu *et al.*, 2012) as well as scales of Nile tilapia (Kittiphattanabawon *et al.*, 2019). Despite the ease of extraction of marine collagen and abundance of collageneous raw materials, the collagen presents some limitations in their applications, due to its low denaturation temperature (Benjakul *et al.*, 2012c).

1.2.3.1.1. Preparation of raw material

The skin is first processed to remove residual meat and cleaning is performed to eliminate other contaminants. Reduction of the size of raw material was also reported to ease further chemical treatment as well as extraction of collagen (Benjakul *et al.*, 2012c; Rizk and Mostafa, 2016).

1.2.3.1.2. Pretreatment of raw material

Generally, the raw material such as fish skin and scales contains some undesired components including non-collagenous proteins, pigments, lipids and minerals, etc. (Savedboworn *et al.*, 2017; Sinthusamran *et al.*, 2013). Calcium, mainly in the form of Ca-hydroxyapatite or other inorganic matters, are found in bone and scale (Arpi and Novita, 2018; Kittiphattanabawon *et al.*, 2019). Appropriate pretreatments have been implemented to remove these undesired contaminants and to increase the purity of extracted collagen. To remove non-collagenous proteins and pigments, alkaline (0.5 or 1 M NaOH) pretreatment is used (Benjakul *et al.*, 2010; Nagai and Suzuki, 2002). However, NaCl and H_2O_2 have also been employed to remove pigments and non-collagenous proteins, respectively (Wang *et al.*, 2007). Few raw materials including bones (Kittiphattanabawon *et al.*, 2005) and scales from carp (Chuaychan *et al.*, 2015), etc. contain a highly significant amount of calcium. Those raw materials are efficiently decalcified by employing inorganic acid, especially hydrochloric acid or ethylenediaminetetraacetic acid (EDTA). Therefore, the decalcified porous raw material with the increased surface area can be readily subjected to collagen extraction.

1.2.3.1.3. Acid soluble collagen extraction

Solubilization of collagen using acid has been extensively used for collagen extration (Table 2). The collagen can be recovered in acid solution, mainly acetic acid and the obtained collagen is referred to as “acid-soluble collagen, ASC” (Wang *et al.*, 2008). Typically, collagen is extracted employing 0.5 M acetic acid treatment at 4 °C for 24–48 h (Sinthusamran *et al.*, 2013; Wang *et al.*, 2018; Wang *et al.*, 2008), in which the tropocollagen is exists in its triple helix form with insignificant changes. After extraction, the undesired non-collagenous proteins are eliminated by

means of salt precipitation or dialysis, therefore increasing collagen purity (Jongjareonrak *et al.*, 2005). Nalinanon *et al.* (2008) documented that, when extraction time was increased from 6 to 48 h, the yield efficieny of ASC improved with an increase from 12.32% to 34.90% (based on hydroxyproline content) from threadfin bream skin. Similar observation were made from bigeye snapper skin, where the yield raised from 7.3% to 9.3% corresponding to the increse in extraction time from 24 to 48 h (Nalinanon *et al.*, 2007). In addtion, the concentration of acid is another dependent factor governing the yield of collagen. The increase in concentration of acetic acid (0.1 to 0.5 M) could result in increased yield of ASC from cod skin, in which the yield increased from 52% to 59% (dry weight basis). Re-extraction of ASC from the residual mass using 0.5 M acetic acid was achieved to increase the yield, mainly in carp bone (Duan *et al.*, 2009), bigeye snapper skin and bone (Kittiphattanabawon *et al.*, 2005). The Fourier transform infrared (FTIR) spectroscopy of collagen from skin and swim bladder of seabass (Sinthusamran *et al.*, 2013), and circular dichroism (CD) spectroscopy of collagen from the scales of *Pagrus major* and *Oreochromis niloticas* extracted using acetic acid apparently demonstraged the triple-helical structure of ASC (Ikoma *et al.*, 2003). Nontheless, yield of ASC is also dependent on the animal species and the age and parameters of extraction used (Savedboworn *et al.*, 2017; Wang *et al.*, 2008).

1.2.3.1.4. Pepsin soluble collagen extraction

Typical acid extraction method renders a low yield of collagen. To overcome this problem, pepsin has been successfully employed, due to it can specifically cleave peptide in telopeptide region of mother collagen, leading to the increased extraction efficiency (Benjakul *et al.*, 2010). The collagen obtained with pepsin treatment is referred to as “pepsin-soluble collagen, PSC” (Nalinanon *et al.*, 2007). Pepsin hydrolyzes some of the non-collagenous proteins and telopeptides of mother collagen, thus increasing the solubility of collagen sample in acid solution. As a result, the improved extraction efficiency was obtained (Iswariya *et al.*, 2017). Shoulders and Raines (2009) documented that most of and inter- and intra-molecular cross-links in collagen occur through the telopeptide region. Therefore, the use of pepsin during collagen extraction could influence the composition of resulting collagen. Generally, β- (dimmer) and γ-chains (trimer) found in PSC might decrease, compared

to those found in ASC (Wu *et al.*, 2014). As the cleavage of telopeptide is more likely results in the breakdown of cross-links, such as β- and γ-chains, to the α-chain, which can be of ease for extraction (Benjakul *et al.*, 2012c). Pepsin, predominantly from porcine, has been employed to increase the extraction efficiency of collagen from several species such as bigeye snapper skin (Benjakul *et al.*, 2010; Nalinanon *et al.*, 2007), *Pagrus major* and *Oreochromis niloticas* scales (Ikoma *et al.*, 2003) and deep-sea redfish skin (Wang *et al.*, 2007). Additionally, fish pepsin has also been used for the extraction of PSC from fish skin (Nalinanon *et al.*, 2010). The skin of bigeye snapper was pre-swelled using 0.5 M acetic acid, followed by pepsin hydrolysis. The samples treated in this two-step manner generally resulted in higher extraction yield of collagen (Benjakul *et al.*, 2010). Via this two-step method, the highest extraction yield of collagen was reported for the skins of bigeye snapper up to ~53%, when the extraction time employed was 48 h, irrespective of the preswelling time used (Nalinanon *et al.*, 2007). Kittiphattanabawon *et al.* (2010a) documented that ASC and PSC from the skin of brownbanded bamboo shark had a yield of 9.3% and 8.8% (based on the wet weight), respectively.

1.2.3.1.5. Recovery of collagen

Recovery of collagen after extraction is mainly carried out by precipitating the collagen in the presence of high salt concentration. Commonly, NaCl to a final concentration of 2.6 M is added to the collagen extract by pre-adjusting the pH of the extract to 7.5 using 0.05 M Tris(hydroxymethyl)aminomethane to precipitate solubilized collagen (Benjakul *et al.*, 2010; Kittiphattanabawon *et al.*, 2005; Nagai and Suzuki, 2002). However, varying concentrations of NaCl ranging from 0.9 to 2.6 M, to precipitate collagen and eliminate the impurities (Kittiphattanabawon *et al.*, 2019; Rizk and Mostafa, 2016; Sadowska *et al.*, 2003). Thereafter, the precipitated collagen is pelleted and dialyzed with 0.1 M acteic acid, followed by dialysis against distilled water (Iswariya *et al.*, 2017; Sinthusamran *et al.*, 2013). The obtained dialysate is subjected to freeze-drying to obtain the collagen (Liang *et al.*, 2014; Schmidt *et al.*, 2016).

Table 2. Sources, type and yield of collagens extracted from different fish species

Fish species	Source	Collagen types	Yield (%)	References
Nile tilapia (*Oreochromis niloticus*)	Scales	ASC PSC	0.77 0.71	Kittiphattanabawon *et al.* (2019)
loach (*Misgurnus anguillicaudatus*)	Skin	ASC PSC	22.42 27.32	Wang *et al.* (2018)
Puffer fish (*Lagocephalus inermis*)	Skin	ASC PSC	43.1 56.6	Iswariya *et al.* (2017)
Seabass (*Lates calcarifer*)	Scales	ASC PSC	0.38 1.06	Chuaychan *et al.* (2015)
Yellowfin tuna (*Thunnus albacares*)	Swim bladder	ASC PSC	1.07 12.10	Kaewdang *et al.* (2014)
Amur sturgeon (*Acipenser schrenckii*)	Cartilage	ASC PSC	27.04 55.92	Liang *et al.* (2014)
Bigeye snapper (*Priacanthus tayenus* and *Priacanthus macracanthus*)	Skin	PSC	7.74 7.06	Benjakul *et al.* (2010)
Brownbanded bamboo shark (*Chiloscyllium punctatum*) and blacktip shark (*Carcharhinus limbatus*)	Cartilage	ASC PSC	1.27 9.59 1.04 10.30	Kittiphattanabawon *et al.* (2010c)
Carp (*Cyprinus carpio*)	Skin Scales Bones	ASC	41.3 1.35 1.06	Duan *et al.* (2009)

1.2.3.2. Properties and characteristics of fish collagens

Collagen from fish has been reported to exhibit varying properties as affected by the extraction process and the sources (Benjakul *et al.*, 2012c; Schmidt *et*

al., 2016). Collagens from shellfish and finfish are generally classified into type I and type V (Bateman *et al.*, 1996).

1.2.3.2.1. Protein patterns and types

Collagen from skin and bones of bigeye snapper (*P. tayenus*) contained at least two different α-chains, named α_1 and α_2. (Benjakul *et al.*, 2012c). Similarly, collagens from skin, scales and bone from other fish species consisted of α_1 and α_2-chains (Chuaychan *et al.*, 2015; Rizk and Mostafa, 2016; Sinthusamran *et al.*, 2013). Fish collagen is defined as type I, in which α_1 and α_2 are found as a major component with dimerization of α_2-chain to from β-chain or β_{12}-dimer (Sadowska *et al.*, 2003). As reported by Benjakul *et al.* (2010), PSCs from bigeye snapper, *P. tayenus* and *P.* macracanthus were extracted with the aid of porcine pepsin and tongol tuna pepsin. Among these PSC extracted using porcine pepsin had a lower proportion of α-chains, but the higher content of β-chain compared with those extracted with tuna pepsin. The electrophoretic patterns of collagens from the skin of bigeye snapper examined under reducing and nonreducing conditions were similar, suggesting that no disulfide bonds were present in those collagens (Nalinanon *et al.*, 2007). In addition, Kittiphattanabawon *et al.* (2010a) reported collagens extracted from brownbanded bamboo shark including ASC and PSC had α- and β-chains as their major components and were identified as type I collagen. Wang *et al.* (2007) documented that ASC from grass carp contained significantly higher population of cross-linked chains (β and γ) than that of PSC, suggesting that the extent of the intra- and/or intermolecular cross-link in ASC was higher than in PSC, since N-and C-terminus non-helical domains in PSC were removed by pepsin. Similarly collagens (ASC and PSC) from scales of various fish species including seabass, bighead carp, Nile tilapia, spotted golden goatfish, etc. are characterized to be type I collagen (Chuaychan *et al.*, 2015; Kittiphattanabawon *et al.*, 2019; Matmaroh *et al.*, 2011; Tu *et al.*, 2015).

1.2.3.2.2. Amino acid compositions

Collagen has a unique amino acid composition, unlike other proteins. Collagen consists of glycine, proline and alanine as an abundant amino acid, low or no cysteine and tryptophan content. Tyrosine and histidine are relatively found in low

abundance in collagen. Two amino acids including hydroxyproline and hydroxylysine substantially present in collagen, but are not commonly available in other proteins (Wang *et al.*, 2007). Collagen consists of glycine almost to the one-third of total amino acid residues, which is present in every third position over all the α-chain (Benjakul *et al.*, 2012c). However, glycine is absent in first ten amino acid residues of C-terminus and first 14 residues from N-terminus; these positions are termed as "telopeptide" regions (Foegeding *et al.*, 1996). The occurrence of glycine at every third residue in α-chain is a crucial requirement to form triple helix structure (Regenstein and Zhou, 2007). As glycine is devoid of side chain, which reduces the hindrance between two α-chains to come in close vicinity and from the superhelix structure with close packing (Shoulders and Raines, 2009). The formation of superhelix is facilitated by the occurrence of proline (Pro) and hydroxyproline (Hyp) at X and Y-positions in Gly-X-Y repeats situated in polypeptide α-chain (Johnston-Banks, 1990). Hydroxyproline is located at Y-position, while proline can be found in either the X- or Y-positions (Johnston-Banks, 1990). Similar amino acid compositions of collagens from various fish species such as bigeye snapper skin and bones (Kittiphattanabawon *et al.*, 2005), seabass scales (Chuaychan *et al.*, 2015; Sinthusamran *et al.*, 2013), Nile tilapia skin (Zeng *et al.*, 2009) have been reported. Benjakul *et al.* (2010) reported that collagens from bigeye snapper contained glycine as the most dominant amino acid (325–330 residues per 1000 residues).

1.2.3.2.3. Fourier Transform Infrared (FTIR) Spectroscopy

Collagens from skin of various fish sources including bigeye snapper, rohu, seabass and puffer fish demonstrated similar FTIR spectra with major absorption bands including amide band I, II, III, A and B (Benjakul *et al.*, 2010; Iswariya *et al.*, 2017; Savedboworn *et al.*, 2017; Sinthusamran *et al.*, 2013). However, a subtle change in FTIR spectra between ASC and PSC from seabass scales (Chuaychan *et al.*, 2015) and brownbanded bamboo shark (Kittiphattanabawon *et al.*, 2010a) was documented, representing slight differences in their functional groups and secondary structure. Amide band A is related to the N–H stretching vibration, which demonstrates the existence of hydrogen bonds. When the NH group of a peptide chain is involved in a hydrogen bonding, the position amide band A is shifted to lower frequencies

(Kittiphattanabawon *et al.*, 2010a). Amide B band is associated with CH_2 irregular stretching vibration (Muyonga *et al.*, 2004). The amind band I associated with the triple helix absorption of collagens is situated at the wavenumber 1637 cm^{-1} (Petibois *et al.*, 2006). Amide II is associated with N-H bending coupled with C-N stretching (Woo *et al.*, 2008). Amide III band of collagens is related to C–N stretching and N–H in-plane bending from amide linkages as well as absorptions arising from wagging vibrations from CH_2 groups from the glycine backbone and proline side chains are involved in the triple-helical structure of collagen (Lebon *et al.*, 2016). In addition, the triple helix structure of collagen can be confirmed by determining the ratio between amide band III and the band occurring at the wavenumber 1450 cm^{-1}, which is almost near to the value 1.0 (Benjakul *et al.*, 2012c; Duan *et al.*, 2009).

1.2.3.2.4. Thermal stability

Thermal stability of collagen superhelix structure is mainly associated to the hydrogen bonding arbitrated to the presence of water molecules, which forms a bridge link between amide carboxyl of the main chain with that of hydroxyl group of hydroxyproline of another chan (Shoulders and Raines, 2009). Thus, the imino acids, proline and hydroxyproline are mainly characterized the thermal stability of collagen molecules. Therefore the content of imino acid is a crucial factor required for the stabilization of collagen structure (Persikov *et al.*, 2004). Generally, fish collagen obtained from fish living in a warm environment have higher hydroxyproline content than those obtained from cold environments (Muyonga *et al.*, 2004). Thus, the thermal stability and imino acid content of fish collagens are mainly related to their habitat (Foegeding *et al.*, 1996). Muyonga *et al.* (2004) documented that ASC from the skin of young and adult Nile perch contained different imino acid contents 19.3% and 20.0%, respectively, corresponding to their age and was higher than that from other fish species. In addition, the thermal stability of triple helix structure of collagen is linked to the hydrogen bonding by hydroxyl group of hydroxyproline and is governed by the restriction caused by the pyrrolidine rings of hydroxyproline located and proline in the secondary structure (Benjakul *et al.*, 2010; Lebon *et al.*, 2016). T_{max} of collagen from skin of different species can be varied, i.e. ASC from skin of puffer fish (*Lagocephalus inermis*) (78.9 °C) (Iswariya *et al.*, 2017), ASC from skin of marine eel-fish (*Evenchelys*

macrura) (38.5 °C) (Veeruraj *et al.*, 2013) and ASC from skin of seabass (*Lates calcarifer*) (33.33 °C) (Sinthusamran *et al.*, 2013).

1.2.3.2.5. Circular dichroism (CD) spectroscopy

Circular dichroism (CD) spectroscopy is a powerful tool for studying the folding of collagen and other model triple-helical peptide systems (Brodsky and Ramshaw, 1997). In the case of the triple helix, the unique supercoiled polyproline type II secondary structure of the protein backbone exhibits the sharp CD transitions, including a positive band at 222 nm and a negative band at 195 nm (Greenfield, 2006). Under acidic conditions, collagen exists primarily as a soluble triple helix. The CD spectrum of collagen (ASC and PSC) from black drum and sheepshead skin, at 15 °C, showed a positive peak at 220 nm and a negative peak at 201 nm, which were characteristic of collagen triple helical structure and were similar to that of calf skin collagen (Ogawa *et al.*, 2003). Veeruraj *et al.* (2013) reported that the triple helical structure of pig and calf collagen was more stable over a temperature range of 25-40 ºC, compared to cold water fish collagens. CD analysis revealed a refolding of denatured collagen chains into the typical triple helix conformation upon cooling and, conversely, unfolding upon reheating (Drzewiecki *et al.*, 2016).

1.2.4. Fish gelatin

Gelatin can be produced by thermal denaturation or partial hydrolysis of fibrous collagen (Muyonga *et al.*, 2004). During the transition process the week bonds along with some covalent bond are destabilized, which results in formation of amorphous form so-called gelatin (Foegeding *et al.*, 1996). Gelatin as a vital hydrocolloid has numerous applications in food industry as a gelling agent, thickening agent and stabilizer in ice cream or salad dressing and as a texturizer in confectionaries (Badii and Howell, 2006; Saha and Bhattacharya, 2010; Zubair and Ullah, 2019). In addition, gelatin has numerous emerging applications in biomedical, pharmaceuticals, cosmetics, biomaterial-based packaging industries and nano-technology based industry (Ali *et al.*, 2018; Duan *et al.*, 2018; Kang *et al.*, 2019; Karim and Bhat, 2009). Gelatin contains all the essential amino acids except tryptophan (Benjakul *et al.*, 2012a). Moreover, due to its surface-active properties, gelatin has been used in a wide range of

applications including foaming, emulsifying and wetting agents in food, and has more significant role in pharmaceutical and medical applications owing to its surface-active properties (Duan *et al.*, 2018; Nagarajan *et al.*, 2012b).

Typically, gelatin is extracted largely from mammalian sources, particularly cow and pig from their skin and bones. However, gelatin from both the sources have restrictions, due to the occurrence of bovine spongiform encephalopathy (BSE) causes mad cow disease and the pig gelatin has cultural and religious constraint and cannot be used in kosher and halal foods (Regenstein and Zhou, 2007). Thus, increasing attention of consumers towards health issues has resulted in higher demands of gelatin from fish (Kittiphattanabawon *et al.*, 2010c). To tackle this problem, gelatin production from alternative sources have been intensively increased, chiefly from processing by-products including fish skin, scales, bone due to their abundance and low cost (Khiari *et al.*, 2017; Nagarajan *et al.*, 2017). Properties and composition of fish gelatin are mainly governed by the raw material. The processing parameters including pretreatments, hot extraction, bleaching and drying could influence the functional and chemical properties of resulting gelatin (Duan *et al.*, 2018; Nagarajan *et al.*, 2012a; Sae-Leaw *et al.*, 2016). Generally, gelatin from fish has been reported to exert inferior functional properties compared to those of mammalian counterparts, therefore limiting their application (Benjakul *et al.*, 2012a). Several approaches have been therefore established to improve the functional properties of gelatin from fish via chemical modification and enzymatic processes to broaden their applications in a wide range of industries (Bitencourt *et al.*, 2014; Choi *et al.*, 2018; Huang *et al.*, 2019; Kaewruang *et al.*, 2014; Staroszczyk *et al.*, 2012).

1.2.4.1. Production of gelatin

Gelatin production involves three main stages (1) pretreatment, (2) extraction, and (3) purification and drying. All these processes have been known to influence the yield and properties of gelatin. Optimization of extraction process has been done using raw materials from different sources as shown in Table 3.

Table 3. Procedures employed for pretreatment and extraction of fish gelatin

Sources	Pretreatment	Extraction condition	References
Whiptail stingray (*Dasyatis brevis*)	1) Treated with 0.1 M NaOH (1:6 w/v) for 1 h. 2) Soaked in different acids HCl or acetic acid at different concentrations (0.01, 0.025, 0.05, 0.075, 0.1, 0.15, and 0.2 M)	Distilled water at 60 °C for 3 h	Sántiz-Gómez *et al.* (2019)
Channel catfish (*Ictalurus punctatus*)	1)Treated with 0.1 M NaOH (1:10 w/v) for 6 h at 4 ºC 2) Soaked in 10% butyl alcohol (1:10 w/v) overnight	Distilled water at 45 ± 1 °C for 12 h	Duan *et al.* (2018)
Tilapia (*Oreochromis niloticus*)	1) Treated with 0.5-1.5 N NaOH (1:5 w/v) at 4 ± 1 °C for 1 h 2) Soak in 0.01 to 1 N HCl (1:5 w/v) for 1 h at 25 °C	Distilled water at 30 to 65 °C for 3 h	Arpi and Novita (2018)
Mackerel	1) Treated with 0.1 N NaOH for 1 h 30 min at 4 °C 2) Soak in different concentrations (25, 50 or 100 mM) of different organic acids (acetic, citric, lactic, malic or tartaric acid) 4 h at 4 °C	Distilled water at 45 °C for 18 h	Khiari *et al.* (2017)
Seabass (*L. calcarifer*)	1) Treated with 0.1 M NaOH (1:10 w/v) for 3 h at 25 ºC 2) Soak in 0.5 M of acetic acid or citric acid for 2 h 3) Soak in 30% isopropanol (1:10 w/v) for 1 h	Distilled water at 55 °C for 6 h	Sae-Leaw *et al.* (2016)
Cobia (*Rachycentron canadum*)	1) Treated 3 M NaOH (1:1 ratio) for 60 mon 2) Soak in 3 M HCl (1:1 ratio) for 15 min at room temperature	Distilled water at 52 °C for 2 h	Silva *et al.* (2014)
Unicorn leatherjacket (*Aluterus monoceros*)	1) Treated with 0.1 M NaOH (1:10 w/v) for 4 h at room temperature 2) Soak in 0.5 M of phosphoric acid for 6 h	Distilled water at 65 °C for 12 h	Kaewruang *et al.* (2014)

Table 3. (continued)

Sources	Pretreatment	Extraction condition	References
Seabass (*L. calcarifer*)	1) Treated with 0.1 M NaOH (1:10 w/v) for 3 h at room temperature 2) Soak in 0.5 M of acetic acid or citric acid for 2 h 3) Soak in 30% isopropanol (1:10 w/v) for 1 h	Distilled water at 45 and 55 °C for 3, 6 and 12 h	Sinthusamran *et al.* (2014)
Tilapia (*Oreochromis niloticus*)	1) Treated with tap water (1:6 w/v) for 10 min 2) Soak in 0.3 M NaOH (1:6 w/v) for 1 h 3) Soak in 0.01 to 0.2 M acetic acid, citric acid HCl for 1 h	Distilled water at 50 °C for 3 h	Niu *et al.* (2013)
Splendid squid (*Loligo formosana*)	1) Treated with 0.1 M NaOH (1:10 w/v) for 6 h at room temperature 2) Soak in 0.5 M of phosphoric acid (1:10 w/v) for 24 h at 4 °C	Distilled water at 50, 60, 70 and 80 °C for 12 h	Nagarajan *et al.* (2012b)
Farmed giant catfish (*Pangasianodon gigas*)	1) Treated with 0.2 mol l^{-1} NaOH (1:10 w/v) at 4 ± 1 °C for 1 h 30 min 2) Soak in 0.05 mol l^{-1} acetic acid (1:10 w/v) for 3 h at 25 °C	Distilled water at 45 ± 1 °C for 12 h	Jongjareonrak *et al.* (2010)

1.2.4.1.1. Pretreatment

Pretreatment of raw material is commonly carried out to increase the purity of resulting gelatin. Primarily, non-collagenous proteins are eliminated by treating the raw material with alkaline solution, in which considerable amount of interchain cross-links are broken down (Regenstein and Zhou, 2007). Type of alkali used does not have any difference in pretreatment process, though the concentration of alkali used is the crucial factor for consideration (Arpi and Novita, 2018; Zhou and Regenstein, 2005a). Besides the removal of non-collagenous proteins, alkali also targets to telopeptide region of tropocollagen. Thus some collagen gets solubilized in alkaline solution. Overall, the longer treatment time or high alkaline concentration

decreased the yield of gelatin from swim bladder of yellowfin tuna (Kaewdang *et al.*, 2016).

Raw materials such as fish skin with high-fat content can readily undergo oxidation, especially during hot extraction, thus resulting in lipid oxidation in gelatin and development of off odors/flavors (Sae-leaw and Benjakul, 2015). Additionally, alkaline pretreatment could form soap and can contaminate the resulting gelatin. Removal of fat has been performed by several researchers, using a different solvent system. Muyonga *et al.* (2004) degreased bone of Nile perch by tumbling in warm (35 °C) water. The skins of channel catfish (*Ictalurus punctatus*) were then soaked in 10% butyl alcohol with a solid/solvent ratio of 1:10 (w/v) overnight to remove fat (Duan *et al.*, 2018).

1.2.4.1.2. Swelling of pretreated raw material (acid process)

Before thermal extraction, it is generally important to loosen the skin matrix, which could increase extraction efficiency. Swelling of raw material is essential because this can favor proteins to unfold through destabilization of noncovalent bonding and disrupt the collagen molecules for subsequent extraction by solubilization using hot water (Stainsby, 1987). The pretreatment is intended to transform tropocollagen to be more suitable for extraction. Nagarajan *et al.* (2012b) reported that the covalent linkages of tropocollagen must be principally disrupted to allow the release of free α-chains during gelatin extraction process. During this process, other organic substances are removed along with partial inactivation of endogenous proteases responsible for degradation (Benjakul *et al.*, 2012a). Moreover, the concentration and type of acid affect the yield and properties of gelatin. Gudmundsson and Hafsteinsson (1997) reported that yield and properties of resulting gelatin from cod skin were influenced by the concentration of H^+ used. Gómez-guillœn and Montero (2001) documented that megrim skin swollen using acetic and propionic acid at the concentration of 0.05 M yielded gelatins with superior rheological properties and gel strength to those pretreated using other acids or concentrations. Pretreatment employing citric acid yielded gelatin with lowest turbidity, while those pretreated with propionic acid had the most turbid gelatin solution (Fernandez-Dıaz *et al.*, 2001). Gómez-Guillén

et al. (2011) documented that pretreatment using lactic acid at the concentration of 25 mM could substitute the swelling process achieved by using 50 mm acetic acid with negligible change in properties of resulting gelatin. Generally, gelatin extracted employing acid process is known as a type A gelatin (Johnston-Banks, 1990). Nalinanon *et al.* (2008) documented the gelatin extracted with the aid of pepsin from bigeye snapper skin in combination with a protease inhibitor had higher bloom strength than compared to the conventional extraction method. Sae-Leaw *et al.* (2016) reported that gelatin from skin pretreated with citric acid had lower fishy odor/flavor than that from skin pretreated using acetic acid.

1.2.4.1.3. Gelatin extraction

After pretreatment, the hot extraction process is generally employed for gelatin extraction. During hot extraction process when the heat is applied to the collagen molecule, the fibrils undergo shrinkage to one-third of its original size, the temperature is termed as shrinkage temperature (Foegeding *et al.*, 1996). The process involves the destruction of collagen triple helical structure follwed by separation of fibers (Chiou *et al.*, 2008). During the transition, most of the weak interaction mainly H-bonds are broken along with few strong covalent bonding, in addition some insignificant number of peptide linkages are also cleaved (Johnston-Banks, 1990). Nonetheless, the higher degree of hydrolysis could results in completed destruction of collagen molecule, as a result glue is from instead of gelatin. Thus with influence of this process parameters, gelatin is extracted with varying yield, mass, which is is also depends on the presence of indigenous proteinases (Carvalho *et al.*, 2008b; Karim and Bhat, 2009). The gelatin typically contains the fractions with wide range of molecular distribution from 15 to 400 kDa (Foegeding *et al.*, 1996).

The main objective of extraction process is to achieve the highest yield efficiency without altering the desirable physiochemical properties. Generally, extraction can be achieved depending on the pH of extraction medium, which can be either low or neutral pH to achieve the desirable physical properties (Johnston-Banks, 1990). Effective pretreatment could be performed at lower temperatures to minimize the loss of properties of resulting gelatin, especially the gel strength (Benjakul *et al.*,

2012a). Generally, a shorter extraction time related with a higher temperature at neutral pH could result in gelatin with lower gel strength (Johnston-Banks, 1990). Gel strength of channel catfish reduced when the extraction temperature was increased from (Yang *et al.*, 2008). Arpi and Novita (2018) investigated the effect of NaOH and HCl concentrations during pretreatment of tilapia skin. Lower NaOH concentrations (0.77 N) provided proper pH for gelatin extraction, especially when combined with higher extraction temperatures (66.80 ºC). Similarly, Kittiphattanabawon *et al.* (2010b) documented that the reduction of α-, β- and γ -chains band intensity of gelatin extracted from blacktip shark and brownbanded bamboo shark skin was noticed when the extraction was performed at the higher temperatures as well as there was a significant increase in the low molecular weight components. This major changes could result in the inferior gel properties due to the shorter chain fragments could not form stronger gel networks. Sinthusamran *et al.* (2018) reported that the yield and recovery of gelatin from swim bladder (44.83–71.95% and 49.08–74.83%, based on dry weight) increased with increasing extraction temperatures. Additionally, FTIR and CD spectra revealed the loss of triple helix during heating via breaking down hydrogen bonds between α-chains.

1.2.4.1.4. Filtration and drying

After completion of extraction process, a significant amount of residue is leftover in the form of insoluble matter, which can be separated by means of filtration using double layered cheesecloth (Kittiphattanabawon *et al.*, 2016; Sinthusamran *et al.*, 2018). Furthermore, the solution was clarified using Diatomaceous earth or activated carbon (Kaewruang *et al.*, 2013; Sae-leaw and Benjakul, 2015), followed by centrifugation and filtration by filter paper (Muyonga *et al.*, 2004; Sinthusamran *et al.*, 2018). Those processes above are employed to minimize the loss of functional property of gelatin, which eliminates the contaminants (Johnston-Banks, 1990). Drying is another crucial process to obtain dry gelatin with long shelf-life. Nevertheless, it can affect the yield and properties of gelatin. Kwak *et al.* (2009) compared three drying methods for gelatin from shark cartilage including (1) spray-drying, (2) freeze-drying, and (3) hot-air drying. The freeze-drying process yielded gelatin with superior gel properties with excellent foaming ability. Nevertheless, gelatins from spray-drying

method exhibited the best emulsion capacities. Sae-Leaw *et al.* (2016) studied the effect of different drying methods on the functional property as well as the quality of resulting gelatin film from seabass skin. It was found that the freeze-dried gelatin had better gel strength in compared to that of spray-dried gelatin. However, spray dried gelatins had lower fishy odor/flavor with coincidentally lower abundance of volatile compounds, including aldehydes, ketones, and alcohols, etc., in comparison with its freeze-dried counterpart.

1.2.4.2. Physicochemical and functional properties of gelatin

The most important properties of gelatin for food applications are gel strength, viscosity, gelling and melting points. These properties are affected by many physical and chemical factors, such as the average molecular weight and molecular weight distribution, concentration of the gelatin solution, gel maturation time, gel maturation temperature, pH, salt content and amino acid composition (Benjakul *et al.*, 2009; Regenstein and Zhou, 2007).

1.2.4.2.1. Amino acid compositions

The amino acid composition of gelatin primarily depends on the tropocollagen of fish and is further affected by the method of extraction. As reported by Karim and Bhat (2009), fish skin gelatin shows a wider variety of amino acids than mammalian gelatins. Hydroxyproline and proline contents are lower than those in mammalian collagens, and this is compensated by higher serine and threonine contents. In general, denaturation temperature is related to the imino acid content. Based on the amino acid composition of gelatin, glycine, alanine, proline and hydroxyproline were found at the highest residues from the total amino acids residues in blacktip shark and brownbanded bamboo shark gelatin (Kittiphattanabawon *et al.*, 2010b). The amino acid composition particularly imino acid (proline and hydroxyproline) of gelatin is one of the important factors affecting the functional properties of resulting gelatin, especially gel-forming properties (Benjakul *et al.*, 2009). The lower denaturation temperature of fish gelatin than mammalian counterpart is primarily related to the lower imino acid content of fish gelatin (Badii and Howell, 2006). Gelatin gel strength is correlated with the Imino acid content of the gelatin. The hydroxyproline in the peptide chain of gelatin

has an important role in gel formation and its properties, it stabilizes the triple helix structure by from inter-chain hydrogen bond to the carbonyl group as well as forms a bridge in the presence of water molecule (Balti *et al.*, 2011; Benjakul *et al.*, 2012a). Moreover, the imino acid contents of warm-water fish gelatins (such as bigeye-tuna and tilapia) were higher than those of cold-water fish (such as cod, whiting and halibut) gelatins (Karim and Bhat, 2009). The proline and hydroxyproline contents are approximately 30% for mammalian gelatins, 17% for cold-water fish gelatin (cod) and 22–25% for warm-water fish gelatins (tilapia and Nile perch), and (Muyonga *et al.*, 2004). However, both cold-water fish and mammalian gelatins have the similar proportion of alanine, glutamic acid, cysteine, isoleucine, tyrosine, phenylalanine, hydroxylysine, lysine, and arginine residues (Lin *et al.*, 2017).

1.2.4.2.2. Gelation

Gelation is one of the most important functional properties of gelatin, which is influenced by raw material, the occurrence of an indigenous protease in raw material and extraction conditions employed, especially the temperature used for extraction of gelatin (Karim and Bhat, 2009; Kittiphattanabawon *et al.*, 2010b). An aqueous solution of gelatin forms a low viscous solution at a temperature above 40 °C. During the cooling process, when the temperature is below the setting temperature the solution turns to transparent gels with thermo-reversible gel properties (Czerner *et al.*, 2016). The gelling or setting temperature of fish gelatin varies with fish species. In general, gelling temperatures of fish gelatin are lower than those of mammalian counterparts (Sinthusamran *et al.*, 2014). During the setting of gel, the transition from disordered structure to ordered structure occurs by increased interactions, in which the gelatin molecules in random coil conformation eventually turn to more ordered superhelical structure. This results in the formation of higher inter junction zones with reversible cross-linkages via hydrogen bonding (Kaewruang *et al.*, 2014; Liu *et al.*, 2019). The amino acid composition and amount of β- and γ-components were considered as factors governing gelation of gelatin (Nagarajan *et al.*, 2012b). Imino acids, especially hydroxyproline, are associated with the gel formation of gelatin by hydrogen bonding through the hydroxyl group (Johnston-Banks, 1990). Also,

Kittiphattanabawon *et al.* (2016) reported that gelatin with a large amount of α-, β- and γ-chains yielded gel network with strong strands.

Additionally, the extraction conditions have been known to determine the gelling property of gelatin. Nagarajan *et al.* (2012b) extracted the gelatin from splendid squid skin at different temperatures (50, 60, 70 and 80 °C). Gelatin extracted with extraction temperature of 50 °C exhibited the highest gel strength. Higher extraction temperature could lead to the formation of considerable portion of hydrolyzed gelatin with lower molecular weight fragments. As a result, gel with inferior gelling ability is formed (Duan *et al.*, 2018). Kittiphattanabawon *et al.* (2016) also reported that increasing extraction temperature and time decreased gel strength of gelatin from clown featherback skin. Additionally, gelling temperature also decreased when extraction temperature and time were increased. Kaewruang *et al.* (2013) documented that gelatin from the skin of unicorn leatherjacket extracted at 45 and 55 °C had the lower gel strength than gelatin extracted at 65 °C, mainly caused by endogenous heat-stable proteases. In addition, several organic acids including acetic, lactic, formic, propionic, citric, malic and tartaric acids) employed for pretreatment had diverse effects on functional properties of gelatin gels (Gómez-Guillén *et al.*, 2011; Sántiz-Gómez *et al.*, 2019). Gelatins with formic acid or lactic acid pretreatment showed higher gel strength than those pretreated with other acids (Zhao *et al.*, 2019). Kaewruang *et al.* (2014) documented that pretreatment with phosphoric acid could render gel with higher gel strength than pretreated with acetic acid, which could be linked to the negative charges on phosphate which could interact with protein and from protein aggregation.

1.2.5. Biodegradable films

Biodegradable coating or packaging has received immense attention due to their biocompatibility and as a substitute to synthetic petrochemical-based packaging (Han *et al.*, 2018). Most of food packaging is usually made of synthetic polymers, which are non-degradable and exert significant impact on the environment by contributing to pollution (Wróblewska-Krepsztul *et al.*, 2018). Biodegradable materials or polymers used for the preparation of biodegradable packaging are classified in

hydrocolloids (carbohydrates and proteins), composites, resins and lipids (Elizabeth A *et al.*, 2011). The chemical and physical properties these polymers directly influence the properties of resulting films (Elizabeth A *et al.*, 2011; Nagarajan *et al.*, 2012a). In past few decades, natural or renewable polymers have gained wide interest in the preparation of biodegradable films or coating. Among all, proteins have gained increasing interest owing to their functional properties and biodegradability (Chentir *et al.*, 2019; Murrieta-Martínez *et al.*, 2018). In addition, protein-based films have good nutritional value and have excellent gas barrier properties with impressive mechanical properties (Chuaynukul *et al.*, 2018; Nilsuwan *et al.*, 2019). Generally, protein-based films are brittle and require plasticizers to enhance flexibility by reducing the protein-protein interactions (Hoque *et al.*, 2011). Moreover, biodegradable films can also be added with various compound to increase their applicability (Hoque *et al.*, 2011; Jongjareonrak *et al.*, 2008). Biodegradable films can be obtained from various sources (Figure 1).

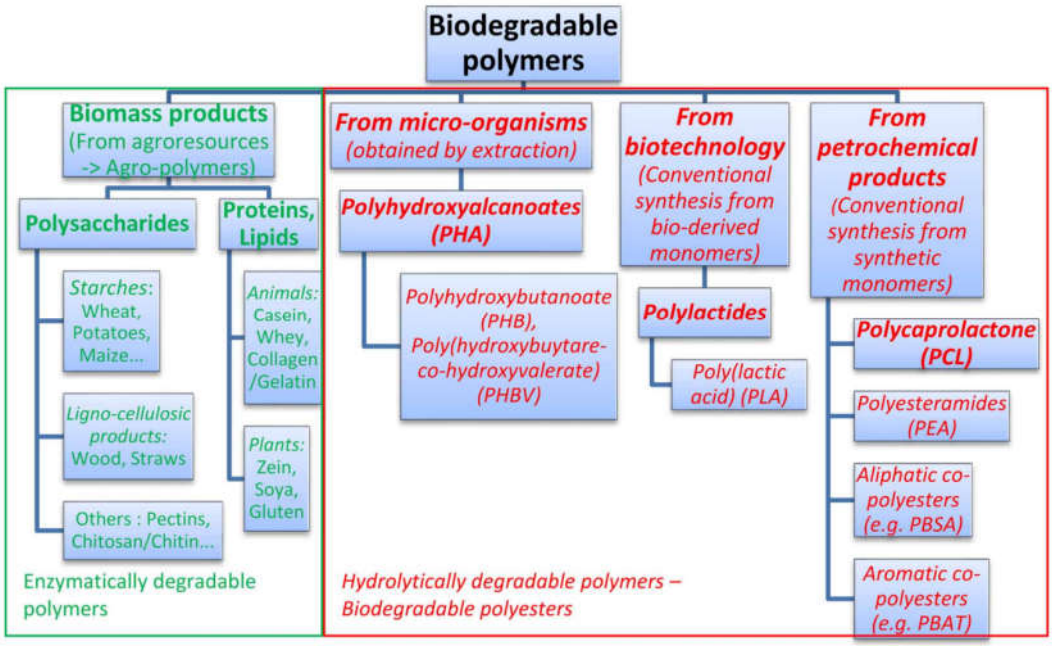

Figure 1. Classification of the biodegradable polymers.

Source: Avérous (2004)

1.2.5.1. Protein as a film forming material

Proteins are biopolymers capable of forming film and coating. The ability of various proteins to form films is extremely dependent on the molecular properties: conformations, molecular weight, electrical properties (charge vs pH), thermal stabilities and flexibilities (Hernandez-Izquierdo and Krochta, 2008). The characteristic properties of proteins make them excellent materials for film preparation. Their structure comprises of 20 different monomers, which provide a broader range functional properties, can from intermolecular binding at different position of polypeptide chain, and can capable of participating in a wide range of interactions and chemical reactions (Wihodo and Moraru, 2013). The unique property of proteins compared to other film-forming materials are electrostatic charges, conformational denaturation and amphiphilic nature (Gennadios *et al.*, 1996). Moreover, various factors can influence the conformation those include hydrophilic-hydrophobic balance, charge density, which can affect the mechanical and physical of prepared films (Elizabeth A *et al.*, 2011). Nonetheless, the properties of proteins based films are influenced by different factors including pH of protein solution, formation process, plasticizers, additives incorporated, film thickness as well the source of protein (Benjakul *et al.*, 2008; Nagarajan *et al.*, 2012a).

1.2.5.1.1. Types of proteins used

1.2.5.1.1.1. Cereal/legume proteins

Soy proteins consist of globulins and albumins, which exhibit excellent film forming property with lower oxygen permeation. However, films made of soy proteins have poor mechanical properties and heat sealability, compared to the synthetic polymer (Wang and Wang, 2017). Guerrero *et al.* (2010) documented that soy protein isolate (SPI) based films are biodegradable and eco-friendly and come from renewable sources, but they are brittle.

Wheat gluten (WG) proteins are insoluble in water and require a complex solvent system with basic or acidic conditions in the presence of alcohol. A plasticizer, usually glycerol is added to reduce film brittleness and ensure the formation of free-standing films. However, some amino acid sequences in gliadin and glutenin

proteins are responsible for celiac toxicity and wheat allergies (Murrieta-Martínez *et al.*, 2018). Nonetheless, wheat gluten films are poor water vapor barriers because of the inherent hydrophilicity of the proteins (Gennadios, 2002).

Zein protein is a valuable by-product from ethanol production from corn. It has been linked to various functional properties, which also includes the film-forming ability. Relatively, zine protein has high hydrophobicity and thermoplastic property, which is linked to the higher residues of non-polar amino acids like leucine, alanine and proline (Shukla and Cheryan, 2001). The biodegradable films made of zine protein are reported exert high barrier properties, compared to films from other proteins (Parris and Coffin, 1997).

1.2.5.1.1.2. Milk protein

Milk proteins are generally composed of whey protein and casein. Edible films made of milk protein are known to have high mechanical strength and show excellent barrier against aroma, oxygen and lipid. Moreover, whey protein films are transparent and flexible. Nevertheless, their hydrophilic nature exhibits poor barrier against moisture vapors (McHugh and Krochta, 1994). Improved physical properties through heat denaturation were reported in whey protein films (Boyacı *et al.*, 2016). Films made from casein have high tensile strength (TS) and have various other advantages such as they are readily available, inexpensive, non-toxic and highly stable. Casein film exhibited high TS (Ridout *et al.*, 2015).

1.2.5.1.1.3. Egg white protein

Egg white consists of 90% moisture and 10% of dissolved proteins (albumins, globulins and mucoproteins). Ovalbumin, which constitutes a dominant protein in egg white, is the only fraction that contains free sulphydryl (SH) groups. Other proteins, such as ovomucoid, ovotransferrin and lysozyme, which contain disulphide (S-S) linkage (Stevens, 1991). Gennadios *et al.* (1996) prepared films from egg white protein by denaturing egg white protein by alkaline solubilization or heat treatment. Egg white films prepared at pH 10.5–12.0 were smooth and homogeneous but the films prepared at pH 3 had rough and gritty surface. Mechanical and water vapor barrier properties of cast albumen films plasticized with glycerol, sorbitol, or

polyethylene glycol were studied. Mecitoğlu *et al.* (2006) prepared active packaging by adding lysozyme from egg white into zein based film to inhibit the bacteria *Bacillus subtilis* and *Lactobacillus plantarum*.

1.2.5.1.1.4. Muscle proteins

Muscle proteins are classified into 3 types, myofibrillar, sarcoplasmic and stromal proteins. Stromal proteins comprise of collagen and elastin. Sarcoplasmic proteins include myoglobulin, cytoplasmic proteins and enzymes. Myofibrillar proteins include myosin, actin, tropomyosin, and troponins Dangaran *et al.* (2009). However, stromal and myofibrillar proteins are mostly utilized for making edible films and coatings (Sothornvit and Krochta, 2005).

Actin and myosin (500 kDa) are the main myofibrillar proteins found in muscle (mammalian or fish). These proteins are extracted after eliminating other components, such as blood, myoglobin, lipids, and collagen, over a series of washing treatments. Fibrous proteins (myosin, F-actin) can form films with good mechanical properties, while globular proteins such as G-actin need to be unfolded before film formation (Prodpran *et al.*, 2012). Tongnuanchan *et al.* (2011) prepared fish myofibrillar protein based film. It was found that films had high mechanical property. However, film made from fish mince had the yellowish color due to Maillard reaction. The use of fish protein isolate prepared from pre-washed mince of red tilapia could reduce or prevent yellow discoloration of film during the extended storage.

1.2.5.2. Plasticizers

Plasticizers have a significant role in films prepared from polysaccharides and proteins. Film prepared from aforementioned sources are stiff and brittle due to the occurrence of extensive interaction among the polymer molecules (Choi *et al.*, 2018; Vieira *et al.*, 2011). Generally, plasticizers are low molecular weight compounds which can be easily incorporated between the polymers during preparation of film, which decrease characteristic brittleness of films by lowering the intermolecular interactions, therefore reduce the glass transition of the resulting polymers (Prodpran *et al.*, 2007). Owing to the smaller size, plasticizers can situate themselves between polymer molecules, increase the flexibility and processability by

increasing the mobility of polymeric chains (Andreuccetti *et al.*, 2009; Murrieta-Martínez *et al.*, 2018). Most plasticizers are highly hygroscopic and hydrophilic in nature. Water molecules in the films also act as plasticizers. Water is essentially a good plasticizer. Nonetheless it can easily be lost by dehydration at low relative humidity. Therefore, the addition of hydrophilic plasticizers to films can reduce their loss from film, but still maintains a high water activity (Gennadios *et al.*, 1996).

1.2.5.2.1. Types of plasticizer

Sothornvit and Krochta (2005) classified plasticizers into two modes of action:

1) The capability of forming numerous hydrogen bonds with the polymers by restricting polymer-polymer interaction and maintaining the distance between polymer chains.
2) The retention of water through establishing large number of interaction with water molecules, leading to retention of higher moisture content.

Due to hydrophilic property of water, plasticizers and biopolymers, and the abundance of hydrogen bonds within their structure, it is very difficult to differentiate these linked components by above mentioned mechanisms.

Types and amount of plasticizers directly affect the properties of resulting films. Presently, polyols and hydroxyl compounds are often used as good plasticizers, especially in the films prepared with protein. Among plasticizers, glycerol is the most commonly used (Gheribi *et al.*, 2018). Jongjareonrak *et al.* (2006a) studied the effects of various plasticizers (ethylene glycol, sorbitol, glycerol, polyethylene glycol 200 and 400 on the gelatin films, found that various plasticizers had varying effect on properties of gelatin films. The polyethylene glycol of a smaller size was more effective in interacting with fish gelatin molecules respectively. Plasticizer have no tendency to undergo crystallization in the film matrix. Thus significantly alters the film properties, such as flexibility, susceptibility to humidity, interactions between chains. Furthermore, the concentration of plasticizer has higher effects on the films than the plasticizer type (Bergo *et al.*, 2013). Rivero *et al.* (2010) documented that water vapor permeability (WVP) of gelatin film was also related to the level of glycerol used as

plasticizer (0–100% based on protein mass). The film added with 20 g glycerol 100 g^{-1} gelatin exerted the lowest WVP compared to the other films, and the flexibility was increased from 2.2% to 180.9% when compared to that of films without glycerol. Thus due to the hydrophilic property of glycerol, addition at higher quantities not be preferable, besides the properties are not modified and moreover it is not profitable. As a new approach, Nuanmano *et al.* (2015) studied the effect of fish gelatin hydrolysates with varying degree of hydrolysis (DH: 23, 61 and 95%) as plasticizer at various concentrations (30–60%) used in fish myofibrillar protein (FMP) film in comparison with glycerol. FMP films added with gelatin hydrolysate exhibited the decreased stiffness i.e. elastic modulus (EM) and TS with higher levels of gelatin hydrolysate. Addition of hydrolysate efficiently improved moisture vapor barrier property of FMP film, compared to the use of glycerol at the same level.

1.2.5.3. Film formation

1.2.5.3.1. Protein-based films

Film formation is carried out with dry and wet process (Guerrero *et al.*, 2010) (Figure 2). Regardless of the film-forming process either dry or wet casting, a structural rearrangement of all the compounds incorporated in film-forming solution including biopolymers, plasticizers, solvent and rest of other additives (Elizabeth A *et al.*, 2011; Hernandez-Izquierdo and Krochta, 2008). Edible films are generally dried and composed of extensive interactions among the biopolymers. In dry casting process, the drying involves the application of heat (temperature higher than melting point of film-forming materials) which caused the flow of materials during with water or solvent are eliminated from the matrixes. On the other hand, wet casting process requires solvents for dispersion of film-forming materials, which is later removed through the mild drying process to form a film structure (Gheribi *et al.*, 2018; Rhim and Ng, 2007). For edible films, those prepared by wet process, selection of solvent is one of the considerable factor, water, ethanol or their mixtures are mostly preferred (Umaraw and Verma, 2017). All the components should be dissolved or homogeneously dispersed in the solvents to produce film-forming solutions (Elizabeth A *et al.*, 2011).

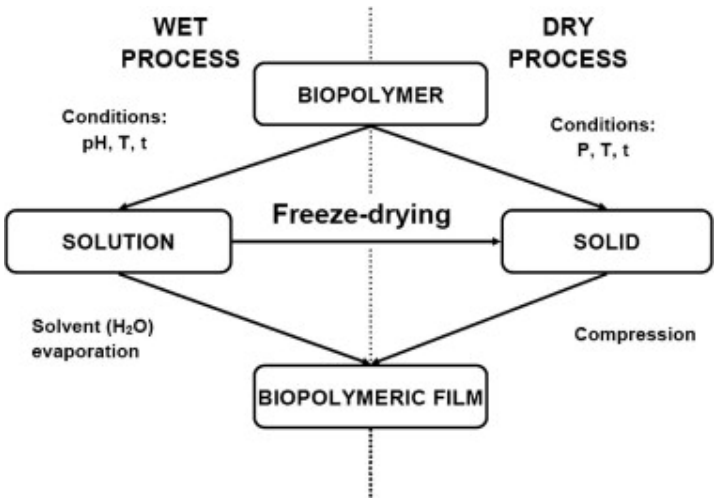

Figure 2. Processing methods of film formation

Source: Guerrero *et al.* (2010)

Most of protein-based films prepared from the proteins from various aquatic sources, including brown stripe red snapper and bigeye snapper (Jongjareonrak *et al.*, 2006a), round scad (*Decapterus maruadsi*) muscle protein (Benjakul *et al.*, 2008), cuttlefish (*Sepia pharaonis*) skin gelatin (Hoque *et al.*, 2011), splendid squid (*Loligo formosana*) and tilapia skin gelatin (Nagarajan *et al.*, 2014), through wet casting methods. In addition, a molten casting method using extrusion has been employed to make films from soy protein (Guerrero *et al.*, 2010) and other food hydrocolloids (Liu *et al.*, 2008). Chuaynukul *et al.* (2018) investigated the properties and characteristics of films from bovine and fish gelatins prepared by compression molding and solution casting methods. Both gelatin films made from compression molding had lower strength, stiffness and tensile toughness, but higher extensibility, water–vapor barrier property and yellowness than those made from casting method.

1.2.5.3.2. Fish gelatin based film

Edible film and coating materials have been widely used as tools in food packaging to extend the shelf-life and improve the quality of food systems by acting as a barrier to moisture and oxygen (Jongjareonrak *et al.*, 2008; Ramos *et al.*, 2016). Films from different gelatins generally exhibit different properties as affected by raw material source, extraction method, molecular weight and structure, amino acid compositions,

film preparation method and type/level of plasticizer (Ramos *et al.*, 2016). However, fish gelatin film is of poor water vapor barrier property (WVP), leading to the limited application of gelatin-based film as food packaging (Nagarajan *et al.*, 2014). However, gelatins from fish have been known to have excellent film forming ability with some advantages those included the resulting films are colorless, transparent and highly extensibility (Jongjareonrak *et al.*, 2006a). Additionally, smart packaging can be implemented, in which the antimicrobials or antioxidants can be incorporated (Jongjareonrak *et al.*, 2008; Wang and Wang, 2017). Fish gelatin-based films have been reported to own excellent oxygen barrier property, which could prevent the oxidation of lipids in the food system (Nagarajan *et al.*, 2014; Nilsuwan *et al.*, 2019). Also, the biodegradable gelatin films prepared from gelatin of various fish species including cuttlefish, tilapia, carp, etc. render superior UV barrier properties (Hoque *et al.*, 2011; Santos *et al.*, 2018; Theerawitayaart *et al.*, 2019; Umaraw and Verma, 2017). Gelatin film is known to effectively prevent lipid oxidation, which is induced by UV light (Limpisophon *et al.*, 2009).

The characteristics of gelatin film mainly correlate to the properties of gelatin used as a film forming material. Generally, the extraction process including pretreatment, extraction, purification and drying conditions could affect the properties of gelatin and influence characteristics of resulting gelatin film (Ansorena *et al.*, 2018; Hoque *et al.*, 2011; Murrieta-Martínez *et al.*, 2018). Niu *et al.* (2013) documented that the gelatin extracted with pretreatment using 0.03 M citric acid, acetic acid and HCl acid exerted films with different properties. Citric acid pretreated gelatin films had superior barrier properties to gelatin films pretreated with acetic or HCl acids. Wang and Wang (2017) studied the effect of varying extraction pHs on the resulting gelatin films. Films prepared with gelatin extracted at pH 5 had the highest TS. Moreover higher or lower pH resulted in the reduced TS. Nuanmano *et al.* (2015) documented that gelatin films prepared from hydrolyzed gelatin exerted decrease in thickness than that of film prepared with native gelatin (without hydrolysis), and the film network was stabilized mainly the hydrogen bonding and hydrophobic interactions. Other factors such as concentration of protein, type and level of plasticizer used could influence the properties of resulting gelatin film (Ansorena *et al.*, 2018; McHugh and Krochta, 1994).

Limpisophon *et al.* (2009) studied the effect of blue shark (*Prionace glauca*) skin gelatin concentration of 1, 2 and 3% on the properties of the resulting film. The film prepared at the concentration of 2% exhibited highest TS than other concentrations used, while the EAB and WVP increased with increasing concentration of protein used.

Moreover, the mechanical properties of gelatin-based film were also affected by glycerol content. The increases in glycerol could lower the interaction between chains by preventing protein-protein interaction. TS and increased elongation at break (EAB) of films from splendid squid (*Loligo formosana*) decreased as the extraction temperature increased (Nagarajan *et al.*, 2012a).

In addition, Limpisophon *et al.* (2009) reported that incorporation of glycerol could enhance the flexibility and also improve the UV light barrier property, the WVP and transparency gradually increased with increasing level of glycerol incorporation. Similarly, TS of gelatin film prepared from bigeye snapper (*Priacanthus macracanthus*) and brownstripe red snapper (*Lutjanus vitta*) skin gelatin reduced with higher incorporation of glycerol levels up to 75% (Jongjareonrak *et al.*, 2006a). Moreover, Cao *et al.* (2009) documented that nature of plasticizer could also affect the properties of gelatin film. Gelatin films plasticized with glycerol exhibited highest EAB, but the film plasticized with ethylene glycol had highest TS and lower EAB. Glycerol exerted superior plasticizing effect, while ethylene glycol had film strengthening effect that plasticizing effect. In addition, due to the hydrophilic plasticizers added and the hygroscopic nature of gelatin, films generally render lower water vapor barrier property (Gheribi *et al.*, 2018; Vieira *et al.*, 2011). Bergo *et al.* (2013) reported that incorporation of higher level of hydrophilic plasticizers could increase the moisture content and WVP of resulting gelatin film.

The chain length of gelatin is a factor determining the property of film. Hoque *et al.* (2011) prepared the films from gelatin of cuttlefish skin with different degrees of hydrolysis (DHs) containing glycerol at varying levels. All films showed different properties and molecular characteristics. Gelatin molecules with the shorter chain had low film-forming properties, owing to the lower junction zones mainly via hydrogen bond. This led to reduction in mechanical properties and thermal stability of their film. Higher content of low molecular weight in gelatin extracted at higher

temperature could impair the formation of junction zones. WVP value of films from splendid squid also increased with increasing extraction temperatures (Nagarajan *et al.*, 2012a). Gelatin film from Atlantic halibut skin extracted at higher temperature with higher degree of lower molecular weight peptides resulted in poor moisture vapor barrier property than that of films prepared with lower content of lower molecular weight peptide chains (Carvalho *et al.*, 2008a). Nagarajan *et al.* (2012a) studied the mechanical property and WVP of gelatin films prepared from splendid squad skin gelatin prepared using different extraction temperatures ranging from 50–80 °C. Gelatin extracted at higher temperature showed decreased TS and EAB, but higher WVP. The loss of properties was associated with the with highly degraded α-chains in the film could form loosened film network which directly influenced the properties of gelatin film.

1.2.5.4. Enhancement of property of gelatin-based film

Properties of gelatin film have been enhanced by means of different treatments such as employing enzymes, mixing with various biopolymers, and chemical treatment, and other approaches including the incorporation with different compounds of interest such as phenols/plant extracts and hydrophobic substances (Ansorena *et al.*, 2018; Jongjareonrak *et al.*, 2008; Ridout *et al.*, 2015; Wang and Wang, 2017). Enzyme or chemical treatments have been employed to modify the gelatin film networks to increase number of cross-linkage of gelatin chain in the film matrix to render films with higher film strength (Bae *et al.*, 2009; Santos *et al.*, 2018). Generally, the cross-linking agents are known to render stronger films with reduced elasticity and solubility in water. Natural or synthetic cross-linkers are known to form new covalent intra- and/or intermolecular linkages between the gelatin chins and thereby strengthen the film network (Chiou *et al.*, 2008; Prodpran *et al.*, 2012; Santos *et al.*, 2018). Incorporation of hydrophilic and hydrophobic clays was also reported to improve water vapor barrier property of squid skin gelation based films (Nagarajan *et al.*, 2014). Bae *et al.* (2009) reported that composite film prepared by cross-linking of gelatin with nanoclay employing microbial transglutaminase increased the viscosity of film-forming solution, and the films with decreased TS could be formed. Nevertheless, oxygen permeability and WVP of cross-linked composite film remained unchanged. Natural plant phenolic

compounds have been used to improve the properties of gelatin film. Rattaya *et al.* (2009) documented that incorporation of seaweed (*Turbinaria ornata*) in fish skin gelatin film at pH 9 and 10 could from non-disulfide covalent bond in film matrix caused by the interaction between gelatin molecule and oxidized seaweed phenols. WVP of seaweed extract incorporated film decreased, however no differences in TS and transparency were observed. Likely, Choi *et al.* (2018) reported that oxidized phenolic substances from caffeic acid, tannic acid and green tea extract increased TS but reduced EAB, WVP and water solubility of gelatin film. Recently, Nilsuwan *et al.* (2019) documented that the incorporation of epigallocatechin gallate (EGCG) could enhance thermal and mechanical properties of gelatin film. The resulting films showed substantial antioxidant activity.

1.2.5.4.1. Use of oils and fatty acids in protein-based films

Recently, the edible materials have been focused on composite or multicomponent films to explore the complementary advantages of each component as well as to minimize their disadvantages (Bae *et al.*, 2009; Dangaran *et al.*, 2009; Nagarajan *et al.*, 2017). Most composite films or coatings having a hydrophilic structural matrix are incorporated with a hydrophobic lipid compound to increase moisture barrier properties. Bilayer film (gelatin film/emulsion film) based on gelatin with the improved water barrier property was successfully developed (Nilsuwan *et al.*, 2018). Composite materials can be obtained as either bi-layers or emulsions. In a bi-layer composite system, the film forming emulsion forms the second layer over the polysaccharide or protein layer (Nilsuwan *et al.*, 2018). In the emulsified film forming solution, the lipid is dispersed in the biopolymer matrix (Tongnuanchan *et al.*, 2014). The main disadvantage of bi-layers films is that the preparation process consists of four stages those are two casting and two drying stages. Thus, laminated films are less popular in the food industry, albeit providing good barriers against water vapor (Sothornvit and Krochta, 2005). Some bi-layer films tend to delaminate over time, develop pinholes or cracks and had rough surface and cohesion characteristics (Ramos *et al.*, 2016).

Emulsion-based edible films and coatings have been introduced in fresh and processed food products, cheeses, meat, sausages, bakery products, fruits and vegetables. Composite emulsion-based edible materials produced from hydrocolloids and lipids result in the improved functionality than those prepared with one component, especially concerning the moisture vapor barrier properties (Murrieta-Martínez *et al.*, 2018). The use of hydrophobic plasticizers has been implemented to improve the moisture vapor barrier property of gelatin films, though resulting film demonstrate varying properties.

The hygroscopic nature of gelatin molecules and the hydrophilic plasticizer used yield the film with poor moisture vapor barrier property, therefore limiting their applications in packaging, especially dry or moist food. To overcome this drawback, the addition of hydrophobic substances such as edible oils, essential oils, waxs and fatty acids have been employed (Galus and Kadzińska, 2015; Sothornvit and Krochta, 2005; Theerawitayaart *et al.*, 2019; Zhang *et al.*, 2018). As reported by Andreuccetti *et al.* (2010), the incorporation of hydrophobic plasticizers including tributyl citrate – TB acetyltributyl citrate – ATB, and acetyltriethyl citrate – ATC in the gelatin film up to 75% (based on protein content) using saponin as an emulsifying agent significantly reduced WVP. WVP of all the gelatin film incorporated with TB, ATB and ATC were 0.07, 0.08 and 0.06 g mm m^{-2} h^{-1} kPa^{-1}, though the SEM analysis demonstrated that no homogenous dispersion of hydrophobic plasticizers occurred. Incorporation of carnauba wax and beeswax at the level of 5, 10 and 15% (w/w) based on protein content improved barrier properties against WVP and UV/visible, but increased the yellowness and opacity of resulting gelatin films (Zhang *et al.*, 2018). Furthermore, incorporation of rapenseed oil, amaranth oil, ozococerite, beeswax and lanolin at the level of 10% could efficiently reduce WVP by 15, 42, 36, 53 and 37% of gelatin film, further reduction in WVP was noticed till the incorporation level of 60%. But the higher level of incorporation led to the loss lipids from the film matrix, the addition of lecitine into the film forming emulsion could prevent the migration of lipids to the surface of the gelatin film (Sztuka and Kołodziejska, 2009). Various edible oils have been used to improve the moisture vapor barrier property of gelatin film. Tongnuanchan *et al.* (2015) reported that incorporation of palm oil at different levels

(25%, 50%, 75% and 100%, based on protein) had reduced EM and TS but a higher EAB was noticed with increasing level of palm oil incorporation. Incorporation of palm oil reduced gelatin-gelatin interactions in the film network and resulted in films with lower thermal stability, as noticed by lower degradation temperatures and glass-transition of the resulting gelatin films. The increased hydrophobicity was noticed with increasing level of palm oil incorporation and as the homogenous dispersion of oil droplets was noticed, regardless of oil levels used.

Addition of fatty acids and their esters influences properties of the gelatin film. Gelatin film incorporated with stearic acid reduced WVP more efficiently than compared to the addition of oleic acid at the same fatty acid concentration was used (Karnnet *et al.*, 2005). Higher level of both fatty acids decreased TS. However, a increased in EAB due to their plasticizing effect. Oleic acid gave a greater plasticizing effect than did stearic acid, at the same concentration (Limpisophon *et al.*, 2010). Jongjareonrak *et al.* (2006b) reported that WVP of gelatin film mainly depends to the functional properties and composition proteins used for film preparation, while the increased hydrophobicity could be improved with addition of hydrophobic substance like long-chain fatty acid to improve the water vapor barrier properties of the resulting gelatin films. Moreover, addition of oil and fatty acids into gelatin film can act as an excellent UV light barrier, therefore prevention lipid oxidation induced by UV light (Jongjareonrak *et al.*, 2006b; Pérez-Mateos *et al.*, 2009). In a recent study, Theerawitayaart *et al.* (2019) reported that molecular modification of gelatin (MG) with oxidized linoleic acid exhibited the reduced TS, EM but increased EAB and yellowness. MG film had the decreased WVP up to 30% compared to that of gelatin film without any modification. In addition, incorporation of oxidized linoleic acid efficiently reduced the migration of lipid to the film matrix.

Essential oil is known to possess varying odor, color, flavor and aroma. Besides these properties, essential oils are known to show beneficial properties including antioxidant and antimicrobial activities (Hashemi *et al.*, 2017b; Sapper *et al.*, 2018). Essential oils from different sources have been employed as an additive in active or smart packaging, through which the characteristics properties of film such as WVP linked to hydrophobic property of oil has also been improved (Gennadios, 2002; Ramos

et al., 2016; Sapper *et al.*, 2018). Addition of lavender essential oil (OEL) to gelatin film increased thickness and decreased solubility and water absorption. Degree of swelling of the film decreased with increasing concentration of oils. TS considerably reduced with increasing concentration of oil, which resulted in lower mechanical strength, whereas, the EAB was unaffected (Jamróz *et al.*, 2018). Similarly, TS was decreased when gelatin film was added with three types of root essential oils (turmeric, ginger and play) at three levels (25%, 50% and 100%, (w/w) based on protein content), but higher EAB was obtained with increasing amount of essential oils. Film added with turmeric and play essential oils demonstrated the higher antioxidant activity (ABTS radical scavenging activity and DPPH activity), compared with that of ginger essential oil added film and control film. Distribution of essential oil droplets in film and their interaction with protein molecules governed by surfactants are illustrated in Figure 3. Tongnuanchan *et al.* (2014) demonstrated that the morphological, structural and thermal properties of fish skin gelatin films incorporated with basil and citronella essential oils at a ratio of 1:1 (w/w) was mainly influenced by various surfactants (Tween-20, Tween-80 and soy lecithin at 25% based on essential oil) (Figure 3). Among the surfactants employed, soy lecithin was found to be highly appropriate due to its enhancement of stability of emulsion and homogenous dispersion of oil droplets in the gelatin film matrix.

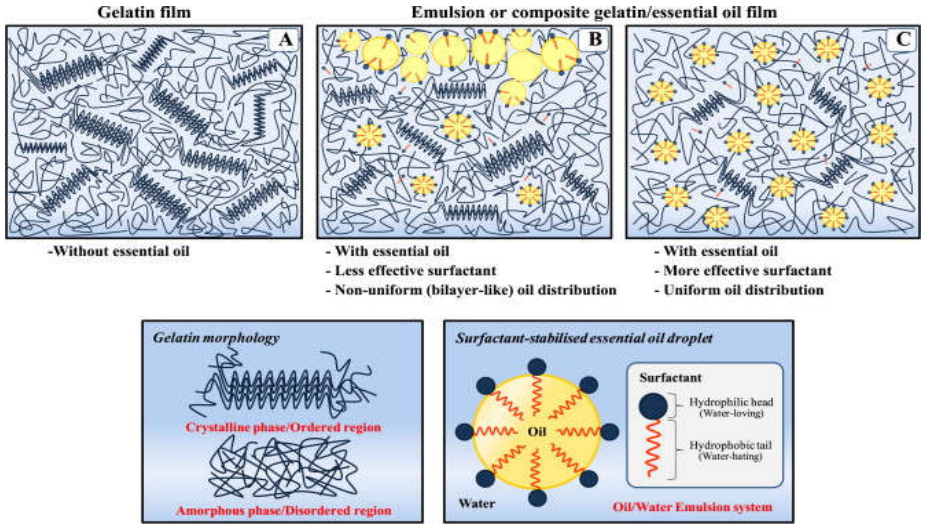

Figure 3. Simplified illustration of gelatin film matrix without and with essential oils in the presence of different surfactants.

Source: Tongnuanchan *et al.* (2014)

1.2.5.4.2. Techniques used for emulsion formation in composite film

The emulsification for homogeneous dispersion of lipid phase in aqueous phase is important during film formation and before casting. The size of droplet is the governing factor for the stability of emulsion and it also affects the viscosity and other related properties. To prepare the film forming emulsions different homogenization techniques have been employed. Most commonly used method for preparation of film-forming emulsion is by employing rotor-stator homogenizers, in which a particle size can be effectively reduced up to 1 μm (Gómez-Estaca *et al.*, 2009; Tongnuanchan *et al.*, 2013). Which can be further reduced by using high-pressure homogenizers to the system (Bonilla *et al.*, 2012). The other technique such as microfluidization can from emulsions having the particles with narrow size distribution generated by high shearing force of ultrahigh-pressure as well as severe stress of head-on collision (Sherwin *et al.*, 1998). In addition to this, the combination of microfluidization and sonification can generate nanoemulsions with particle size ranging from 150 to 700 nm, the size of particles decrease in correspondence with the increase in pressure and time of microfluidization or with the increased sonification time (Mahdi *et al.*, 2006). Figure 4 shows the difference in particle size and distribution of emulsion and nanoemulsion produced by rotor-stator and ultrahigh homogenization method, respectively.

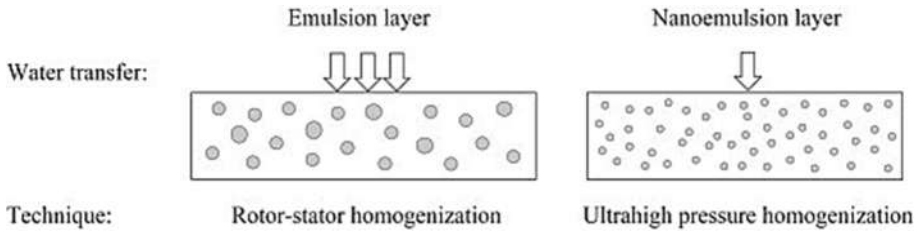

Figure 4. Emulsion layer formation

Source: Mahdi *et al.* (2006)

1.2.6. Squalene

Squalene is a highly hydrophobic lipid with the formula $C_{30}H_{50}$. It is an intermediate for the biosynthesis of phytosterol or cholesterol in plants/animals and humans. Squalene is a triterpenoid in nature with six conjugated double bonds (Spanova and Daum, 2011). Double-bonded configuration allows squalene to occurs in two configurations e.g., stretched or coiled form (Figure 5) (Naziri and Tsimidou, 2013). The first one (Figure 5A) is expected in a hydrophobic system and the second one is found in aqueous media (Van Tamelen, 1968). Squalene was discovered in 1906 by the Japanese researcher Dr. Mitsumaru Tsujimoto (Tsujimoto, 1906). The unsaponifiable fraction from the shark liver oil "kurokozame" showed the existence of a highly unsaturated hydrocarbon (Tsujimoto, 1916). The greatest concentration of squalene can be found in the liver of certain species of fish, especially sharks living in the sea at depth under 400 m. The other rich sources include olive oil, amaranth seed oil and rice bran oil (Spanova and Daum, 2011). In humans, squalene is present at its highest concentration in sebum (~13%) (Boussouira and Pham, 2016). Squalene is synthesized in all types of cells because it is a key intermediate in the formation of eukaryotic sterols and bacterial hopanoids (Xu *et al.*, 2004).

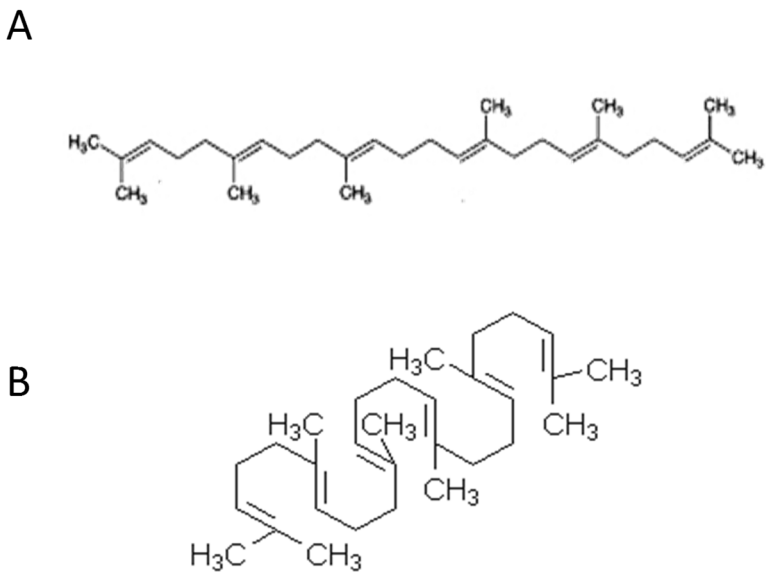

Figure 5: Chemical structure of squalene A, stretched form and B, coiled form

Source: Spanova and Daum (2011)

Squalene has several beneficial properties. It is a natural antioxidant (Kohno *et al.*, 1995a). It also serves in skin hydration, as an efficient quencher of singlet oxygen in UV-associated skin damage and has been used as emollient in adjuvants for vaccines (Huang *et al.*, 2009). Squalene from olive oil also has a preventive effect on possesses tumor-protective, breast cancer and cardio-protective properties and reduces the serum cholesterol level (Newmark, 1999; Reddy and Couvreur, 2009; Spanova and Daum, 2011). Furthermore, squalenoylation has become the most common technique for delivering prodrugs into cells (Fox, 2009).

Antimicrobial activity toward virulence factors was documented (Bindu *et al.*, 2015). Despite these beneficial properties, the formulated food applications of squalene have not been reported.

1.2.6.1. Extraction of squalene

Squalene can be extracted from few shark species as well as from different commercially available fresh and marine water fish species. In the case of deep-sea sharks, liver is the main organ for lipid storage and the unsaponifiable matter represents 50–80% of the liver mass. Thankappan and Gopakumar (1991) reported that the unsaponifiable matter from liver of *Centrophorus artomarginatus* (deep-sea sharks) contained 71% squalene. Whereas, no squalene was obtained from other shark species such as *Scoliodon sp*, *Sphyrna zygaena*, *Carcharhinus limbatus* and *Chiloscyllium griseum* (Dog shark), when saponification was employed as separation method. Bakes and Nichols (1995) determined the fatty acid and squalene composition of liver oil from six deep-sea shark species namely *Somniosus pacificus, Centroscymnus plunketi*, *Centroscymnus crepidater*, *Etmopterus granulosus*, *Deania calcea and Centrophorus scalpratus*. Not all shark species contain squalene at higher amounts. Some contained higher amount of diacylglyceryl esters (DAGE) with high squalene content and some contained higher amounts of DAGE and without squalene. Among these six species, only four species contained squalene higher than 500 mg g^{-1} oil. *Centroscymnus plunketi* contained no squalene and *Somniosus pacificus* contained 9 milligrams of squalene per gram oil. KopiCoVá and VaVreiNoVá (2007) studied the occurrence of squalene in twenty different commercially available freshwater fish from the Czech

Republic. Squalene was determined in the unsaponifiable matter of muscular and visceral fat by a capillary gas chromatography method using a flame ionization detector and cholesterol was also determined using cholesterol assay kit. The quantity of squalene in muscle ranged from 98.0 to 1536.8 mg kg^{-1} and from 70.1 to 1803.8 mg kg^{-1} in visceral fat. Cholesterol ranged from 0.011% to 0.170% from 0.104% to 0.297% in muscle and visceral fat, respectively. Bavisetty and Narayan (2015) modified a fractional crystallization method using absolute ethanol as a solvent to obtain a fraction of squalene and cholesterol in the oil extracted from different body parts of fresh and marine water fish species. Among all the species, tilapia (*Oreochromis mossambicus*) and mackerel (Rastrelliger kanagurta) contained higher amounts of squalene 5-55 µg and 35-95 µg, respectively, per gram of oil.

The first step in squalene recovery from animal or plant source is generally carried out by extracting oil. Czaplicki *et al.* (2012) studied the content of squalene from amaranth oil obtained by three different methods, supercritical fluid extraction, cold pressing extraction, and extraction with chloroform/methanol. The best results expressed as squalene concentration were obtained by SFE. For aquatic sources, oil extraction has been conducted using solvents such as hexane, petroleum ether/acetone (2:1 v/v), methanol/chloroform/water extraction (2:l:0.8 v/v/v) for recovery of squalene (Bakes and Nichols, 1995; Bavisetty and Narayan, 2015; Catchpole *et al.*, 1997).

1.2.6.2. Analysis of squalene

Conventional sample preparation involves multi-step sample preparations, including saponification followed by extraction of unsaponifiable matter using solvents fractionating through column chromatography and many more tedious methods. Analysis of squalene has been achieved by several techniques, including chemical and physical methods such as titrimetric, colorimetric, molecular distillation (Popa *et al.*, 2015), supercritical fluid extraction (SFE), supercritical fluid chromatography (Güçlü-Üstündağ and Temelli, 2005), short path distillation (Pietsch and Jaeger, 2007), fractional crystallization (Bavisetty and Narayan, 2015) and chromatographic methods like high-speed counter-current chromatography (Lu *et al.*,

2003), and high resolution gas chromatography and capillary column gas chromatography (Villén *et al.*, 1998). For all the reported methods, tedious multi-step sample preparation methods seem to be inevitable. For instance, the colorimetric method includes tedious drying process since a trace amount of solvents interfere with color development.

Gas chromatographic method for separation of squalene from animal sources requires triacylglyceride removal, followed by fractionation of unsaponifiable matter into several classes of compounds. This method was preceded by sample preparation such as derivatization, separation into several classes of compounds using column chromatography or TLC. The existing HPLC methods including the complex sample preparation procedures, e.g. alkaline digestion and distillation have been employed for normal and reverse phase chromography. A more recent methodology involves sample preparation using ethanol fractionation and simultaneous determination of squalene and cholesterol by RP-HPLC, which could be advantageous for determination of squalene due to its simplicity and rapid determination (Bavisetty and Narayan, 2015). Another analytical method for analysis of squalene is thin layer chromatography with flame ionization detection (Wetherbee and Nichols, 2000). However, this approach is not specific and cannot differentiate squalene properly from other hydrocarbons that are present in the oil. Furthermore, in order to avoid the use of toxic solvents and high process temperatures a “green extraction technology”, SFE as solvent, supercritical carbon dioxide (SC-CO_2) is usually used. This process yields to high-quality squalene without use of toxic unallowable solvents. As a disadvantage, SFE-CO_2 is high cost of production and holds the complicated operating parameters (high-pressure operation) when it comes to recovery of squalene from shark liver oil and olive oil deodorization distillate (OODD), at both laboratory and pilot scale (Catchpole *et al.*, 1997). The other major disadvantage of SFE, is the coelution of fatty acids, which needs further supplementary steps of purification in order to obtain pure squalene.

A large-scale concentration of squalene from animal and plant sources is generally carried out using short-path distillation at a range of temperatures starting from 70 to 260 ºC. The purity of squalene obtained by this method was found to be in

the range of 76-97%, depending on the source (Popa *et al.*, 2015). Recently, Nam *et al.* (2017) reported the use of nuclear magnetic resonance spectroscopy (NMR) for direct quantification of squalene in olive oil without saponification, extraction, or fractionation of the samples. Squalene accounted for 0.35–0.83% of the whole of the olive oil composition. Based on NMR result reported by Rotondo *et al.* (2017), the signals of terminal methyl groups got resolved at 1.67 ppm of squalene regardless of hydrophobic group. However, NMR displayed low intrinsic sensitivity, acceptable accuracy (<4%) and reproducibility (<6%). Besides this, squalene could undergo oxidation or thermal degradation under harsh environmental condition during extraction or processing. Ortega *et al.* (2012) study the decay of squalene and the formation of trans fatty acids (TFAs) in the amaranth oil extracted with hexane with and without heat. The squalene content was not affected by the application of heat during the oil extraction process in amaranth, this was identified by the presence of well-defined peak at 968 cm^{-1} for both the oil extracts (with and without heat). However, there is always a demand for novel extraction techniques for production of sensitive compounds such as squalene as they have many food and pharmaceutical applications.

1.2.7. Ultrasound

Ultrasound has been considered an advanced and promising technology of the 21st century, with plentiful applications in the chemistry, alimentary, pharmaceutical and cosmetic fields (Marić *et al.*, 2018). Ultrasound has been successfully employed for laboratory scale or the pilot procedures. Various industries have been employing sonication technique in extraction, food processing and preservation. The use of ultrasound in food processing is of wide interest based on the physical effects of ultrasound. Sonication has been efficiently used for degassing, cutting, filtration, freezing, defoaming, cooking, sterilization, drying, homogenization and emulsification (Bermúdez-Aguirre *et al.*, 2011).

Also, the sonication technique has been implemented for the extraction of wide range of compounds of interest from different matrixes. The ultrasound assisted extraction is linked to numerous advantages such as it enhances extraction yield,

reduces the overall time of extraction, options to use various alternative solvents, cost-effective, improve the extraction efficiency of heat liable compounds (Vilkhu *et al.*, 2008). Moreover, sonication provides the facility to have milder process conditions, shorten the processing time when compared to conventional techniques, which results in improved quality of products with a less cost (Hashemi *et al.*, 2017a).

1.2.7.1. Principle of ultrasound

Ultrasound is a mechanical wave that needs an elastic medium to pass over and it is different from audible sounds based on the frequency. The frequency of ultrasound range from 20 kHz to 10 MHz, while the audible frequencies of humans rest between 16 Hz and 20 kHz. The important parameters that describe ultrasound are the frequency (in Hz), wavelength (in cm) and power (in W), through which the ultrasonic intensity (I) can be calculated (in W cm^{-2}). Ultrasound can be classified into two distinct categories, based on the frequency range. Those include high frequency (100 kHz to 1 MHz) low power (<1 W cm^{-2}) and low frequency (20–100 kHz) high power (10–1000 W cm^{-2}). The former is more commonly used for the evaluation of physicochemical properties of food, whereas the latter is mostly employed for either physical or chemical modification of food (Chemat and Khan, 2011; Lavilla and Bendicho, 2018; Soria and Villamiel, 2010).

Ultrasound directly contributes to the cavitation effect, the phenomenon of generation, growing and eventual collapse of the bubbles associated with the rapidly alternating high-amplitude pressure waves. Vapor or gas bubbles are created by the change of average distance between molecules and decrease in pressure. The bubbles grow in areas of low pressure and collapses violently when passing to high-pressure areas. During the collapse of bubble, energy release causes rise in pressure at level more than 1000 atm and in temperatures close to 5000K (Figure 6) (Soria and Villamiel, 2010). In a liquid medium, the molecules are linked togother by various attractive forces, which are affected or broken by the effect of ultrasound through the longitudinal displacement when the ultrasound waves pass through the elastic medium, resulting from a succession of compression and rarefaction phases (Figure 6). However, heat produced by the implosion of the bubbles is instantly dissipated. Consequently, there is

no substantial temperature rise in the medium (Lavilla and Bendicho, 2018). Collapse of bubble increases with increasing intensity, which results in high energy during explosion of bubble. The efficiency of cavitation mechanism depends on the frequency and intensity of the transmitted ultrasound waves, as well as on the physical properties of the sample subjected to ultrasound. Additionally, propagation of ultrasound wave causes oscillation and collapse of bubbles, thus providing mechanical effects associated with collapse pressure, turbulences, and shear stresses (Yusaf and Al-Juboori, 2014). In addition to cavitation effect, ultrasound also generates agitation, turbulence and interparticle collision, which enhances the extraction process (Tiwari, 2015).

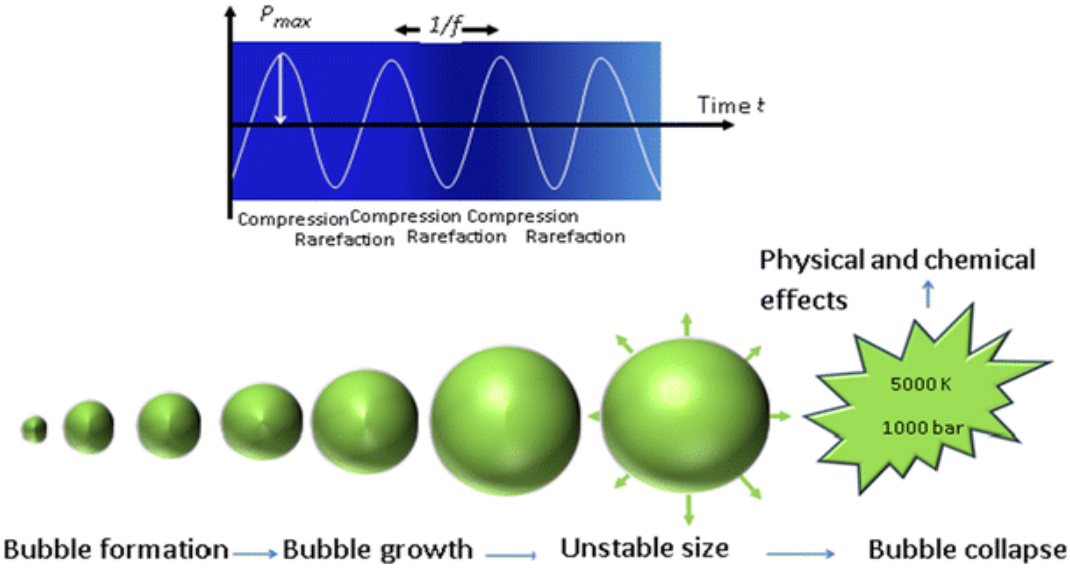

Figure 6: Schematic representation of the acoustic cavitation mechanism

Source: Kumari *et al.* (2018)

1.2.7.2. Ultrasound-assisted process for recovery of collagen and gelatin

Conventional extraction methods for collagen (ASC and PSC) and gelatin are time-consuming with low yield. Additionally, a considerable amount of insoluble collagen becomes leftover (Benjakul *et al.*, 2012b). To improve the extraction efficiency from different processing by-products, ultrasound with optimized conditions has been employed. Extraction time was reduced by 16-fold as the ultrasonication at 80% amplitude was applied. The components of collagen α_1 (α_3), α_2 and β-subunits remained intact. Nevertheless, most of the collagen was degraded throughout sonication

process when longer extraction time (24 h) was used (Kim *et al.*, 2012). Zou *et al.* (2017a); Zou *et al.* (2017b) reported that amino acid compositions of ASC and UASC (with ultrasound treatment) from soft-shell turtle calipash were not affected, and both the collagens contained α_1, α_2 and β-subunits as the major components.

Typically, gelatin (type A) from fish sources is produced by a mild acid pretreatment, followed by extraction in hot extraction process. As there are higher cross-linkages present in tropocollagen, which are stable to thermal and acid treatment (Zhou and Regenstein, 2005b), a lower yield is generally obtained. To increase the extraction efficiency, ultrasonication has been employed during extraction process. Tu *et al.* (2015) compared the water bath (WB) and ultrasound bath (UB) for extraction of gelatin from the scales of bighead carp at 60 °C for 1 h, 3 h and 5 h without acid pretreatment. Gelatin obtained using UB had much higher yield (30.94-46.67 %) than that of WB (19.15-36.39 %). All the gelatins contained α-and β-chains as the predominant components. The gelatins extracted using UB for longer time exhibited lower gel strength and melting point, mainly caused by degradation of gelatin components as observed by FTIR, from which free amino group content was increased.

1.3. Objectives

1) To extract and characterize acid and pepsin soluble collagen from skin and scales of golden carp.

2) To study the extraction efficiency and characteristics of acid and pepsin soluble collagens from the skin of golden carp as affected by ultrasonication.

3) To examine physicochemical and molecular properties of gelatin from skin of golden carp as influenced by acid pretreatment and ultrasonication.

4) To recover and characterize of squalene from the liver of different fish species

5) To investigate the effect of squalene as plasticizer replacer on water vapor barrier, mechanical and sealing properties of edible gelatin film.

6) To study storage stability of deep fried crackers packed in the developed squalene/gelatin bag.

1.4. References

Ali, E., Sultana, S., Hamid, S. B. A., Hossain, M., Yehya, W. A., Kader, A. and Bhargava, S. K. 2018. Gelatin controversies in food, pharmaceuticals, and personal care products: Authentication methods, current status, and future challenges. Critical Reviews in Food Science and Nutrition. 58: 1495-1511.

Andreuccetti, C., Carvalho, R. A. and Grosso, C. R. 2010. Gelatin-based films containing hydrophobic plasticizers and saponin from *Yucca schidigera* as the surfactant. Food Research International. 43: 1710-1718.

Andreuccetti, C., Carvalho, R. A. and Grosso, C. R. F. 2009. Effect of hydrophobic plasticizers on functional properties of gelatin-based films. Food Research International. 42: 1113-1121.

Ansorena, M. R., Pereda, M. and Marcovich, N. E. 2018. Edible films. *In* Polymers for food applications. (Gutiérrez, T. J., ed.). p. 5-24. Springer International Publishing. Cham, Switzerland.

Arpi, N. and Novita, M. 2018. Isolation of fish skin and bone gelatin from tilapia (*Oreochromis niloticus*): Response surface approach. *In* IOP Conference Series: Materials Science and Engineering. Vol. 334. (Arpi, N., ed.). p. 1-7. IOP Publishing Ltd. Bandung, Indonesia.

Avérous, L. 2004. Biodegradable multiphase systems based on plasticized starch: a review. Journal of Macromolecular Science Polymer Reviews. 44: 231-274.

Badii, F. and Howell, N. K. 2006. Fish gelatin: structure, gelling properties and interaction with egg albumen proteins. Food Hydrocolloids. 20: 630-640.

Bae, H. J., Darby, D. O., Kimmel, R. M., Park, H. J. and Whiteside, W. S. 2009. Effects of transglutaminase-induced cross-linking on properties of fish gelatin–nanoclay composite film. Food Chemistry. 114: 180-189.

Baird, I. G. 2006. *Probarbus jullieni* and *Probarbus labeamajor*: the management and conservation of two of the largest fish species in the Mekong River in southern Laos. Aquatic Conservation: Marine and Freshwater Ecosystems. 16: 517-532.

Bakes, M. J. and Nichols, P. D. 1995. Lipid, fatty acid and squalene composition of liver oil from six species of deep-sea sharks collected in Southern Australian

waters. Comparative Biochemistry and Physiology, Part B: Biochemistry and Molecular Biology. 110: 267-275.

Balti, R., Jridi, M., Sila, A., Souissi, N., Nedjar-Arroume, N., Guillochon, D. and Nasri, M. 2011. Extraction and functional properties of gelatin from the skin of cuttlefish (*Sepia officinalis*) using smooth hound crude acid protease-aided process. Food Hydrocolloids. 25: 943-950.

Bateman, J. F., Lamande, S. R. and Ramshaw, J. A. 1996. Collagen superfamily. Extracellular matrix. 2: 22-67.

Bavisetty, S. C. B. and Narayan, B. 2015. An improved RP-HPLC method for simultaneous analyses of squalene and cholesterol especially in aquatic foods. Journal of Food Science and Technology. 52: 6083-6089.

Bechtel, P. J. 2003. Properties of different fish processing by-products from pollock, cod and salmon. Journal of Food Processing and Preservation. 27: 101-116.

Benjakul, S., Artharn, A. and Prodpran, T. 2008. Properties of protein-based film from round scad (*Decapterus maruadsi*) muscle as influenced by fish quality. LWT-Food Science and Technology. 41: 753-763.

Benjakul, S., Kittiphattanabawon, P. and Regenstein, J. M. 2012a. Fish gelatin. *In* Food Biochemistry and Food Processing, Second Edition. (Simpson, B. K., ed.). p. 388-405. Wiley-Blackwell. Iowa, USA.

Benjakul, S., Nalinanon, S. and Shahidi, F. 2012b. Fish collagen. Food Biochemistry and Food Processing, Second Edition. 365-387.

Benjakul, S., Nalinanon, S. and Shahidi, F. 2012c. Fish Collagen. *In* Food Biochemistry and Food Processing, Second Edition. (Simpson, B. K., ed.). p. 365-387. Wiley-Blackwell. Iowa, USA.

Benjakul, S., Oungbho, K., Visessanguan, W., Thiansilakul, Y. and Roytrakul, S. 2009. Characteristics of gelatin from the skins of bigeye snapper, *Priacanthus tayenus* and *Priacanthus macracanthus*. Food Chemistry. 116: 445-451.

Benjakul, S., Thiansilakul, Y., Visessanguan, W., Roytrakul, S., Kishimura, H., Prodpran, T. and Meesane, J. 2010. Extraction and characterisation of pepsin solubilised collagens from the skin of bigeye snapper (*Priacanthus tayenus* and

Priacanthus macracanthus). Journal of the Science of Food and Agriculture. 90: 132-138.

Bergo, P., Moraes, I. and Sobral, P. 2013. Effects of plasticizer concentration and type on moisture content in gelatin films. Food Hydrocolloids. 32: 412-415.

Bermúdez-Aguirre, D., Mobbs, T. and Barbosa-Cánovas, G. V. 2011. Ultrasound applications in food processing. *In* Ultrasound technologies for food and bioprocessing. (Hao, F. *et al.*, eds.). p. 65-105. Springer. New York, NY.

Bigi, A., Burghammer, M., Falconi, R., Koch, M. H. J., Panzavolta, S. and Riekel, C. 2001. Twisted plywood pattern of collagen fibrils in teleost scales: An X-ray diffraction investigation. Journal of Structural Biology. 136: 137-143.

Bindu, B. S. C., Mishra, D. P. and Narayan, B. 2015. Inhibition of virulence of *Staphylococcus aureus* – a food borne pathogen – by squalene, a functional lipid. Journal of Functional Foods. 18: 224-234.

Bitencourt, C. M., Fávaro-Trindade, C. S., Sobral, P. J. A. and Carvalho, R. A. 2014. Gelatin-based films additivated with curcuma ethanol extract: Antioxidant activity and physical properties of films. Food Hydrocolloids. 40: 145-152.

Bonilla, J., Atarés, L., Vargas, M. and Chiralt, A. 2012. Edible films and coatings to prevent the detrimental effect of oxygen on food quality: possibilities and limitations. Journal of Food Engineering. 110: 208-213.

Boussouira, B. and Pham, D. M. 2016. Squalene and skin barrier function: From molecular target to biomarker of environmental exposure. *In* Skin Stress Response Pathways. (Georg T, W., ed.). p. 29-48. Springer, Cham. Switzerland.

Boyacı, D., Korel, F. and Yemenicioğlu, A. 2016. Development of activate-at-home-type edible antimicrobial films: An example pH-triggering mechanism formed for smoked salmon slices using lysozyme in whey protein films. Food Hydrocolloids. 60: 170-178.

Brodsky, B. and Ramshaw, J. A. M. 1997. The collagen triple-helix structure. Matrix Biology. 15: 545-554.

Cao, N., Yang, X. and Fu, Y. 2009. Effects of various plasticizers on mechanical and water vapor barrier properties of gelatin films. Food Hydrocolloids. 23: 729-735.

Carvalho, R., Sobral, P., Thomazine, M., Habitante, A., Giménez, B., Gómez-Guillén, M. and Montero, P. 2008a. Development of edible films based on differently processed Atlantic halibut (*Hippoglossus hippoglossus*) skin gelatin. Food Hydrocolloids. 22: 1117-1123.

Carvalho, R. A., Sobral, P. J. A., Thomazine, M., Habitante, A. M. Q. B., Giménez, B., Gómez-Guillén, M. C. and Montero, P. 2008b. Development of edible films based on differently processed Atlantic halibut (*Hippoglossus hippoglossus*) skin gelatin. Food Hydrocolloids. 22: 1117-1123.

Catchpole, O. J., Von Kamp, J.-C. and Grey, J. B. 1997. Extraction of squalene from shark liver oil in a packed column using supercritical carbon dioxide. Industrial and Engineering Chemistry Research. 36: 4318-4324.

Chemat, F. and Khan, M. K. 2011. Applications of ultrasound in food technology: processing, preservation and extraction. Ultrasonics Sonochemistry. 18: 813-835.

Chentir, I., Kchaou, H., Hamdi, M., Jridi, M., Li, S., Doumandji, A. and Nasri, M. 2019. Biofunctional gelatin-based films incorporated with food grade phycocyanin extracted from the *Saharian cyanobacterium Arthrospira sp*. Food Hydrocolloids. 89: 715-725.

Chiou, B.-S., Avena-Bustillos, R. J., Bechtel, P. J., Jafri, H., Narayan, R., Imam, S. H., Glenn, G. M. and Orts, W. J. 2008. Cold water fish gelatin films: Effects of cross-linking on thermal, mechanical, barrier, and biodegradation properties. European Polymer Journal. 44: 3748-3753.

Choi, I., Lee, S. E., Chang, Y., Lacroix, M. and Han, J. 2018. Effect of oxidized phenolic compounds on cross-linking and properties of biodegradable active packaging film composed of turmeric and gelatin. LWT. 93: 427-433.

Chuaychan, S., Benjakul, S. and Kishimura, H. 2015. Characteristics of acid- and pepsin-soluble collagens from scale of seabass (*Lates calcarifer*). LWT-Food Science and Technology. 63: 71-76.

Chuaynukul, K., Nagarajan, M., Prodpran, T., Benjakul, S., Songtipya, P. and Songtipya, L. 2018. Comparative characterization of bovine and fish gelatin

films fabricated by compression molding and solution casting methods. Journal of Polymers and the Environment. 26: 1239-1252.

Czaplicki, S., Ogrodowska, D., Zadernowski, R. and Derewiaka, D. 2012. Characteristics of biologically-active substances of amaranth oil obtained by various techniques. Polish Journal of Food and Nutrition Sciences. 62: 235-239.

Czerner, M., Fasce, L. A., Martucci, J. F., Ruseckaite, R. and Frontini, P. M. 2016. Deformation and fracture behavior of physical gelatin gel systems. Food Hydrocolloids. 60: 299-307.

Dangaran, K., Tomasula, P. M. and Qi, P. 2009. Structure and function of protein-based edible films and coatings. *In* Edible films and coatings for food applications. (Embuscado, M. and Kerry C, H., eds.). p. 25-56. Springer. New York, USA.

Drzewiecki, K. E., Grisham, D. R., Parmar, A. S., Nanda, V. and Shreiber, D. I. 2016. Circular dichroism spectroscopy of collagen fibrillogenesis: A new use for an old technique. Biophysical Journal. 111: 2377-2386.

Duan, R., Zhang, J., Du, X., Yao, X. and Konno, K. 2009. Properties of collagen from skin, scale and bone of carp (*Cyprinus carpio*). Food Chemistry. 112: 702-706.

Duan, R., Zhang, J., Liu, L., Cui, W. and Regenstein, J. M. 2018. The functional properties and application of gelatin derived from the skin of channel catfish (*Ictalurus punctatus*). Food Chemistry. 239: 464-469.

Elizabeth A, B., Robert, H. and Jinhe, B. 2011. Edible coatings and films to improve food quality. CRC Press. Baca Raton, Florida, USA.

Erts, D., Gathercole, L. and Atkins, E. 1994. Scanning probe microscopy of intrafibrillar crystallites in calcified collagen. Journal of Materials Science: Materials in Medicine. 5: 200-206.

Fernandez-Dıaz, M., Montero, P. and Gomez-Guillen, M. 2001. Gel properties of collagens from skins of cod (*Gadus morhua*) and hake (*Merluccius merluccius*) and their modification by the coenhancers magnesium sulphate, glycerol and transglutaminase. Food Chemistry. 74: 161-167.

Foegeding, E., Lanier, T. and Hultin, H. 1996. Characteristics of edible muscle tissues. Food Chemistry. 3: 879-942.

Fox, C. B. 2009. Squalene emulsions for parenteral vaccine and drug delivery. Molecules. 14: 3286-3312.

Galus, S. and Kadzińska, J. 2015. Food applications of emulsion-based edible films and coatings. Trends in Food Science and Technology. 45: 273-283.

Gennadios, A. 2002. Proteins as raw materials for films and coatings: definitions, current status, and opportunities. *In* Protein-based films and coatings. (Aristippos, G., ed.). p. 21-62. CRC press. Boca Raton, Florida, USA.

Gennadios, A., Hanna, M. A. and Kurth, L. B. 1997. Application of edible coatings on meats, poultry and seafoods: a review. LWT- Food Science and Technology. 30: 337-350.

Gennadios, A., Weller, C., Hanna, M. and Froning, G. 1996. Mechanical and barrier properties of egg albumen films. Journal of Food Science. 61: 585-589.

Gheribi, R., Puchot, L., Verge, P., Jaoued-Grayaa, N., Mezni, M., Habibi, Y. and Khwaldia, K. 2018. Development of plasticized edible films from *Opuntia ficus-indica mucilage*: A comparative study of various polyol plasticizers. Carbohydrate Polymers. 190: 204-211.

Giraud-Guille, M.-M., Besseau, L., Chopin, C., Durand, P. and Herbage, D. 2000. Structural aspects of fish skin collagen which forms ordered arrays via liquid crystalline states. Biomaterials. 21: 899-906.

Glover, C. N., Bucking, C. and Wood, C. M. 2013. The skin of fish as a transport epithelium: a review. Journal of Comparative Physiology. B: Biochemical, Systemic, and Environmental Physiology. 183: 877-891.

Gómez-Estaca, J., Bravo, L., Gómez-Guillén, M. C., Alemán, A. and Montero, P. 2009. Antioxidant properties of tuna-skin and bovine-hide gelatin films induced by the addition of oregano and rosemary extracts. Food Chemistry. 112: 18-25.

Gómez-Guillén, M., Giménez, B., López-Caballero, M. a. and Montero, M. 2011. Functional and bioactive properties of collagen and gelatin from alternative sources: A review. Food Hydrocolloids. 25: 1813-1827.

Gómez-guillœn, M. and Montero, P. 2001. Extraction of gelatin from megrim (*Lepidorhombus boscii*) skins with several organic acids. Journal of Food Science. 66: 213-216.

Greenfield, N. J. 2006. Using circular dichroism spectra to estimate protein secondary structure. Nature Protocols. 1: 2876-2890.

Güçlü-Üstündağ, Ö. and Temelli, F. 2005. Solubility behavior of ternary systems of lipids, cosolvents and supercritical carbon dioxide and processing aspects. The Journal of Supercritical Fluids. 36: 1-15.

Gudmundsson, M. and Hafsteinsson, H. 1997. Gelatin from cod skins as affected by chemical treatments. Journal of Food Science. 62: 37-39.

Guerrero, P., Retegi, A., Gabilondo, N. and De la, C. K. 2010. Mechanical and thermal properties of soy protein films processed by casting and compression. Journal of Food Engineering. 100: 145-151.

Han, J.-W., Ruiz-Garcia, L., Qian, J.-P. and Yang, X.-T. 2018. Food Packaging: A Comprehensive Review and Future Trends. Comprehensive Reviews in Food Science and Food Safety. 17: 860-877.

Hashemi, S. M. B., Mousavi Khaneghah, A., Koubaa, M., Barba, F. J., Abedi, E., Niakousari, M. and Tavakoli, J. 2017a. Extraction of essential oil from *Aloysia citriodora* Palau leaves using continuous and pulsed ultrasound: Kinetics, antioxidant activity and antimicrobial properties. Process Biochemistry. 65: 197-204.

Hashemi, S. M. B., Mousavi Khaneghah, A., Koubaa, M., Barba, F. J., Abedi, E., Niakousari, M. and Tavakoli, J. 2017b. Extraction of essential oil from Aloysia citriodora Palau leaves using continuous and pulsed ultrasound: Kinetics, antioxidant activity and antimicrobial properties. Process Biochemistry. 65: 197-204.

Hernandez-Izquierdo, V. and Krochta, J. 2008. Thermoplastic processing of proteins for film formation-a review. Journal of Food Science. 73: 30-39.

Hogan, Z., Baird, I. G. and Phanara, T. 2009. Threatened fishes of the world: *Probarbus jullieni* Sauvage, 1880 (*Cypriniformes: Cyprinidae*). Environmental Biology of Fishes. 84: 291-292.

Hoque, M. S., Benjakul, S. and Prodpran, T. 2011. Effects of partial hydrolysis and plasticizer content on the properties of film from cuttlefish (*Sepia pharaonis*) skin gelatin. Food Hydrocolloids. 25: 82-90.

Huang, T., Tu, Z.-c., Shangguan, X., Sha, X., Wang, H., Zhang, L. and Bansal, N. 2019. Fish gelatin modifications: A comprehensive review. Trends in Food Science and Technology. 86: 260-269.

Huang, Z.-R., Lin, Y.-K. and Fang, J.-Y. 2009. Biological and pharmacological activities of squalene and related compounds: potential uses in cosmetic dermatology. Molecules. 14: 540.

Hulmes, D., Wess, T., Prockop, D. and Fratzl, P. 1995. Radial packing, order, and disorder in collagen fibrils. Biophysical Journal. 68: 1661-1670.

Ikoma, T., Kobayashi, H., Tanaka, J., Walsh, D. and Mann, S. 2003. Physical properties of type I collagen extracted from fish scales of *Pagrus major* and *Oreochromis niloticas*. International Journal of Biological Macromolecules. 32: 199-204.

Ishida, K., Kuroda, R., Miwa, M., Tabata, Y., Hokugo, A., Kawamoto, T., Sasaki, K., Doita, M. and Kurosaka, M. 2007. The regenerative effects of platelet-rich plasma on meniscal cells in vitro and its in vivo application with biodegradable gelatin hydrogel. Tissue Engineering. 13: 1103-1112.

Iswariya, S., Velswamy, P. and Uma, T. S. 2017. Isolation and characterization of biocompatible collagen from the skin of puffer fish (*Lagocephalus inermis*). Journal of Polymers and the Environment. 26: 2086–2095.

Jamróz, E., Juszczak, L. and Kucharek, M. 2018. Investigation of the physical properties, antioxidant and antimicrobial activity of ternary potato starch-furcellaran-gelatin films incorporated with lavender essential oil. International Journal of Biological Macromolecules. 114: 1094-1101.

Johnston-Banks, F. A. 1990. Gelatine. *In* Food Gels. (Harris, P., ed.). p. 233-289. Springer. Dordrecht, Netherlands.

Jongjareonrak, A., Benjakul, S., Visessanguan, W., Prodpran, T. and Tanaka, M. 2006a. Characterization of edible films from skin gelatin of brownstripe red snapper and bigeye snapper. Food Hydrocolloids. 20: 492-501.

Jongjareonrak, A., Benjakul, S., Visessanguan, W. and Tanaka, M. 2005. Isolation and characterization of collagen from bigeye snapper (*Priacanthus macracanthus*) skin. Journal of the Science of Food and Agriculture. 85: 1203-1210.

Jongjareonrak, A., Benjakul, S., Visessanguan, W. and Tanaka, M. 2006b. Fatty acids and their sucrose esters affect the properties of fish skin gelatin-based film. European Food Research and Technology. 222: 650-657.

Jongjareonrak, A., Benjakul, S., Visessanguan, W. and Tanaka, M. 2008. Antioxidative activity and properties of fish skin gelatin films incorporated with BHT and α-tocopherol. Food Hydrocolloids. 22: 449-458.

Jongjareonrak, A., Rawdkuen, S., Chaijan, M., Benjakul, S., Osako, K. and Tanaka, M. 2010. Chemical compositions and characterisation of skin gelatin from farmed giant catfish (*Pangasianodon gigas*). LWT-Food Science and Technology. 43: 161-165.

Kaewdang, O., Benjakul, S., Kaewmanee, T. and Kishimura, H. 2014. Characteristics of collagens from the swim bladders of yellowfin tuna (*Thunnus albacares*). Food Chemistry. 155: 264-270.

Kaewdang, O., Benjakul, S., Prodpran, T., Kaewmanee, T. and Kishimura, H. 2016. Characteristics of gelatin extracted from the swim bladder of yellowfin tuna (*Thunnus albacores*) as affected by alkaline pretreatments. Journal of Aquatic Food Product Technology. 25: 1190-1201.

Kaewruang, P., Benjakul, S. and Prodpran, T. 2013. Molecular and functional properties of gelatin from the skin of unicorn leatherjacket as affected by extracting temperatures. Food Chemistry. 138: 1431-1437.

Kaewruang, P., Benjakul, S., Prodpran, T., Encarnacion, A. B. and Nalinanon, S. 2014. Impact of divalent salts and bovine gelatin on gel properties of phosphorylated gelatin from the skin of unicorn leatherjacket. LWT-Food Science and Technology. 55: 477-482.

Kang, M. G., Lee, M. Y., Cha, J. M., Lee, J. K., Lee, S. C., Kim, J., Hwang, Y.-S. and Bae, H. 2019. Nanogels derived from fish gelatin: application to drug delivery system. Marine Drugs. 17: 246.

Karim, A. A. and Bhat, R. 2009. Fish gelatin: properties, challenges, and prospects as an alternative to mammalian gelatins. Food Hydrocolloids. 23: 563-576.

Karnnet, S., Potiyaraj, P. and Pimpan, V. 2005. Preparation and properties of biodegradable stearic acid-modified gelatin films. Polymer Degradation and Stability. 90: 106-110.

Kelly, G. 1999. Squalene and its potential clinical uses. Alternative Medicine Review. 4: 29-36.

Khiari, Z., Rico, D., Martin-Diana, A. B. and Barry-Ryan, C. 2017. Valorization of fish by-products: rheological, textural and microstructural properties of mackerel skin gelatins. Journal of Material Cycles and Waste Management. 19: 180-191.

Kim, H. K., Kim, Y. H., Kim, Y. J., Park, H. J. and Lee, N. H. 2012. Effects of ultrasonic treatment on collagen extraction from skins of the sea bass *Lateolabrax japonicus*. Fisheries Science. 78: 485-490.

Kittiphattanabawon, P., Benjakul, S., Sinthusamran, S. and Kishimura, H. 2016. Gelatin from clown featherback skin: Extraction conditions. LWT-Food Science and Technology. 66: 186-192.

Kittiphattanabawon, P., Benjakul, S., Visessanguan, W., Kishimura, H. and Shahidi, F. 2010a. Isolation and characterisation of collagen from the skin of brownbanded bamboo shark (*Chiloscyllium punctatum*). Food Chemistry. 119: 1519-1526.

Kittiphattanabawon, P., Benjakul, S., Visessanguan, W., Nagai, T. and Tanaka, M. 2005. Characterisation of acid-soluble collagen from skin and bone of bigeye snapper (*Priacanthus tayenus*). Food Chemistry. 89: 363-372.

Kittiphattanabawon, P., Benjakul, S., Visessanguan, W. and Shahidi, F. 2010b. Comparative study on characteristics of gelatin from the skins of brownbanded bamboo shark and blacktip shark as affected by extraction conditions. Food Hydrocolloids. 24: 164-171.

Kittiphattanabawon, P., Benjakul, S., Visessanguan, W. and Shahidi, F. 2010c. Isolation and characterization of collagen from the cartilages of brownbanded bamboo shark (*Chiloscyllium punctatum*) and blacktip shark (*Carcharhinus limbatus*). LWT-Food Science and Technology. 43: 792-800.

Kittiphattanabawon, P., Sriket, C., Kishimura, H. and Benjakul, S. 2019. Characteristics of acid and pepsin solubilized collagens from Nile tilapia

(*Oreochromis niloticus*) scale. Emirates Journal of Food and Agriculture. 31: 95-01.

Kohno, Y., Egawa, Y., Itoh, S., Nagaoka, S.-i., Takahashi, M. and Mukai, K. 1995a. Kinetic study of quenching reaction of singlet oxygen and scavenging reaction of free radical by squalene in n-butanol. Biochimica et Biophysica Acta (BBA)-Lipids and Lipid Metabolism. 1256: 52-56.

Kohno, Y., Egawa, Y., Itoh, S., Nagaoka, S.-i., Takahashi, M. and Mukai, K. 1995b. Kinetic study of quenching reaction of singlet oxygen and scavenging reaction of free radical by squalene in n-butanol. Biochimica et Biophysica Acta, Lipids and Lipid Metabolism. 1256: 52-56.

KopiCoVá, Z. and VaVreiNoVá, S. 2007. Occurrence of squalene and cholesterol in various species of Czech freshwater fish. Czech Journal of Food Sciences. 25: 195-201.

Kumari, B., Tiwari, B. K., Hossain, M. B., Brunton, N. P. and Rai, D. K. 2018. Recent advances on application of ultrasound and pulsed electric field technologies in the extraction of bioactives from agro-industrial by-products. Food and Bioprocess Technology. 11: 223-241.

Kwak, K. S., Cho, S. M., Ji, C. I., Lee, Y. B. and Kim, S. B. 2009. Changes in functional properties of shark (*Isurus oxyrinchus*) cartilage gelatin produced by different drying methods. International Journal of Food Science and Technology. 44: 1480-1484.

Lavilla, I. and Bendicho, C. 2018. Fundamentals of Ultrasound-Assisted Extraction. *In* Water Extraction of Bioactive Compounds. (Herminia Dominguez, G. and María Jesús González, M., eds.). p. 291-316. Elsevier. Philadelphia, St. Louis, N.Y.

Lebon, M., Reiche, I., Gallet, X., Bellot-Gurlet, L. and Zazzo, A. 2016. Rapid quantification of bone collagen content by ATR-FTIR spectroscopy. Radiocarbon. 58: 131-145.

Li, Z. R., Wang, B., Chi, C. F., Zhang, Q. H., Gong, Y. D., Tang, J. J., Luo, H. Y. and Ding, G. F. 2013. Isolation and characterization of acid soluble collagens and

pepsin soluble collagens from the skin and bone of Spanish mackerel (*Scomberomorous niphonius*). Food Hydrocolloids. 31: 103-113.

Liang, Q., Wang, L., Sun, W., Wang, Z., Xu, J. and Ma, H. 2014. Isolation and characterization of collagen from the cartilage of Amur sturgeon (*Acipenser schrenckii*). Process Biochemistry. 49: 318-323.

Limpisophon, K., Tanaka, M. and Osako, K. 2010. Characterisation of gelatin–fatty acid emulsion films based on blue shark (*Prionace glauca*) skin gelatin. Food Chemistry. 122: 1095-1101.

Limpisophon, K., Tanaka, M., Weng, W., Abe, S. and Osako, K. 2009. Characterization of gelatin films prepared from under-utilized blue shark (*Prionace glauca*) skin. Food Hydrocolloids. 23: 1993-2000.

Lin, L., Regenstein, J. M., Lv, S., Lu, J. and Jiang, S. 2017. An overview of gelatin derived from aquatic animals: Properties and modification. Trends in Food Science and Technology. 68: 102-112.

Liu, D., Liang, L., Regenstein, J. M. and Zhou, P. 2012. Extraction and characterisation of pepsin-solubilised collagen from fins, scales, skins, bones and swim bladders of bighead carp (*Hypophthalmichthys nobilis*). Food Chemistry. 133: 1441-1448.

Liu, L., Jin, T., Liu, C.-K., Hicks, K., Mohanty, A. K., Bhardwaj, R. and Misra, M. 2008. A preliminary study on antimicrobial edible films from pectin and other food hydrocolloids by extrusion method. Journal of Natural Fibers. 5: 366-382.

Liu, Y., Cheong Ng, S., Yu, J. and Tsai, W.-B. 2019. Modification and crosslinking of gelatin-based biomaterials as tissue adhesives. Colloids and Surfaces B: Biointerfaces. 174: 316-323.

Lu, H.-T., Jiang, Y. and Chen, F. 2003. Application of high-speed counter-current chromatography to the preparative separation and purification of baicalin from the Chinese medicinal plant *Scutellaria baicalensis*. Journal of Chromatography A. 1017: 117-123.

Mahdi, J. S., He, Y. and Bhandari, B. 2006. Nano-emulsion production by sonication and microfluidization-a comparison. International Journal of Food Properties. 9: 475-485.

Marić, M., Grassino, A. N., Zhu, Z., Barba, F. J., Brnčić, M. and Brnčić, S. R. 2018. An overview of the traditional and innovative approaches for pectin extraction from plant food wastes and by-products: Ultrasound-, microwaves-, and enzyme-assisted extraction. Trends in Food Science and Technology. 76: 28-37.

Matmaroh, K., Benjakul, S., Prodpran, T., Encarnacion, A. B. and Kishimura, H. 2011. Characteristics of acid soluble collagen and pepsin soluble collagen from scale of spotted golden goatfish (*Parupeneus heptacanthus*). Food Chemistry. 129: 1179-1186.

McHugh, T. H. and Krochta, J. M. 1994. Sorbitol-vs glycerol-plasticized whey protein edible films: integrated oxygen permeability and tensile property evaluation. Journal of Agricultural and Food Chemistry. 42: 841-845.

Mecitoğlu, Ç., Yemenicioğlu, A., Arslanoğlu, A., Elmacı, Z. S., Korel, F. and Çetin, A. E. 2006. Incorporation of partially purified hen egg white lysozyme into zein films for antimicrobial food packaging. Food Research International. 39: 12-21.

Murrieta-Martínez, C., Soto-Valdez, H., Pacheco-Aguilar, R., Torres-Arreola, W., Rodríguez-Felix, F. and Márquez Ríos, E. 2018. Edible protein films: Sources and behavior. Packaging Technology and Science.

Muyonga, J., Cole, C. and Duodu, K. 2004. Fourier transform infrared (FTIR) spectroscopic study of acid soluble collagen and gelatin from skins and bones of young and adult Nile perch (*Lates niloticus*). Food Chemistry. 86: 325-332.

Nagai, T. and Suzuki, N. 2002. Preparation and partial characterization of collagen from paper nautilus (*Argonauta argo, Linnaeus*) outer skin. Food Chemistry. 76: 149-153.

Nagarajan, M., Benjakul, S., Prodpran, T. and Songtipya, P. 2012a. Properties of film from splendid squid (*Loligo formosana*) skin gelatin with various extraction temperatures. International Journal of Biological Macromolecules. 51: 489-496.

Nagarajan, M., Benjakul, S., Prodpran, T. and Songtipya, P. 2014. Characteristics of bio-nanocomposite films from tilapia skin gelatin incorporated with hydrophilic and hydrophobic nanoclays. Journal of Food Engineering. 143: 195-204.

Nagarajan, M., Benjakul, S., Prodpran, T., Songtipya, P. and Kishimura, H. 2012b. Characteristics and functional properties of gelatin from splendid squid (*Loligo formosana*) skin as affected by extraction temperatures. Food Hydrocolloids. 29: 389-397.

Nagarajan, M., Prodpran, T., Benjakul, S. and Songtipya, P. 2017. Properties and characteristics of multi-layered films from tilapia skin gelatin and poly (lactic acid). Food Biophysics. 12: 222-233.

Nalinanon, S., Benjakul, S. and Kishimura, H. 2010. Collagens from the skin of arabesque greenling (*Pleurogrammus azonus*) solubilized with the aid of acetic acid and pepsin from albacore tuna (*Thunnus alalunga*) stomach. Journal of the Science of Food and Agriculture. 90: 1492-1500.

Nalinanon, S., Benjakul, S., Visessanguan, W. and Kishimura, H. 2007. Use of pepsin for collagen extraction from the skin of bigeye snapper (*Priacanthus tayenus*). Food Chemistry. 104: 593-601.

Nalinanon, S., Benjakul, S., Visessanguan, W. and Kishimura, H. 2008. Improvement of gelatin extraction from bigeye snapper skin using pepsin-aided process in combination with protease inhibitor. Food Hydrocolloids. 22: 615-622.

Nam, A.-M., Bighelli, A., Tomi, F., Casanova, J. and Paoli, M. 2017. Quantification of squalene in olive oil using 13C nuclear magnetic resonance spectroscopy. Magnetochemistry. 3: 34.

Naziri, E. and Tsimidou, Z. M. 2013. Formulated squalene for food related applications. Recent Patents on Food, Nutrition and Agriculture. 5: 83-104.

Newmark, H. L. 1999. Squalene, olive oil, and cancer risk: review and hypothesis. Annals of the New York Academy of Sciences. 889: 193-203.

Nilsuwan, K., Benjakul, S. and Prodpran, T. 2018. Physical/thermal properties and heat seal ability of bilayer films based on fish gelatin and poly(lactic acid). Food Hydrocolloids. 77: 248-256.

Nilsuwan, K., Benjakul, S., Prodpran, T. and de la Caba, K. 2019. Fish gelatin monolayer and bilayer films incorporated with epigallocatechin gallate: Properties and their use as pouches for storage of chicken skin oil. Food Hydrocolloids. 89: 783-791.

Niu, L., Zhou, X., Yuan, C., Bai, Y., Lai, K., Yang, F. and Huang, Y. 2013. Characterization of tilapia (*Oreochromis niloticus*) skin gelatin extracted with alkaline and different acid pretreatments. Food Hydrocolloids. 33: 336-341.

Nuanmano, S., Prodpran, T. and Benjakul, S. 2015. Potential use of gelatin hydrolysate as plasticizer in fish myofibrillar protein film. Food Hydrocolloids. 47: 61-68.

Ogawa, M., Moody, M. W., Portier, R. J., Bell, J., Schexnayder, M. A. and Losso, J. N. 2003. Biochemical properties of black drum and sheepshead seabream skin collagen. Journal of Agricultural and Food Chemistry. 51: 8088-8092.

Ortega, J., Zavala, A. M., Hernández, M. and Reyes, J. D. 2012. Analysis of trans fatty acids production and squalene variation during amaranth oil extraction. Open Chemistry. 10: 1773-1778.

Parris, N. and Coffin, D. R. 1997. Composition factors affecting the water vapor permeability and tensile properties of hydrophilic zein films. Journal of Agricultural and Food Chemistry. 45: 1596-1599.

Pérez-Mateos, M., Montero, P. and Gómez-Guillén, M. 2009. Formulation and stability of biodegradable films made from cod gelatin and sunflower oil blends. Food Hydrocolloids. 23: 53-61.

Persikov, A. V., Xu, Y. and Brodsky, B. 2004. Equilibrium thermal transitions of collagen model peptides. Protein Science. 13: 893-902.

Petibois, C., Gouspillou, G., Wehbe, K., Delage, J.-P. and Déléris, G. 2006. Analysis of type I and IV collagens by FT-IR spectroscopy and imaging for a molecular investigation of skeletal muscle connective tissue. Analytical and Bioanalytical Chemistry. 386: 1961-1966.

Pietsch, A. and Jaeger, P. 2007. Concentration of squalene from shark liver oil by short-path distillation. European Journal of Lipid Science and Technology. 109: 1077-1082.

Pingret, D., Fabiano-Tixier, A. S. and Chemat, F. 2013. Ultrasound-assisted extraction. *In* Natural product extraction. Vol. 21. (Juliana M, P. and Mauricio A, R., eds.). p. 89-112. Royal Society of Chemistry. Thomas Graham House, Cambridge, UK.

Popa, O., Băbeanu, N. E., Popa, I., Niță, S. and Dinu-Pârvu, C. E. 2015. Methods for obtaining and determination of squalene from natural sources. BioMed Research International. 2015: 1-16.

Prodpran, T., Benjakul, S. and Artharn, A. 2007. Properties and microstructure of protein-based film from round scad (*Decapterus maruadsi*) muscle as affected by palm oil and chitosan incorporation. International Journal of Biological Macromolecules. 41: 605-614.

Prodpran, T., Benjakul, S. and Phatcharat, S. 2012. Effect of phenolic compounds on protein cross-linking and properties of film from fish myofibrillar protein. International Journal of Biological Macromolecules. 51: 774-782.

Ramos, M., Valdés, A., Beltrán, A. and Garrigós, M. 2016. Gelatin-based films and coatings for food packaging applications. Coatings. 6: 41-61.

Rattaya, S., Benjakul, S. and Prodpran, T. 2009. Properties of fish skin gelatin film incorporated with seaweed extract. Journal of Food Engineering. 95: 151-157.

Reddy, L. H. and Couvreur, P. 2009. Squalene: A natural triterpene for use in disease management and therapy. Advanced Drug Delivery Reviews. 61: 1412-1426.

Regenstein, J. M. and Zhou, P. 2007. Collagen and gelatin from marine by-products *In* Maximising the Value of Marine By-Products. (Shahidi, F., ed.). p. 279-303. Woodhead Publishing. Abington, Cambridge, England.

Rhim, J.-W. and Ng, P. K. 2007. Natural biopolymer-based nanocomposite films for packaging applications. Critical Reviews in Food Science and Nutrition. 47: 411-433.

Ridout, M. J., Paananen, A., Mamode, A., Linder, M. B. and Wilde, P. J. 2015. Interaction of transglutaminase with adsorbed and spread films of β-casein and κ-casein. Colloids and Surfaces B: Biointerfaces. 128: 254-260.

Rivero, S., García, M. and Pinotti, A. 2010. Correlations between structural, barrier, thermal and mechanical properties of plasticized gelatin films. Innovative Food Science and Emerging Technologies. 11: 369-375.

Rizk, M. A. and Mostafa, N. Y. 2016. Extraction and characterization of collagen from buffalo skin for biomedical applications. Oriental Journal of Chemistry. 32: 1601-1609.

Roberts, T. 1993. Artisanal fisheries and fish ecology below the great waterfalls of the Mekong River in southern Laos. Natural History Bulletin of the Siam Society. 41: 31-62.

Rotondo, A., Salvo, A., Gallo, V., Rastelli, L. and Dugo, G. 2017. Quick unreferenced NMR quantification of Squalene in vegetable oils. European Journal of Lipid Science and Technology.

Sadowska, M., Kołodziejska, I. and Niecikowska, C. 2003. Isolation of collagen from the skins of Baltic cod (*Gadus morhua*). Food Chemistry. 81: 257-262.

Sae-leaw, T. and Benjakul, S. 2015. Physico-chemical properties and fishy odour of gelatin from seabass (*Lates calcarifer*) skin stored in ice. Food Bioscience. 10: 59-68.

Sae-Leaw, T., Benjakul, S. and O'Brien, N. M. 2016. Effect of pretreatments and drying methods on the properties and fishy odor/flavor of gelatin from seabass (*Lates calcarifer*) skin. Drying Technology. 34: 53-65.

Saha, D. and Bhattacharya, S. 2010. Hydrocolloids as thickening and gelling agents in food: a critical review. Journal of Food Science and Technology. 47: 587-597.

Sai-Ut, S., Jongjareonrak, A. and Rawdkuen, S. 2012. Re-extraction, recovery, and characteristics of skin gelatin from farmed giant catfish. Food and Bioprocess Technology. 5: 1197-1205.

Sántiz-Gómez, M. A., Mazorra-Manzano, M. A., Ramírez-Guerra, H. E., Scheuren-Acevedo, S. M., Navarro-García, G., Pacheco-Aguilar, R. and Ramírez-Suárez, J. C. 2019. Effect of acid treatment on extraction yield and gel strength of gelatin from whiptail stingray (*Dasyatis brevis*) skin. Food Science and Biotechnology. 28: 751-757.

Santos, J. P., Esquerdo, V. M., Moura, C. M. and Pinto, L. A. A. 2018. Crosslinking agents effect on gelatins from carp and tilapia skins and in their biopolymeric films. Colloids and Surfaces A: Physicochemical and Engineering Aspects. 539: 184-191.

Sapper, M., Wilcaso, P., Santamarina, M. P., Roselló, J. and Chiralt, A. 2018. Antifungal and functional properties of starch-gellan films containing thyme (*Thymus zygis*) essential oil. Food Control. 92: 505-515.

Savedboworn, W., Kittiphattanabawon, P., Benjakul, S., Sinthusamran, S. and Kishimura, H. 2017. Characteristics of collagen from rohu (*Labeo rohita*) skin. Journal of Aquatic Food Product Technology. 26: 248-257.

Schmidt, M., Dornelles, R., Mello, R., Kubota, E., Mazutti, M., Kempka, A. and Demiate, I. 2016. Collagen extraction process. International Food Research Journal. 23: 913-922.

Sherwin, C. P., Smith, D. E. and Fulcher, R. G. 1998. Effect of fatty acid type on dispersed phase particle size distributions in emulsion edible films. Journal of Agricultural and Food Chemistry. 46: 4534-4538.

Shirsath, S., Sonawane, S. and Gogate, P. 2012. Intensification of extraction of natural products using ultrasonic irradiations-a review of current status. Chemical Engineering and Processing: Process Intensification. 53: 10-23.

Shoulders, M. D. and Raines, R. T. 2009. Collagen structure and stability. Annual Review of Biochemistry. 78: 929-958.

Shukla, R. and Cheryan, M. 2001. Zein: the industrial protein from corn. Industrial crops and products. 13: 171-192.

Silva, R. S., Bandeira, S. F. and Pinto, L. A. 2014. Characteristics and chemical composition of skins gelatin from cobia (*Rachycentron canadum*). LWT-Food Science and Technology. 57: 580-585.

Sinthusamran, S., Benjakul, S., Hemar, Y. and Kishimura, H. 2018. Characteristics and properties of gelatin from seabass (*Lates calcarifer*) swim bladder: Impact of extraction temperatures. Waste and Biomass Valorization. 9: 315-325.

Sinthusamran, S., Benjakul, S. and Kishimura, H. 2013. Comparative study on molecular characteristics of acid soluble collagens from skin and swim bladder of seabass (*Lates calcarifer*). Food Chemistry. 138: 2435-2441.

Sinthusamran, S., Benjakul, S. and Kishimura, H. 2014. Characteristics and gel properties of gelatin from skin of seabass (*Lates calcarifer*) as influenced by extraction conditions. Food Chemistry. 152: 276-284.

Soria, A. C. and Villamiel, M. 2010. Effect of ultrasound on the technological properties and bioactivity of food: a review. Trends in Food Science and Technology. 21: 323-331.

Sothornvit, R. and Krochta, J. M. 2005. Plasticizers in edible films and coatings. *In* Innovations in food packaging. (Han, J. H., ed.). p. 403-433. Elsevier Acadamic Press. San Diego, California, USA.

Spanova, M. and Daum, G. 2011. Squalene–biochemistry, molecular biology, process biotechnology, and applications. European Journal of Lipid Science and Technology. 113: 1299-1320.

Stainsby, G. 1987. Gelatin gels. *In* Advances in meat research (USA). Vol. 4. (A. M. Pearson, T. R. D., and A. J. Bailey, Allen J., ed.). p. 209–222. Van Nostrand Reinhold Company Inc. New York.

Staroszczyk, H., Pielichowska, J., Sztuka, K., Stangret, J. and Kołodziejska, I. 2012. Molecular and structural characteristics of cod gelatin films modified with EDC and TGase. Food Chemistry. 130: 335-343.

Stevens, L. 1991. Egg white proteins. Comparative Biochemistry and Physiology. Part B: Biochemistry and Molecular Biology. 100: 1-9.

Sztuka, K. and Kołodziejska, I. 2009. The influence of hydrophobic substances on water vapor permeability of fish gelatin films modified with transglutaminase or 1-ethyl-3-(3-dimethylaminopropyl) carbodiimide (EDC). Food Hydrocolloids. 23: 1062-1064.

Thankappan, T. and Gopakumar, K. 1991. A rapid method of seperation and estimation of squalene from fish liver oils using latroscan analyser. Fishery Technology. 28: 63-66.

Theerawitayaart, W., Prodpran, T., Benjakul, S. and Sookchoo, P. 2019. Properties of films from fish gelatin prepared by molecular modification and direct addition of oxidized linoleic acid. Food Hydrocolloids. 88: 291-300.

Tiwari, B. K. 2015. Ultrasound: A clean, green extraction technology. TrAC Trends in Analytical Chemistry. 71: 100-109.

Tongnuanchan, P., Benjakul, S. and Prodpran, T. 2011. Roles of lipid oxidation and pH on properties and yellow discolouration during storage of film from red tilapia (*Oreochromis niloticus*) muscle protein. Food Hydrocolloids. 25: 426-433.

Tongnuanchan, P., Benjakul, S. and Prodpran, T. 2013. Physico-chemical properties, morphology and antioxidant activity of film from fish skin gelatin incorporated with root essential oils. Journal of Food Engineering. 117: 350-360.

Tongnuanchan, P., Benjakul, S. and Prodpran, T. 2014. Structural, morphological and thermal behaviour characterisations of fish gelatin film incorporated with basil and citronella essential oils as affected by surfactants. Food Hydrocolloids. 41: 33-43.

Tongnuanchan, P., Benjakul, S., Prodpran, T. and Nilsuwan, K. 2015. Emulsion film based on fish skin gelatin and palm oil: Physical, structural and thermal properties. Food Hydrocolloids. 48: 248-259.

Tsujimoto, M. 1906. About kuroko-zame shark oil. Journal of the Society of Chemical Industry. 9: 953-958.

Tsujimoto, M. 1916. A highly unsaturated hydrocarbon in shark liver oil. Industrial and Engineering Chemistry. 8: 889-896.

Tu, Z.-c., Huang, T., Wang, H., Sha, X.-m., Shi, Y., Huang, X.-q., Man, Z.-z. and Li, D.-j. 2015. Physico-chemical properties of gelatin from bighead carp (Hypophthalmichthys nobilis) scales by ultrasound-assisted extraction. Journal of Food Science and Technology. 52: 2166-2174.

Umaraw, P. and Verma, A. K. 2017. Comprehensive review on application of edible film on meat and meat products: An eco-friendly approach. Critical Reviews in Food Science and Nutrition. 57: 1270-1279.

Van Tamelen, E. 1968. Bioorganic chemistry: sterols and acrylic terpene terminal expoxides. Accounts of Chemical Research. 1: 111-120.

Veeruraj, A., Arumugam, M. and Balasubramanian, T. 2013. Isolation and characterization of thermostable collagen from the marine eel-fish (*Evenchelys macrura*). Process Biochemistry. 48: 1592-1602.

Vieira, M. G. A., da Silva, M. A., dos Santos, L. O. and Beppu, M. M. 2011. Natural-based plasticizers and biopolymer films: A review. European Polymer Journal. 47: 254-263.

Vilkhu, K., Mawson, R., Simons, L. and Bates, D. 2008. Applications and opportunities for ultrasound assisted extraction in the food industry-A review. Innovative Food Science and Emerging Technologies. 9: 161-169.

Villén, J., Blanch, G. P., Ruiz del, C., María, L. and Herraiz, M. 1998. Rapid and simultaneous analysis of free sterols, tocopherols, and squalene in edible oils by coupled reversed-phase liquid chromatography− gas chromatography. Journal of Agricultural and Food Chemistry. 46: 1419-1422.

Wang, H. and Wang, L. 2017. Developing a bio-based packaging film from soya by-products incorporated with valonea tannin. Journal of Cleaner Production. 143: 624-633.

Wang, J., Pei, X., Liu, H. and Zhou, D. 2018. Extraction and characterization of acid-soluble and pepsin-soluble collagen from skin of loach (*Misgurnus anguillicaudatus*). International Journal of Biological Macromolecules. 106: 544-550.

Wang, L., An, X., Xin, Z., Zhao, L. and Hu, Q. 2007. Isolation and characterization of collagen from the skin of deep-sea redfish (*Sebastes mentella*). Journal of Food Science. 72:

Wang, L., Yang, B., Du, X., Yang, Y. and Liu, J. 2008. Optimization of conditions for extraction of acid-soluble collagen from grass carp (*Ctenopharyngodon idella*) by response surface methodology. Innovative Food Science and Emerging Technologies. 9: 604-607.

Wetherbee, B. M. and Nichols, P. D. 2000. Lipid composition of the liver oil of deep-sea sharks from the Chatham Rise, New Zealand. Comparative Biochemistry and Physiology B: Biochemistry and Molecular Biology. 125: 511-521.

Wihodo, M. and Moraru, C. I. 2013. Physical and chemical methods used to enhance the structure and mechanical properties of protein films: A review. Journal of Food Engineering. 114: 292-302.

Woo, J.-W., Yu, S.-J., Cho, S.-M., Lee, Y.-B. and Kim, S.-B. 2008. Extraction optimization and properties of collagen from yellowfin tuna (*Thunnus albacares*) dorsal skin. Food Hydrocolloids. 22: 879-887.

Wróblewska-Krepsztul, J., Rydzkowski, T., Borowski, G., Szczypiński, M., Klepka, T. and Thakur, V. K. 2018. Recent progress in biodegradable polymers and nanocomposites based packaging materials for sustainable environment. International Journal of Polymer Analysis and Characterization.

Wu, G. P., Wang, X. M., Lin, L. P., Chen, S. H. and Wu, Q. Q. 2014. Isolation and characterization of pepsin-solubilized collagen from the skin of black carp (Mylopharyngdon piceus). Advances in Bioscience and Biotechnology. 5: 642.

Xu, R., Fazio, G. C. and Matsuda, S. P. 2004. On the origins of triterpenoid skeletal diversity. Phytochemistry. 65: 261-291.

Yakimets, I., Wellner, N., Smith, A. C., Wilson, R. H., Farhat, I. and Mitchell, J. 2005. Mechanical properties with respect to water content of gelatin films in glassy state. Polymer. 46: 12577-12585.

Yang, H., Wang, Y., Zhou, P. and Regenstein, J. M. 2008. Effects of alkaline and acid pretreatment on the physical properties and nanostructures of the gelatin from channel catfish skins. Food Hydrocolloids. 22: 1541-1550.

Yusaf, T. and Al-Juboori, R. A. 2014. Alternative methods of microorganism disruption for agricultural applications. Applied Energy. 114: 909-923.

Zeng, S.-k., Zhang, C.-h., Lin, H., Yang, P., Hong, P.-z. and Jiang, Z. 2009. Isolation and characterisation of acid-solubilised collagen from the skin of Nile tilapia (*Oreochromis niloticus*). Food Chemistry. 116: 879-883.

Zhang, Y., Simpson, B. K. and Dumont, M.-J. 2018. Effect of beeswax and carnauba wax addition on properties of gelatin films: A comparative study. Food Bioscience. 26: 88-95.

Zhao, X., Wu, J. e., Chen, L. and Yang, H. 2019. Effect of vacuum impregnated fish gelatin and grape seed extract on metabolite profiles of tilapia (Oreochromis niloticus) fillets during storage. Food Chemistry.

Zhou, P. and Regenstein, J. M. 2005a. Effects of alkaline and acid pretreatments on Alaska pollock skin gelatin extraction. Journal of Food Science. 70: 392-396.

Zou, Y., Wang, L., Cai, P., Li, P., Zhang, M., Sun, Z., Sun, C., Xu, W. and Wang, D. 2017a. Effect of ultrasound assisted extraction on the physicochemical and

functional properties of collagen from soft-shelled turtle calipash. International Journal of Biological Macromolecules. 105: 1602-1610.

Zou, Y., Xu, P., Li, P., Cai, P., Zhang, M., Sun, Z., Sun, C., Xu, W. and Wang, D. 2017b. Effect of ultrasound pre-treatment on the characterization and properties of collagen extracted from soft-shelled turtle (*Pelodiscus sinensis*). LWT-Food Science and Technology. 82: 72-81.

Zubair, M. and Ullah, A. 2019. Recent advances in protein derived bionanocomposites for food packaging applications. Critical Reviews in Food Science and Nutrition. 1-29.

Zunying, L., Oliveira, A. C. and Su, Y.-C. 2009. Purification and characterization of pepsin-solubilized collagen from skin and connective tissue of giant red sea cucumber (*Parastichopus californicus*). Journal of Agricultural and Food Chemistry. 58: 1270-1274.

CHAPTER 2

EXTRACTION AND CHARACTERIZATION OF COLLAGEN FROM THE SKIN OF GOLDEN CARP (*PROBARBUS JULLIENI*), A PROCESSING BY-PRODUCT

2.1. Abstract

Acid solubilized collagen (ASC) and pepsin solubilized collagen (PSC) were isolated from the skin of golden carp with the yields of 21.16% and 39.05%, respectively, based on dry weight. Both ASC and PSC were composed of α1 and α2 chains and were characterized as type I collagen. Both collagens also had β-chain at a high content. Imino acid contents of ASC and PSC were 197 and 199 residues (1000 residues)$^{-1}$, respectively. Glycine constituted approximately 1:3 of total amino acid residues. No cysteine was present, indicating the absence of disulfide bonds. Fourier transform infrared (FTIR) and Circular dichroism (CD) spectra were almost similar between ASC and PSC. Thus, pepsin hydrolysis had no marked effect on triple helical structure. ASC and PSC showed T_{max} of 36.28 °C and 37.87 °C, respectively, which were higher than those of most temperate and cold-water fish collagens. The maximum solubility for both collagens was found at pH 3 and the drastic decrease in solubility was observed at neutral pH. Skin of golden carp, a by-product from fish processing, could therefore serve as an alternative source of collagen.

2.2. Introduction

Golden carp (*Probarbus jullieni*) is one of popular freshwater fish and primarily aquacultured in Thailand and Lao. Golden carp is also distributed in South-East Asian river basins with increasing demand of farmed freshwater fish consumption, the considerable amount of by-products (60–70%) including bones, skins, scales and fins are generated and usually used as animal feed or manure. Those underutilized bio-resources are gaining attention as a raw material for marketable value-added products, especially for the production of collagen and gelatin (Ashokkumar *et al.*, 2010;

Benjakul *et al.*, 2010; Elavarasan *et al.*, 2017). The value-added products, particularly collagen, can increase the revenue of producer and the alternative biomaterial can be produced.

Approximately 27 types of collagens with varying structural complexity and diversity have been reported (Birk and Bruckner, 2005). The traditional sources of collagen are porcine/bovine skin and bones. In general, porcine collagen has restrictions for some religions and socio-culture (Chakka *et al.*, 2017). Collagen from bovine origin is at risk of contamination with bovine spongiform encephalopathy (BSE) (Venien and Levieux, 2005). As a consequence, collagen from the fish skin and bones has become the promising alternative (Kittiphattanabawon *et al.*, 2005). Collagen content in fish is mainly dependent on fish species, age and seasons (Nagai and Suzuki, 2000). Additionally, collagen from different fish species and habitats might possess various molecular composition and physical properties (Benjakul *et al.*, 2012).

Collagen is traditionally extracted with the acid. However, it has a low yield. Pepsin, which is able to cleave peptides at telopeptide region, is therefore employed to increase the extraction efficiency of collagen (Benjakul *et al.*, 2010; Nagai and Suzuki, 2000). Both marine and freshwater fish skins have been used for collagen extraction (Duan *et al.*, 2009; Muyonga *et al.*, 2004). However, no information on collagen from golden carp exists.

2.3. Objective

To extract and characterize acid and pepsin soluble collagen from skin of golden carp.

2.4. Materials and methods

2.4.1. Chemicals

Sodium hydroxide and acetic acid were obtained from Merck (Darmstadt, Germany). Pepsin from porcine (EC3.4.23.1; 516 U mg^{-1} dry matter) and protein molecular weight markers were purchased from GE Healthcare UK (Aylesbury, UK). Coomassie Blue R-250, sodium dodecyl sulphate (SDS), and *N,N,N',N'*-

tetramethylethylenediamine (TEMED) were procured from Bio-Rad Laboratories (Hercules, CA, USA). All chemicals were of analytical grade.

2.4.2. Extraction of collagen

2.4.2.1. Preparation of fish skin

Fresh skins of golden carp (*Probarbus jullieni*) having an average body weight of 6-8 kg were obtained from fish dock, Samut Sakhon province, Thailand. The skins (30 kg) were packed in a polyethylene bag (5 kg bag^{-1}) were placed in polystyrene box and embedded in ice (1:3; w/w). Skins were transported to the Department of Food Technology, Prince of Songkla University, Hat Yai. The residual meat and scales were manually removed, and the skins were washed thoroughly with cold water. The prepared skins were cut into 0.5 × 0.5 cm^2 pieces and packed in polyethylene bags and stored at -20 °C for not longer than 2 months. Golden carp skin contained 67.35 ± 1.58% moisture, 24.21 ± 0.26% protein, 6.43 ± 0.35% fat, and 1.86 ± 0.18% ash as determined by the method of AOAC (2000).

2.4.2.2. Pretreatment of fish skin

All the processes were carried out at 4 °C. Non-collagenous proteins were removed by soaking skins in 0.1 M NaOH using skin/alkali ratio of 1:10 (w/v) for 6 h. The mixture was stirred continuously using an overhead stirrer model W20.n (IKA®-Werke GmbH & CO.KG, Stanfen, Germany) and the alkaline solution was changed every 2 h. After treatment, alkaline solution was drained off and residual skins were washed with chilled water until the wash water had the neutral pH. Skins were then defatted using 10% butanol with a skin/solvent ratio of 1:10 (w/v) for 9 h and the solvent was changed every 3 h. The solvent was discarded, and the defatted skins were washed with 10 volumes of chilled water for 5 times to completely remove butanol

2.4.2.3. Preparation of acid soluble collagen (ASC)

Pretreated skins were soaked in 0.5 M acetic acid using a skin/acid solution ratio of 1:15 (w/v) for 48 h under stirring condition. The mixture was then filtered with two-layered cheese cloth. The collagen in the filtrate was precipitated

using 2.5 M NaCl in the presence of 0.05 M tris (hydroxymethyl) aminomethane (pH 7.0). The precipitated collagen was collected by centrifugation at 15,000 ×g for 1 h at 4 °C using a refrigerated centrifuge model CR 22GIII (Hitachi, Tokyo, Japan). The obtained pellet was dissolved in minimal volume of 0.5 M acetic acid and dialyzed in 20 volume of 0.1 M acetic acid for 48 h. Dialysis was further performed using 20 volumes of distilled water. The obtained collagen was freeze-dried using a freeze-dryer (CoolSafe 55, ScanLaf A/S, Lynge, Denmark). The obtained dry matter was termed as ASC and subjected to analysis.

2.4.2.4. Preparation of Pepsin Soluble Collagen (PSC)

PSC was extracted from the residue obtained from ASC extraction. The residue was soaked in 0.5 M acetic acid containing porcine pepsin (50 unit g^{-1} residue) at a matter/solution ratio of 1:15 (w/v). The mixture was stirred continuously for 24 h, followed by filtration and precipitation as mentioned above. The precipitate was dialyzed and freeze-dried in the same manner. PSC was then analyzed.

2.4.3. Analysis

2.4.3.1. Yield

The yield of ASC and PSC was calculated based on a wet weight of starting material.

$$\text{Yield (\%)} = \frac{\text{Weight of freeze} - \text{dried collagen (g)}}{\text{Weight of initial dry skin (g)}} \times 100$$

2.4.3.2. Protein patterns

Sodium dodecyl sulphate-polyacrylamide gel electrophoresis (SDS-PAGE) was carried out by the method of Laemmli (1970) as described by Benjakul *et al.* (2010). Samples solubilized in 5% SDS (12 mg) were loaded onto polyacrylamide gel comprising 4% stacking gel and 7.5% running gel. After being separated, gels were stained and destained. MW of protein bands was estimated. Proteins in the gel were quantified using public domain digital analysis software, ImageJ (ImageJ 1.42q, National Institutes of Health, Bethesda, MD, USA).

2.4.3.3. Amino acid composition

Amino acid composition was determined according to the method described by Nagarajan *et al.* (2012) with a slight modification. In brief, the samples were hydrolyzed at low pressure in 4 M methanesulphonic acid containing 0.2% (v/v) 3-2(2-aminoethyl) indole at 115 °C for about 24 h. The hydrolysates were neutralized with 3.5 M NaOH and then diluted with 0.2 M citrate buffer (pH 2.2). An aliquot of 0.04 mL was applied to an amino acid analyser (MLC-703; Atto Co., Tokyo, Japan). An automated liquid chromatography system was used along with ninhydrin post column derivitization. The analysis was performed in duplicate.

2.4.3.4. Fourier transform infrared (FTIR) spectroscopy

FTIR spectroscopy of ASC and PSC were determined as described by Sinthusamran *et al.* (2013) using a FTIR spectrometer (Model Equinox 55, Bruker, Ettlingen, Germany) equipped with a horizontal ATR trough plate crystal cell (45 ZnSe; 80 mm long, 10 mm wide and 4 mm thick) (PIKE Technology Inc., Madison, WI, USA). Freeze-dried samples were placed in the crystal cell and the spectra were recorded over the wavenumber range of 650–4000 cm^{-1} at room temperature. The spectra were collected for 32 scans at a resolution of 4 cm^{-1}. The spectrum of clean empty cell was considered as background. Spectral data was analyzed by using OPUS 3.0 data collection software programme (Bruker, Ettlingen, Germany).

2.4.3.5. Circular dichroism (CD) spectroscopy

Samples were dissolved in 0.5 M acetic acid, stirred continuously for 4 h and centrifuged at 10000 ×g for 5 min at 4 °C. A final concentration of 2.0×10^{-4} g ml^{-1} was used for analysis. The analysis was carried out using a JASCO J-801 spectrometer (Jasco Corp, Tokyo, Japan). The prepared samples were scanned at the wavelength range of 190–240 nm with a bandwidth of 1 nm using nitrogen as atmosphere at room temperature. The spectral data obtained for 0.5 M acetic acid was

considered as blank and was subtracted with that of sample. The results were expressed as the molar residual ellipticity.

2.4.3.6. Zeta potential

ASC and PSC were dissolved in 0.05 M acetic acid (w/v) to obtain the final concentration of 0.04%. The mixtures were stirred continuously at 4 °C using a magnetic stirrer model BIG SQUID (IKA–Werke GmbH & CO.KG, Stanfen, Germany) until the samples were completely dissolved. Twenty millilitre of dissolved solution was subjected to auto titrator model BI-ZTU (Brookhaven Instruments Co., Holtsville, NY, USA), in which the desired pHs ranging from 2 to 12 were obtained using 1.0 M nitric acid or 1.0 M KOH. Zeta potential of pH adjusted sample was measured by Zeta potential analyser, model ZetaPALs (Brookhaven Instruments Co., Holtsville, NY, USA). The isoelectric point (pI) was determined from the pH showing zero zeta potential.

2.4.3.7. Thermal transition

Samples were prepared according to Kittiphattanabawon *et al.* (2005). ASC and PSC were dissolved in deionised water at a solid/solution ratio of 1:40 (w/v). The mixture was allowed to stand for 24 h at 4 °C. The samples were accurately weighed into aluminium pans and sealed. The scan was performed in the temperature range of 25-45 °C with the increasing rate of 1 °C min^{-1}, using a differential scanning calorimeter model DSC7 (Perkin–Elmer, Norwalk, CA, USA). Iced water was used as the cooling medium. An empty pan was used as a reference and the temperature was calibrated using indium thermogram. Total denaturation enthalpy (ΔH) was determined by measuring the peak area of DSC thermogram and the maximum transition temperature (T_{max}) was estimated from the endothermic peak of thermogram.

2.4.3.8. Solubility

Collagen dissolved in 0.5 M acetic acid (3 mg ml^{-1}) was adjusted to the pHs ranging from 1 to 10, using 6 N NaOH or 6 N HCl. Then the solutions were stirred for 30 min at 4 °C, followed by centrifugation at 10,000 ×g for 30 min at 4 °C. The supernatant was collected and protein content was determined using the Lowry method

[15]. Bovine serum albumin was used as a standard. Relative solubility was calculated in comparison with that of pH rendering the highest solubility.

2.4.4. Statistical Analysis

All the experiments were performed in triplicate and a completely randomised design (CRD) was used. Data was presented in mean ± standard deviation. Analysis of variance (ANOVA) was performed and mean comparison was done by the Duncan's multiple range tests. The analysis was performed using SPSS software (SPSS 11.0 for Windows, SPSS Inc, Chicago, IL, USA).

2.5. Results and discussion

2.5.1. Yield

ASC from the skin of golden carp had the yield of 22.16 ± 1.53% (based on dry weight). The result suggested that collagen was solubilized in acid to the low extent. Similarly, Nalinanon *et al.* (2007) reported the incomplete solubilization of bigeye snapper skin in 0.5 M acetic acid. The presence of cross-linkages at the telopeptide and inter-molecular region is associated with the difficulty in collagen extraction by acid alone (Zhang *et al.*, 2007). The yield of PSC was 39.05 ± 2.31%, which was 1.7–fold higher than that of ASC. The increase in solubilization of collagen in the residue from ASC extraction was achieved with the aid of pepsin. Pepsin was able to cleave specifically the cross-linkages at telopeptide, thereby facilitating the solubilization of collagen by acid (Benjakul *et al.*, 2012). Thus, collagen in the skin of golden carp could be more extracted when pepsin was present.

2.5.2. Protein patterns

Protein patterns of ASC and PSC under non-reducing condition are shown in Figure 1. Both collagens contained α_1- and α_2-chains at a ratio of 2:1, indicating that collagen from skin of golden carp belonged to type 1. The type I collagen consists of two identical α_1-chains and one α_2-chain (Gómez-Guillén *et al.*, 2011). Fish skins such as seabass (Sinthusamran *et al.*, 2013) and rohu (Savedboworn *et al.*, 2017) have been reported to contain type I collagen as the major constituent. β-chain (dimer)

was found at a high content. Crosslinks including γ-component as well as high-molecular-weight components were also observed. It was noted that α-chains of PSC showed slightly lower MW than those of ASC. Telopeptide was cleaved to some degree, resulting in slightly shorter chain length of PSC. Kittiphattanabawon *et al.* (2005) also reported that MW of α-chains of PSC from the skin of bamboo shark decreased slightly, compared to that of ASC.

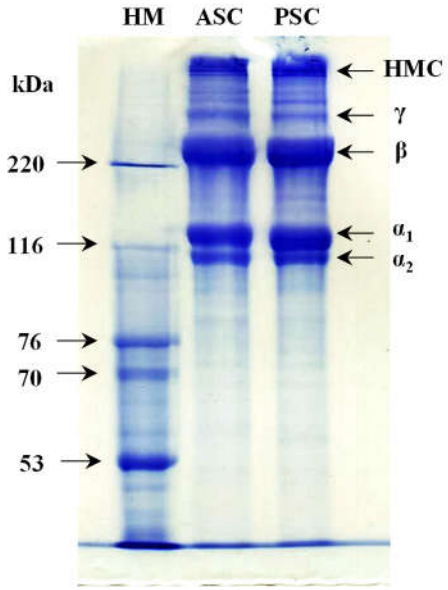

Figure 7. Protein patterns of acid soluble collagen (ASC) and pepsin soluble collagen (PSC) from golden carp skin. HMC high molecular weight component, HM high molecular weight marker.

2.5.3. Amino acid composition

ASC and PSC showed a similar profile of amino acid composition (Table 1). Both collagens had glycine (329-336 residues (1000 residues)$^{-1}$) as the major amino acid. Generally, glycine occurs at every third residue in peptide chain of collagen except for the first 14 amino acid residues from the N-terminus and the first 10 residues from the C-terminus (Benjakul *et al.*, 2012). With some removal of telopeptide, PSC showed higher number of glycine restudies (336 residues (1000 residues)$^{-1}$), compared to ASC (329 residues (1000 residues)$^{-1}$). Proline (117 and 120 residues (1000 residues)$^{-1}$) and alanine (112 and 120 residues (1000 residues)$^{-1}$) were also dominant in both ASC and PSC. Hydroxyproline contents of ASC and PSC were 80 and 79 residues (1000

residues)$^{-1}$, respectively. The imino acid (proline + hydroxyproline) contents of ASC and PSC were 197 and 199 residues (1000 residues)$^{-1}$, respectively, which were higher than those of bigeye snapper skin collagen (193 residues (1000 residues)$^{-1}$) (Kittiphattanabawon *et al.*, 2005), grass carp skin collagen (186 residues (1000 residues)$^{-1}$) (Zhang *et al.*, 2007) were much higher than that of cod skin collagen (154 residues (1000 residues)$^{-1}$) (Duan *et al.*, 2009). The difference in imino acid content among collagens from different species is most likely due to the difference in living environment and temperature.

Table 4. Amino acid composition of acid soluble collagen (ASC) and pepsin soluble collagen (PSC) from golden carp skin.

Amino acids	**(Residues (1000 residues)$^{-1}$)**	
	ASC	**PSC**
Alanine	112	120
Arginine	53	53
Aspartic acid/asparagine	51	48
Cysteine	0	0
Glutamine/glutamic acid	70	68
Glycine	329	336
Histidine	4	4
Isoleucine	13	11
Leucine	23	22
Lysine	28	26
Hydroxylysine	6	6
Methionine	12	12
Phenylalanine	14	13
Hydroxyproline	80	79
Proline	117	120
Serine	36	35
Threonine	25	23
Tyrosine	4	3
Valine	23	21
Imino acid	197	199
Total residues	1000	1000

In general, the imino acids contribute to thermal stability of collagen via maintaining the integrity of triple helix through hydrogen bonds (Benjakul *et al.*, 2010). As a consequence, ASC and PSC from golden carp skin were more likely stable than those of other fish species. Both collagens contained no cysteine, confirming the absence of disulphide bonds. Other amino acids such as arginine, aspartic acid, glutamic acid, leucine and lysine were present at lower amounts in both ASC and PSC. PSC contained a lower content of acidic amino acids (aspartic and glutamic acids) than ASC. This was possibly due to the removal of telopeptide, which might consist of those acidic amino acids. Thus, pepsin treatment had the influence on the amino acid composition of collagen to some degree.

2.5.4. FTIR spectra

FTIR spectra of ASC and PSC from the skin of golden carp are shown in Figure 2. Both samples had amide I (1600 to 1700 cm^{-1}), amide II (1500 to 1600 cm^{-1}) and amide III (1200 to 1300 cm^{-1}) bands, which were in accordance with the report of Muyonga *et al.* (2004). Amide I, II and III bands of ASC were found at wavenumbers of 1639, 1541 and 1236 cm^{-1}, respectively. PSC showed absorption bands at wavenumbers of 1633, 1538 and 1236 cm^{-1}, respectively. Amide I bands are associated with C=O stretching vibrations coupled to N-H bending vibrations and C-N stretching (Payne and Veis, 1988). Amide I band of PSC had lower wavenumber than ASC, indicating the higher interaction of C=O with the adjacent chains of the latter associated with the higher compactness of PSC. This was related with the removal of telopeptide. Similarly, amide II band of PSC also shifted to lower wavenumber than that of ASC. Amide II represents the N-H bending vibrations coupled to C-N stretching vibrations (Li *et al.*, 2004), suggesting the presence of more inter-molecular hydrogen bonds in PSC, specifically at helical portion of collagen structure. The amide III represents the combination peaks between C-H stretching vibrations and N-H deformation involved in inter-molecular interaction in triple helical structure (Muyonga *et al.*, 2004). ASC and PSC showed the same wavenumbers of amide III. The triple helical structure of ASC and PSC was confirmed by the IR ratio between amide III and 1450 cm^{-1} band (Duan *et al.*, 2009), which were found to be approximately 0.98 and 1, respectively. PSC, therefore, had slightly higher ordered triple helical structure than ASC.

Amide A, associated with the stretching vibrations of N-H group, appeared at 3294 and 3301 cm^{-1} for ASC and PSC, respectively. The shift of wavenumber to lower frequency is typically due to the involvement of N-H group in hydrogen bond (Kittiphattanabawon *et al.*, 2005). Thus, hydrolysis of telopeptide region by pepsin might cause some destruction of hydrogen bonds as indicated by higher wavenumber of PSC. The amide B was observed with similar wavenumber for ASC (2924 cm^{-1}) and PSC (2923 cm^{-1}). Amide B corresponds to asymmetric stretch vibration of =C-H and NH_3^+ (Abe and Krimm, 1972). The FTIR spectra indicated that both ASC and PSC were most likely in native triple helical conformation. However, some differences in inter- and intra-molecular interactions existed between both collagens

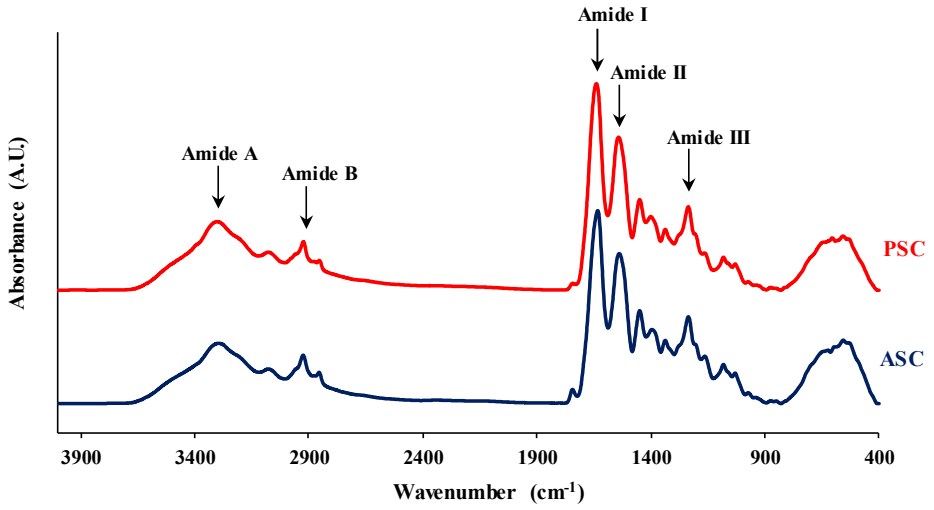

Figure 8. Fourier transform infrared spectra of acid soluble collagen (ASC) and pepsin soluble collagen (PSC) from golden carp skin.

2.5.5. CD spectroscopy

CD spectra of collagens extracted from skins of golden carp are shown in Figure 3. CD spectroscopy is mainly used to investigate the secondary structure of proteins. Native collagen is optically active protein, which has triple helical conformation with a negative peak at 196-198 nm and a positive peak at 200 nm (Tifany and Krimm, 1972). Rotatory maxima of positive peak of ASC and PSC were found at 220.6 and 220.8 nm, respectively. In general, the molar ellipticity of positive peak of

PSC was slightly higher than ASC, suggesting that PSC possessed a higher degree of triple helical structure. Nevertheless, the rotatory minimum of negative peak of both collagens was found at the same wavelength (198 nm). Therefore, the slight difference in ellipticity of both collagens could be due to the removal of telopeptide region in PSC. Partially denatured collagen is found to give lower intensity band (Tifany and Krimm, 1972). The ratio of positive and negative peak (Rpn) of ASC and PSC was 0.107 and 0.109, respectively. The obtained values of Rpn were in agreement with previously reported for native collagen (Usha and Ramasami, 2005). The results of both CD and FTIR spectra demonstrated that ASC and PSC were helical in structure.

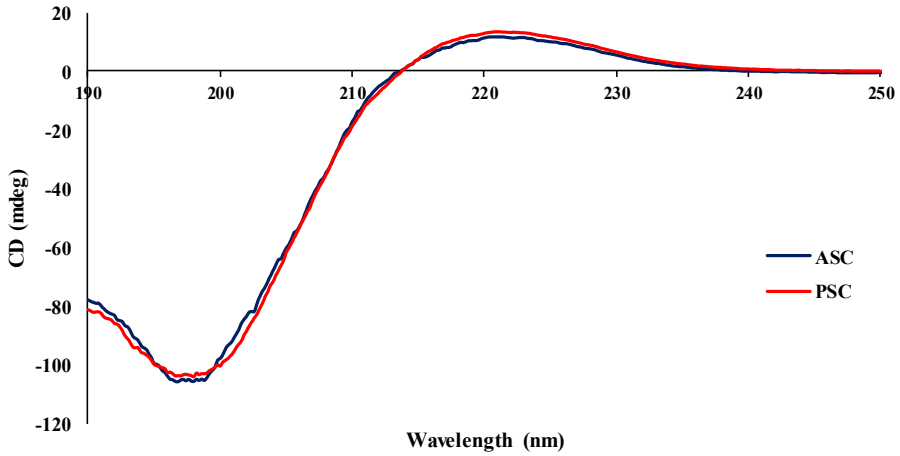

Figure 9. Circular dichroism spectra of acid soluble collagen (ASC) and pepsin soluble collage (PSC) from golden carp skin.

2.5.6. Zeta potential

Zeta potential of ASC and PSC from the skin of golden carp at different pHs is shown in Figure 4. At acidic pH (2–6) both collagens were positively charged. The charge decreased with continuous increase in pHs. Zero surface net charge of ASC and PSC was observed at pH 6.54 and 6.79, respectively, which were estimated to be their isoelectric points (pI). The pIs of both collagens were found at slightly acidic pH. This might be attributed to the higher content of acidic amino acids including aspartic acid and glutamic acid, compared to basic amino acids, involving lysine, histidine and arginine (Nalinanon *et al.*, 2011). Furthermore, the slight difference in pI of both collagens might be due to the difference in distribution and composition of amino acid

residues, particularly on the surface domains of collagen molecules (Kittiphattanabawon *et al.*, 2010b). At pHs above the pI, both collagens became negatively charged. Slightly increase in negative charge was noticeable as pH increased. The obtained pI values were in accordance with those of collagens from skin of seabass (6.46) (Sinthusamran *et al.*, 2013) and skin of bamboo shark (6.56) (Kittiphattanabawon *et al.*, 2010b).

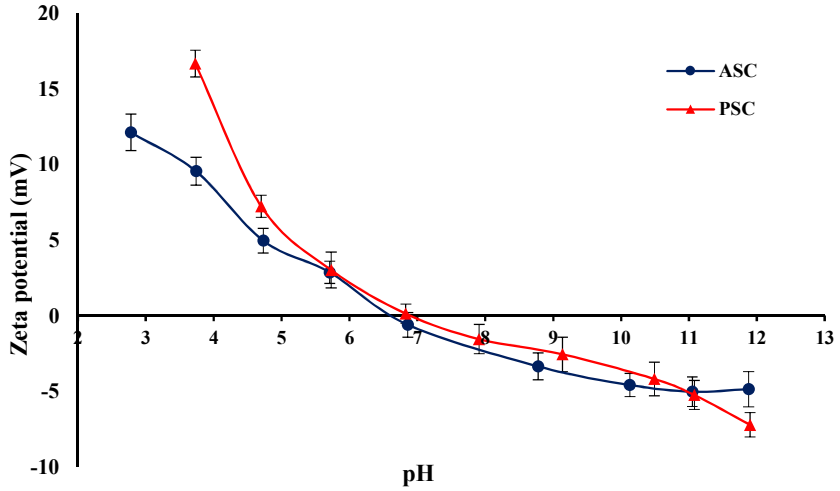

Figure 10. Zeta potential of acid soluble collagen (ASC) and pepsin soluble collagen (PSC) from golden carp skin at different pHs. Bars represent the standard deviation (n:3).

2.5.7. Thermal transition

DSC thermograms of collagens from the skin of golden carp rehydrated in deionized water are shown in Figure 5. The endothermic peak of ASC was observed with T_{max} of 36.28 °C, which was slightly lower than that of PSC (37.87 °C). Higher T_{max} of PSC might be caused by the removal of non-helical region, associated with more ordered and compact structure. Different T_{max} have been reported for collagens from skins of bigeye snapper (30.80 °C) (Kittiphattanabawon *et al.*, 2005), bullhead shark (25 °C), chub mackerel (25.6 °C) and seabass (26.5 °C) (Nagai and Suzuki, 2000). Those were lower than T_{max} of collagens from skin of golden carp. However, T_{max} values of both collagens from golden carp skin were lower than that of calf skin collagen (41 °C). Enthalpy of PSC was also higher than ASC, suggesting higher

stability of the former. Thermal stability of collagen is attributed by the hydrogen bonded triple helix structure mediated by hydroxyl group of hydroxyproline in one strand to the main chain carboxyl group of another chain (Kittiphattanabawon *et al.*, 2010a; Nalinanon *et al.*, 2011). The higher thermal stability of PSC was also demonstrated by the higher content of imino acids, especially hydroxyproline content (Table 1).

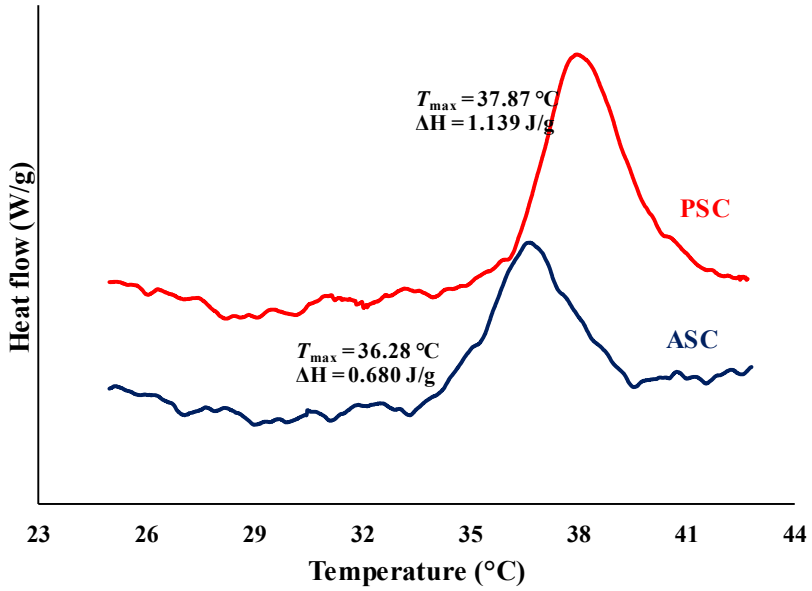

Figure 11. Differential scanning calorimeter thermogram of acid soluble collagen (ASC) and pepsin soluble collagen (PSC) from golden carp skin.

2.5.8. Solubility

Effect of pH on the solubility of ASC and PSC is depicted in Figure 6. Both collagens were highly solubilized at the pH range of 1–3, with relative solubility greater than 95%. Both collagens showed almost similar pattern of solubility. There was a sharp decrease in solubility above pH 3, in which solubility was approximately 20% at pH 6 or 7. Similar results were reported for the collagens from the skin of bamboo shark (Kittiphattanabawon *et al.*, 2010b). The decrease in solubility might be due to the hydrophobic and hydrophobic interaction of collagen molecules at pH close to pI (Sinthusamran *et al.*, 2013). When pH increased from 7 to 10, a slight increase in solubility of ASC and PSC was found. This might be due to the increased repulsion of

collagen molecules with increasing negative charge. At pH 10, relative solubility of 35 and 29%, respectively, was obtained. Thus, both collagens were highly soluble at very acidic pH range.

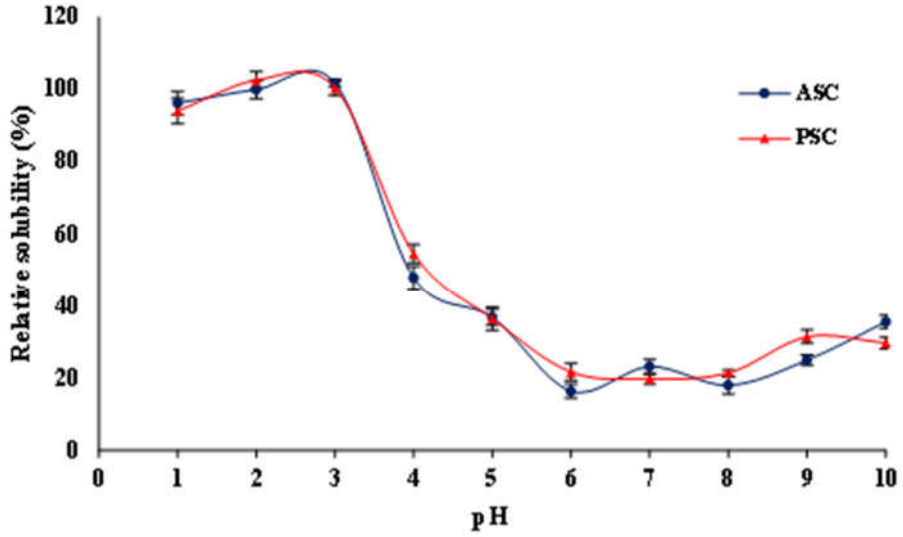

Figure 12. Relative solubility of acid soluble collagen (ASC) and pepsin soluble collagen (PSC) from golden carp skin at different pHs. Bars represent the standard deviation (n:3).

2.6. Conclusion

ASC and PSC could be extracted from the skin of golden carp and classified to be type I. Telopeptides of collagen was cleaved by pepsin, resulting in the increased yield of PSC. PSC showed higher integrity of triple helical structure than ASC. Both ASC and PSC had higher T_{max} and imino acid composition. Both collagens showed higher solubility in acidic pH (1-3). Thus, the skin of golden carp could be an alternative source of thermal stable collagen.

2.7. References

Abe, Y. and Krimm, S. 1972. Normal vibrations of crystalline polyglycine I. Biopolymers: Original Research on Biomolecules. 11: 1817-1839.

AOAC. 2000. Official Methods of Analysis. 17 th ed. *In* Association of Official Analytical Chemists. Arlington, VA.

Ashokkumar, M., Thanikaivelan, P., Murali, R. and Chandrasekaran, B. 2010. Preparation and characterization of composite sheets from collagenous and chromium–collagen complex wastes using polyvinylpyrrolidone: two problems, one solution. Waste Biomass Valorization. 1: 347-355.

Benjakul, S., Nalinanon, S. and Shahidi, F. 2012. Fish Collagen. *In* Food Biochemistry and Food Processing, Second Edition. (Simpson, B. K., ed.). p. 365-387. Wiley-Blackwell. Iowa, USA.

Benjakul, S., Thiansilakul, Y., Visessanguan, W., Roytrakul, S., Kishimura, H., Prodpran, T. and Meesane, J. 2010. Extraction and characterisation of pepsin solubilised collagens from the skin of bigeye snapper (*Priacanthus tayenus* and *Priacanthus macracanthus*). Journal of the Science of Food and Agriculture. 90: 132-138.

Birk, D. E. and Bruckner, P. 2005. Collagen suprastructures. *In* Collagen. (Brinckmann, J. *et al.*, eds.). p. 185-205. Springer. Berlin, Heidelberg.

Chakka, A. K., Muhammed, A., Sakhare, P. and Bhaskar, N. 2017. Poultry processing waste as an alternative source for mammalian gelatin: Extraction and characterization of gelatin from chicken feet using food grade acids. Waste Biomass Valorization. 8: 2583-2593.

Duan, R., Zhang, J., Du, X., Yao, X. and Konno, K. 2009. Properties of collagen from skin, scale and bone of carp (*Cyprinus carpio*). Food Chemistry. 112: 702-706.

Elavarasan, K., Kumar, A., Uchoi, D., Tejpal, C., Ninan, G. and Zynudheen, A. 2017. Extraction and characterization of gelatin from the head waste of tiger tooth croaker (*Otolithes ruber*). Waste Biomass Valorization. 8: 851-858.

Gómez-Guillén, M., Giménez, B., López-Caballero, M. a. and Montero, M. 2011. Functional and bioactive properties of collagen and gelatin from alternative sources: A review. Food Hydrocolloids. 25: 1813-1827.

Kittiphattanabawon, P., Benjakul, S., Visessanguan, W., Kishimura, H. and Shahidi, F. 2010a. Isolation and characterisation of collagen from the skin of brownbanded bamboo shark (*Chiloscyllium punctatum*). Food Chemistry. 119: 1519-1526.

Kittiphattanabawon, P., Benjakul, S., Visessanguan, W., Nagai, T. and Tanaka, M. 2005. Characterisation of acid-soluble collagen from skin and bone of bigeye snapper (*Priacanthus tayenus*). Food Chemistry. 89: 363-372.

Kittiphattanabawon, P., Benjakul, S., Visessanguan, W. and Shahidi, F. 2010b. Isolation and characterization of collagen from the cartilages of brownbanded bamboo shark (*Chiloscyllium punctatum*) and blacktip shark (*Carcharhinus limbatus*). LWT-Food Science and Technology. 43: 792-800.

Laemmli, U. K. 1970. Cleavage of structural proteins during the assembly of the head of bacteriophage T4. Nature. 227: 680-685.

Li, H., Liu, B., Gao, L. and Chen, H. 2004. Studies on bullfrog skin collagen. Food Chemistry. 84: 65-69.

Muyonga, J., Cole, C. and Duodu, K. 2004. Fourier transform infrared (FTIR) spectroscopic study of acid soluble collagen and gelatin from skins and bones of young and adult Nile perch (*Lates niloticus*). Food Chemistry. 86: 325-332.

Nagai, T. and Suzuki, N. 2000. Isolation of collagen from fish waste material—skin, bone and fins. Food Chemistry. 68: 277-281.

Nagarajan, M., Benjakul, S., Prodpran, T., Songtipya, P. and Kishimura, H. 2012. Characteristics and functional properties of gelatin from splendid squid (*Loligo formosana*) skin as affected by extraction temperatures. Food Hydrocolloids. 29: 389-397.

Nalinanon, S., Benjakul, S., Kishimura, H. and Osako, K. 2011. Type I collagen from the skin of ornate threadfin bream (*Nemipterus hexodon*): Characteristics and effect of pepsin hydrolysis. Food Chemistry. 125: 500-507.

Nalinanon, S., Benjakul, S., Visessanguan, W. and Kishimura, H. 2007. Use of pepsin for collagen extraction from the skin of bigeye snapper (*Priacanthus tayenus*). Food Chemistry. 104: 593-601.

Payne, K. and Veis, A. 1988. Fourier transform IR spectroscopy of collagen and gelatin solutions: deconvolution of the amide I band for conformational studies. Biopolymers: Original Research on Biomolecules. 27: 1749-1760.

Savedboworn, W., Kittiphattanabawon, P., Benjakul, S., Sinthusamran, S. and Kishimura, H. 2017. Characteristics of collagen from rohu (*Labeo rohita*) skin. Journal of Aquatic Food Product Technology. 26: 248-257.

Sinthusamran, S., Benjakul, S. and Kishimura, H. 2013. Comparative study on molecular characteristics of acid soluble collagens from skin and swim bladder of seabass *(Lates calcarifer*). Food Chemisty. 138: 2435-2441.

Tifany, M. L. and Krimm, S. 1972. Effwct of temperature on the circular dichroism spectra of polypeptides in the extended state. Biopolymers: Original Research on Biomolecules. 11: 2309-2316.

Usha, R. and Ramasami, T. 2005. Structure and conformation of intramolecularly cross-linked collagen. Colloids Surface B: Biointerfaces. 41: 21-24.

Venien, A. and Levieux, D. 2005. Differentiation of bovine from porcine gelatines using polyclonal anti-peptide antibodies in indirect and competitive indirect ELISA. Journal of Pharmaceutical and Biomedical Analysis. 39: 418-424.

Zhang, Y., Liu, W., Li, G., Shi, B., Miao, Y. and Wu, X. 2007. Isolation and partial characterization of pepsin-soluble collagen from the skin of grass carp (*Ctenopharyngodon idella*). Food Chemistry. 103: 906-912.

CHAPTER 3

MOLECULAR CHARACTERISTICS OF ACID AND PEPSIN SOLUBLE COLLAGENS FROM THE SCALES OF GOLDEN CARP (*PROBARBUS JULLIENI*)

3.1. Abstract

Acid soluble collagen (ASC) and pepsin soluble collagen (PSC) were isolated from the scales of golden carp (*Probarbus jullieni*). Both ASC and PSC consisted of α- and β-chains as the major constituent and were identified as type I collagen. The yields of ASC and PSC were 0.42 and 1.16 g 100 g^{-1} (dry weight basis), respectively. Amino acid composition revealed that glycine constituted 1/3 of total amino acid residues and no cysteine was found. ASC and PSC had imino acid contents of 197 and 202 residues (1000 residues)$^{-1}$, respectively. Fourier transform infrared spectroscopy (FTIR) and Circular dichroism (CD) spectra indicated high integrity of the triple helical structure of both ASC and PSC. Based on Differential scanning calorimetry (DSC), T_{max} of ASC and PSC were 37.67 and 37.83 °C, respectively. Both collagens exhibited high solubility at acidic pH (1–3) and the solubility was decreased in the presence of NaCl at concentrations above 30 g l^{-1}. The overall results demonstrated that scales of golden carp could serve as another source of collagen.

3.2. Introduction

Collagen constitutes as a major component of extracellular matrix and serves a mechanical protection as well as regulates cell from the environment (Kielty et al., 1993). Collagen is a fibrous protein, constituting about 30% of total protein. There are over 28 types of collagen distributed in cartilage, tendons, ligaments, skins, bones, and other organs (Jongjareonrak et al., 2005). Collagen, especially type I, has a wide range of applications in food, pharmaceutical, biomedical and cosmetic industries. This attributes to its excellent biocompatibility/biodegradability and weak antigenicity (Rizk

and Mostafa, 2016). Since collagen from porcine or bovine sources has the limitation due to religious concern (Kittiphattanabawon et al., 2005), demand for alternative commercial sources of collagen is increasing.

Fish processing generates a considerable amount of organic by-products up to 50-70%, depending on fish species. To increase the value of those by-products, marketable value-added products, especially collagen and gelatin, have gained increasing interest for manufacturers. Collagens from skin of bigeye snapper (Benjakul et al., 2010), skin, scale, and bone of carp (*Cyprinus carpio*) (Duan et al., 2009), scale of snakehead (*Ophiocephalus argus*) (Liu et al., 2008) and swim bladder of seabass (Sinthusamran et al., 2013) have been extracted. Nevertheless, biochemical properties of collagen can be influenced by species, extraction procedures and other factors. Due to the lack of disease transmission and no dietary restriction, collagens from aquatic animals are gaining attention for various potential applications (Liu et al., 2012).

Golden carp (*Probarbus jullieni*) is a freshwater fish, commonly distributed in Southeast Asian river basins. Golden carp is very popular and primarily aquacultured in Thailand and Lao PDR. The global aquaculture production has the annual growth rate of 3.86 % from 3077 metric ton in 2005 to 5500 metric ton in 2010 (FAO 2016). During descaling process, scales are generated as leftover (Zall, 2004). Scales are usually considered as low-value feed material or dumped as a waste, causing a pollution. Those scales can be used for collagen extraction. Nevertheless, no information on the isolation and characterisation of collagen from scales of golden carp has been reported.

3.3. Objective

To extract and characterize acid and pepsin soluble collagen from scales of golden carp which could serve as a substitute for mammalian collagen.

3.4. Material and methods

3.4.1. Chemicals

Sodium hydroxide and acetic acid were obtained from Merck (Darmstadt, Germany). Pepsin from porcine (EC3.4.23.1; 516 U mg^{-1} dry matter) and

protein molecular weight markers were purchased from GE Healthcare UK (Aylesbury, UK). Coomassie Blue R-250, sodium dodecyl sulphate (SDS), and *N,N,N',N'*-tetramethylethylenediamine (TEMED) were procured from Bio-Rad Laboratories (Hercules, CA, USA). All chemicals were of analytical grade.

3.4.2. Extraction of golden carp scales collagen

3.4.2.1. Preparation of golden carp scales

The scales of golden carp (*Probarbus jullieni*) were obtained from the fish dock in Mahachai, Samut sakhon province, Thailand. The packaging, transportation and storage were carried out as described in section *2.4.2.1*. Scales of golden carp contained 16.24 ± 0.18% moisture, 40.36 ± 0.27% protein, 0.62 ± 0.1% fat, and 42.16 ± 0.21% ash as determined by AOAC method (AOAC, 2000). Hydroxyproline content of scale was 22.46 ± 0.82 mg g^{-1} of sample as analyzed by the method of Bergman and Loxley (1963).

3.4.2.2. Extraction of acid soluble collagen (ASC)

Extraction was done according to the method described by Chuaychan et al. (2015) with a slight modifications. Before extraction, non-collagen proteins were removed by treating the scales with 0.1 M NaOH at the scale/solution ratio of 1:10 (w/v) for 8 h. The process was carried out with continuous stirring using an overhead stirrer model W20.n (IKA®-Werke GmbH & CO.KG, Stanfen, Germany) and the alkaline solution was changed after 4 h. Thereafter, the scales were thoroughly washed using chilled water until the wash water had the neutral pH. Subsequently, these scales were demineralized with 0.5 M EDTA-2Na salt solution (pH 7.4) at the ratio of 1:10 (w/v) for about 48 h under stirring condition. EDTA solution was changed after 24 h. Finally, the demineralized scales were washed with cold water until pH of wash water turned to be neutral.

The demineralized scales were subjected to ASC extraction with 0.5 M acetic acid using the scale/acid solution ratio of 1:15 (w/v). The extraction process was continued for 48 h with continuous stirring. Thereafter, the mixture was filtered with two-layered cheesecloth. The collagen in the filtrate was precipitated by salting out. To

the filtrate, 0.05 M tris (hydroxymethyl) aminomethane (pH 7.0) was added, and NaCl was added slowly to obtain the final concentration of 2.5 M. The precipitate was collected by centrifugation at 15,000 ×g at 4 °C for 1 h using a refrigerated centrifuge model CR 22GIII (Hitachi, Tokyo, Japan). The collected pellet was dissolved in the minimal volume of 0.5 M acetic acid and subsequently dialyzed in 20 volumes of 0.1 M acetic acid for about 48 h, followed by 20 volumes of distilled water for another 72 h. Collagen was freeze-dried using a freeze-dryer (CoolSafe 55, ScanLaf A/S, Lynge, Denmark). The matter termed 'acid soluble collagen; ASC' was analyzed.

3.4.2.3. Extraction of pepsin soluble collagen (PSC)

PSC was extracted from the undissolved residue obtained after acid soluble collagen extraction. To the residue, 0.5 M acetic acid consisting of 1% pepsin was added (w/w) at a residue/solution ratio of 1:10 (w/v). The extraction was performed with the aid of continuous stirring for 24 h at 4 °C. After extraction, the collagen was filtered and precipitated in the same manner. Dialysis and lyophilisation were carried out as previously described. The obtained collagen referred to as 'pepsin soluble collagen, PSC' was subjected to analysis.

3.4.3. Analysis

Both ASC and PSC were calculated for yield and further analyzed.

3.4.3.1. Yield

The yield of ASC and PSC was calculated based on dry weight of starting material.

$$\text{Yield (\%)} = \frac{\text{Weight of freeze} - \text{dried collagen (g)}}{\text{Weight of initial dry scales (g)}} \times 100$$

3.4.3.2. Protein patterns (*section 2.4.3.2*)

3.4.3.3. Amino acid composition (*section 2.4.3.3*)

3.4.3.4. Fourier transform infrared spectroscopy (FTIR) spectroscopy (*section 2.4.3.4*)

3.4.3.5. Circular dichroism (CD) spectroscopy (*section 2.4.3.5*)

3.4.3.6. Zeta potential (*section 2.4.3.6*)

3.4.3.7. Differential scanning calorimetry (DSC) (*section 2.4.3.7*)

3.4.3.8. Solubility

Solubility of ASC and PSC at different pH was determined as mention in section *2.4.3.8*. The effect of NaCl at different final concentrations (0, 10, 20, 30, 40, 50 and 60 g l^{-1}) on solubility of collagen solution (3 mg ml^{-1}) was also examined. After the aliquots were prepared for both pH and salt solubility tests, the mixtures were stirred for 1 h at 4 °C and centrifuged at 8500 ×g for 20 min. The obtained supernatant was analyzed for protein content by the Lowry method (Lowry et al., 1951) using bovine serum albumin as a standard.

3.4.4. Statistical Analysis

Optimization of extraction was analyzed using CCD as mentioned above. All experiments were run in triplicate. Data were subjected to analysis of variance. Comparison of means was carried out by the Duncan's multiple range tests (Steel and Torrie, 1980). T-test was used for pair comparison. Analysis was performed using a SPSS package (SPSS 22 for Windows, SPSS Inc., Chicago, IL, USA).

3.5. Results and discussion

3.5.1. Yield of ASC and PSC

The yield of ASC from scales of golden carp was 0.42 g 100 g^{-1} (dry weight basis), which was slightly high than that reported for ASC from seabass scales

(0.38 g 100 g^{-1}) (Chuaychan et al., 2015) but was slightly lower than that of ASC extracted from golden goatfish scales (0.46 g 100 g^{-1}) (Matmaroh et al., 2011). Relatively high yield (about 5 g 100 g^{-1}) was reported for ASC from rohu scales (Pati et al., 2010). Accordingly, the difference in yield of ASC depends on the type of fish, age and structure of collagen in scale matrix, etc (Duan et al., 2009). PSC generally had higher yield (1.16 g 100 g^{-1}), compared to ASC. The yield was increased up to 3.8 folds when pepsin was used as the extraction aid. Pepsin was able to cleave specifically at the telopeptide region of collagen (Nalinanon et al., 2007) and the collagen was released at molecules in a significant amount. This result indicated that pepsin had the efficiency in increasing the yield of collagen extracted from the scales of golden carp.

3.5.2. Protein patterns

The protein patterns of ASC and PSC from golden carp scales analyzed by SDS–PAGE under non-reducing condition are depicted in Figure 1. α-chain and β-chain were found as the dominant components in both ASC and PSC. α_1 and α_2 chains of ASC had MW of 117 and 108 kDa, respectively. For PSC, both α_1 and α_2 chains showed slightly lower MW (114 and 106 kDa, respectively), compared to those of ASC. The obtained results were in agreement with Nalinanon et al. (2010) who found that α_1 and α_2 chains of PSC from the skin of arabesque greenling had marginally lower MW than those of ASC. Pepsin is able to cleave the peptides restricted at the telopeptide region. As a result, some part of the peptide was removed, thereby shortening the chain. It was noted that ratio of α_1/α_2 chain was 2:1, suggesting that both ASC and PSC belonged to type I. ASC from scales of different species including seabass (Chuaychan et al., 2015), snakehead fish (Liu et al., 2008), rohu and catla (Pati et al., 2010) were classified as type I collagen. Furthermore, β-chain and γ-chain representing dimer and trimer, respectively, were also observed in both ASC and PSC. The result indicated that collagen from scales contained high MW cross-links. The band intensity of γ-chain in both ASC and PSC were similar, but the band intensity of β-chain and α-chain of PSC was more intense than that found in ASC (Nalinanon et al., 2007). This could suggest that pepsin is more likely cleave the telopeptide region, in which α- and β-chains were more released as evidenced by the increased band intensity of both chains in PSC. Moreover, there were no low MW proteins in both ASC and PSC. This indicated that

no degradation took place and there was negligible contamination of non-collagenous proteins in both collagens.

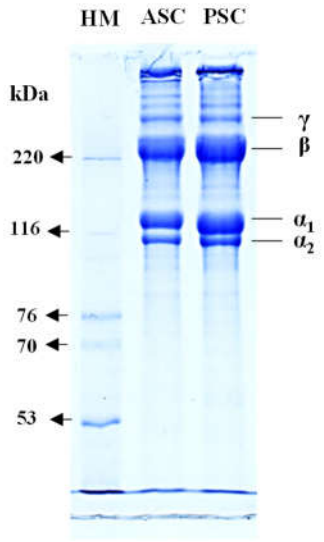

Figure 13. SDS–PAGE patterns of acid soluble collagen (ASC) and pepsin soluble collagen (PSC) from scales of golden carp. HM: high molecular weight marker.

3.5.3. Amino acid compositions

Amino acid compositions of both ASC and PSC from the scales of golden carp are expressed as residues per 1000 amino acid residues as shown in Table 1. For both ASC and PSC, glycine constituted approximately one-third of total amino acids (330–333 residues (1000 residues)$^{-1}$). The presence of glycine in α-chain at every third position shows a major role in sinking the steric interference and providing an inter-chain hydrogen-bond perpendicular to the helix axis of collagen (Fontaine-Vive et al., 2009). No cysteine was present in both collagens. This confirmed that there were no disulfide bonds in the collagen. Imino acid (proline and hydroxyproline) content in ASC (197 residues (1000 residues)$^{-1}$) was slightly lower than that of PSC (202 residues (1000 residues)$^{-1}$). The removal of telopeptide caused by pepsin more likely affected imino acids of collagen to some degree. The imino acid contents of collagen form golden carp scales were higher than those of seabass (193 and 195 residues (1000 residues)$^{-1}$) (Chuaychan et al., 2015), bighead carp scale collagen (156 residues (1000 residues)$^{-1}$) (Liu et al., 2012) and carp scale collagen (192 residues (1000 residues)$^{-1}$) (Duan et al., 2009).

Table 5. Amino acid composition of acid soluble collagen (ASC) and pepsin soluble collagen (PSC) from the scales of golden carp.

Amino acids	(Residues (1000 residues)$^{-1}$)	
	ASC	PSC
Alanine	120	115
Arginine	52	49
Aspartic acid/asparagine	48	45
Cysteine	0	0
Glutamine/glutamic acid	69	69
Glycine	330	333
Histidine	4	6
Isoleucine	12	13
Leucine	23	23
Lysine	26	25
Hydroxylysine	7	8
Methionine	12	11
Phenylalanine	14	13
Hydroxyproline	80	86
Proline	118	116
Serine	36	36
Threonine	24	25
Tyrosine	4	4
Valine	22	22
Imino acid	197	202

In general, imino acids contribute to the thermal stability of collagens (Liu et al., 2012). Hydroxyproline and proline are strengthening units in triple helix via hydrogen bonds (Li et al., 2008). Alanine (115-120 residues (1000 residues)$^{-1}$), arginine (49-52 residues (1000 residues)$^{-1}$), asparagine/asparatic acid (45-48 residues (1000 residues)$^{-1}$), and glutamine/glutamic acid (69 residues (1000 residues)$^{-1}$) were present at high amount. However, tyrosine (4 residues (1000 residues)$^{-1}$) and histidine (4-13 residues (1000 residues)$^{-1}$) were found at very low amount in both ASC and PSC. The lysine contents in ASC and PSC were 26 and 25 residues (1000 residues)$^{-1}$, respectively. Hydroxylysine was present at small amounts (7-8 residues (1000 residues)$^{-1}$). Lysine and hydroxylysine in the telopeptide region have been known to involve in cross-linkage of collagen (Knott and Bailey, 1998). Thus, slight differences in amino acid

composition between ASC and PSC might be owing to the removal of some portions of telopeptides induced by pepsin (Matmaroh et al., 2011).

3.5.4. FTIR spectra

FTIR spectra of ASC and PSC depicted in Figure 2 confirmed the characteristic peaks for amide I, II, III as well as amide A and B. In general, amide I, II, and III bands are known to be responsible for the degree of molecular order found in collagen, and to be involved in the formation of its triple helical structure, which results from C=O stretching, and N-H bending and C-N stretching, respectively (Chen et al., 2016). Amide I characteristic wavenumber ranging from 1600 to 1700 cm^{-1}, is mainly associated with backbone C=O stretching vibrational (Payne and Veis, 1988). The absorption peaks for ASC and PSC were found at 1637 and 1631 cm^{-1}, respectively. The formation of hydrogen bond between N-H stretch (X position) and C=O (Gly) of the fourth residue is responsible for introducing triple helix (Zanaboni et al., 2000). The higher wavenumber observed in ASC suggested that the removal of telopeptide could lower the C=O of PSC. Amide II-bond is responsible for the combination of N-H in-plane bend and the C-N stretching vibration (Barth and Zscherp, 2002). Amide II wavenumber of ASC and PSC were at 1548 and 1540 cm^{-1}, respectively. Amide II bands of PSC also showed the lower wavenumber as compared to that of ASC. This suggested that there is more proportion of hydrogen bonds present in PSC due to the removal of amorphous telopeptide. This result confirmed that pepsin was able to cleave non-helical portion of telopeptide regions, leading to the increased molecular integrity of collagen structure. Furthermore, amide III is related with intermolecular interactions in collagen, consisting of components from C-N stretching and N-H in plane bending of amide linkages. Amide III bands for ASC and PSC were found at similar wavenumbers of (1237 and 1236 cm^{-1}). The absorption band pattern of amide III was also arising from wagging vibrations from CH_2 groups from the glycine backbone and proline side-chains (Guzzi Plepis et al., 1996).

Amide A bands of ASC and PSC were found at wavenumbers of 3295 and 3292 cm^{-1}, respectively. These bands are associated with N-H stretching vibration. However, a free N-H stretching vibration occurs in the range of 3400–3440 cm^{-1}. When

the NH group of a peptide is involved in a hydrogen bond, the position is shifted to a lower frequency (Fontaine-Vive et al., 2009). This result indicated that N-H was involved in H-bond stabilizing helical structure. The amide B peaks of ASC and PSC were found at 2920 and 2924 cm^{-1}, respectively. The amide B bands are associated with an asymmetrical stretch of CH_2 (Abe and Krimm, 1972). A distinct absorption peaks around 1451–1450 cm^{-1} were also observed in PSC and ASC. This peak corresponds to pyrrolidine ring vibration of proline and hydroxyproline as described by Matmaroh et al. (2011). The ratio of peaks between amide III and 1454 cm^{-1} band was 0.98 and 0.99 for both ASC and PSC, respectively. The absorption ratio of approximately 1.0 indicates the presence of triple-helical structure (Benjakul et al., 2010). The results indicated that both ASC and PSC were most likely in the native triple helical structure.

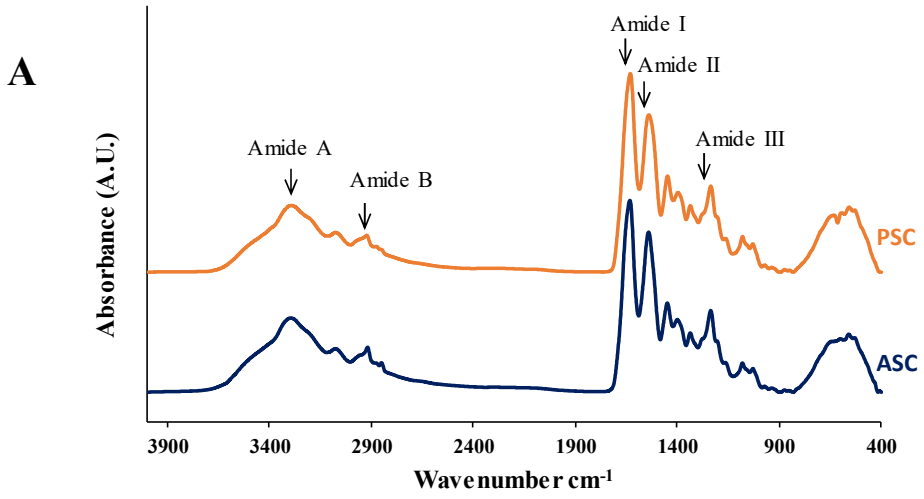

Figure 14. Fourier transform infrared spectra of acid soluble collagen (ASC) and pepsin soluble collagen (PSC) from scales of golden carp.

3.5.5. CD spectroscopy

CD spectra of ASC and PSC from scales of golden carp are shown in Figure 3. The spectra were scanned in the range of 190-250 nm. The rotatory maxima of ASC and PSC were observed at 220.8 and 221 nm, respectively. The negative peak of both samples was found at 198 nm. Overall, ASC and PSC showed similar spectra having positive and negative peaks at 221 and 198 nm, which is a characteristic feature of triple helical conformation of the protein (Tifany and Krimm, 1972). CD spectra

represent the absorption region for peptide linkage and imitate the backbone configuration of protein. A slight difference in ellipticity between ASC and PSC suggested that there was some difference in the secondary conformation of both collagens, more likely due to telopeptide removal in PSC (Ogawa et al., 2004). On the other hand, the denatured collagen showed more distorted spectrum, as evidenced by the absence of positive peak at 221 nm. Additionally, the negative peak shifts to the lower absorption than 198 nm, (Tifany and Krimm, 1972). The results confirmed that ASC and PSC had high structural integrity without denaturation.

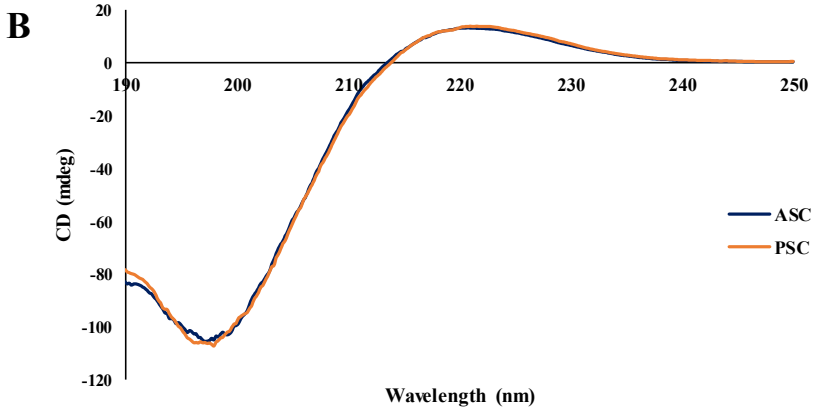

Figure 15. Circular dichroism spectra of acid soluble collagen (ASC) and pepsin soluble collagen (PSC) from scales of golden carp.

3.5.6. Zeta potential

Zeta potential of ASC and PSC from golden carp scales at pHs ranging from 2 to 12 is shown in Figure 4 with pH range of 2–6, both the collagen samples were positively charged, and the charge decreased continuously with increasing pHs. Zero surface net charge of ASC and PSC was observed at pH 6.04 and 6.22, respectively. These specific points were estimated to be their isoelectric points (pI), which were in acidic pH range. This might be contributed to the carboxylic group of acidic amino acids such as aspartic and glutamic acid, which were found at higher extent (Table 1). At pHs above the pI, both the samples had the shift in electric charge from positive to negative, and there was a further increase in negative charge as pH increased. The change in electric charge was governed by protonation and deprotonation of amino acids at different pHs as reported by Benjakul et al. (2010). Collagens from different

sources showed different pIs. ASC from striped catfish skin had pI at 4.72 (Singh et al., 2011), while ASC from seabass skin had higher pI (6.64) (Sinthusamran et al., 2013). The slight differences in pI between collagens might be due to the difference in their amino acid compositions and distribution of amino acid residues, particularly on the surface domains of the collagen molecule.

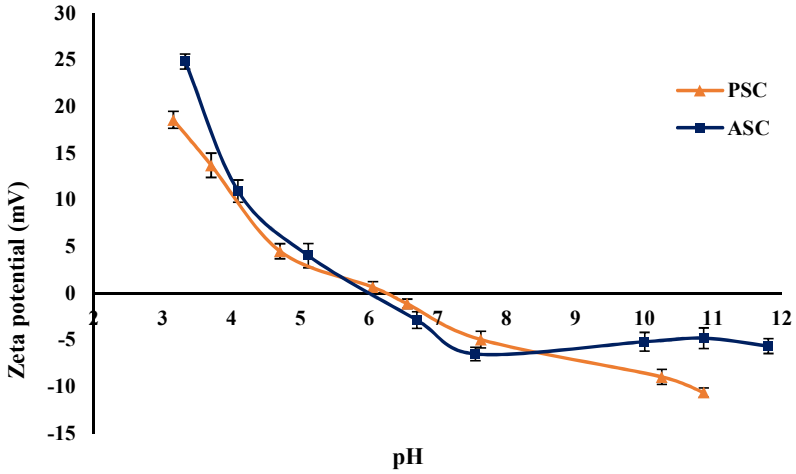

Figure 16. Zeta potential of acid soluble collagen (ASC) and pepsin soluble collagen (PSC) from scales of spotted golden carp at different pHs. Bars represent the standard deviation (n = 3).

3.5.7. Thermal transition

The thermograms of ASC and PSC from scales of golden carp are shown in Figure 5. T_{max} of ASC and PSC were 37.67 and 37.83 °C, respectively. Similar T_{max} values between ASC and PSC suggested the similar secondary structure of both samples. The thermal stability of collagen was directed by the pyrrolidine rings of proline and hydroxyproline and partially attributed to the hydrogen bonds of the hydroxyl group of hydroxyproline (Benjakul et al., 2010). It was noted that PSC had slightly higher ΔH values when compare to ASC. The removal of non-helical telopeptides possibly resulted in more ordered and compact structure of PSC. As a result, PSC needed higher energy for destabilization. This observation was also reflected by the higher content of imino acids, especially hydroxyproline content in PSC (Table 1). T_{max} values of ASC and PSC from golden carp scale, were lower than those of type I collagens from scales of spotted golden goatfish (41.58 °C) (Matmaroh

et al., 2011) and seabass scales (39.32 °C) (Chuaychan et al., 2015). Nevertheless, ASC and PSC from golden carp scales had higher T_{max} values when compared to PSC from the scale of bighead carp (35.2 °C) (Liu et al., 2012), ASC from scale of rohu and catla (36.5 °C) (Pati et al., 2010), and ASC and PSC from silver carp scales (29 °C) (Zhang et al., 2010). Generally, the collagens from fish living in cold environment have a lower content of hydroxyproline and therefore exhibit low thermal stability than those from fish living in warm environment (Muyonga et al., 2004). Varying denaturation temperatures depend on various factors, such as habitat temperature, seasons, fish species, age, etc. (Duan et al., 2009; Muyonga et al., 2004).

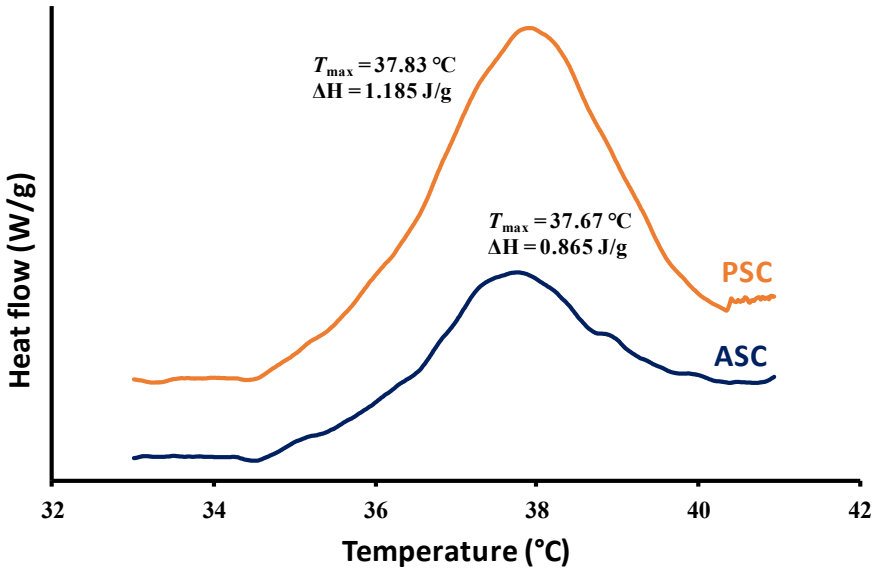

Figure 17. Differential scanning calorimeter thermogram of acid soluble collagen (ASC) and pepsin soluble collagen (PSC) from scales of golden carp.

3.5.8. Solubility test

3.5.8.1. Effect of pH

The solubility of ASC and PSC from scales of golden carp at different pHs is shown in Figure 6(A). pH had the marked effect on the relative solubility of both collagens. Both samples showed similar solubility pattern. Overall, both collagens were highly soluble within the pH range of 1–3. Similar results were reported for ASC and PSC from scales of snakehead and seabass (Chuaychan et al., 2015; Liu et al., 2012).

At pH higher than 3, there was a sharp decrease in solubility, and very low solubility was observed at pH 5 and 6. This reduction in solubility might be due to the hydrophobic interaction amongst the collagen molecules in a solution as described by Sinthusamran et al. (2013). Furthermore, there was a slight increase in solubility at alkaline pH. The repulsive force of collagen molecules mediated by the negatively charged domains at pH above pI of both collagens contributed to the slight increase in solubility. Slight difference in solubility pattern between ASC and PSC was probably governed by a difference in chain length, amino acid composition, molecular properties and conformation of both collagens (Kittiphattanabawon et al., 2005).

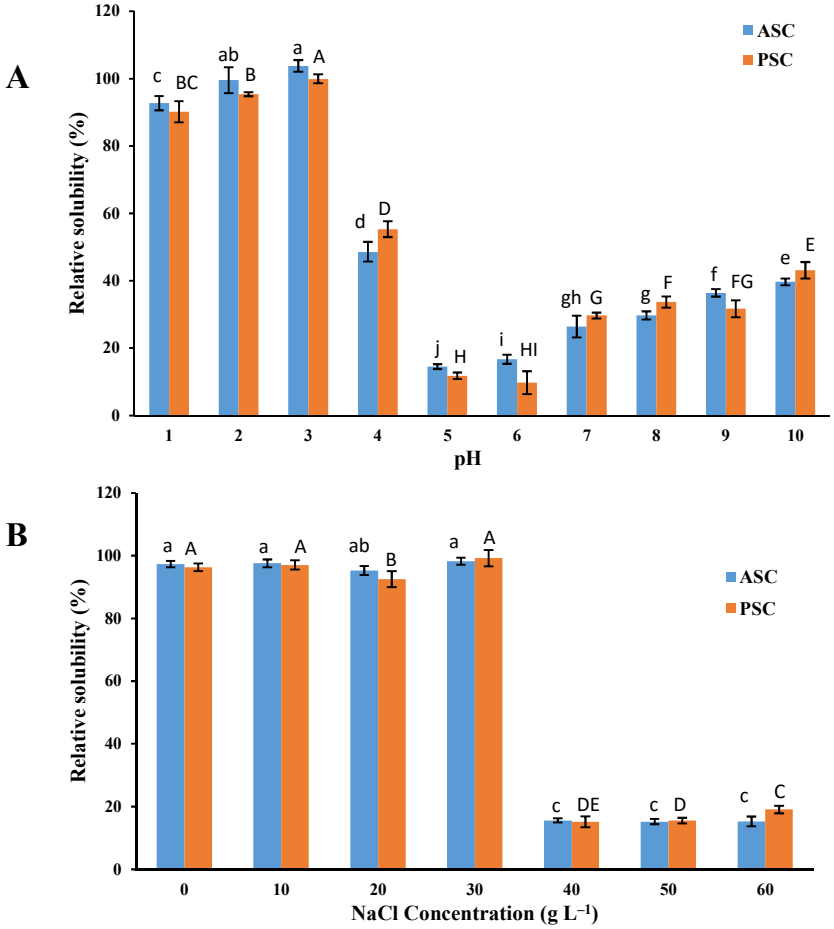

Figure 18. Relative solubility of acid soluble collagen (ASC) and pepsin soluble collagen (PSC) from scales of golden carp at different pHs (A) and NaCl concentrations, (B). Different lowercase or uppercase letters on the bars within the same sample indicate significance difference ($p < 0.05$).

3.5.8.2. Effect of NaCl

The effect of NaCl on solubility of ASC and PSC is shown in Figure 6(B). High solubility was observed in the presence of NaCl up to 30 g l^{-1} ($p < 0.05$). There was no difference in solubility between ASC and PSC ($p > 0.05$). At a lower concentration of NaCl, salt ions have weak interactions with the charge groups on proteins surface (Damodaran, 1996). Thus, low salt concentration did not have the effect on charge as well as solubility of collagen. Conversely, NaCl at high concentrations led to the sharp decrease in solubility of both ASC and PSC. This drastic decrease in solubility might be due to the salting out effect of collagen (Bae et al., 2008). At high salt concentration, hydrophobic interaction between proteins chains was enhanced. Simultaneously, the water was bound with salt to a higher extent. This resulted in precipitation of collagen (Damodaran, 1996).

3.6. Conclusion

ASC and PSC extracted from scales of golden carp were characterised as type I collagen. The aid of pepsin helped in increasing the yield of collagen up to 3.8 folds. Based on FTIR, CD and SDS-PAGE analyses, ASC and PSC were in triple helical structure. There was a slight difference in amino acid composition as well as enthalpy for thermal transition between ASC and PSC, mainly caused by the removal of telopeptide by pepsin. Thus, collagen from scales of golden carp could serve as an alternative to mammalian counterpart, in which the limitation of the latter associated with religious constraint and safety can be conquered.

3.7. References

Abe, Y. and S. Krimm, 1972. Normal vibrations of crystalline polyglycine I. Biopolymers: Original Research on Biomolecules. 11: 1817–1839.

AOAC. 2000. Official methods of analysis. 17th ed. Association of Official Ananlytical Chemists. Arlington, VA.

Bae, I., K. Osatomi, A. Yoshida, K. Osako, A. Yamaguchi and K. Hara. 2008. Biochemical properties of acid-soluble collagens extracted from the skins of underutilised fishes. Food Chemistry. 108: 49–54.

Barth, A. and C. Zscherp. 2002. What vibrations tell about proteins. Quarterly Reviews of Biophysics. 35: 369–430.

Benjakul, S., Y. Thiansilakul, W. Visessanguan, S. Roytrakul, H. Kishimura, T. Prodpran and J. Meesane. 2010. Extraction and characterisation of pepsin-solubilised collagens from the skin of bigeye snapper (*Priacanthus tayenus* and *Priacanthus macracanthus*). Journal of the Science of Food and Agriculture. 90: 132–138.

Bergman, I. and R. Loxley. 1963. Two improved and simplified methods for the spectrophotometric determination of hydroxyproline. Analytical Chemistry. 35: 1961–1965.

Chen, J., L. Li, R. Yi, N. Xu, R. Gao and B. Hong. 2016. Extraction and characterization of acid-soluble collagen from scales and skin of tilapia (*Oreochromis niloticus*). LWT- Food Science and Technology. 66: 453–459.

Chuaychan, S., S. Benjakul and H. Kishimura. 2015. Characteristics of acid- and pepsin-soluble collagens from scale of seabass (*Lates calcarifer*). LWT- Food Science and Technology. 63: 71–76.

Damodaran, S. 1996. Amino acids, peptides, and proteins, in: O. R. Fennema, editors. Food chemistry. Marcel Dekker, Inc., N. Y., pp. 321–429.

Duan, R., J. Zhang, X. Du, X. Yao and K. Konno. 2009. Properties of collagen from skin, scale and bone of carp (*Cyprinus carpio*). Food Chemistry. 112: 702–706.

FAO (2016) Fishery and aquaculture statistics 2014. Food and Agricultural Organization of the United Nation, Rome, pp 189–194.

Fontaine-Vive, F., F. Merzel, M. R. Johnson and G. J. Kearley. 2009. Collagen and component polypeptides: Low frequency and amide vibrations. Chemical Physics. 355: 141–148.

Gornall, A. G., Bardawill, C. J. and David, M. M. 1949. Determination of Serum proteins by means of the Biuret reaction. The Journal of Biological Chemistry. 177: 751–766.

Guzzi Plepis, A. M. D., G. Goissis, and D. K. Das-Gupta. 1996. Dielectric and pyroelectric characterization of anionic and native collagen. Polymer Engineering and Science. 36: 2932–2938.

Jongjareonrak, A., S. Benjakul, W. Visessanguan, T. Nagai and M. Tanaka. 2005. Isolation and characterisation of acid and pepsin-solubilised collagens from the skin of brownstripe red snapper (*Lutjanus vitta*). Food Chemistry. 93: 475–484.

Kielty, C. M., I. Hoplinson and M. E. Grant. 1993. Part I: connective tissue and its heritable disorders, in: Royce, P. M. and B. Steinmann, editors. Wiley-Interscience, N. Y., pp. 103–147.

Kittiphattanabawon, P., S. Benjakul, W. Visessanguan, T. Nagai and M. Tanaka. 2005. Characterisation of acid-soluble collagen from skin and bone of bigeye snapper (*Priacanthus tayenus*). Food Chemistry. 89: 363–372.

Knott, L. and A. J. Bailey. 1998. Collagen cross-links in mineralizing tissues: A review of their chemistry, function, and clinical relevance. Bone 22: 181–187.

Laemmli, U.K. 1970. Cleavage of structural proteins during the assembly of the head of bacteriophage T4. Nature. 227: 680–685.

Li, C., Z. Zhong, Q. Wan, H. Zhao, H. Gu and S. Xiong. 2008. Preparation and thermal stability of collagen from scales of grass carp (*Ctenopharyngodon idellus*). European Food Research and Technology. 227: 1467–1473.

Liu, D., L. Liang, J. M. Regenstein and P. Zhou. 2012. Extraction and characterisation of pepsin-solubilised collagen from fins, scales, skins, bones and swim bladders of bighead carp (*Hypophthalmichthys nobilis*). Food Chemistry. 133: 1441–1448.

Liu, W.T., Y. Zhang, G. Y. Li, Y. Q. Miao and X. H. Wu. 2008. Structure and composition of teleost scales from snakehead *Channa argus* (Cantor) (Perciformes: Channidae). Journal of Fish Biology. 72: 1055–1067.

Lowry, O.H., N. J. Rosebrough, A. L. Farr and R. J. Randall. 1951. Protein measurement with the folin phenol reagent. Journal of Biological Chemistry. 193: 265–275.

Matmaroh, K., S. Benjakul, T. Prodpran, A. B. Encarnacion and H. Kishimura. 2011. Characteristics of acid soluble collagen and pepsin soluble collagen from scale of spotted golden goatfish (*Parupeneus heptacanthus*). Food Chemistry. 129: 1179–1186.

Muyonga, J.H., C. G. B. Cole and K. G. Duodu. 2004. Characterisation of acid soluble collagen from skins of young and adult Nile perch (*Lates niloticus*). Food Chemistry. 85: 81–89.

Nagarajan, M., S. Benjakul, T. Prodpran, P. Songtipya and H. Kishimura. 2012. Characteristics and functional properties of gelatin from splendid squid (*Loligo formosana*) skin as affected by extraction temperatures. Food Hydrocolloids. 29: 389–397.

Nalinanon, S., S. Benjakul and H. Kishimura. 2010. Collagens from the skin of arabesque greenling (*Pleurogrammus azonus*) solubilized with the aid of acetic acid and pepsin from albacore tuna (*Thunnus alalunga*) stomach. Journal of the Science of Food and Agriculture. 90: 1492–1500.

Nalinanon, S., S. Benjakul, W. Visessanguan and H. Kishimura. 2007. Use of pepsin for collagen extraction from the skin of bigeye snapper (*Priacanthus tayenus*). Food Chemistry. 104: 593–601.

Ogawa, M., R. J. Portier, M. W. Moody, J. Bell, M. A. Schexnayder and J. N. Losso. 2004. Biochemical properties of bone and scale collagens isolated from the subtropical fish black drum (*Pogonia cromis*) and sheepshead seabream (*Archosargus probatocephalus*). Food Chemistry. 88: 495–501.

Pati, F., B. Adhikari and S. Dhara. 2010. Isolation and characterization of fish scale collagen of higher thermal stability. Bioresource Technology. 101: 3737–3742.

Payne, K.J. and A. Veis. 1988. Fourier transform ir spectroscopy of collagen and gelatin solutions: Deconvolution of the amide I band for conformational studies. Biopolymers. 27: 1749–1760.

Rizk, M.A. and N. Y. Mostafa. 2016. Extraction and characterization of collagen from buffalo skin for biomedical applications. Oriental Journal of Chemistry. 32: 1601–1609.

Singh, P., S. Benjakul, S. Maqsood and H. Kishimura. 2011. Isolation and characterisation of collagen extracted from the skin of striped catfish (*Pangasianodon hypophthalmus*). Food Chemistry. 124: 97–105.

Sinthusamran, S., S. Benjakul and H. Kishimura. 2013. Comparative study on molecular characteristics of acid soluble collagens from skin and swim bladder of seabass (*Lates calcarifer*). Food Chemistry. 138: 2435–2441.

Tifany, M. L. and S. Krimm. 1972. Effect of temperature on the circular dichroism spectra of polypeptides in the extended state. Biopolymers. 11: 2309–2316.

Zall, R. R. 2004. Unconventional techniques to deal with waste recovery or treatment schemes, in: Zall, R.R., editors. Managing food industry waste. Blackwell Publishing, Iowa, pp. 105–113.

Zanaboni, G., A. Rossi, A. M. T. Onana and R. Tenni. 2000. Stability and networks of hydrogen bonds of the collagen triple helical structure: influence of pH and chaotropic nature of three anions. Matrix Biology. 19: 511–520.

Zhang, J., R. Duan, C. Ye and K. Konno. 2010. Isolation and characterization of collagens from scale of silver carp (*hypophthalmichthys Molitrix*). Journal of Food Biochemistry. 34: 1343–1354.

CHAPTER 4

EXTRACTION EFFICIENCY AND CHARACTERISTICS OF ACID AND PEPSIN SOLUBLE COLLAGENS FROM THE SKIN OF GOLDEN CARP (*PROBARBUS JULLIENI*) AS AFFECTED BY ULTRASONICATION

4.1. Abstract

Extraction efficiency and physiochemical properties of acid and pepsin soluble collagens from the skin of golden carp (*Probarbus jullieni*) as influenced by ultrasonication were studied. The ultrasound treatment (20 kHz) with increasing amplitudes from 20 to 80% increased the yield of acid soluble collagen (ASC) ($p < 0.05$). When the ultrasound at an amplitude of 80% was employed in combination with pepsin (0.1. 0.5 and 1%), the marked increase in pepsin soluble collagen (PSC) was obtained when pepsin level increased ($p < 0.05$). The yield of ASC and PSC increased as ultrasonication time increased ($p < 0.05$). ASC and PSC with the ultrasound aided process, named as UASC and UPSC, had the yields of 81.53 and 94.88%, while ASC and PSC prepared with typical method showed the yields of 51.90 and 79.27%, respectively. All the collagens, with similar amino acid composition, contained α- and β-chains and were type I. Based on circular dichroism (CD) and fourier transform infrared spectroscopy (FTIR), all the collagens had the triple helical structure. T_{max} of PSC and UPSC were higher than those of ASC and UASC. Overall, ultrasound treatment under appropriate condition effectively improved the extraction efficiency of ASC and PSC without affecting their physiochemical properties.

4.2. Introduction

Collagen is a major structural protein of animal origin and constitutes about 30% of total protein. There are at least 27 types of collagens with different structure and molecular properties (Benjakul *et al.*, 2010). Amongst all the collagens, type I collagen is most widely found in fish and some mammals. Type I collagen is

triple helical in a structure, which is stabilized by interchain hydrogen bonds between glycine and amide groups in the polypeptide chains (Shoulders and Raines, 2009). Due to wide acceptability and safety concern, collagen from fish sources is receiving greater interest in a broad range of applications (Schmidt *et al.*, 2016). Collagen, primarily type I is widely used in food and nutraceutical industries (Lafarga and Hayes, 2014). For pharmaceutical and biomedical uses, collagen is used as a substitute for blood vessels, human skin, wound dressing, a vehicle for drugs, etc. (Kim and Mendis, 2006; Yuan *et al.*, 2015).

Collagen in its native form is insoluble and successive pretreatment makes it suitable for extraction (Benjakul *et al.*, 2010; Nalinanon *et al.*, 2007). Generally, the important sources of commercial collagen are from porcine and bovine origins (Liu *et al.*, 2007). However, due to environmental management and economic valorization of industrial waste, especially from fish processing industry, there has been increasing interest in collagen from various aquatic sources (Schmidt *et al.*, 2016). Traditionally, collagen is extracted in an acidic solution such as 0.5 M acetic acid (Benjakul *et al.*, 2010). Acid soluble collagen (ASC) is generally of lower yield. To tackle the problem, pepsin has been employed to increase the extraction yield, while the triple helical structure of pepsin soluble collagen remained substantially unaffected (Ali *et al.*, 2017a). However, these typical extraction methods are time consuming and a significant amount of insoluble collagen is still retained.

In recent years, high-intensity ultrasound (20 kHz) has been widely studied to accelerate the mass transfer, in which mixing, drying, homogenization and extraction can be improved (Pingret *et al.*, 2013). The mechanism of ultrasound in a liquid system is mainly due to the cavitation process (Schmidt *et al.*, 2016). When the waves generate regions of high and low pressure, this attributes to quick formation and collapse of cavitation bubbles (Pingret *et al.*, 2013). Ultrasound has been used to improve the availability and functional properties of proteins from soy, milk, eggs and poultry (Zou *et al.*, 2017). Presently, ultrasound assisted extraction (UAE) has been introduced for recovery of biomolecules from different sources (Vilkhu *et al.*, 2008). Generally, ultrasonication has been successfully used to improve the extraction efficiency of phenolic compounds, oils and some organic acids from various plant

sources (Hashemi *et al.*, 2017; Pingret *et al.*, 2013; Shirsath *et al.*, 2012). Moreover, a few reports on the extraction yield of ultrasound assisted acid soluble collagen exist (Kim *et al.*, 2012; Zou *et al.*, 2017). However, no scientific information on the extraction of collagen using ultrasonication in conjunction with pepsin treatment exists. Additionally, the molecular properties of collagen, especially pepsin soluble collagen from fish skin as affected by ultrasound assisted extraction has not been reported.

Golden carp is a freshwater fish, commonly found in Southeast Asian river basins and are primarily aquacultured in Thailand and Lao. Based on the FAO statistics, aquaculture production of golden carp is growing at an annual rate of 3.86% globally (FAO, 2016), as an outcome of an increase in demand of freshwater fish consumption. During processing, a considerable amount of by-products (60-70%) is generated. Those are commonly considered to be a low market value feedstock or discarded as waste. Golden carp skin alone constitutes around 4-5% of body weight. Due to the abundance and availability, its skin can be used for extraction of value added product, especially collagen. To enhance the extraction efficiency of collagen associated with high yield, the application of pepsin for cleavage of telopeptide region prior to ultrasonication under appropriate condition could be a promising means.

4.3. Objective

To increase the extraction yield and to study the molecular properties of collagen prepared using ultrasound pretreatment, particularly in conjugation with pepsin treatment, from golden carp skin.

4.4. Materials and methods

4.4.1. Chemicals and enzyme

Acetic acid and sodium hydroxide were obtained from Merck (Darmstadt, Germany). Porcine pepsin (EC3.4.23.1) and protein molecular weight markers were procured from Sigma Chemicals (St. Louis, MO, USA). All chemicals for electrophoresis including sodium dodecyl sulphate (SDS), *N,N,N′,N′*-tetramethylethylenediamine (TEMED) and Coomassie Blue R-250 were obtained from

Bio-Rad Laboratories (Hercules, CA, USA). All chemicals used in this study were of analytical grade.

4.4.2. Collection and preparation of golden carp skin

Collection, transportation, preparation and storage of golden carp skin was carried out as described in the section *2.4.2.1*.

4.4.3. Extraction of collagen

4.4.3.1. Pretreatment of fish skin (*section 2.4.2.2*)

4.4.3.2. Conventional method

Conventional extraction process of acid soluble collagen (ASC) and pepsin soluble collagen (PSC) from golden carp skin were carried out as described in section *2.4.2.3* and *2.4.2.4*. All operations were performed at 4 ºC to avoid the denaturation of collagens.

4.4.3.3. Ultrasound assisted methods

Skin (100 g) was soaked in 0.5 M acetic acid with a skin/acid solution ratio of 1:15 (w/v). The skin was allowed to swell partially by holding the mixture for 30 min at 4 ºC. The mixture was subjected to ultrasonication using an ultrasound reactor model Vibra–Cell (Sonics & Material, Inc, Newtown, CT, USA) with a flat tip probe of 25 mm diameter. The reaction was carried out at a power of 750 W, working at a single frequency of 20 kHz. The temperature of the sample was maintained at 4 ºC using an ice bath. Temperature was monitored using a digital thermometer (model DE-3004 Type K, DER EE Electrical Instruments Co., Ltd., Chung Ho, Taipei, Taiwan). To avoid overheating, the ultrasound was operated in a pulse mode at 5 sec acting and 5 sec resting time. The treatment was conducted at different levels of amplitude (20, 50 and 80%) for various times (10, 20, 30 min). After the treatment, further extraction was carried out for 48 h by continuous stirring. Collagen was precipitated, dialyzed and freeze-dried as mentioned above. The obtained collagen was termed as ‘UASC’.

For PSC, skin (100 g) was suspended in 0.5 M acetic acid solution with a skin/acid solution ratio of 1/15 (w/v). The mixture was added with pepsin at various levels (0.1, 0.5 and 1%). The skin was allowed to partially swell as stated above and subjected to ultrasonication at 80% amplitude for 30 min using the pulse mode as described previously. Further extraction was done and PSC was collected, dialyzed and dried. The obtained matter was referred to as 'UPSC'.

4.4.3.4. Determination of extraction yield

Extraction yield was determined by estimating the content of hydroxyproline released into the extract. Hydroxyproline content was determined every 6 h up to 48 h of extraction.

Hydroxyproline content was determined as described by Bergman and Loxley (1963). Sample (500 µL) was firstly hydrolyzed in 6 M hydrochloric acid at 110 ºC in an oil bath (model B-490, BUCHI, Flawil, Switzerland) for 24 h and the hydrolysate was clarified using activated charcoal. The hydrolysate was filtered using a Whatman filter paper No. 4 and then neutralised with 3 M NaOH. The reaction was initiated by adding 0.2 ml of isopropanol to 0.1 ml of sample and 0.1 ml of oxidant solution. Finally, 1.3 ml of Ehrlich's reagent was added. The mixture was mixed well and incubated at 60 ºC for 25 min. The reaction was cooled, and 5 ml of isopropanol was added before reading the absorbance at 558 nm. Hydroxyproline standard curve was constructed using hydroxyproline standard ranging from 10 to 60 ppm. Hydroxyproline content was calculated. Collagen was then calculated from hydroxyproline content by using a factor of 7.7 (Nalinanon *et al.*, 2007). The extraction yield was expressed as mg collagen g^{-1} dry skin.

4.4.4. Characterization of selected collagens

ASC and PSC were subjected to characterization. UASC extracted with the aid of ultrasound at 80% amplitude for 30 min and UPSC extracted with the aid of 1% pepsin in combination with ultrasound (80% amplitude for 30 min) were also characterized. Both UASC and UPSC were extracted for 48 h.

4.4.4.1. Protein patterns (*section 2.4.3.2*)

4.4.4.2. Amino acid compositions (*section 2.4.3.3*)

4.4.4.3. Fourier transform infrared (FTIR) spectroscopy (*section 2.4.3.4*)

4.4.4.4. Differential scanning calorimetry (DSC) (*section 2.4.3.7*)

4.4.4.5. Circular dichroism (CD) spectroscopy (*section 2.4.3.5*)

4.4.4.6. Zeta potential (*section 2.4.3.6*)

4.4.5. Statistical analysis

Experiments were conducted in triplicates with completely randomized design (CRD). Analysis of variance (ANOVA) was performed and comparison of mean values was accomplished using Duncan's multiple range tests. SPSS 11.0 (SPSS Inc., Chicago, IL, USA) software was used for experimental analysis and the results were represented as means ± standard deviation.

4.5. Results and discussion

4.5.1. Extraction yield

The extraction yield of ASC as a function of ultrasound pretreatment (time and amplitude) and extraction time is shown in Figure 1. For the raw skin (without pretreatment), the hydroxyproline and collagen contents were 37.41 ± 1.23 and 288.06 ± 9.47 mg g^{-1} (dry weight basis), respectively. Overall, extraction yield increased as the extraction time increased for skin without and with ultrasound treatment. When comparing the extraction yield for ASC from the conventional method and those of ASC prepared by an ultrasound aided process, ASC from conventional extraction method demonstrated the lower yield at all the extraction time used. At the same amplitude of ultrasound used for pretreatment, the longer ultrasonication time rendered the higher yield ($p < 0.05$) at all extraction times used. At the same treatment time skin subjected to ultrasonication at higher amplitude showed the higher extraction yield ($p < 0.05$), when the same ultrasonication time was applied. Ultrasound at varying

amplitudes and times therefore affected the yield differently. The yield was noted to be proportional to amplitude and time for ultrasound treatment.

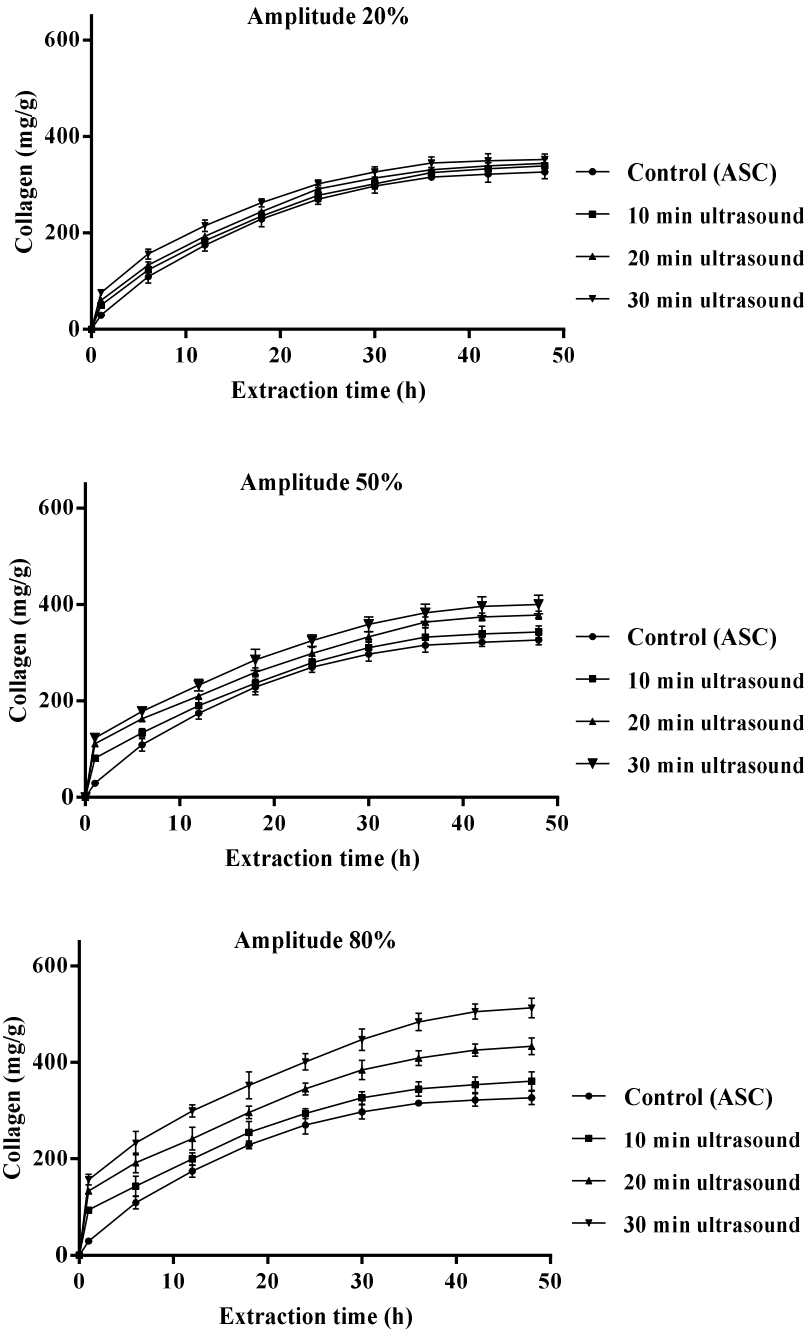

Figure 19. Extraction yield of acid soluble collagen from the skin of golden carp treated with ultrasound at various amplitude and time as a function of extraction time. Control: without ultrasound treatment. Bars represent the standard deviation (n=3).

The highest yield of UASC was obtained when ultrasound at amplitude 80% and time of 30 min was applied and the extraction time of 48 h was used. The yield in terms of collagen content of UASC was recorded as 512.65 ± 19.95 mg g^{-1} (based on the dry pretreated skin). Application of ultrasonication increased the yield of UASC up to 81.53%. The yield of UASC from the skin of golden carp was much higher than collagen extracted from soft-shelled turtle using ultrasound (16.3%) (Zou *et al.*, 2017), suggesting that ultrasonication was more effective for extraction of collagen from fish skin. Thus, ultrasound with cavitation effect more likely loosened the pretreated skin. As a consequence, acetic acid could penetrate through the skin more effectively and was able to extract collagen more potentially. Ultrasound has been employed for extraction of polyphenolic compounds, oil, carotenoids and chlorophylls and some organic acids from different sources (Pingret *et al.*, 2013; Shirsath *et al.*, 2012; Vilkhu *et al.*, 2008).

PSC from golden carp skin had the yield of 498.38 ± 16.88 mg g^{-1}, which was 79.27% higher than that of ASC when the extraction time of 48 h was used, as shown in Figure 2. It was also noted that there was a marginal difference between the yield of PSC, compared to that of UASC. For UPSC from golden carp skin, extraction yield was increased when skin was subjected to ultrasound ($p < 0.05$). It was shown that increasing pepsin concentrations could enhance the extraction efficiency of UPSC. In the presence of 1% pepsin, the yield was drastically increased in comparison with those of skin treated with a lower level of pepsin. Also, the extraction time was another prime factor determining the yield of collagen. With sufficient time, pepsin could hydrolyze telopeptide region to a greater extent, especially for ultrasound treated skin, in which the looser structure was attained. This was evidenced by a marked increase in extraction yield in the presence of pepsin at a higher level. The obtained results of UPSC was in agreement with collagen extracted from bovine tendon with the aid of ultrasound (Li *et al.*, 2009). Pepsin has been known to increase the extraction of collagen by cleavage of telopeptide region of tropocollagen (Nalinanon *et al.*, 2007). Ultrasound technology generates the mechanical effect, resulting in molecular motion of the solution (Pingret *et al.*, 2013). This combined effect facilitated the penetration of pepsin and simultaneously enhanced mass transfer from the matrix of skin. The results showed

that the use of ultrasound treatment in combination with pepsin at a sufficient amount effectively extracted collagen by increasing the yield and reducing the process time. UPSC prepared by treatment of skin using ultrasound at amplitude 80% for 30 min in conjugation with the use of pepsin at the level of 1% had the highest yield, which was 180% and 120% higher than that of ASC and PSC prepared by the conventional method with the extraction time of 48 h.

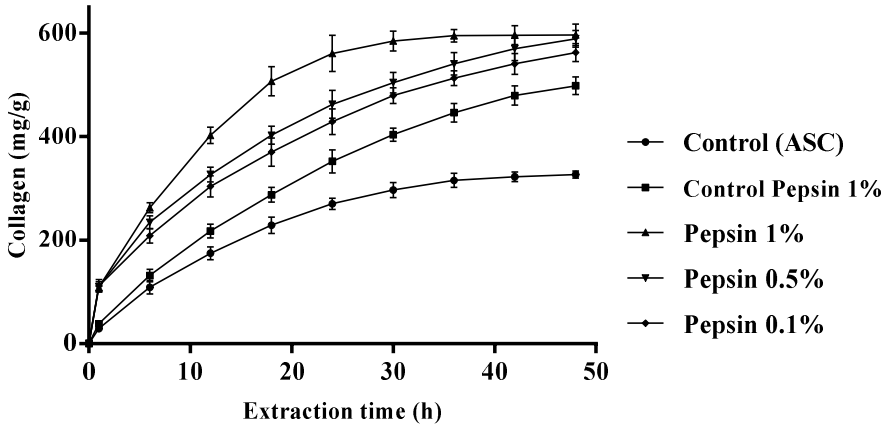

Figure 20. Extraction yield of pepsin soluble collagen from the skin of golden carp treated with ultrasound at 80% amplitude for 30 min in the presence of pepsin at different level as a function of extraction time. Control: without ultrasound treatment. Bars represent the standard deviation (n=3).

4.5.2. Protein patterns

Based on electrophoretic patterns of all collagens, they were composed of α_1- α_2- and β-chains, a dimer, as the major components (Figure 3). Since the α_1/α_2-chains ratio was about 2:1, they were classified as type I collagen (Benjakul *et al.*, 2010; Shoulders and Raines, 2009). The α_1 and α_2 bands of ASC and UASC (amplitude of 50 and 80% for 30 min) showed similar molecular weight (MW) of ~117 and ~108 kDa, respectively. The results demonstrated that ultrasonic treatment did not affect protein pattern of ASC and UASC, in terms of MW or intensity of each band. Kim, Kim, Kim, Park and Lee reported the degradation of α_1 and α_2 chains of ASC from seabass skin when the samples were subjected to ultrasonication for very long time (24 h) (Kim *et al.*, 2012). For PSC and UPSC (pepsin at 0.5 and 1%; with a fixed amplitude of 80%

and time for 30 min), they had the slightly lower MW of α_1- and α_2-chains. However higher intensities of α-chains were obtained, when compared to those of ASC or UASC. Pepsin was able to cleave telopeptide region to some extent, resulting in shortening of chain length (Ali *et al.*, 2017b). It was noted that UPSC prepared using 1% pepsin has a lower intensity of β-chain band when compared to UPSC with 0.5% pepsin or PSC from the conventional method. This might be due to the enhancement of pepsin activity by ultrasound treatment (Yu *et al.*, 2014), which potentially loosened skin matrix caused by cavitation effect (Zou *et al.*, 2017). For PSC and UPSC, the ratio of α_1/α_2-chains was also found to be 2:1. Moreover, β-chains (dimer) and γ-chains (trimer) in all collagens extracted were also present, suggesting that all the collagens have high molecular cross-linkages (Shoulders and Raines, 2009). Negligible low MW proteins were observed. The result indicated that no degradation took place and there was negligible contaminated non-collagenous protein in collagen, especially as induced by ultrasound treatment.

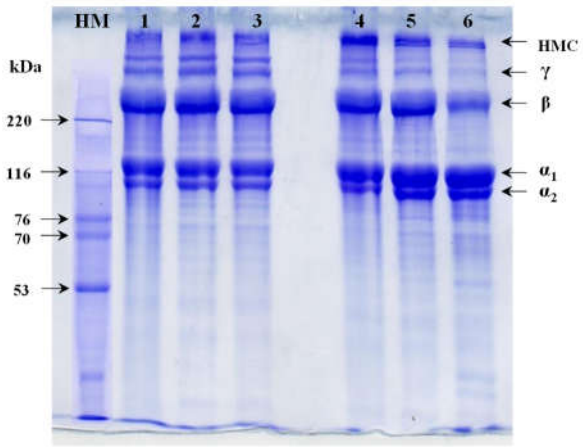

Figure 21. Protein patterns of acid and pepsin soluble collagens from the skin of golden carp under different extraction conditions. 1) acid soluble collagen (ASC). 2) and 3) acid soluble collagen with ultrasound assisted method (UASC) using the amplitude of 50 and 80%, respectively for 30 min. 4) pepsin soluble collagen (PSC). 5) and 6) pepsin soluble collagen extracted using 0.5 and 1% of pepsin with ultrasound assisted method (UPSC) at amplitude 80% for 30 min. HM: high molecular weight marker.

4.5.3. Amino acid compositions

Amino acid compositions of ASC and PSC prepared by the conventional method and UASC (using the amplitude of 80% for 30 min) and UPSC (using the amplitude of 80% for 30 min with 1% pepsin), expressed as residues (1000 residues)$^{-1}$ are shown in Table 1. All the collagens had glycine as the most abundant amino acid, accounting 325–336 residues (1000 residues)$^{-1}$. Glycine constitutes one-third of the total amino acid residues, excluding the first fourteen residues from N-terminal and the last ten residues from the C-terminal in a polypeptide chain (Shoulders and Raines, 2009). Glycine is mainly involved in formation of inter-chain hydrogen bonds, which stabilizes the α-chain (Zanaboni *et al.*, 2000). Both ASC and UASC, showed lower glycine residues (325–327 residues (1000 residues)$^{-1}$), compared to that of PSC and UPSC (332–336 residues (1000 residues)$^{-1}$). A similar effect was observed in imino acids (proline and hydroxyproline), where PSC and UPSC (197 and 202 residues (1000 residues)$^{-1}$, respectively) possessed a higher number of residues, compared to ASC and UASC (194 and 194 residues (1000 residues)$^{-1}$, respectively). Pyrrolidine ring of the imino acids has been known to strengthen the triple helix through interchain hydrogen bonding (Nalinanon *et al.*, 2007; Zanaboni *et al.*, 2000). This suggested that the use of ultrasonication in conjugation with pepsin slightly affected amino acid composition of collagen. Moreover, the imino acid contents of golden carp collagens were higher than those from big eye snapper and ocellate pufferfish (193 and 170 residues (1000 residues)$^{-1}$) (Zhang *et al.*, 2007), but lower than porcine dermis collagen (220 residue (1000 residues)$^{-1}$) (Ikoma *et al.*, 2003). Other amino acids including alanine (111–122 residues (1000 residues)$^{-1}$), glutamic acid/glutamine (68–72 residues (1000 residues)$^{-1}$), arginine (53 residues (1000 residues)$^{-1}$) and aspartic acid/asparagine (48–51 residues (1000 residues)$^{-1}$) were found at a high amount. On the other hand, histidine (4 residues/1000 residues) and tyrosine (3–4 residues (1000 residues)$^{-1}$) were present in very low amount in all the collagens. It was noted that lysine (25–28 residues (1000 residues)$^{-1}$) and hydroxylysine (5–7 residues (1000 residues)$^{-1}$) in both PSC or UPSC were lower than those of ASC and UASC. Since lysine and hydroxylysine are known to participate in cross-linkage at telopeptide region, partial elimination of telopeptide might result in some difference in these amino acids (Ali *et al.*, 2017b).

Table 6. Amino acid composition of acid and pepsin soluble collagens from skin of golden carp extracted with conventional method and ultrasound assisted extraction method.

Amino acids	(Residues (1000 residues)$^{-1}$)			
	ASC	**UASC**	**PSC**	**UPSC**
Alanine	111	121	122	120
Arginine	53	53	53	53
Aspartic acid/asparagine	51	50	48	49
Cysteine	0	0	0	0
Glutamine/glutamic acid	72	70	68	68
Glycine	327	325	336	332
Histidine	4	4	4	4
Isoleucine	13	12	11	10
Leucine	25	24	22	23
Lysine	28	27	26	25
Hydroxylysine	7	7	6	5
Methionine	12	12	12	12
Phenylalanine	14	14	13	13
Hydroxyproline	78	77	79	81
Proline	116	117	118	121
Serine	37	37	35	36
Threonine	25	24	23	23
Tyrosine	4	4	3	3
Valine	23	22	21	22
Total residues	1000	1000	1000	1000
Imino acid	194	194	197	202

ASC: acid soluble pepsin collagen extracted by conventional method

PSC: pepsin soluble collagen extracted by conventional method

UASC: acid soluble collagen extracted by ultrasound assisted method (amplitude 80% and time 30 min)

UPSC: pepsin soluble collagen extracted by ultrasound assisted method (pepsin 1%, amplitude 80% and time 30 min).

When comparing the amino acid composition of all the collagens, ultrasonic treatment under the condition used in the present study had no pronounced effect on the amino acid composition of resulting collagens.

4.5.4. FTIR spectra

FTIR spectra of ASC, PSC and the selected UASC and UPSC demonstrated the presence of characteristic peaks related to amide bands A, B, I, II and III (Figure 4). The FTIR spectra of collagens were similar to those of other fish skin collagens such as ASC from seabass and channel catfish (Liu *et al.*, 2007; Sinthusamran *et al.*, 2013). Amide I, II and III band vibration are typical for collagen (Benjakul *et al.*, 2010). It was noted that, amide bands I, II and III of collagens showed vibrations in the range of 1600 to 1700 cm^{-1}, 1500 to 1600 cm^{-1} and 1200 to 1300 cm^{-1}, respectively (Fontaine-Vive *et al.*, 2009). It is well established that amide band I is associated with stretching vibration of C═O. Amide I bands of ASC, UASC, PSC and UPSC were found at 1639, 1636, 1631 and 1630 cm^{-1}, respectively. Lower wavenumber of PSC and UPSC confirms the formation of hydrogen bond between N─H stretch, where the CO residue is responsible for stabilizing triple helix structure (Wu *et al.*, 2014; Zanaboni *et al.*, 2000). For amide II band representing N─H bending, PSC and UPSC (1541 and 1538 cm^{-1}, respectively) had lower wavenumber, when compared to those of ASC and UASC (1545 and 1544 cm^{-1}, respectively). Thus, amide I and II bands of PSC and UPSC shifted to lower wavenumber, suggesting more hydrogen bond formation in triple helical structure. High ordered structure of collagen was due to the fact that non-helical region was removed by pepsin. Amide III is the combination of C─N stretching and N─H deformation, which involves in the complex inter-molecular interactions in collagen (Sinthusamran *et al.*, 2013). All the collagens displayed the same wavenumber of 1236 cm^{-1}, representing hydrogen bonds involved in maintaining the native structure.

The absorption band of amide A, associated with N─H stretching vibration occurred in the range of 3400–3440 cm^{-1} (Ikoma *et al.*, 2003). ASC, UASC, PSC and UPSC had the wavenumbers of 3301, 3300, 3296 and 3295 cm^{-1}, respectively. Observed shift in wavenumber to lower frequency suggested that the NH group was involved in hydrogen bonding (Fontaine-Vive *et al.*, 2009). The results of amide A

were in accordance with amide band I as discussed earlier. The amide band B associated with asymmetrical stretching of CH_2 of PSC and UPSC (2924 and 2924 cm^{-1}, respectively) was similar to that of ASC and UASC (2923 and 2923 cm^{-1}, respectively). The triple helix structure of collagen was determined by the intensity ratio between amide III and 1450 cm^{-1} band (Benjakul *et al.*, 2010). The ratio values were approximately 1.0 for all the collagens, confirming that triple helical structure of collagens still existed. The result implied that ultrasound under the condition used for skin pretreatment and pepsin had no impact on the native structure of collagen. Thus, collagen structure remained intact even after ultrasound or pepsin treatment, whereas a drastic increase in extraction yield was attained.

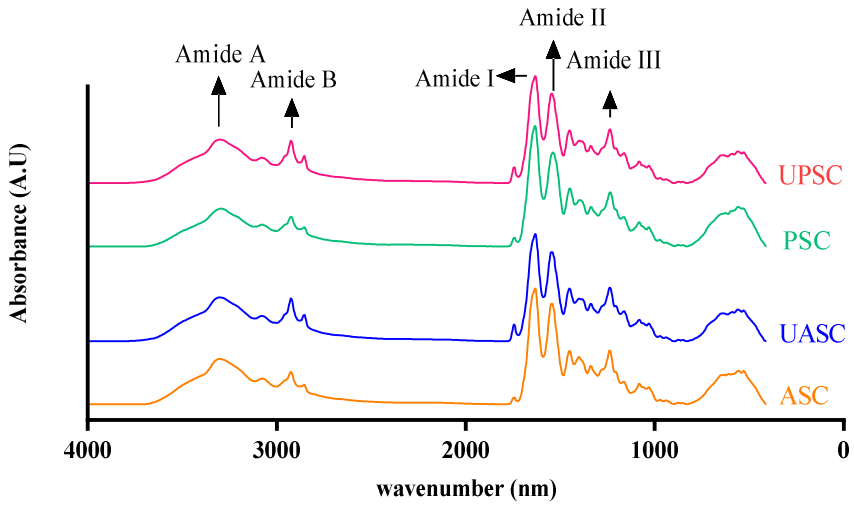

Figure 22. Fourier transform infrared spectra of acid soluble collagen (ASC), acid soluble collagen extracted using ultrasound assisted method (amplitude 80% and time 30 min) (UASC), pepsin soluble collagen (PSC) and pepsin soluble collagen extracted using ultrasound assisted method (pepsin 1%, amplitude 80% and time 30 min) (UPSC) from the skin of golden carp.

4.5.5. Thermal transition

Thermal transition expressed as T_{max} and enthalpy of all the collagens rehydrated in deionized water are presented in Table 2. PSC and UPSC showed the endothermic peak with T_{max} of 38.27 and 40.82 ºC, which were higher than ASC and UASC (36.91 and 36.14 ºC) ($p < 0.05$). The higher T_{max} of PSC might be due to the

removal of non-helical telopeptide region by pepsin, resulting in more ordered and compact structure of collagen (Benjakul *et al.*, 2010). It was noted that T_{max} of UPSC was higher than PSC. Ultrasound with cavitation effect might open up the structure of skin and facilitated pepsin to pass through and cleave telopeptide region effectively. Moreover, a small difference between T_{max} of ASC and UASC suggested that ultrasound alone could not alter physical/chemical properties of collagen as indicated by unchanged thermal stability. Comparatively, PSC and UPSC showed slightly higher ΔH values than ASC and UASC ($p < 0.05$). Higher thermal stability of both PSC and UPSC was governed by the higher imino acid content, particularly hydroxyproline which could donate hydroxyl group in the formation of hydrogen bond (Wu *et al.*, 2014; Zanaboni *et al.*, 2000). According to the previous reports, collagens from golden carp skins had higher T_{max} when compared to those extracted from temperate or cold water fish (Matmaroh *et al.*, 2011). Furthermore, higher T_{max} of UPSC indicated that ultrasonication in conjugation with pepsin exhibited a beneficial effect via increasing thermal stability.

Table 7. Thermal transition temperatures and enthalpy of acid and pepsin soluble collagens from skin of golden carp extracted with conventional method and ultrasound assisted extraction method.

Sample	T_{max} (ºC)	ΔH (J g^{-1})
ASC	36.91 ± 0.23^{a}	0.873 ± 0.02^{a}
UASC	36.14 ± 0.45^{a}	0.896 ± 0.02^{a}
PSC	38.27 ± 1.21^{a}	1.236 ± 0.08^{b}
UPSC	40.82 ± 1.44^{b}	1.420 ± 0.13^{c}

ASC: acid soluble pepsin collagen extracted by conventional method
PSC: pepsin soluble collagen extracted by conventional method
UASC: acid soluble collagen extracted by ultrasound assisted method (amplitude 80% and time 30 min)
UPSC: pepsin soluble collagen extracted by ultrasound assisted method (pepsin 1%, amplitude 80% and time 30 min)
Different lowercase superscripts in the same column indicate the significant differences ($P<0.05$).

4.5.6. CD spectroscopy

The triple helical conformation of ASC, UASC, PSC and UPSC was confirmed by CD spectra in Figure 5. A distinctive positive peak at 221 nm and a negative peak at 198 nm are ideal for collagen (Tifany and Krimm, 1972). The rotatory maxima of the positive peak of ASC and UASC were at 220 and 219.9. The similar molar ellipticity between ASC and UASC indicated no difference in the secondary structure. Thus, ultrasound treatment had no impact on the secondary structure of resulting collagen. For PSC and UPAC, positive peaks were at 220.8 and 221. The molar ellipticity of UPAC was higher than that of PSC, ASC and UASC. This result indicated that UPSC had more compact triple helical structure. It has been reported that PSC has more ordered secondary structure than that of ASC, as the pepsin removes non-helical telopeptide region from the molecules (Liang *et al.*, 2014).

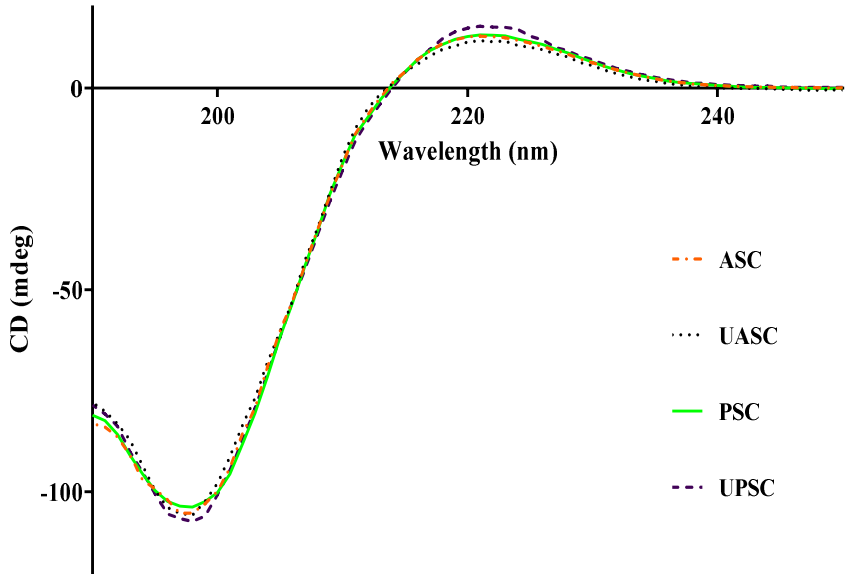

Figure 23. Circular dichroism spectra of acid soluble collagen (ASC), acid soluble collagen extracted using ultrasound assisted method (amplitude 80% and time 30 min) (UASC), pepsin soluble collagen (PSC) and pepsin soluble collagen extracted using ultrasound assisted method (pepsin 1%, amplitude 80% and time 30 min) (UPSC) from the skin of golden carp.

In the present study, it was observed that cavitation induced by ultrasound facilitated pepsin to cleave telopeptide region more effectively. As a result,

more amounts of collagen were released (Yu *et al.*, 2014; Zou *et al.*, 2017). All the collagens also showed a negative peak at 198 nm. The CD spectra of denatured collagen have the disappearance of the positive peak and the shift of negative peak to the lower wavelength (Tifany and Krimm, 1972). The CD measurement demonstrated that all the collagens were in native secondary structure, triple helical. Therefore, the use of ultrasound for collagen extraction in combination with pepsin was able to increase the extraction yield and had no adverse effect on the molecular integrity of collagen.

4.5.7. Zeta Potential

Zeta potential of ASC, UASC, PSC and UPSC at the pH range of 2–12 is shown in Figure 6. In the acidic pH (2 to 6), all collagens had net positive charge. With increasing pH values, the charge of collagen was reduced and isoelectric point (pI) of all collagens was attained within the pH range of 6 to 7, where the net charge of zero was found. The surface net zero charge of ASC, UASC, PSC and UPSC were obtained at pH 6.11, 6.02, 6.21 and 6.56, respectively. The obtained pIs were similar to those of collagen from golden carp (Ali *et al.*, 2017b) and seabass (Sinthusamran *et al.*, 2013). pIs of PSC and UPSC were higher than those of ASC and UASC. This was more likely owing to the removal of some amino acids in the non-helical region of collagen in PSC and UPSC.

Difference in pI between the collagens was plausibly due to the difference in charged amino acids, especially glutamic acid, lysine and aspartic acid as reported by Benjakul *et al.* (2010). At pH above pI, collagens showed the negative charge. The more basic the pH, higher the values of negative charge was attained. The difference in zeta potential profile within the collagen molecule might be associated with the dissimilar distribution of amino acid, mainly on the surface of collagens (Ali *et al.*, 2017a). Thus, the pIs of collagens were not affected much by ultrasonication, whereas pepsin treatment showed some impact on pI of resulting collagen.

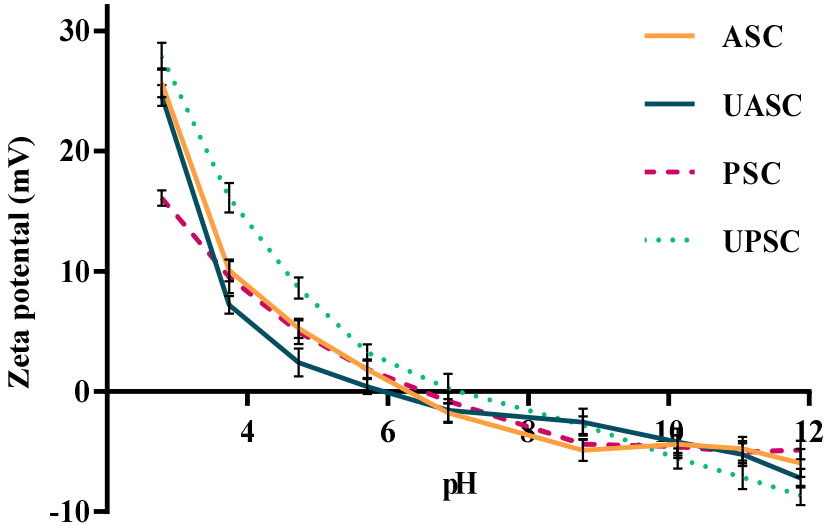

Figure 24. Zeta potential of acid soluble collagen (ASC), acid soluble collagen extracted using ultrasound assisted method (amplitude 80% and time 30 min) (UASC), pepsin soluble collagen (PSC) and pepsin soluble collagen extracted using ultrasound assisted method (pepsin 1%, amplitude 80% and time 30 min) (UPSC) from the skin of golden carp at different pHs. Bars represent the standard deviation (n=3).

4.6. Conclusions

The aid of ultrasound in conjugation with pepsin improved the yield of collagen from skin of golden carp. The use of ultrasound (20 kHz, amplitude 80% for 30 min) could increase the yield of ASC to 81.53%, which was 150% higher than that extracted using conventional method. Ultrasonication (20 kHz, amplitude 80% for 30 min) in combination with pepsin (1%) could increase the yield up to 94.88%, which was 180% and 120% higher than ASC and PSC. Protein pattern, FTIR and CD spectra confirmed that all the collagens had the native triple helical conformation. However, a minor difference was observed in amino acid composition and T_{max} amongst all the collagens. Thus, UASC or UPSC could be utilized as a potential source of collagen that can be applied in food and pharmaceutical industries.

4.7. References

Ali, A. M. M., Benjakul, S. and Kishimura, H. 2017a. Molecular characteristics of acid and pepsin soluble collagens from the scales of golden carp (*Probarbus jullieni*). Emirates Journal of Food and Agriculture. 29: 450-457.

Ali, A. M. M., Benjakul, S., Prodpran, T. and Kishimura, H. 2017b. Extraction and characterisation of collagen from the skin of golden carp (*Probarbus Jullieni*), a processing by-product. Waste Biomass Valorization. 9: 783–791.

Benjakul, S., Thiansilakul, Y., Visessanguan, W., Roytrakul, S., Kishimura, H., Prodpran, T. and Meesane, J. 2010. Extraction and characterisation of pepsin-solubilised collagens from the skin of bigeye snapper (*Priacanthus tayenus* and *Priacanthus macracanthus*). Journal of the Science of Food and Agriculture. 90: 132-138.

Bergman, I. and Loxley, R. 1963. Two improved and simplified methods for the spectrophotometric determination of hydroxyproline. Analytical Chemistry. 35: 1961-1965.

Fontaine-Vive, F., Merzel, F., Johnson, M. and Kearley, G. 2009. Collagen and component polypeptides: Low frequency and amide vibrations. Chemical Physics. 355: 141-148.

Hashemi, S. M. B., Mousavi Khaneghah, A., Koubaa, M., Barba, F. J., Abedi, E., Niakousari, M. and Tavakoli, J. 2017. Extraction of essential oil from Aloysia citriodora Palau leaves using continuous and pulsed ultrasound: Kinetics, antioxidant activity and antimicrobial properties. Process Biochemistry. 65: 197-204.

Ikoma, T., Kobayashi, H., Tanaka, J., Walsh, D. and Mann, S. 2003. Physical properties of type I collagen extracted from fish scales of *Pagrus major* and *Oreochromis niloticas*. International Journal of Biological Macromolecules. 32: 199-204.

Kim, H. K., Kim, Y. H., Kim, Y. J., Park, H. J. and Lee, N. H. 2012. Effects of ultrasonic treatment on collagen extraction from skins of the sea bass *Lateolabrax japonicus*. Fisheries Science. 78: 485-490.

Kim, S. K. and Mendis, E. 2006. Bioactive compounds from marine processing byproducts–a review. Food Research International. 39: 383-393.

Lafarga, T. and Hayes, M. 2014. Bioactive peptides from meat muscle and by-products: generation, functionality and application as functional ingredients. Meat Science. 98: 227-239.

Li, D., Mu, C., Cai, S. and Lin, W. 2009. Ultrasonic irradiation in the enzymatic extraction of collagen. Ultrasonics Sonochemistry. 16: 605-609.

Liang, Q., Wang, L., Sun, W., Wang, Z., Xu, J. and Ma, H. 2014. Isolation and characterization of collagen from the cartilage of Amur sturgeon (Acipenser schrenckii). Process Biochemistry. 49: 318-323.

Liu, H., Li, D. and Guo, S. 2007. Studies on collagen from the skin of channel catfish (*Ictalurus punctaus*). Food Chemistry. 101: 621-625.

Matmaroh, K., Benjakul, S., Prodpran, T., Encarnacion, A. B. and Kishimura, H. 2011. Characteristics of acid soluble collagen and pepsin soluble collagen from scale of spotted golden goatfish (*Parupeneus heptacanthus*). Food Chemistry. 129: 1179-1186.

Nalinanon, S., Benjakul, S., Visessanguan, W. and Kishimura, H. 2007. Use of pepsin for collagen extraction from the skin of bigeye snapper (*Priacanthus tayenus*). Food Chemistry. 104: 593-601.

Schmidt, M., Dornelles, R., Mello, R., Kubota, E., Mazutti, M., Kempka, A. and Demiate, I. 2016. Collagen extraction process. International Food Research Journal. 23: 913-922.

Shirsath, S., Sonawane, S. and Gogate, P. 2012. Intensification of extraction of natural products using ultrasonic irradiations—a review of current status. Chemical Engineering and Processing: Process Intensification. 53: 10-23.

Shoulders, M. D. and Raines, R. T. 2009. Collagen structure and stability. Annual Review of Biochemistry. 78: 929-958.

Sinthusamran, S., Benjakul, S. and Kishimura, H. 2013. Comparative study on molecular characteristics of acid soluble collagens from skin and swim bladder of seabass (*Lates calcarifer*). Food Chemistry. 138: 2435-2441.

Tifany, M. L. and Krimm, S. 1972. Effect of temperature on the circular dichroism spectra of polypeptides in the extended state. Biopolymers. 11: 2309-2316.

Vilkhu, K., Mawson, R., Simons, L. and Bates, D. 2008. Applications and opportunities for ultrasound assisted extraction in the food industry — A review. Innovative Food Science and Emerging Technologies. 9: 161-169.

Wu, G. P., Wang, X. M., Lin, L. P., Chen, S. H. and Wu, Q. Q. 2014. Isolation and characterization of pepsin-solubilized collagen from the skin of black carp (Mylopharyngdon piceus). Advances in Bioscience and Biotechnology. 5: 642.

Yu, Z.-L., Zeng, W.-C., Zhang, W.-H., Liao, X.-P. and Shi, B. 2014. Effect of ultrasound on the activity and conformation of α-amylase, papain and pepsin. Ultrasonics Sonochemistry. 21: 930-936.

Yuan, T., He, L., Yang, J., Zhang, L., Xiao, Y., Fan, Y. and Zhang, X. 2015. Conjugated icariin promotes tissue-engineered cartilage formation in hyaluronic acid/collagen hydrogel. Process Biochemistry. 50: 2242-2250.

Zanaboni, G., Rossi, A., Onana, A. M. T. and Tenni, R. 2000. Stability and networks of hydrogen bonds of the collagen triple helical structure: influence of pH and chaotropic nature of three anions. Matrix Biology. 19: 511-520.

Zhang, Y., Liu, W., Li, G., Shi, B., Miao, Y. and Wu, X. 2007. Isolation and partial characterization of pepsin-soluble collagen from the skin of grass carp (*Ctenopharyngodon idella*). Food Chemistry. 103: 906-912.

Zou, Y., Wang, L., Cai, P., Li, P., Zhang, M., Sun, Z., Sun, C., Xu, W. and Wang, D. 2017. Effect of ultrasound assisted extraction on the physicochemical and functional properties of collagen from soft-shelled turtle calipash. International Journal of Biological Macromolecules. 105: 1602-1610.

CHAPTER 5

PHYSICOCHEMICAL AND MOLECULAR PROPERTIES OF GELATIN FROM SKIN OF GOLDEN CARP (*PROBARBUS JULLIENI)* AS INFLUENCED BY ACID PRETREATMENT AND PRIOR-ULTRASONICATION

5.1. Abstract

Gelatins from golden carp skin pretreated using different acids (acetic acid and sulfuric acid + acetic acid), with and without prior-ultrasonication, extracted at 55 ºC for 3 and 6 h, were characterized. Different extraction efficiency and gelatin properties were obtained with different acid pretreatments. Prior-ultrasonication (20 kHz) with amplitude of 80% increased the yield of gelatins from acetic acid and sulfuric acid + acetic acid pretreated skins by 110.9% and 174.8%, respectively compared with the corresponding controls (without prior-ultrasonication), when extracted for 6 h. All the gelatin samples had α- and β-chain as the major components. The gelatins extracted from skin with prior-ultrasonication showed slightly higher content of imino acids, compared to those produced by conventional method, regardless of acid pretreatments. Moreover, gelatin extracted by prior-ultrasonication had higher gelling and melting temperature than those produced by conventional method by 9.1-12.0 and 8.2-12.2%, respectively. FTIR spectra revealed that the formers had the higher cross-links stabilized by hydrogen bond than the latter. Based on microstructure study, the formers had higher number of interjunction zones with finer networks. Overall, pretreatment with sulfuric acid/acetic acid in combination with prior-ultrasonication effectively improved the extraction efficiency and gelling properties of gelatin from golden carp skin.

5.2. Introduction

Gelatins is a high molecular weight (MW) protein manuufactued by thermal denaturation of collagen (Kaewruang *et al.*, 2013). Gelatin in food industry has

been used as thickening agent in gravy and desserts, stabilizer in ice cream and texturizer in confectionaries, salad dressing, gelling agent as well as employed as food foams (Badii and Howell, 2006; Saha and Bhattacharya, 2010). Moreover, gelatin has numerous and emerging applications in cosmetics, pharmaceuticals, biomedical and biomaterial-based packaging industries (Gennadios *et al.*, 1997; Ishida *et al.*, 2007; Yakimets *et al.*, 2005). Generally, commercial sources of gelatin production is porcine as well bovine skin and bones (Khiari *et al.*, 2017). Albeit its wide applications, a strong concern of gelatin over the consumers still persists, mainly due to the religious restrictions or health issues (Benjakul *et al.*, 2010). However, the annual usage of gelatin is increasing worldwide. The estimated usage food industry alone is about 200,000 metric tons per year, which is chiefly from mammalian origins (Badii and Howell, 2006).

Gelatin from fish processing byproduct has gained interest as an alternative for mammalian gelatin (Gudmundsson, 2002). Generally, gelatin (type A gelatin) from fish sources is produced by a mild acid pretreatment (Giménez *et al.*, 2005; Khiari *et al.*, 2017). Gelatin from several fish skins such as unicorn leatherjacket (Kaewruang *et al.*, 2013), mackerel (Khiari *et al.*, 2017), blacktip shark and brownbanded bamboo shark (Kittiphattanabawon *et al.*, 2010) and channel catfish (Yang *et al.*, 2008) have been extracted by the conventional method including acid pretreatment and extraction using hot water. Since the cross-links of collagen molecules are stable to thermal and acid treatment (Zhou and Regenstein, 2005), a lower yield is generally obtained. To increase the extraction yield of gelatin, some proteases were employed to destabilize collagen before extraction (Chomarat *et al.*, 1994). Pretreatment using different acids was optimized (Yang *et al.*, 2008; Zhou and Regenstein, 2005) and appropriate extraction temperature was employed (Kittiphattanabawon *et al.*, 2010). These methods increased the yield to some degrees, but the resulting gelatin had inferior gelling property. Appart from the tissue or species from which gelatin is extracted, peoperties of gelatin were influenced by the extraction conditions (Khiari *et al.*, 2017; Zhou and Regenstein, 2005).

Recently, ultrasound has become the emerging technology for extraction of biologically important molecules to increase the extraction efficiency and shorten

the extraction time (Jiang *et al.*, 2014; Pingret *et al.*, 2013). The improvement of yield by ultrasound is due to the physical disruption of wall/matrix and the increaed mass transfer. This is caused by the regions of high and low pressure, mainly due to the cavitation process (Pingret *et al.*, 2013). Additionally, ultrasound has been reported to enhance the functional properties (emulsifying, solubility, rheological and others) of proteins, caused by induced changes in conformation (Arzeni *et al.*, 2012; Soria and Villamiel, 2010). Fish skin is a complex matrix containing acid and thermo-stable cross-linkages. This is associated with the reduced extraction efficiency (Nagarajan *et al.*, 2012). Owing to cavitation effect, ultrasound could be introduced to enhance extraction efficiency. Prior-ultrasonication of acid treated skin could loosen skin matrix, thus enhancing extraction by hot water.

Golden carp (*Probarbus jullieni*) is a freshwater fish, habitually distributed in Southeast Asian river basins and is primarily aquacultured in Thailand and Lao PDR. According to FAO, aquaculture production of golden carp has the annual growth rate of 3.86% (FAO, 2016). Skin of golden carp constitutes around 4–5% of body weight. Its skins can be utilized for production of gelatin, particularly using the appropriate and effective extraction method.

5.3. Objective

To investigate the effect of acid pretreatment and prior-ultrasonication on characteristics, yield and gel properties of gelatin produced from golden carp skin.

5.4. Materials and methods

5.4.1. Chemicals

Sulfuric acid, sodium hydroxide and acetic acid were purchased from Merck (Darmstadt, Germany). High molecular weight protein marker was obtained from Sigma Chemicals (St. Louis, MO, USA). Coomassie Blue R-250, *N,N,N',N'* - tetramethylethylenediamine (TEMED) and sodium dodecyl sulfate (SDS) were procured from Bio-Rad Laboratories (Hercules, CA, USA). All the chemical used were of analytical grade.

5.4.2. Collection and preparation of golden carp skin

Collection, transportation, preparation and storage of golden carp skin was carried out as described in the section *2.4.2.1*.

5.4.2.1. Pretreatment of golden carp skin

Removal of non-collagenous proteins was carried out by soaking golden carp skins in 0.1 M NaOH with a skin/alkaline solution ratio of 1:10 (w/v). The mixture was stirred for 6 h at room temperature (28–30 ºC) using an overhead stirrer model W20.n, (IKA®-Werke GmbH & CO.KG, Staufen, Germany). Fresh alkaline solution was replaced every 2 h for totally 3 times. The treated skin was washed with tap water until pH of wash water became neutral or faintly basic. Thereafter, the skin was defatted by soaking in 10% butyl alcohol at a skin/solvent ratio of 1:15 (w/v) for 6 h by replacing the fresh solvent after 3 h. Defatted skins were washed in a running tap water and drained on a screen.

5.4.2.2. Acid pretreatment

The first portion of prepared skin was pretreated using acetic acid. The skin (100 g) was soaked in 0.05 M acetic acid (pH 3.4) at a sample/acid solution ratio of 1:10 (w/v). The mixture was stirred at 150 rpm for 2 h at room temperature. Subsequently, the skins were washed with a running tap water until the wash water had neutral pH. Finally, the pretreated skin was drained on a screen.

For the second portion, the skin (100 g) was suspended in 0.02 M sulfuric acid (pH 1.7) at the sample/solution ratio of 1:10 (w/v). The mixture was stirred for 15 min continuously at room temperature, followed by washing and draining of skin as described before. The skin was further soaked in 0.05 M acetic acid at a sample/acid solution ratio of 1:10 (w/v) for 15 min (without stirring). Thereafter, the residue was washed in tap water until the pH of wash water was neutral and the residue was drained on the screen.

The third portion of skin (without acid pretreatment) was used as a negative control.

5.4.2.3. Ultrasound assisted pretreatment

Prior to ultrasonication, the skins with and without acid pretreatments (100 g) were mixed with distilled water at a skin/water ratio of 1:10 (w/v). The mixture was subjected to ultrasonication using a reactor Vibra–Cell (Sonics & Material, Inc, Newtown, CT, USA) equipped with 25 mm diameter probe, working at a fixed frequency and power (20 kHz and 750 W, respectively). Ultrasonication was operated at an amplitude of 80% for 30 min. Temperature of sample was maintained at 25 ± 2 ºC using an iced bath containing 2% NaCl and the temperature was monitored using a digital thermometer (model DE-3004 Type K, DER EE Electrical Instruments Co., Ltd., Chung Ho, Taipei, Taiwan). The reaction was performed in a pulsed mode at 5 sec acting and 5 sec resting time.

5.4.2.4. Gelatin extraction

Gelatin was extracted following the method of Sinthusamran *et al.* (2014). Skin samples (without and with acid pretreatments), without and with prior-ultrasonication, added with water at a ratio of 1:10 (w/v) were incubated at 55 ºC with continuous stirring. The extraction times of 3 and 6 h were used. After the designated time, the extract was filtered using two layers of cheesecloth. The filtrate was mixed with 1% activated carbon, followed by filtration using Buchner funnel with Whatman filter paper No. 4 (Whatman International, Ltd., Maidstone, England). The obtained gelatin samples were freeze-dried using a freeze-dryer, model CoolSafe 55 (ScanLaf A/S, Lynge, Denmark). The obtained gelatin samples were calculated for yield and subjected to analysis. Scheme for gelatin production under different conditions are presented in Figure 1.

5.4.2.5. Yield

The yield of gelatin was calculated, based on the dry weight of the initial skin according to the Eq. (1):

$$\text{Yield (\%)} = \frac{\text{Weight of freeze–dried gelatin (g)}}{\text{Weight of initial dry skin (g)}} \times 100 \qquad (1)$$

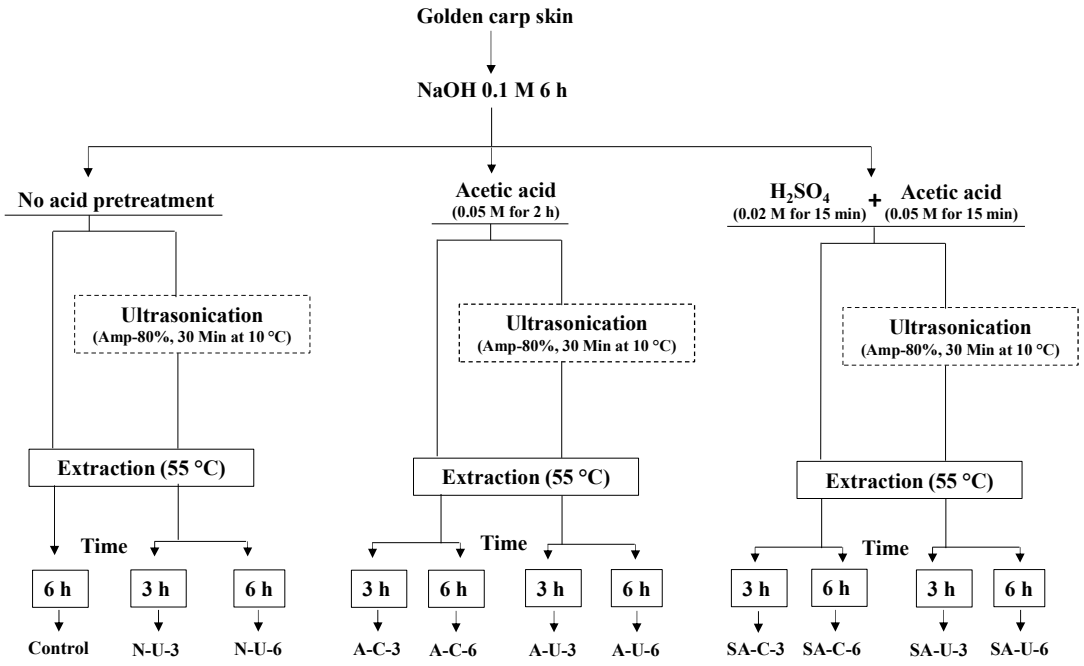

Figure 25. Overview of different extraction condition of gelatin from skin of golden carp. Control: without acid/ultrasound pretreatment, N-U: prior-ultrasonication without acid pretreatment, A-C: acetic acid pretreatment, A-U: acetic acid pretreatment and prior-ultrasonication, SA-C: sulfuric acid + acetic acid pretreatment, SA-U: sulfuric acid + acetic acid pretreatment and prior-ultrasonication.

5.4.3. Characterization of selected gelatins

The samples prepared under the extracting conditions rendering the highest yield and gel strength were selected for characterization. Those included gelatin extracted from skin pretreated with acetic acid and sulfuric acid + acetic acid by the conventional method (A-C-6 and SA-C-6) and by the extraction method with prior-ultrasonication (A-U-6 and SA-U-6). The gelatin from skin without acid pretreatment, prepared by the extraction method with prior-ultrasonication (N-U-6) was also characterized.

5.4.3.1. Protein patterns (*section 2.4.3.2*)

5.4.3.2. Amino acid compositions (*section 2.4.3.3*)

5.4.3.3. Fourier transform infrared (FTIR) spectroscopy (*section 2.4.3.4*)

5.4.3.4. Gelling and melting temperatures

Gelling and melting temperatures were measured using a controlled stress rheometer model HAAKE RheoStress 1 (Thermo Fisher Scientific, Karlsruhe, Germany) as described by Sinthusamran *et al.* (2014). The solution was loaded on the parallel plates with diameter of 35 mm and the gap was set at 1.0 mm. The program was initiated by preheating the solution at 40 ºC for 15 min, followed by cooling period from 40 to 5 ºC and heating from 5 to 40 ºC at the rate of 0.5 ºC min^{-1}. The oscillating stress of 3 Pa was applied with a frequency of 1 Hz. Finally, the gelling and melting temperatures were identified when tan δ reached the value of 1.

5.4.4. Determination of gel properties

5.4.4.1. Color

Color of gelatin gels of (6.67%, w/v) were measured using a Hunter lab colorimeter (color Flex, Hunter Lab Inc., Reston, VA, USA). L^*, a^* and b^* representing lightness/brightness, redness/greenness and yellowness/blueness, respectively, were recorded. The color difference value (ΔE^*) was calculated according to the Eq. (2) (Gornall *et al.*, 1949):

$$\Delta E^* = \sqrt{(\Delta L^*)^2 + (\Delta a^*)^2 + (\Delta b^*)^2} \qquad (2)$$

where ΔL^*, Δa^* and Δb^* are the differences corresponding to color parameter of sample to that of the white standard (L^* = 93.6, a^* = −0.94 and b^* = 0.40).

5.4.4.2. Gel strength

Gel strength of gelatin samples was determined according to the British Standard 757: 1975 method (B.S.I, 1975) with a slight modification. Gelatins were dissolved in distilled water at 60 ºC to obtain a final concentration of 6.67% (w/v). After

complete solubilization, the solution was transferred to a cylindrical mold (height 2.5 cm and diameter 3 cm) and incubated at 4 ºC for 16–18 h to set the gel. Gel strength was determined at 8–10 ºC using a texture analyzer model TA.XT Plus (Stable Micro System, Surrey, UK) equipped with a 1.27 cm diameter flat-faced cylindrical Teflon® plunger and with a load cell of 5 kg. The maximum force (grams) was recorded at a cross head speed of 1 mm s^{-1} until the plunger penetrated 4 mm into the gelatin gel.

5.4.4.3. Microstructure

Microstructure of gelatin gels was visualized using a scanning electron microscopy (SEM). Gelatin gels were cut into strips of 2–3 mm width and 1-2 mm thickness. These were immersed in liquid nitrogen and broken into small pieces. Specimens were fixed with 2.5% (v/v) glutaraldehyde in 0.2 M phosphate buffer (pH 7.2) for 12 h. Specimens were then rinsed using distilled water for 1 h and dehydrated using ethanol in a sequential concentration of 50%, 70%, 80%, 90% and 100% each for 15 min. Dried samples were mounted on a bronze stab and sputter-coated with gold (Sputter coater SPI-Module, West Chester, PA, USA). The specimens were observed with a scanning electron microscope (JEOL JSM-5800 LV, Tokyo, Japan) at an acceleration voltage of 20 kV.

5.4.5. Statistical analysis

The experiments were conducted in triplicates with completely randomized design (CRD). The difference between means were tested by the Duncan's multiple range test. The data was presented as means ± standard deviation. Statistical analysis was performed using the SPSS 11.0 software (SPSS Inc., Chicago, IL, USA).

5.5. Results and discussion

5.5.1. Extraction yield

Yields of gelatin from golden carp skin under different acid pretreatments and prior-ultrasonication are presented in Table 1. Yields of gelatin with respect to different conditions varied from 9.34 to 62.12%. Gelatin from skin without acid pretreatment and without prior-ultrasonication (control) had very low yield

(1.47%). This could be related to the cross-linkages present in the skin matrix. Without swelling using acid or ultrasound to loosen the skin matrix, it was difficult to extract gelatin. In general, a mild acid treatment is necessary to destabilize these cross-links and facilitate the extraction (Benjakul *et al.*, 2010). For gelatin extracted from skin without acid pretreatment, the prior-ultrasonication followed by heating was found to increase the yield of gelatin, with increasing extraction time from 3 to 6 h ($p < 0.05$). Overall, the recovery of gelatin increased ($p < 0.05$), particularly when the extraction time was increased from 3 to 6 h, regardless of acid types for pretreatment and prior-ultrasonication. The obtained results were in accordance with Sinthusamran *et al.* (2014) who testified the increased yield from seabass skin when extraction time was increased. For acid pretreatments, acetic acid pretreated skin showed higher yield ($p < 0.05$) than that from skin pretreated with sulfuric acid + acetic acid. Swelling process of skin was affected by type of acid used, mainly depending on the total H^+ concentration and the final pH of the solution (Zhou and Regenstein, 2005).

Moreover, acetic acid pretreatment was reported to render gelatin with higher yield and quality, compared to pretreatment using other organic and inorganic acids (Khiari *et al.*, 2017; Kittiphattanabawon *et al.*, 2010; Zhou and Regenstein, 2005). For the same acid pretreatment, extraction yields of gelatin from conventional method was lower than those with prior-ultrasonication ($p < 0.05$). Prior-ultrasonication in conjunction with acid pretreatment using two acids increased the yield effectively. The highest yield (62.12%) was obtained when prior-ultrasonication was applied to sulfuric acid + acetic acid pretreated samples, followed by extraction for 6 h. Prior-ultrasonication increased the yield of gelatins by 110.9% (acetic acid pretreated) and 174.8% (sulfuric acid + acetic acid pretreated), compared to that of corresponding gelatins extracted by conventional method, when extracted for 6 h. The increase in yield was suggested to be due to the cavitation and mechanical effect of ultrasound (Jiang *et al.*, 2014; Pingret *et al.*, 2013). The cavitation effect facilitated the loosening of pretreated skin. During subsequent extraction, penetration of hot water into the matrix of loosened skin was enhanced (Soria and Villamiel, 2010). This result indicated that prior-ultrasonication along with the increased extraction time were able to destabilize collagen structure, thus inducing helix to coil transition of collagen to soluble gelatin

(Nagarajan *et al.*, 2012). When comparing the yield of gelation from skin without acid pretreatment, prior-ultrasonication alone could also assist the extraction of gelatin to some extent but efficiency of extraction was lower, compared to that of skin pretreated using acid in combination with prior-ultrasonication.

Table 8. Extraction yield (%, dry weight basis), gelling and melting temperature of gelatin from the skin of golden carp with different pretreatment and extraction conditions.

Sample	Time (h)	Yield (%)	Gelling temperature (°C)	Melting temperature (°C)
Control	6	1.47 ± 0.26^{i}	-	-
N-U	3	5.84 ± 0.38^{h}	-	-
	6	9.34 ± 1.31^{g}	13.26 ± 0.27^{d}	24.25 ± 0.34^{e}
A-C	3	24.65 ± 1.83^{e}		
	6	52.38 ± 2.34^{bc}	19.78 ± 0.25^{bc}	28.73 ± 0.35^{c}
A-U	3	33.68 ± 0.76^{de}		
	6	58.12 ± 1.56^{b}	21.76 ± 0.25^{a}	32.74 ± 0.37^{a}
SA-C	3	18.54 ± 1.21^{f}		
	6	35.54 ± 0.85^{de}	18.26 ± 0.32^{c}	27.76 ± 0.28^{cd}
SA-U	3	37.79 ± 1.44^{d}		
	6	62.12 ± 1.52^{a}	20.76 ± 0.38^{b}	30.25 ± 0.31^{b}

Mean ± SD from triplicate determination.

Different superscript letters in the same column indicate significant difference ($p < 0.05$).

Control: without acid/ultrasound pretreatment, N-U: prior-ultrasonication without acid pretreatment, A-C: acetic acid pretreatment, A-U: acetic acid pretreatment and prior-ultrasonication, SA-C: sulfuric acid + acetic acid pretreatment, SA-U: sulfuric acid + acetic acid pretreatment and prior-ultrasonication.

Number of 3 and 6 represents the extraction time (3 and 6 h).

5.5.2. Protein patterns

The protein patterns of gelatin from the golden carp skin extracted using various pretreatments and extracting conditions are presented in Figure 2. All the gelatin samples comprised α_1 (MW: ~117 kDa), α_2 (MW: ~108 kDa) and β (MW: ~193 kDa) chains as the major constituents. The protein patterns were similar to those found in gelatin from of seabass skin (Sinthusamran *et al.*, 2014). The band intensity of α- and β-chain in gelatin from acetic acid pretreated skin showed similar pattern, regardless of prior-ultrasonication. Similar protein patterns were also obtained for gelatin obtained from pretreatment using sulfuric acid + acetic acid, extracted by conventional method. Nevertheless, the reduction in band intensity of β-chain and disappearance of α_2-band in gelatin prepared by sulfuric acid + acetic acid pretreatment was noted. This suggested that sulfuric acid pretreatment in conjugation with prior-ultrasonication possibly loosened the skin matrix to higher extent and a partial hydrolysis occurred during extraction. This coincided with the presence of protein band with a MW of 76-78 kDa. Prior-ultrasonication might induce the degradation of gelatin component in skin pretreated with acetic acid and sulfuric acid + acetic acid to some extent. Similarly, Zhou and Regenstein (2005) reported that the quality of gelatin from mackerel skin was affected by the type of acid used for pretreatment. Degradation of gelatin from blacktip shark and brownbanded bamboo shark skin was increased when the temperature or time of extraction was increased (Kittiphattanabawon *et al.*, 2010). The results indicated that prior-ultrasonication had the impact on protein patterns of gelatin, particularly those from skin pretreated with sulfuric acid + acetic acid. Moreover, the bands corresponding to α- and β-chains were observed when skin without acid pretreatment but subjected to prior-ultrasonication and extracted for 6 h. The result indicated that prior-ultrasound treatment assisted in loosening the skin matrix and facilitated mass transfer (Soria and Villamiel, 2010). Moreover, ultrasound might inactivate indigenous proteases to some degree. Ultrasonication has been reported to inactivate proteases and lipases to higher rate than heat denaturation in a biological system (Vercet *et al.*, 2001). Kaewruang *et al.* (2013) testified no α- and β-chains were remained in gelatin from unicorn leather jacket, due to hydrolysis caused by endogenous heat-stable proteases.

Therefore, prior-ultrasonication improved the extraction efficiency of gelatin from skin, especially with acid pretreatments, in which the major components were still retained.

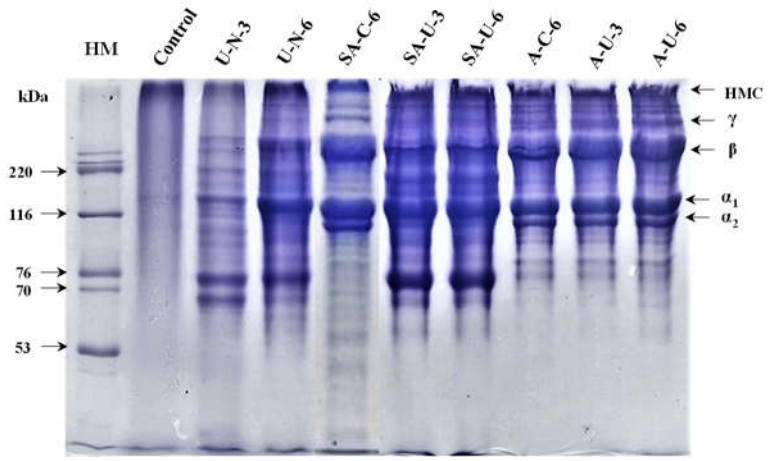

Figure 26. SDS-PAGE patterns of gelatin from the skin of golden carp with the selected pretreatment and extraction conditions. Control: without acid/ultrasound pretreatment (6 h), N-U: prior-ultrasonication without acid pretreatment, A-C: acetic acid pretreatment, A-U: acetic acid pretreatment and prior-ultrasonication, SA-C: sulfuric acid + acetic acid pretreatment, SA-U: sulfuric acid + acetic acid pretreatment and prior-ultrasonication.

Number of 3 and 6 represents the extraction time (3 and 6 h).

5.5.3. Amino acid compositions

Amino acid compositions of selected gelatins including N-U-6, A-C-6, SA-C-6, A-U-6 and SA-U-6 from the skins of golden carp are presented in Table 2. Among all the gelatins, glycine was present as the major amino acid ranging from 327 to 336 residues (1000 residues)$^{-1}$. Generally, glycine is known to be present at every one-third residue of α-chain and is principally involved in intermolecular H-bonding perpendicular to the helical axis, thereby stabilizing collagen structure (Benjakul *et al.*, 2010). This indicates that the prepared gelatin from golden carp skin was derived from tropocollagen. It was noted that A-U-6 and SA-U-6 (336 and 336 residues (1000 residues)$^{-1}$, respectively) had higher number of glycine residues, compared to that of A-C-6 and SA-C-6 (333 and 334 residues (1000 residues)$^{-1}$, respectively). Similar effect was observed in imino acids (proline and hydroxyproline), where A-U-6 and SA-U-6

(204 and 201 residues (1000 residues)$^{-1}$, respectively) had higher imino acid residues than A-C-6 and SA-C-6 (199 and 197 residues (1000 residues)$^{-1}$, respectively). The results suggested that pretreatment with acid in combination with prior-ultrasonication could loosen the skin matrix (Soria and Villamiel, 2010). Moreover, N-U-6 sample had the lowest imino acid content (194 residues (1000 residues)$^{-1}$). The imino acids composition of gelatin from the skin of golden carp were comparable to that of seabass skin (198–202 residues (1000 residues)$^{-1}$) (Sinthusamran *et al.*, 2014) but were higher than those from skin of dover sole (173–183 residues (1000 residues)$^{-1}$) (Giménez *et al.*, 2005), bigeye snapper (186–187 residues (1000 residues)$^{-1}$) (Benjakul *et al.*, 2010), mackerel (154–169 residues (1000 residues)$^{-1}$) (Khiari *et al.*, 2017). The different imino acid content is anticipated to be governed by species and living environment. Imino acids including hydroxyproline have a role in stabilizing gelatin gel by forming a hydrogen bond from their hydroxyl group (Kittiphattanabawon *et al.*, 2010). Thus hydroxyproline as a H-donor is an significant factor in determining gelatin gel strength (Benjakul *et al.*, 2010). Furthermore, alanine (112–123 residues (1000 residues)$^{-1}$) was found at high extent, regardless of the extraction conditions. Gelatin with higher alanine content has been known to possess better viscoelastic property (Giménez *et al.*, 2005). Arginine, glutamine/glutamic acid and asparagine/aspartic acid were also present at high amounts. However, no marked difference in charged amino acids (glutamic acid, aspartic acid, lysine and arginine) was observed between gelatin from skin without (A-C-6 and SA-C-6) and with prior-ultrasonication (A-U-6 and SA-U-6). Other amino acids such as phenylalanine, isoleucine, leucine, serine, threonine and valine were present at lower amounts in all the gelatins. Sinthusamran *et al.* (2014) reported similar results for gelatin from the seabass skin. All the gelatin samples contained no cysteine, confirming that the gelatin extracted possessed no disulfide linkages (Morales *et al.*, 2000). Therefore, amino acid composition of extracted gelatin was not drastically affected by both the acid pretreatment, prior-ultrasonication and extraction conditions.

Table 9. Amino acid composition of gelatin from the skin of golden carp with the selected pretreatment and extraction conditions.

Amino acids	(Residues (1000 residues)$^{-1}$)				
	N-U-6	**A-C-6**	**A-U-6**	**SA-C-6**	**SA-U-6**
Alanine	112	123	121	123	122
Arginine	53	52	52	53	52
Aspartic acid/asparagine	51	47	47	48	47
Cysteine	0	0	0	0	0
Glutamine/glutamic acid	72	69	68	68	68
Glycine	327	333	336	334	336
Histidine	4	4	4	4	4
Isoleucine	13	11	10	11	11
Leucine	25	23	21	22	22
Lysine	28	26	26	26	26
Hydroxylysine	6	6	6	6	6
Methionine	12	12	12	12	12
Phenylalanine	14	13	13	13	13
Hydroxyproline	78	81	84	79	82
Proline	116	118	120	118	119
Serine	37	35	35	35	35
Threonine	25	23	23	23	23
Tyrosine	4	3	3	3	3
Valine	23	21	19	22	19
Total residues	1000	1000	1000	1000	1000
Imino acid	194	199	204	197	201

N-U: prior-ultrasonication without acid pretreatment, A-C: acetic acid pretreatment, A-U: acetic acid pretreatment and prior-ultrasonication, SA-C: sulfuric acid + acetic acid pretreatment, SA-U: sulfuric acid + acetic acid pretreatment and prior-ultrasonication. Number of 6 represents the extraction time (6 h).

5.5.4. ATR-FTIR

FTIR spectra of N-U-6, A-C-6, SA-C-6, A-U-6 and SA-U-6 are depicted in Figure 3. All the samples exhibited similar spectral profile. The spectra of all golden carp skin gelatins had the major peaks associated with amide bands I, II, III, A and B, which were similar to those of gelatin from other aquatic sources (Kittiphattanabawon

et al., 2010; Sinthusamran *et al.*, 2014). It is well established that amide I band is associated with C═O stretching vibration coupled to CN stretch and NH bending modes occurring in the range of 1600 to 1700 cm^{-1} (Nagarajan *et al.*, 2012). N-U-6, A-C-6, A-U-6, SA-C-6 and SA-U-6 showed the presence of amide band I at the wavenumber of 1642.3, 1633.6, 1632.9, 1636.7 and 1633.1 cm^{-1}, respectively. Yakimets *et al.* (2005) testified that absorption band of amide I at wavenumber of 1634.7 cm^{-1} represents gelatin with distinctive coiled conformation. The differences in frequency of amide I among the samples were mainly attributed to the dissimilar conformation of polypeptide chains. The lower wavenumber of A-C-6, A-U-6 and SA-U-6, compared to those of N-U-6 and SA-C-6 indicated that C═O stretching vibration was reduced, possibly due to the occurrence of hydrogen bond between N─H bonding responsible for stabilizing triple helical structure (Zanaboni *et al.*, 2000). Higher wavenumber of SA-C-6 was due to the lower molecular order as affected by the type of acid (H^+ concentration and final pH of solution) used for pretreatment (Al-Saidi *et al.*, 2012).

The amide II bands of N-U-6, A-C-6, A-U-6, SA-C-6 and SA-U-6 were found at the wavenumbers of 1549.7, 1543.8, 1540.5, 1546.4 and 1543.4 cm^{-1}, respectively. Amide II vibration ranged from 1500 to 1600 cm^{-1}, attributing to stretching vibration of C─N groups and in-plane bending modes of N─H of the peptide groups (Al-Saidi *et al.*, 2012). The frequency of A-C-6, A-U-6 and SA-U-6 were lower, compared to N-U-6 and SA-C-6, indicating that more proportion of N─H was involved in hydrogen bonding with that of adjacent α-chains. Moreover, amide III band was observed at 1246.7, 1239.2, 1239.4, 1239.0 and 1239.1 cm^{-1} for N-U-6, A-C-6, A-U-6, SA-C-6 and SA-U-6, respectively. The amide III is the combination of N─H deformation and C─N stretching as well as wagging vibrations of CH_2 groups. The amplitude of amide III vibrations of A-C-6, A-U-6, SA-C-6 and SA-U-6 were similar to those of gelatins from unicorn leatherjacket skin (Kaewruang *et al.*, 2013) and bigeye snapper (Benjakul *et al.*, 2010), and were higher than collagen from golden carp skin (Ali *et al.*, 2017). The higher amplitude was suggested to be due to conversion of α-helix structure to random coils upon heating. The changes were linked to the denaturation of collagen to gelatin with the loss in triple helical structure (Nagarajan *et al.*, 2012).

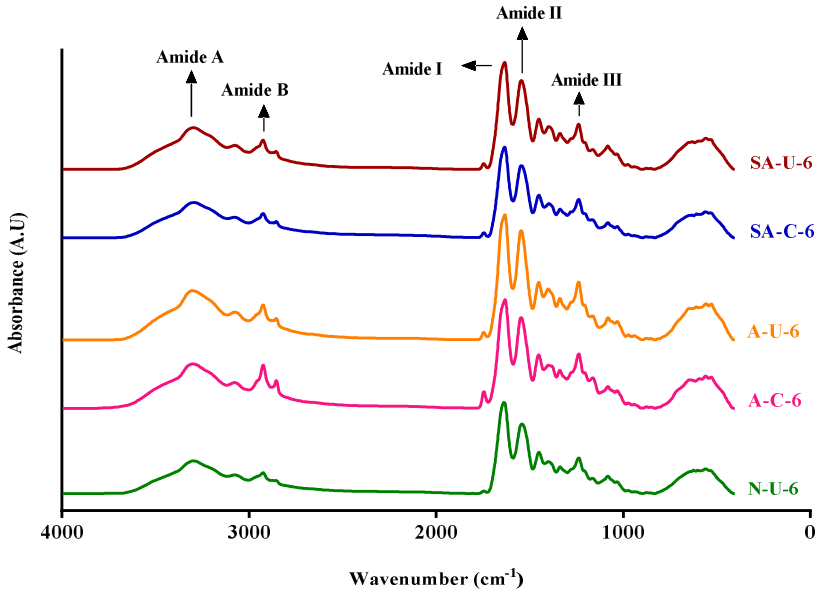

Figure 27. FTIR spectra of gelatin from the skin of golden carp with the selected pretreatment and extraction conditions. N-U: prior-ultrasonication without acid pretreatment, A-C: acetic acid pretreatment, A-U: acetic acid pretreatment and prior-ultrasonication, SA-C: sulfuric acid + acetic acid pretreatment, SA-U: sulfuric acid + acetic acid pretreatment and prior-ultrasonication.

Number of 6 represents the extraction time (6 h).

Amide A band, corresponding to the stretching vibrations of N─H group, appeared at 3297.1, 3290.8, 3287.4, 3296.6 and 3293.8 cm^{-1} for N-U-6, A-C-6, A-U-6, SA-C-6 and SA-U-6, respectively. Normally, stretching vibration of free N─H group occurs within the range of 3400─3440 cm^{-1} (Sinthusamran *et al.*, 2014). When the N─H group of peptide is involved in a hydrogen bonding, the wavenumber shifts to lower frequency (Zanaboni *et al.*, 2000). Varying wavenumbers among samples suggested the formation of hydrogen bonding at different degrees in various samples. The amide band B was observed in 2924.1, 2924.4, 2924.7, 2924.5 and 2924.5 cm^{-1} for N-U-6, A-C-6, A-U-6, SA-C-6 and SA-U-6, respectively, due to asymmetrical stretching of both ═C─H and $─NH_3^+$. The comparable frequency of all the samples suggested that the molecular structure and functional groups of golden carp skin gelatins were not drastically affected by the ultrasound waves or acids used for pretreatment.

5.5.5. Gelling and melting temperature

The gelling and melting temperatures of N-U-6, A-C-6, SA-C-6, A-U-6 and SA-U-6 are shown in Table 1. Thermal transition was examined by change in phase angel (δ) while cooling (40–5 °C) and subsequently heating (5–40 °C). Gelling temperatures of all the samples ranged from 13.26 to 21.76 °C. It was noted that gelling temperature was affected by prior-ultrasonication, especially the gelatins from skin with acetic acid pretreatment. Higher gelling temperature was obtained for all samples in comparison with commercial fish gelatin (15.84 °C) (Gudmundsson, 2002). However, gelling temperatures were lower than bovine gelatin (24.71 °C) (Sinthusamran *et al.*, 2014). The gelling temperature of SA-U-6 sample tended to be higher than SA-C-6. Thus, ultrasound had an impact on gelling property of extracted gelatin to some extent. The higher phase transition value indicated the development of three-dimensional network formation of stronger gel matrix through hydrogen bond (Yakimets *et al.*, 2005). Generally, gelling temperature was affected by comparative content and molecular weight of α-, β- and γ-chains (Nagarajan *et al.*, 2012). On the other hand, N-U-6 sample demonstrated the lowest gelling temperature (13.26 ± 0.27 °C), due to the presence of lower MW components (Figure 2). The obtained results were in accordance with Kittiphattanabawon *et al.* (2010) who reported that lower gelling temperature as well as longer gelling time were related with low molecular weight protein components. Melting temperature of A-U-6 and SA-U-6 samples were higher than others ($p < 0.05$). The melting temperatures of samples with prior-ultrasonication process was higher ($p < 0.05$) when compared to commercial fish gelatin (25.10 °C) and comparable to the gelatin from skin of bovine (29.7 °C) and porcine (32.3 °C) (Gudmundsson, 2002). Moreover, the melting temperature of gelatin was reported to relate with the imino acid content in the original collagen (Nagarajan *et al.*, 2012). Thermal stability of gelatin corresponds to the number of imino acids, which is higher in mammals and warm water fish species (Ali *et al.*, 2017; Kaewruang *et al.*, 2013; Zanaboni *et al.*, 2000). The higher gelling and melting point of A-U-6 and SA-U-6 were in agreement with the higher imino acid contents (Table 2). The results suggested that prior-ultrasonication used during extraction process of gelatin affected the gelling and melting point of gelatin from skins of golden carp.

5.5.6. Gel properties

5.5.6.1. Color

Colors of gels prepared with gelatins extracted at different pretreatments and extraction conditions expressed in terms of L^*, a^* and b^* are presented in Table 3. The gelatin from golden carp skin extracted with pretreatment using acetic acid showed higher lightness (L^*) than those from skin pretreated using sulfuric acid + acetic acid. Higher lightness value was detected for gelatin from golden carp skin with prior-ultrasonication ($p < 0.05$). Additionally, the increase in lightness of all gelatin gels was observed when higher extraction time was used. The decrease in a^* and b^* values were obtained in gelatin gels when prior-ultrasonication was implemented. It was noted that greater yellowness (b^*) was detected when the extraction time was increased.

Table 10. Color of gelatin gel from the skin of golden carp with different pretreatment and extraction conditions.

Sample	Time (h)	Color value			
		L^*	a^*	b^*	ΔE^*
Control	6	-	-	-	-
N-U	3	-	-	-	-
	6	42.06 ± 0.06^{bc}	-2.26 ± 0.12^{c}	1.79 ± 0.36^{e}	50.8 ± 0.07^{f}
A-C	3	28.54 ± 0.02^{d}	-1.82 ± 0.03^{d}	1.85 ± 0.11^{cd}	56.81 ± 0.14^{e}
	6	33.88 ± 0.08^{c}	-2.26 ± 0.14^{c}	2.26 ± 0.26^{b}	58.94 ± 0.06^{d}
A-U	3	46.58 ± 0.12^{b}	-3.10 ± 0.42^{b}	1.11 ± 0.08^{f}	46.21 ± 0.61^{g}
	6	59.81 ± 0.23^{a}	-3.97 ± 0.08^{a}	3.48 ± 0.14^{a}	34.06 ± 0.48^{h}
SA-C	3	18.31 ± 0.11^{f}	-0.78 ± 0.07^{e}	1.83 ± 0.13^{cd}	75.32 ± 0.47^{a}
	6	19.24 ± 0.47^{f}	-0.99 ± 0.04^{e}	1.86 ± 0.19^{c}	73.58 ± 0.08^{b}
SA-U	3	20.68 ± 0.05^{ef}	-1.48 ± 0.03^{de}	0.58 ± 0.09^{g}	72.13 ± 0.12^{c}
	6	42.06 ± 0.23^{bc}	-3.19 ± 0.57^{ab}	1.79 ± 0.44^{e}	50.8 ± 0.08^{f}

Mean ± SD from triplicate determination.
Different superscript letters in the same column indicate significant difference ($p < 0.05$).
Control: without acid/ultrasound pretreatment, N-U: prior-ultrasonication without acid pretreatment, A-C: acetic acid pretreatment, A-U: acetic acid pretreatment and prior-ultrasonication, SA-C: sulfuric acid + acetic acid pretreatment, SA-U: sulfuric acid + acetic acid pretreatment and prior-ultrasonication.
Number of 3 and 6 represents the extraction time (3 and 6 h).

Furthermore, longer extraction time at 55 °C more likely generated free amino group to some extent in the resulting gelatin. Those free amino groups could take part in non-enzymatic browning reaction with carbonyl compounds present in skin, resulting in the increase in yellowness of gelatin (Nie *et al.*, 2013). Furthermore, higher extraction time in conjunction with prior-ultrasonication resulted in higher efficiency as evidenced by the increased extraction yield. As a consequence, the gelatins turned to be more yellowish in color. Thus, prior-ultrasonication used as well as longer extraction time affected the gel color of gelatin extracted from skin of golden carp.

5.5.6.2. Gel Strength

Gelatin gels extracted using different acid pretreatments and extraction conditions had varying gel strength (Figure 4). Gel strength increased as the extraction time increased from 3 to 6 h, regardless of pretreatment conditions used ($p < 0.05$). The gel strength of gelatin gel varied substantially with the acid pretreatments used for swelling process. Gel strength of gelatin extracted by conventional method using acetic acid pretreatment with extraction times of 3 and 6 h were 190 and 221 g, respectively. Similar results were also reported for gelatin from skin of mackerel, pretreated using different acids (Khiari *et al.*, 2017). N-U-6 sample exhibited the lowest gel strength (128 g) ($p < 0.05$). For A-C-6 and SA-C-6 samples, similar gel strength was found (221 and 210 g, respectively). Higher gel strength was found for gelatins extracted for skin subjected to prior-ultrasonication for both extraction times of 3 and 6 h. Amongst all the gelatins, the highest gel strength (241 g) was obtained for the sample A-U-6 sample ($p < 0.05$). This could be related with higher proportion of α- and β-chains. Generally, gelatins with the shorter chain length are inefficient to form strong inter-junction zone through hydrogen bond, hydrophobic interaction or ionic interactions. On the other hand, gelatins with longer chain length are able to align or self-aggregate more easily (Kittiphattanabawon *et al.*, 2010; Sinthusamran *et al.*, 2014).

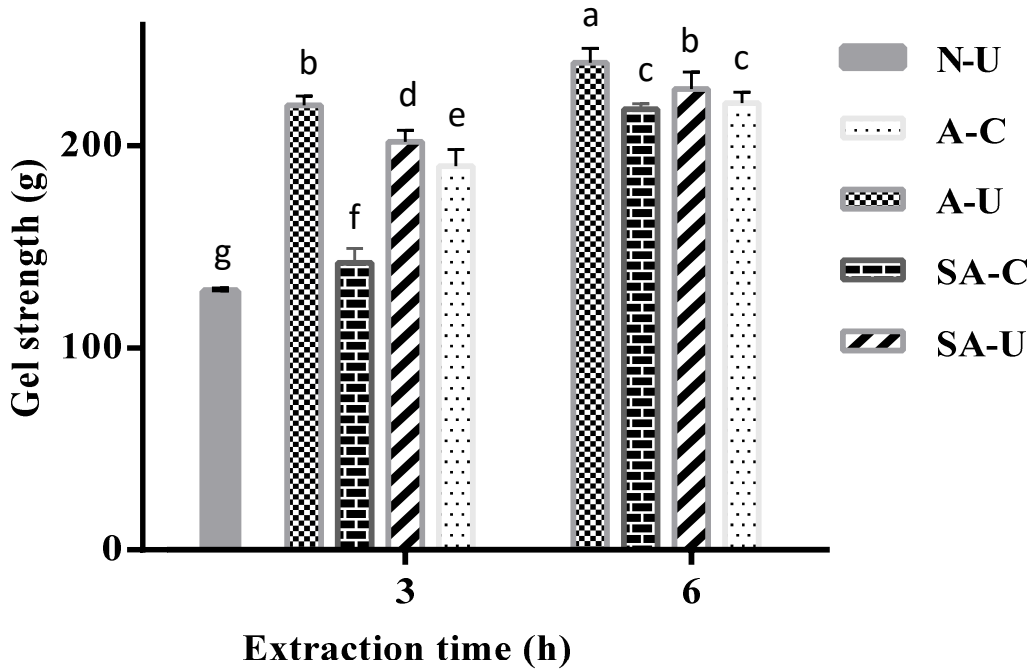

Figure 28. Gel strength of gelatin gels from the skin of golden carp with the selected pretreatment and extraction conditions. Bars represent standard deviation (n = 3). N-U: prior-ultrasonication without acid pretreatment, A-C: acetic acid pretreatment, A-U: acetic acid pretreatment and prior-ultrasonication, SA-C: sulfuric acid + acetic acid pretreatment, SA-U: sulfuric acid + acetic acid pretreatment and prior-ultrasonication.

Moreover, the difference in gel strength and network formation was also governed by the intrinsic factors such as molecular weight distribution and amino acid composition (Sae-leaw and Benjakul, 2015). The increased gel strength was also proportional to the higher imino acid content (proline and hydroxyproline). Particularly, the hydroxyl group of hydroxyproline has an significant role in formation of inter-chain hydrogen bond by means of connecting water molecule and direct hydrogen bonding via carbonyl group (Zanaboni *et al.*, 2000). The slightly lower gel strength of SA-U-6, compared to A-U-6, was reflected by the appearance of protein with MW of 76-78 kDa. Gelatins with longer chain length could form higher gel network, thereby increasing gelling ability. Therefore, extraction time and acid pretreatment as well as prior-ultrasonication demonstrated an important role in gel-forming ability of gelatin from golden carp skin.

5.5.6.3. Microstructures

Microstructures of gels from N-U-6, A-C-6, SA-C-6, A-U-6 and SA-U-6 samples are shown in Figure 5. All the gelatin gels showed different network, thickness of strands and voids. Gelatins from golden carp skin pretreated with acetic acid (A-C-6 and A-U-6) displayed the finer and ordered networks with smaller voids. Conversely, sulfuric acid + acetic acid pretreated gelatins (SA-C-6 and SA-U-6) had slightly coarser structure with larger voids and strands. This result was in agreement with Zhou and Regenstein (2005) who reported that the gel network is dependent on the physicochemical properties of gelatin, which is influenced by the pretreatment conditions. Acid ionization constant and available ionized H concentration during pretreatment probably affected the skin of golden carp differently, leading to difference in release of different components (Zanaboni *et al.*, 2000). Additionally, the gel network of samples from skin with prior-ultrasonication not only exhibited denser and more uniform in structure but also had smaller voids. This was related well with gel strength. Gelatin gels possessing these characteristics are able to form stronger networks (Sinthusamran *et al.*, 2014). It was noted that A-U-6 samples displayed more inter-connected protein chains than A-C-6 samples. This coincided with the stronger gel matrix in the former. It is well known that the gelatin with higher contents of α-, β- and γ-chain are able to form stronger network than those with hydrolyzed/fragmented gelatin molecules (Khiari *et al.*, 2017; Sinthusamran *et al.*, 2014; Zanaboni *et al.*, 2000). The gelatin extracted by mild acid pretreatment in conjugation with prior-ultrasonication could form the inter-connected strands to develop the stronger network as shown by higher gel strength. Compared to other gelatins gels, N-U-6 sample showed the coarser gel with large voids in structure. This result indicated that the improper pretreatment conditions could yield the gelatin which formed a gel with weaker network and less inter-connected zones.

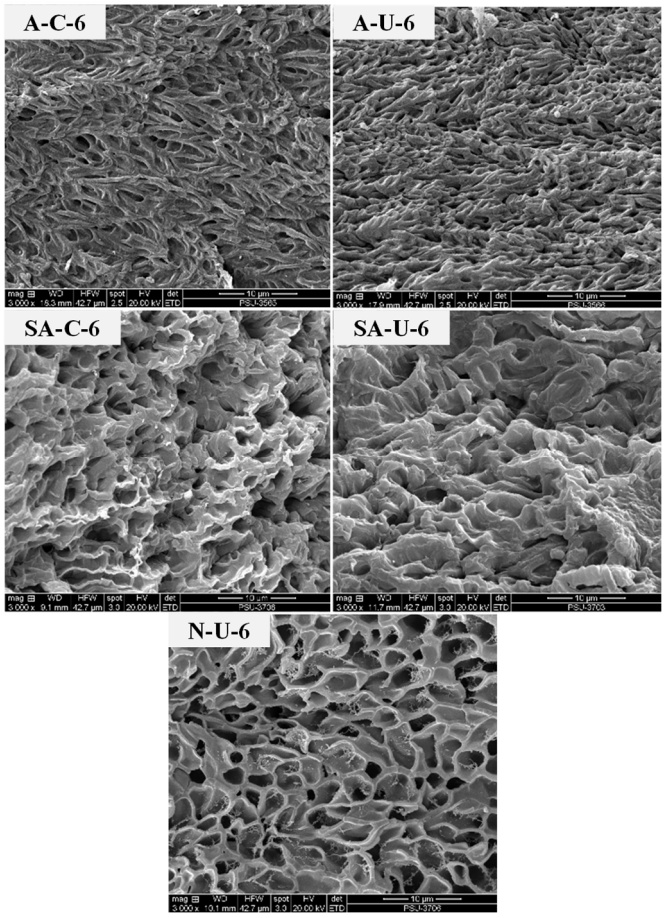

Figure 29. Microstructure of gelatin gels from the skin of golden carp with the selected pretreatment and extraction conditions. Magnification: 3000x. N-U: prior-ultrasonication without acid pretreatment, A-C: acetic acid pretreatment, A-U: acetic acid pretreatment and prior-ultrasonication, SA-C: sulfuric acid + acetic acid pretreatment, SA-U: sulfuric acid + acetic acid pretreatment and prior-ultrasonication.

Number of 6 represents the extraction time (6 h).

5.6. Conclusions

Acid pretreatment in combination with prior-ultrasonication improved the extraction efficiency of gelatin, compared to the conventional method. Acid types and extraction time had the impact on properties of gelatin from golden carp skin. The gelatin extracted without acid pretreatment but with prior-ultrasonication showed negligible yield and poor gel properties. Prior-ultrasonication of both acid pretreated types (A-U-6 and SA-U-6) contained higher amounts of glycine and imino acid

residues. Prior-ultrasonication was found to improve the gelling properties with stronger gel network, regardless of acid types. Gelling and melting temperatures of gelatins from the skin of golden carp were greater than that of commercial fish gelatin. Therefore, prior-ultrasonication in combination with acid pretreatment particularly using sulfuric acid/acetic acid could be a useful technique to enhance the extraction efficiency and gelling properties of gelatin extracted from fish processing byproducts, especially golden carp skin.

5.7. References

Al-Saidi, G., Al-Alawi, A., Rahman, M. and Guizani, N. 2012. Fourier transform infrared (FTIR) spectroscopic study of extracted gelatin from shaari (*Lithrinus microdon*) skin: effects of extraction conditions. International Food Research Journal. 19: 1167-1173.

Ali, A. M. M., Benjakul, S., Prodpran, T. and Kishimura, H. 2017. Extraction and characterisation of collagen from the skin of golden carp (*Probarbus Jullieni*), a processing by-product. Waste and Biomass Valorization. 9: 783-791.

Arzeni, C., Martínez, K., Zema, P., Arias, A., Pérez, O. E. and Pilosof, A. M. R. 2012. Comparative study of high intensity ultrasound effects on food proteins functionality. Journal of Food Engineering. 108: 463-472.

B.S.I. 1975. Methods for Sampling and Testing Gelatine (Physical and Chemical Methods). *In* British Standards Institution.

Badii, F. and Howell, N. K. 2006. Fish gelatin: structure, gelling properties and interaction with egg albumen proteins. Food Hydrocolloids. 20: 630-640.

Benjakul, S., Thiansilakul, Y., Visessanguan, W., Roytrakul, S., Kishimura, H., Prodpran, T. and Meesane, J. 2010. Extraction and characterisation of pepsin solubilised collagens from the skin of bigeye snapper (*Priacanthus tayenus* and *Priacanthus macracanthus*). Journal of the Science of Food and Agriculture. 90: 132-138.

Chomarat, N., Robert, L., Seris, J. and Kern, P. 1994. Comparative efficiency of pepsin and proctase for the preparation of bovine skin gelatin. Enzyme and Microbial Technology. 16: 756-760.

Gennadios, A., Hanna, M. A. and Kurth, L. B. 1997. Application of edible coatings on meats, poultry and seafoods: a review. LWT- Food Science and Technology. 30: 337-350.

Giménez, B., Turnay, J., Lizarbe, M., Montero, P. and Gómez-Guillén, M. 2005. Use of lactic acid for extraction of fish skin gelatin. Food Hydrocolloids. 19: 941-950.

Gornall, A. G., Bardawill, C. J. and David, M. M. 1949. Determination of serum proteins by means of the biuret reaction. Journal of Biological Chemistry. 177: 751-766.

Gudmundsson, M. 2002. Rheological properties of fish gelatins. Journal of Food Science. 67: 2172-2176.

Ishida, K., Kuroda, R., Miwa, M., Tabata, Y., Hokugo, A., Kawamoto, T., Sasaki, K., Doita, M. and Kurosaka, M. 2007. The regenerative effects of platelet-rich plasma on meniscal cells in vitro and its in vivo application with biodegradable gelatin hydrogel. Tissue Engineering. 13: 1103-1112.

Jiang, X., Chang, M., Wang, X., Jin, Q. and Wang, X. 2014. Effect of ultrasound treatment on oil recovery from soybean gum by using phospholipase C. Journal of Cleaner Production. 69: 237-242.

Kaewruang, P., Benjakul, S. and Prodpran, T. 2013. Molecular and functional properties of gelatin from the skin of unicorn leatherjacket as affected by extracting temperatures. Food Chemistry. 138: 1431-1437.

Khiari, Z., Rico, D., Martin-Diana, A. B. and Barry-Ryan, C. 2017. Valorization of fish by-products: rheological, textural and microstructural properties of mackerel skin gelatins. Journal of Material Cycles and Waste Management. 19: 180-191.

Kittiphattanabawon, P., Benjakul, S., Visessanguan, W. and Shahidi, F. 2010. Comparative study on characteristics of gelatin from the skins of brownbanded bamboo shark and blacktip shark as affected by extraction conditions. Food Hydrocolloids. 24: 164-171.

Morales, J., Montero, P. and Moral, A. 2000. Isolation and partial characterization of two types of muscle collagen in some cephalopods. Journal of Agricultural and Food Chemistry. 48: 2142-2148.

Nagarajan, M., Benjakul, S., Prodpran, T., Songtipya, P. and Kishimura, H. 2012. Characteristics and functional properties of gelatin from splendid squid (*Loligo formosana*) skin as affected by extraction temperatures. Food Hydrocolloids. 29: 389-397.

Nie, S., Huang, J., Hu, J., Zhang, Y., Wang, S., Li, C., Marcone, M. and Xie, M. 2013. Effect of pH, temperature and heating time on the formation of furan in sugar–glycine model systems. Food Science and Human Wellness. 2: 87-92.

Sae-leaw, T. and Benjakul, S. 2015. Physico-chemical properties and fishy odour of gelatin from seabass (*Lates calcarifer*) skin stored in ice. Food Bioscience. 10: 59-68.

Saha, D. and Bhattacharya, S. 2010. Hydrocolloids as thickening and gelling agents in food: a critical review. Journal of Food Science and Technology. 47: 587-597.

Sinthusamran, S., Benjakul, S. and Kishimura, H. 2014. Characteristics and gel properties of gelatin from skin of seabass (*Lates calcarifer*) as influenced by extraction conditions. Food Chemistry. 152: 276-284.

Soria, A. C. and Villamiel, M. 2010. Effect of ultrasound on the technological properties and bioactivity of food: a review. Trends in Food Science & Technology. 21: 323-331.

Vercet, A., Burgos, J., Crelier, S. and Lopez-Buesa, P. 2001. Inactivation of proteases and lipases by ultrasound. Innovative Food Science & Emerging Technologies. 2: 139-150.

Yakimets, I., Wellner, N., Smith, A. C., Wilson, R. H., Farhat, I. and Mitchell, J. 2005. Mechanical properties with respect to water content of gelatin films in glassy state. Polymer. 46: 12577-12585.

Yang, H., Wang, Y., Zhou, P. and Regenstein, J. M. 2008. Effects of alkaline and acid pretreatment on the physical properties and nanostructures of the gelatin from channel catfish skins. Food Hydrocolloids. 22: 1541-1550.

Zanaboni, G., Rossi, A., Onana, A. M. T. and Tenni, R. 2000. Stability and networks of hydrogen bonds of the collagen triple helical structure: influence of pH and chaotropic nature of three anions. Matrix Biology. 19: 511-520.

Zhou, P. and Regenstein, J. M. 2005. Effects of alkaline and acid pretreatments on Alaska pollock skin gelatin extraction. Journal of Food Science. 70: 392-396.

CHAPTER 6

SQUALENE FROM FISH LIVERS EXTRACTED BY ULTRASOUND ASSISTED DIRECT *IN-SITU* SAPONIFICATION: PURIFICATION AND MOLECULAR CHARACTERISTICS

6.1. Abstract

Squalene from livers of four fish species *L. calcarifer, K. pelamis, C. sorrah* and *C. griseum* were extracted using ultrasound-assisted direct *in-situ* saponification (U-DS) process, in comparison with the conventional process. Box-Behnken experimental design (BBD) was adopted to optimize the independent variables including biomass/methanol ratio (1:3 to 1:9, w/v), 50% KOH volume (1–12 ml) and sonication time (0–30 min) over the unsaponifiable yield. With conventional process, the yield of squalene was 0.10±0.02 to 5.52±0.06 g (100 g)$^{-1}$, whereas U-DS process rendered the yield of 0.13±0.03 to 6.86±0.05 g (100 g)$^{-1}$, depending on the fish species. After extraction, squalene was further concentrated up to ≥ 60% of purity from all the fish species via fractional crystallization (yield of squalene concentrate ranged from 48.35-74.49%) and purified using a silica gel column with a maximum recovery up to 98%. For all the fractions, components were examined by thin layer chromatography (TLC). Squalene was qualitatively and quantitatively analyzed using reversed-phase high-performance liquid chromatography (RP-HPLC). Entire extraction processes yielded squalene with a purity of ≥ 94%. Fourier transform infrared (FTIR) analysis confirmed the native structure of squalene with six nonconjugated bonds, suggesting no degradation of squalene taken place during U-DS process. Thus U-DS process along with fractionation and purification could be used for recover the squalene from fish livers.

6.2. Introduction

Squalene ($C_{30}H_{50}$) is a triterpene commonly found in plants, animals and humans. Squalene is an acyclic and highly unsaturated hydrocarbon with six nonconjugated double bonds (Nenadis and Tsimidou, 2002). It is pale yellow in color

with low melting and high boiling temperature (-70 °C and 285 °C, respectively) (Ortega *et al.*, 2012). Squalene is a key intermediate in formation of bacterial hopanoids and eukaryotic sterols. In human, squalene is present in sebum at highest concentration (~13%) and play a major role in quenching singlet oxygen in ultraviolet (UV) associated skin damage and lipid peroxidation (Spanova and Daum, 2011). Owing to its unique functional and structural properties, squalene has numerous applications in nutraceutical, pharmaceutical, cosmetics and food industries (Bindu *et al.*, 2015; Spanova and Daum, 2011). Due to its high commercial demand, the global production of squalene has increased to 2500 tons per year in 2013 with a value of 93 million dollars and is expected to rise to 241.9 million dollars by year 2022 (Research, 2017; Rosales-García *et al.*, 2017). Squalene is produced at 1050 ton per year from plants (chiefly from olive oil); 1000 tons per year is recovered from shark liver (a processing by-product) and the remainder (450 tons per year) is produced synthetically via genetically modified microorganisms (e.g. Amyris, Inc. (California, USA) and Biossance (California, USA). Squalene is mainly produced by extraction of oil, followed by molecular distillation, super or sub-critical gases as well as high-pressure column purification method (Ghimire *et al.*, 2016; Popa *et al.*, 2015; Spanova and Daum, 2011). Extraction using super-critical CO_2 with ethanol as extractant was reported to be the cost effective procedure for extraction of squalene from olives (Cristóbal *et al.*, 2018).

Production of squalene from vegetable oil as a minor constituent (10-560 mg $(100\ g)^{-1}$ of oil) with low yield and economic loss (Lozano-Grande *et al.*, 2018). Among the microbial sources, *Saccharomyces cerevisiae* is the most promising strain for squalene production. Nonetheless, it takes a long cultivation time with low yield (1 to 4.6% on the dry weight basis), thus being less suitable for industrial scale (Ghimire *et al.*, 2016). Apart from sharks, fresh and marine water fish have been reported to contain squalene at substantial amounts (70-1803 mg kg^{-1} based on wet weight), especially from the visceral biomass (Bavisetty and Narayan, 2015; KopiCoVá and VaVreiNoVá, 2007). Squalene is chiefly synthesized and accumulated in the liver and transported to the site of requirement (Blondin *et al.*, 1966).

Most of the production cost and time are mainly governed by extraction and concentration steps (using saponification). Another major concern of these steps is related with the large quantities of solvents required (Li *et al.*, 2017). Basically, direct *in-situ* saponification has been implemented, in which fatty acids in biomass are allowed to directly react with alcohol in the presence of alkali catalyst to form soap (Cavonius *et al.*, 2014). Additionally, the elimination of water from biomass is not critical for saponification reaction (He *et al.*, 2002).

Ultrasonication has gained high attention particularly in the field of extraction. When the sound waves generate compression and decompression regions, several mechanisms such as mass transfer, sonoporation, sonocapillary effect, fragmentation, destruction and detexturation occur (Chemat *et al.*, 2017). The overall impact of these mechanisms results in disruption of the cell membrane or modification of compounds, and the extent of action depends on the process parameters. Ultrasonication has been employed to achieve high extraction yield with shorter processing time and is often suitable for recovery of thermolabile and natural antioxidant compounds such as collagen, carotenoids, phenolics and other bioactive compounds (Ali *et al.*, 2018b; Vilkhu *et al.*, 2008). Furthermore, ultrasonication has its ability to generate high-intensity cavitation zones (Peshkovsky *et al.*, 2013). With its advantages, ultrasonication can be a practical approach to achieve simultaneous lipid extraction and saponification in an aqueous environment for production of squalene from fish livers. Thus, the present study aimed to develop ultrasound assisted direct *in-situ* saponification for extraction of unsaponifiable matter (rich in squalene) from spot-tail shark liver (biomass) and to optimize the extraction conditions using response surface methodology (RSM). Additionally, squalene was purified through fractional crystallization and column chromatography, and further characterized.

6.3. Objective

To develop ultrasound assisted direct *in-situ* saponification of wet liver biomass for extraction of squalene and to optimize the reaction conditions using response surface methodology (RSM). Additionally, the squalene was also purified through fractionation and column chromatography, and further characterized.

6.4. Materials and Methods

6.4.1. Chemicals

Analytical grade potassium hydroxide was obtained from Merck (Darmstadt, Germany). Methanol, *n*-hexane and chloroform were procured from RCL Lab-Scan (Bangkok, Thailand). HPLC-grade solvents including acetonitrile, *n*-hexane, ethanol and methanol were purchased from RCL Lab-Scan (Bangkok, Thailand). Squalene (≥98%), cholesterol (≥99%), silica gel (for column chromatography, 70–230 mesh) and Brilliant blue R were procured from Sigma-Aldrich (St. Louis, MO, USA).

6.4.2. Collection of raw material

Sea bass (*Lates calcarifer*) liver was purchased from a local market in Hat Yai (Songkhla, Thailand). Skipjack tuna (*Katsuwonus pelamis*) liver was gifted by Songkla Canning Public Co., Ltd., Songkhla, Thailand. Livers of spot-tail shark (*Carcharhinus sorrah*) and grey bamboo shark (*Chiloscyllium griseum*) were obtained from the fish dock located at Songkhla province, Thailand. The livers (20 kg) were packed in polyethylene bags (5 kg skins bag^{-1}) and then placed in polystyrene box containing ice, with an ice/liver ratio of 3:1 (w/w). The samples were transported to the Department of Food Technology, Prince of Songkla University, Hat Yai, within 2 h. Upon arrival, they were kept at -20 °C until use. The storage time was not longer than a month. Liver samples were ground and determined for proximate composition (Table 1) following the AOAC method (AOAC, 2000).

6.4.3. Extraction of squalene by conventional process

Extraction and saponification experiments were conducted in inert atmosphere by flushing nitrogen gas. All the experiments were carried could in amber glassware to prevent photo oxidation of lipids.

6.4.3.1. Oil extraction

Firstly, oils from different livers were extracted by the Bligh and Dyer method (Bligh and Dyer, 1959). Liver sample (100 g) was homogenized with 400 ml of the solvent mixture of chloroform:methanol:water (1:2:1, v/v/v) at a speed of 14000

rpm using an IKA Labortechnik homogeniser (Selangor, Malaysia) for 3 min at 25 ± 2 °C. To the homogenate, 100 ml of chloroform will be added and homogenized at the same speed for another 2 min and then centrifuged at 3000 ×g for 15 min. The liquid phase was collected and chloroform layer will be separated using separating flask. The separated chloroform phase will be dried with anhydrous sodium sulphate and filtered using Whatman No. 1 filter paper (Whatman International Ltd., Maidstone, England). The solvent was evaporated using a rotary evaporator model EYELA N-1000 (Tokyo Rikakikai, Co., Ltd., Tokyo, Japan) at 37 °C. The obtained oils were then stored in airtight amber bottles at −40 °C after flushing the headspace using nitrogen gas.

6.4.3.2. Saponification

Saponification of liver oils was carried out according to the method of He *et al.* (2002), with some modifications. Liver oil (1 g) was dissolved in 10 ml of 95% methanol and 1.5 ml of 50% aqueous KOH and then refluxed for 60 min at 70 °C. The reaction was ended by diluting with 25 ml of distilled water. The unsaponifiable components were extracted twice with 8 ml of hexane each time and were washed with 25 ml of 10% ethanol until the wash medium had the neutral pH. Filtration and evaporation of hexane fraction were carried out using Whatman No. 1 filter paper (Whatman International Ltd., Maidstone, England). The solvent was evaporated using a rotary evaporator model EYELA N-1000 (Tokyo Rikakikai, Co., Ltd., Tokyo, Japan) at 37 °C and the residual solvent was flushed using nitrogen gas. The unsaponifiable fraction obtained was expressed as g $(100\ g)^{-1}$ of raw liver.

6.4.4. Extraction of squalene by ultrasound-assisted *in-situ* direct saponification (U-DS) process

6.4.4.1. Response surface methodology (RSM)

Spot-tail shark liver was used for optimization experiment. Before extraction, livers were ground using a blender until homogeneity was attained. The experimental plan was designed based on three factors/level design, referred to as a Box-Behnken design (Table 2). Ground liver (100 g) was added with 95% methanol at different biomass/solvent ratios (1:3, 1:6 and 1:9, w/v), 50% aqueous KOH at different

volumes (1–12 ml) in wide mouth glass jar with lid (800 and 1600 ml) and sonicated (0–30 min) in an inert atmosphere. Thereafter, 30 ml of *n*-hexane were added to extract unsaponifiables in the homogenate. The mixture was subjected to ultrasonication at an amplitude of 80%. An ultrasound processor model Vibra–Cell (Sonics & Material, Inc, Newtown, CT, USA) with a 13 mm flat tip prob with a fixed frequency and power of 20 kHz and 750 W, respectively, was used. The temperature of the mixture was maintained at 40 °C using a water bath (EYELA, Tokyo Rikakikai, Co., Ltd., Tokyo, Japan) and was monitored using a digital thermometer (model DE-3004 Type K, DER EE Electrical Instruments Co., Ltd., Chung Ho, Taipei, Taiwan). Ultrasound was operated in a pulse mode at 10 s acting and 5 s resting time, to avoid overheating. The solvent (hexane phase) was separated, washed and dried as described above, and the yield of unsaponifiable matter (dependent variable) was expressed as g (100 g)$^{-1}$ of raw liver.

Analysis of experimental data was done using statistical software Design-Expert 8.0.7.1 (Stat-Ease Inc., Minneapolis, USA). Analysis of experimental data and regression coefficients of linear and quadratic terms were evaluated through ANOVA. Probability (P) and F-test values were determined to assess the statistical implication. The precision of the polynomial model was verified by determination of coefficient (R^2), adjusted determination coefficient (adjR^2) and coefficient of variance (CV%). A quadratic model is given in the Eq. below:

$$Y^e = b_0 + b_1X_1 + b_2X_2 + b_3X_3 + b_{12}X_1X_2 + b_{13}X_1X_3 + b_{23}X_2X_3 + b_{11}X_1^2 + b_{22}X_2^2 + b_{33}X_3^2 \quad (1)$$

where Y^e is the response for extraction yield, b_0 is intercept constant; b_1, b_2 and b_3 are linear and quadratic coefficients of X_1, X_2 and X_3 independent variables, respectively (50% aqueous KOH, biomass/methanol ratio, volume and sonication time, respectively). The polynomial equation was expressed in terms of a contour plot, to explain the relationship between experimental variables and dependent variables.

Table 11. Box-Behnken design for ultrasound assisted direct *in-situ* saponification (U-DS) of liver tissue of spot-tail shark (*C. sorrah*) using random surface methodology (RSM).

Run	Factor X_1 50% aqueous KOH (ml)	Factor X_2 biomass/methanol Ratio (w/v)	Factor X_3 Time (min)
1	3.00	3.00	15.00
2	0.10	6.00	30.00
3	1.55	3.00	30.00
4	3.00	9.00	15.00
5	3.00	6.00	0.00
6	3.00	6.00	30.00
7	0.10	3.00	15.00
8	1.55	9.00	0.00
9	1.55	6.00	15.00
10	1.55	3.00	0.00
11	0.10	6.00	0.00
12	0.10	9.00	15.00
13	1.55	9.00	30.00
14	1.55	6.00	15.00
15	1.55	6.00	15.00

The process conditions were optimized by multiple response analysis using a desirability function (D) to verify if a particular response (Y) was maximized to the target based on the requirement of the process. The desirability was obtained by using the following Eq:

$$D = d_n(Y_i) \quad (2)$$

where D is the desirability function and $d_n(Y_i)$ are the normalized values of each studied responses.

6.4.4.2. Ultrasound energy calculation

The ultrasonic power dissipation (Pdiss) and ultrasonic energy density (UED) in the extraction mixture were calculated as described by Upadhyay *et al.* (2015). Pdiss was calculated as follows:

$$Pdiss = \left(\frac{dT}{dt}\right) \times m \times C_p \quad (3)$$

where dT/dt is the temperature change of mixture when exposed to ultrasound energy; m and C_p are the biomass (kg) and specific heat (J $kg^{-1}K^{-1}$) of the solvents in the mixture, respectively. The UED was determined by dividing the value of Pdiss by total volume of extraction mixture (ml).

6.4.5. Fractionation and purification of squalene

The unsaponifiable matters from livers of all four fish species obtained using conventional and U-DS processes were further purified.

6.4.5.1. Fractional crystallization

The fractional crystallization of unsaponifiable matter obtained by conventional and U-DS processes was performed using the solvent mixture as described by Nenadis and Tsimidou (2002), with some modifications. Unsaponifiable matter (1 g) was mixed thoroughly in 5 ml of methanol/acetone mixture (7:3, v/v) in a glass-stoppered test tube using a vortex for 1 min. The mixture was stored at -22 ± 1°C for 24 h and then subjected to centrifugation at 3000 ×g for 10 min at 4 °C. The supernatant rich in squalene was separated, and the solvent was removed as tailored

above. The concentrated squalene was collected. The yield of squalene concentrate (YSC) recovered was calculated as follows:

$$YSC\ (\%) = \frac{W_f}{W_i} \times 100 \qquad (4)$$

where W_i is the initial weight unsaponifiable matter before fractional crystallization (mg) and W_f is the weight of unsaponifiable after fractional crystallization (mg).

Concentration of squalene in the concentrate was determined based on the standard curve of the respective external standards.

6.4.5.2. Column chromatography

Separation of squalene from uncrystallized fraction from conventional and U-DS processes was carried out on silica gel column. A glass column (300 mm × 20 mm; L × i.d) was equipped with a fraction collector with a controlled flow rate ranging from 0.5 to 6.5 ml. Before packing the column, silica gel (24 g; 70-230 mesh) was activated in hot air oven at 105 ºC for 3 h. About 0.3 g of unsaponifiable fraction obtained after fractional crystallization was dissolved in 0.5 ml of *n*-hexane and loaded onto the column at room temperature (26 ± 2 ºC). The first fraction of the column was eluted with 60 ml of *n*-hexane at the flow rate of 4 ml min^{-1}. The second elution was carried out with 50 ml of a solvent mixture, *n*-hexane:ethanol (95:5, v/v), in an isocratic mode at the same flow rate. The residues in the column was washed with *n*-hexane:ethanol (60:40 %, v/v) and the silica was reconditioned using *n*-hexane. The test tubes (20 ml with screw cap) were used for collecting the eluate. Standard squalene was used as the reference to note the elution time. The eluate was evaporated in vacuum to obtain clear and slight yellow colored squalene, which was then stored in the dark at 4 ºC.

6.4.6. Characterization of fish oil, unsaponifiable matter, fraction obtained after fractional crystallization and pure squalene

6.4.6.1. Thin layer chromatography (TLC)

Components in liver oil, unsaponifiables, uncrystallized compounds after fractional crystallization and squalene were separated on 5 × 5 cm^2 precoated silica

gel 60 F254 plates (0.25 mm, Merck KGaA, Darmstadt, Germany). The separation was carried out using *n*-hexane. The plates were then stained as per the method of Nakamura and Handa (1984) using 0.03% Brilliant blue R in 20% methanol for 1 h and destained in 20% methanol for 30 min. For comparison, the standard squalene (Sigma, >98%) was spotted directly on the plate. The components on the TLC were identified based on the relative mobility value (Rf).

6.4.6.2. Reversed-phase high-performance liquid chromatography (RP-HPLC)

A stock solution of squalene and cholesterol were prepared in ethanol to give a final concentration ranging from 5 to 200 µg ml^{-1}. Test samples (10–30 µg ml^{-1}) were dissolved in hexane and subjected to RP–HPLC model, comprising Waters 2707 autosampler, Waters 1525 binary pump and Waters 2998 photodiode array detector (Milford, MA, USA). The connected series was controlled using Waters Empower™ 3 Chromatography Software. Detection of squalene was carried out according to the method of Bavisetty and Narayan (2015), with some modifications using Waters RP C18 5 µm (150 mm×4.4 mm) column. The injection volume was set at 1-20 µl, and the temperature of the column was maintained at 26 °C for analysis. Acetonitrile (100 %) was used as mobile phase at a flow rate of 1.5 ml min^{-1} in an isocratic mode. Analytes were monitored with a diode array detector at a wavelength of 195 nm. Peaks of squalene and cholesterol in the sample were identified based on the retention time, and were confirmed by spiking with the corresponding commercial standards. Quantification of identified peaks was done based on the standard curve of the respective external standards.

The yield (Y) of squalene was enumerated based on the quantitative data as determined by RP-HPLC and was expressed as g $(100\ g)^{-1}$ of raw liver. Recovery (R) and purity (P) of squalene after column chromatography were calculated as described by Li *et al.* (2017), as given below:

$$R\ (\%) = \frac{W_p \times P_p}{W_c \times P_c} \times 100 \qquad (5)$$

where W_p is the weight of purified squalene (mg), W_c is the weight of unsaponifiable matter after saponification (mg), P_p is HPLC purity of purified squalene (%) and P_c is HPLC purity of unsaponifiable matter after saponification (%).

$$P\ (\%) = \frac{A_1 - A_2}{A_s} \times 100 \qquad (6)$$

where A_1 is the value of peak area of purified squalene, A_2 is the value of peak area of undesired peaks and A_s is the value of peak area of standard squalene (≥98%) at known weight (µg). The values were calculated at five different levels of concentrations at five replications.

6.4.6.3. Fourier transform infrared (FTIR) spectroscopy

Purified squalenes, extracted from livers of spot-tail shark and skip-jack tuna (non-shark species) using conventional and U-DS processes, were selected for FTIR analysis. FTIR spectra was obtained using ATR-FTIR model Equinox 55 (Bruker, Ettlingen, Germany). The scan was performed within the range of 400–4000 cm^{-1}. Analysis and measuring conditions were carried out according to the method of Ali *et al.* (2018a).

6.4.7. Statistical analysis and experimental design

The experiments were conducted in triplicates with completely randomized design (CRD) except for RSM part. The differences between means were tested by the Duncan's multiple range test. The data was presented as means ± standard deviation. Statistical analysis of experimental data was performed using the SPSS 11.0 software (SPSS Inc., Chicago, IL, USA).

6.5. Results and discussion

6.5.1. Squalene extraction using conventional extraction process

Yields of oil extracted from livers of seabass, skipjack tuna, gray bamboo shark and spot-tail shark are 14.75±0.83, 6.34±0.13, 10.25±0.58 and 21.25±0.56 g $(100\ g)^{-1}$, respectively. The highest yield of oil was obtained for spot-tail shark liver ($p < 0.05$), which was in line with the highest lipid content in their liver

(Table 1). Achouri *et al.* (2018) reported the lipid contents of three deep-sea sharks, namely *S. acanthias*, *M. mustelus* and *R. cemiculus* ranged from 64 to 69%, which was higher than those of shark species used in the present study. In general, lipid content of sharks varies depending on species and the depth of their habitat (Bakes and Nichols, 1995). Shark species used in the present study were relatively smaller in size and were from shallow water.

Table 12. Proximate composition of livers from *L. calcarifer, K. pelamis, C. sorrah* and *C. griseum*.

Fish species	% weight/fresh weight			
	Lipids	**Moisture**	**Protein**	**Ash**
Seabass (*L. calcarifer*)	18.72±0.24^{b}	58.02±0.49^{c}	18.57±0.06^{b}	1.69±0.12^{d}
Skipjack tuna (*K. pelamis*)	9.03±0.15^{d}	64.47±0.21^{b}	21.33±0.09^{a}	3.17±0.03^{a}
Gray bamboo shark (*C. sorrah*)	11.52±0.28^{c}	65.01±0.40^{a}	17.81±0.04^{bc}	2.56±0.07^{c}
Spot-tail shark (*C. griseum*)	27.38±0.20^{a}	49.39±0.52^{d}	16.45±0.11^{cd}	2.78±0.06^{b}

Data was presented as proximate composition analyzed by the AOAC method (AOAC, 2000).

Mean ± SD from triplicate determination.

Different lowercase superscripts in the same column indicate the significant differences ($p < 0.05$).

For oil from skipjack tuna liver, which was a lean liver, the lowest yield of 6.34 ± 0.13 g (100 g)$^{-1}$ was found. The obtained result was in agreement with Vlieg and Murray (1988) who reported that oil from albacore tuna viscera extracted using the Folch method had the yield of 4.1%. Conversely, the yield of oil from seabass liver was significantly higher (14.75 ± 0.83 g (100 g)$^{-1}$) when compared to that of gray bamboo shark and skipjack tuna. Apart from liver, the majority of the lipids in Asian seabass were stored in the form of depot fat (Sae-leaw and Benjakul, 2017). Among the traditional extraction methods known, solvent method has been widely used (Adeoti and Hawboldt, 2014).

After oil extraction, squalene in the oil was recovered by hot saponification process. The yields of unsaponifiable fraction obtained from oil extracted using conventional process are summarized in Table 3. Saponification is a

crucial step to recover unsaponifiable fraction containing squalene. To achieve complete saponification, the optimal condition was adopted from that documented by He *et al.* (2002). The results indicated that highest content of unsaponifiable fraction was found in oil from livers of gray bamboo and spot-tail shark (3.47±0.23 and 10.93±0.26 g (100 g)$^{-1}$, respectively) followed by seabass 2.89±0.29 g 100 g^{-1} and skipjack tuna 0.35±0.05 g (100 g)$^{-1}$.

Table 13. Yields of unsaponifiable matter and squalene from fish livers extracted using conventional and ultrasound-assisted direct *in-situ* saponification (U-DS) processes.

Fish species	Yield (g (100 g)$^{-1}$)$^{\#}$			
	Conventional process		Ultrasound-assisted process*	
	Unsaponifiable matter	Squalene	Unsaponifiable matter	Squalene
Seabass	2.89±0.29^{cB}	0.10±0.02^{dD}	3.90±0.18^{cA}	0.13±0.03^{dC}
Skipjack tuna	0.35±0.05^{dB}	0.18±0.04^{cD}	0.43±0.05^{dA}	0.24±0.02^{cC}
Gray bamboo shark	3.47±0.23^{bB}	0.65±0.03^{bD}	4.71±0.10^{bA}	0.73±0.04^{bC}
Spot-tail shark	10.93±0.26^{aB}	5.52±0.06^{aD}	14.62±0.17^{aA}	6.86±0.05^{aC}

$^{\#}$ Yield was determined wet weight basis.

* Yield at optimal condition of U-DS process

Mean ± SD from triplicate determination.

Different lowercase superscripts in the same column indicate the significant differences ($p < 0.05$).

Different uppercase superscripts in the same row under the same parameters tested indicate the significant differences ($p < 0.05$).

The unsaponifiable matter contents of spot-tail shark, gray bamboo shark, seabass and skipjack tuna were 51.4, 33.8, 19.6 and 5.5% respectively, based on the amount of oil extracted. It was suggested that tuna and seabass liver oil contained a relatively higher amount of saponifiable matter, mainly triacylglycerides, diacylglycerides and free fatty acids (Bakes and Nichols, 1995). Czaplicki *et al.* (2011) reported that oils from terrestrial animals usually contain a relatively smaller percentage of unsaponifiable matter (0.5-2%). On the other hand, some marine oils particularly

shark or ray, have comparatively high quantity of unsaponifiable matter up to 80% (Bakes and Nichols, 1995). The yield of squalene using conventional process was 0.10±0.02 to 5.52±0.06 g (100 g)$^{-1}$, depending on the fish species as given in Table 3. The highest yield of squalene was from spot-tail shark (5.52±0.06 g 100 g^{-1}) and the lowest was from seabass (0.10±0.02 g (100 g)$^{-1}$).

6.5.2. Squalene extraction using U-DS process

For optimization of U-DS process, liver of spot-tail shark was selected based on its highest content of unsaponifiable matter. To validate the optimized process, the extraction of unsaponifiable matters from the rest of fish species was also conducted.

6.5.2.1. Optimization of extraction

Three independent variables (biomass/methanol ratio, volume of 50% aqueous KOH and sonication time) were optimized to obtain the maximal unsaponifiable yield as shown in Figure 1. Yield of unsaponifiable fraction from spot-tail shark liver using U-DS process was 14.62 g (100 g)$^{-1}$ of the raw liver, which was significantly higher ($p < 0.05$) than the solvent method (10.93 g (100 g)$^{-1}$). This drastic increase in yield could be due to the intense effect of cavitation, which improved the rate of mass transfer and accelerated the release of target compounds (Peshkovsky *et al.*, 2013). Sonication was performed at fixed frequency and power values (20 kHz and 750 W, respectively), based on the preliminary saponification experiment conducted using single factorial design (data not shown), in which the maximum unsaponifiable yield was obtained at an amplitude of 80% and temperature of 40 °C.

Influence of independent variables was determined through the linear and interactive outcome of independent variables over the response (yield) as shown in three-dimensional (3D) surface plots. These surface plots were used to obtain the optimum process conditions for the maximum yield as shown in Figure 1.

6.5.2.1.1. Effect of KOH volume

In the present study, KOH was used as a catalyst. Alkali catalyst has been reported to induce the rate of saponification more effectively than an acid

counterpart. Additionally, alkali catalyst requires a lower volume of solvent for saponification, compared to the latter (Nagappan *et al.*, 2018). Apart from the saponification reaction, the alkali catalyst was postulated to participate in the extraction process, as the alkali can help break down the cell wall (Li *et al.*, 2012). As a result, solvent can penetrate more easily. The effect of 50% KOH volume on direct saponification of spot-tail shark liver (100g) was studied, at the volume of 1 to 12 ml per reaction. The results indicated that the 50% KOH volume as low as 1 ml yielded 24.94% unsaponifiable matter. Furthermore, the interactive effect of KOH with biomass/methanol ratio and sonication time increased the yield of unsaponifiable matter. The highest amount of 50% KOH (12 ml) resulted in 50% of optimal yield (14.62 g (100 g)$^{-1}$). Perhaps due to the susceptibility of unsaponifiable compounds to harsh high alkali extraction conditions (Li *et al.*, 2017). The optimal level of 50% KOH was 6.5 ml (0.032g KOH g^{-1} of wet biomass) for a biomass/methanol ratio of 1:6 (w/v) and sonication time of 15 min (Fig. 1A and 1C). Consequently, the optimal amount of KOH required during U-DS was lower than that of conventional process but was higher than the molar concentration required for saponification (1:57 w/w), which was computed based on the average molecular weight of total fatty acids (863.47 g mol^{-1}) as determined by gas chromatography (Muhammed *et al.*, 2015). The excess catalyst was participated in the denaturation and solubilization of proteins (Chen *et al.*, 2016) and also saponify free fatty acids (Nagappan *et al.*, 2018). In addition, the cavitation effect is known to enhance protein denaturation as well as saponification of fatty acids (Chemat *et al.*, 2017; Ivanovs and Blumberga, 2017).

6.5.2.1.2. Effect of biomass/methanol ratio

The effect of biomass/methanol ratio (1:3, 1:6 and 1:9 w/v) during U-DS process is shown in Fig 1A and 1B. To achieve complete saponification reaction, the solubility of triacylglycerols is a major factor, requiring a sufficient amount of alcohol. The maximum yield (14.62 g (100 g)$^{-1}$) of unsaponifiable matter was found at the ratio of 1:6 w/v, when volume of 50% KOH and sonication time was 6.5 ml and 15 min, respectively. With a further increase of biomass/methanol ratio, the yield decreased. A higher biomass/methanol ratio can affect the reaction time, since alcohol dilutes the reaction components. Subsequently, the separation of ester phase became

more difficult (Czaplicki *et al.*, 2011). It was also observed that at a higher ratio of biomass/methanol (1:9 w/v), there was a reduction in yield of unsaponifiable matter to some extent. Thus, the negative effect of interaction of biomass/methanol ratio, KOH and sonication time was observed beyond the optimal points of Fig. 1, due to methanol serving as a solvent particularly when sonication was applied, resulting in loss of unsaponifiable matter to the aqueous phase. Nevertheless, at lower biomass/methanol ratio (1:3 w/v), the yield obtained was 5.44 g (100 g)$^{-1}$, which was significantly ($p < 0.05$) lower than the optimal yield, suggesting that reaction was incomplete at the ratio less than 1:6 (w/v). Therefore, the biomass/methanol ratio had affected the U-DS process. However, the amount of alcohol consumed was lower when compared to that used for conventional process.

6.5.2.1.3. Effect of sonication time

The effect of sonication time (0-30 min) over the yield of unsaponifiable matter was determined and the results are plotted as shown in Fig.1B and 1C. The yield of unsaponifiable matter increased when sonication time was increased up to 15 min. A further increase in sonication time led to a decline of yield. During U-DS, complete extraction and saponification took place to a higher degree till 15 min. Cavitation effect had a significant role in breaking the cell wall as well as accelerating the saponification reaction significantly under an appropriate condition such as the amount of catalyst, temperature of reaction and ratio of alcohol (Ivanovs and Blumberga, 2017). Similarly, ultrasonication has been reported to enhance the extraction yield of total lipids from bighead carp viscera and cobia liver in a single solvent system, cyclohexane and hexane, respectively (Kuo *et al.*, 2017; Xiao *et al.*, 2017). Another crucial independent factor of saponification is the degree of mixing, enhanced when sound waves generated an intense amount of turbulence and hence convective mass transfer during the process, resulting in high yield efficiency (Chemat *et al.*, 2017). More importantly, U-DS of raw liver sample reduced the entire processing time from 10-15 h to less than 20 min compared to the conventional solvent extraction method. When the sonication time was above 17 min, the yield decreased slightly. Thus, the prolonged exposure to ultrasonication may result in degradation and loss in structural properties of extracted

compounds. Considering the energy requirement of the extraction system, 15 min was suitable sonication time to complete the reaction at 40 ºC.

From theoretical point of view, extraction and hydrolysis of lipids from the complex aqueous biomass such a liver tissue using a single solvent system is challenging process. Due to the strong molecular association between lipids and other cellular constituents, the complex is resistant to solvent penetration (Bligh and Dyer, 1959), leading to incomplete hydrolysis and reduced extraction efficiency. However, in the present study, it was noticed that hydrolysis and release of cellular components were mainly governed by cavitation effect caused by ultrasound applied. The high intensity cavitation waves were able to enhance the penetration of solvent into the tissue matrix and augment mass transfer. In addition, homogenization of raw liver prior to sonication increased the surface area, which favored the penetration of solvent and improved the extraction efficiency. Similarly, Xiao *et al.* (2017) documented that sonication was highly efficient to recover total lipids from fish visceral biomass using cyclohexane. Additionally, it was also observed that the yield of squalene increased with U-DS treatments when compared to that of conventional method (Kuo *et al.*, 2017). Which is related to the increased degree of hydrolysis, thus enhancing the solvent extraction efficiency. Generally, squalene is available in free form, which can be easily extracted by means of conventional solvent systems (chloroform:methanol). However, substantial amount of squalene is located within bilayer membranes (Lopez *et al.*, 2014), which is not effectively extracted by solvent. Thus, high intensity ultrasound may extensively (hydrolyze the cell and proteins) release the squalene from complex tissue as evidenced by the increased efficiency compared to conventional solvent extraction method (Table 2). In addition, squalene may undergo weak hydrophobic-hydrophobic or van der Waals interactions with denatured cellular components (proteins and carbohydrates) generated during extraction process (Popa *et al.*, 2015; Rosales-García *et al.*, 2017; Spanova and Daum, 2011). These interactions may be destabilized by ultrasonic cavitation, resulting in increased mobility of squalene to interact with the solvent system. The solubilized squalene in solvent system will not further interact with denatured cellular components (Van Tamelen, 1968). Overall, U-DS improve the extraction efficiency of squalene.

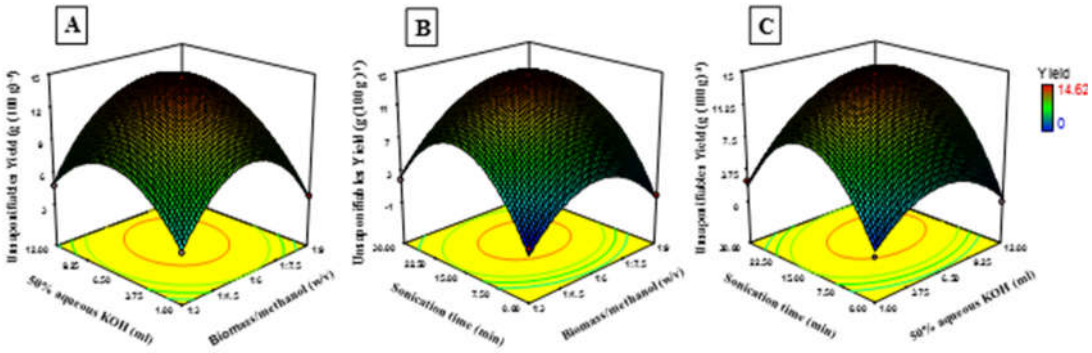

Figure 30. Response surface plots indicating the effect of sonication time, biomass/methanol ratio and volume of 50% KOH on the extraction yield of unsaponifiable matter from spot-tail shark extracted using ultrasound assisted direct in-situ saponification (U-DS) process.

6.5.2.2. Ultrasound energy

During the sonication process, a part of the energy is lost in the form of heat, resulting in raised temperature of extraction medium. This heat dissipated during sonication was determined based on the calorimetric measurements. The value of UED distributed in the medium was calculated as described in Eq. 3. The UED in the present study ranged from 0.056 to 0.265 W cm^{-3}. The UED for optimized U-DS process conditions was estimated to be 0.15 W cm^{-3} when the amplitude of 80% was applied.

6.5.2.3. Validation of U-DS process

Validation of the experiment and adequacy of regression equation was carried out using desirability function (D) for predicting optimal values through 3D plots (Upadhyay *et al.*, 2015). A D value of 0.875 obtained (obtained based on Eq. 2) was reached when the optimal conditions were employed (8.41 ml of 50% KOH, 1:5.99 w/v of biomass/methanol ratio and 16.27 min sonication time). Under optimal conditions, the observed yield was 14.58 g $(100\ g)^{-1}$, which strongly agreed with the predicted yield value (14.62 g $(100\ g)^{-1}$), thereby demonstrating the validity and acceptability of the RSM model.

Additionally, optimal conditions for saponification of spot-tail shark liver were applied to livers from fish species as shown in Table 3. The yield of unsaponifiable matter and squalene from other fish species obtained from U-DS process

was also higher ($p < 0.05$) than that obtained from the conventional process. The results demonstrated that there was a signification ($p < 0.05$) increase in the yield of squalene (0.13±0.03 to 6.86±0.05 g $(100\ g)^{-1}$) among all the fish species under optimal conditions of U-DS process when compared to that of conventional process (0.10±0.02 to 5.52±0.06 g $(100\ g)^{-1}$) as given in Table 3.

Overall, results indicated that the amount of solvent and time consumed in U-DS process were significantly lower ($p < 0.05$) than those used in the conventional process. The traditional method of oil extraction demands higher amounts of toxic chemical solvents. Multistep processing was also required. This could result in loss of yield and provide harsh conditions of extraction. Additionally, convention saponification needs higher temperature (70 ºC) and longer reflux time (1 h) to complete the saponification reaction, compared to the U-DS process, which needed lower temperature (40 ºC) and shorter time (15 min). Overall, net energy and time consumed during U-DS process was significantly lower (85-95%), compared to the conventional process (Xu *et al.*, 2011). Furthermore, U-DS process under optimal conditions provided the milder extraction conditions, lower temperature and amount of KOH used. Ultrasonication also reduced the viscosity of the extraction mixture and facilitated phase separation (Peshkovsky *et al.*, 2013). Reduction of energy, time and solvent with the increased yield was advantageous of U-DS process for extraction of squalene from wet biomass. Additionally, ultrasound has been proven as a potential extraction tool at large scales, irrespective of sources (plants, animals or microbes) Thus, the established U-DS process can be useful technique to extract different unsaponifiable compounds directly from the wet biomass, irrespective of the sample type and can also be scaled up for industrial application. In addition, the present method has an advantage over the residue obtained after U-DS extraction process. The use of non-toxic solvent (hexane and ethanol) makes the U-DS by-product suitable for further application, compared to the by-product from conventional method, in which chloroform or methanol are used. Besides, the U-DS by-product is rich in free fatty acids (including EPA and DHA) as well as extensively denatured or hydrolyzed proteins with high nutritive value. Thus, U-DS by-product can be utilized as an animal

feed or for the development of value-added products with further downstream processing.

6.5.2.4. Model fitting

The polynomial model designed from the obtained data by software Design-Expert using multiple regression analysis between extraction conditions and yield of unsaponifiable matter, calculated based on Eq. 1 is shown below:

$$Y^e = -21.74 + 7.07\,X_1 + 1.61\,X_2 + 1.03\,X_3 + 0.03\,X_1X_2 + 0.01\,X_1X_3 + 0.02\,X_2X_3 - 0.60\,X_1^2 - 0.14\,X_2^2 - 0.03\,X_3^2$$

In the present study, the maximum value for R^2 and adjR^2 were 0.9925 and 0.9790, respectively. Similar, coefficient values indicated the correlation among independent and dependent variables (Upadhyay *et al.*, 2015). The smaller value of coefficient of variation (14.95%) implies a good consistency and accuracy of the experiment. The model exhibited higher F-value (73.48) and relatively lower significant P-value (P<0.0001), representing the importance of the selected model and its fitness to elucidate the variation in response through regression equation.

6.5.3. Fractionation and purification of squalene

6.5.3.1. Fractional crystallization

Fractional crystallization is a mild process of separation, often used in industries. The compounds in a complex mixture are fractionated based on the melting point and difference in solubility (Nenadis and Tsimidou, 2002). In the present study, crystallization was conducted at -22 ºC for 24 h. After incubation, the liquid phase rich in squalene was collected and determined for squalene content using RP-HPLC. Under these conditions, squalene was effectively concentrated up to ≥ 60% purity from all the fish species used. The yield of squalene concentrates from sea bass and skipjack tuna was lower (48.35 and 61.37%, respectively) compared to those from grey bamboo and spot-tail shark (70.26 and 74.49%, respectively) (Table 4). The lower percentage in yield of squalene concentrate suggested that the sample had high proportion of crystalizing compound or contaminants. The difference in degree of

crystallization was purely dependent on the composition of unsaponifiable matter. The chemical composition of unsaponifiable matter is diversified but is majorly classified into hydrocarbons, sterols, triterpenoids, fatty alcohols and tocopherols (Achouri *et al.*, 2018; Bakes and Nichols, 1995).

Table 14. Fractionation and recovery of squalene from unsaponifiable matter of four fish species using fractional crystallization and silica gel column.

Fish samples	Yield of squalene concentrate (%)*	Recovery of squalene (%)#
Sea bass	48.35[d]	92.68[d]
Skipjack tuna	61.37[c]	94.24[c]
Gray bamboo shark	70.26[b]	95.55[b]
Spot-tail shark	74.49[a]	98.32[a]

* Percent yield of squalene concentrate gained after fractional crystallization as determined by Eq: 4. With a concentration of squalene up to ≥ 60% purity.

Percent recovery of squalene using silica gel column chromatography as determined by Eq: 5

Different lowercase superscripts in the same column indicate the significant differences ($p < 0.05$).

Additionally, the unsaponifiable fraction may also contain other compounds such as waxes, tocopherols esters, sterols esters and others with high melting point (Czaplicki *et al.*, 2011). Thus, the higher degree of crystallization from sea bass and skipjack tuna suggested the higher proportion of compound with a higher melting point. Conversely, lower degree of crystallinity from sharks suggests higher proportion compounds with a lower melting point, chiefly the squalene. Among all the compounds in unsaponifiable matter, squalene being highly unsaturated compound with lower melting point (-70 ºC) was present in liquid state and remained soluble in the solvent mixture (methanol/acetone, 7:3), whereas the other compounds with higher melting point were crystallized and could be easily eliminated. Additionally, Nenadis and Tsimidou (2002) reported that a higher degree of crystallization was observed when two-solvent system was used than a single solvent. Moreover, this method is convenient for routine fractionation and could be advantageous when compared to other

sophisticated methods including molecular distillation, supercritical fluid chromatography and others.

6.5.3.2. Column purification

The separation of squalene was carried out employing a two-phase solvent system using activated silica gel column chromatography. The recovery percentage of purified squalene from unsaponifiable matter of four fish species ranged from 92.68 to 98.32% as shown in Table 4. The difference in recovery percentage was more likely related to varying chemical compositions of unsaponifiable matters among the samples. After elution using 60 ml of *n*-hexane, the column was eluted with the mixture of *n*-hexane:ethanol (95:5, v/v). The mixture of *n*-hexane:ethanol (95:5, v/v) could elute squalene without coelution of other compounds. This suggested that squalene was easily eluted when the polarity of mobile phase was slightly increased. Lu *et al.* (2003) partitioned squalene from microalga in several solvent systems and found that *n*-hexane:methanol (2:1) a two-phase solvent system was the best. Nevertheless, unsaponifiable fraction eluted with intermediate polarity (*n*-hexane:methanol, 2:1) demonstrated coelution of squalene with other components (data not shown). Additionally, separation of squalene using highly nonpolar solvents such as dichloromethane, ethyl acetate, petroleum ether and diethyl ether was carried out as described by previous reports (He *et al.*, 2002; Wiesenberg *et al.*, 2004). These methods, however, resulted in early elution of squalene and it was difficult to separate other components from squalene (data not shown), indicating unsuitability of these solvents to purify squalene from unsaponifiable matter on a silica column. Besides, these solvents tended to form column bubbles and, in some case, caused cracks in the column. Thus, the present method on elution using n-hexane (60 ml) followed by mixed solvents (*n*-hexane:ethanol; 95:5%) (50 ml) with low polarity demonstrated the effective separation of squalene from unsaponifiable matter with negligible contaminants, and the column could be reused after washing.

6.5.4. Composition and characteristics of squalene in liver oils and different fractions obtained from various steps of fractionation/purification

6.5.4.1. TLC

Compositional profiles of fish liver oil and different fractions from sequential process of squalene fractionation and purification determined by TLC are shown in Figure 2. The samples were examined using squalene (≥98%) and cholesterol (≥99%) as standards. *n*-hexane was found as an ideal mobile phase with a Rf value of 0.5, demonstrating better separation and visualization of squalene from other components. However, cholesterol did not show any mobility and had an Rf value of 0.0. All the samples contained squalene. Oil from spot-tail shark had the highest concentration of squalene as examined on TLC than oils from other fish species (Figure 2A). Conversely, fish species including sea bass, skip-jack tuna and gray bamboo shark contained other components including cholesterol. Oil from fish liver showed a high proportion of undesired components, which gradually decreased upon saponification and fractional crystallization (Figure 2B and 2C). Concentration of squalene increased significantly on subsequent treatments. The result indicated that both saponification and fractional crystallization were the crucial steps to increase the squalene concentration prior to column purification. TLC profile of unsaponifiables displayed major differences among different fish species. Majority of unidentified compounds in unsaponifiable matter were found at Rf value ranging from 0.1 to 0.42, which were different from that of squalene. Furthermore, patterns of purified squalene spotted on TLC indicated that silica gel column was useful in terms of separating squalene from the complex mixture (Figure 2D). It was also noted that the purity of squalene gained after column chromatography was high (≥94%) with negligible contaminants, which was comparable to the standard squalene, which had ≥98% purity.

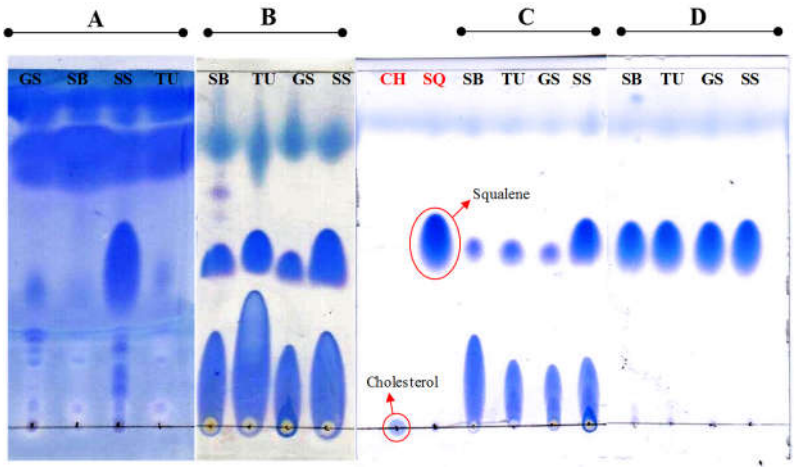

Figure 31. Thin layer chromatographic (TLC) analysis of fish liver oil (A), unsaponifiable matter (B), fraction obtained after fractional crystallization (C) and purified squalenes (D) from four different fish species including seabass (SB), skipjack tuna (TU), gray bamboo shark (GS) and spot-tail shark (SS). The plates were developed using n-hexane and were stained in 0.03% Brilliant blue R in 20% methanol for 1 h. CH and SQ represents the standard cholesterol (purity, ≥99%) and squalene (purity, ≥98%). Fish liver oil was extracted using conventional method, whereas unsaponifiable matter and purified squalene were extracted by means of ultrasound assisted direct in-situ saponification (U-DS).

6.5.4.2. RP-HPLC analysis

The quantification of squalene in fish liver oil, unsaponifiable matter after fractional crystallization and purified squalene was carried out using RP-HPLC as described by Bavisetty and Narayan (2015), using acetonitrile (100%) as a mobile phase for simultaneous detection of squalene and cholesterol. As shown in Figure 3, squalene and cholesterol were eluted at 11.74 and 7.7 min, respectively, at the flow rate of 1.5 ml min^{-1}. The chromatograms displayed a distinct separation of squalene from other components in the lipid. The results were in line with Yuan *et al.* (2017) who reported that squalene could be simultaneously detected with other complex mixture in the oil using a reverse phase column.

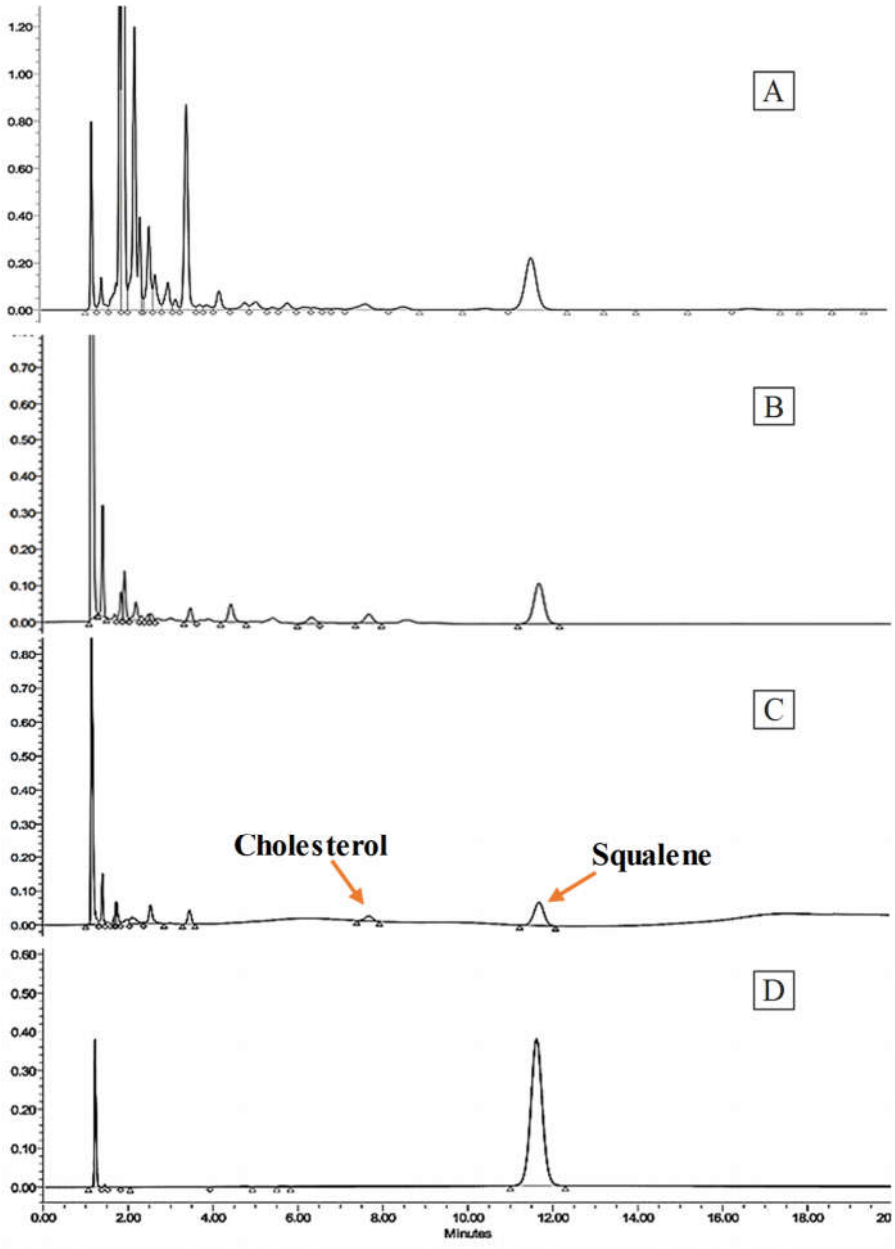

Figure 32. Reversed-phase high-performance liquid chromatograms (RP-HPLC) of oil (A), unsaponifiable matter (B), fraction obtained after fractional crystallization (C) and purified squalene (D) from spot-tail shark liver.

Fish liver oil was extracted using conventional method, whereas unsaponifiable matter and purified squalene were extracted by means of ultrasound assisted direct in-situ saponification (U-DS).

However, a tailing of cholesterol peak was observed, which could be more likely linked to the oxidation and degradation of cholesterol during saponification process (Ramalho *et al.*, 2011). The chromatogram (Figure 3A) of liver oil from spot-

tail shark indicated that both squalene and cholesterol were present at a low concentration, but the other lipid components constituted at high levels. Furthermore, the concentration of squalene increased upon saponification (48.6-94.5% from liver oils, depending on the fish species) and fractional crystallization of unsaponifiable (25.51-58.56% with respect to the volume of unsaponifiable matter). This was related with the reduction of peak number and area of the peaks of unidentified compounds (Figure 3A-3C). Additionally, the squalene obtained after column purification had negligible contaminants including cholesterol (Figure 3D). The purity of recovered squalene was as high as ≥94% (calculated based on Eq. 6).

6.5.4.3. FTIR spectra

Squalene from spot-tail shark and skip-jack tuna (non-shark species), rendering high squalene yield, were selected for FTIR analysis. Figure 4 depicts the infrared spectra of extracted squalenes in comparison with standard squalene. All the samples exhibited similar absorption profile with major absorption bands corresponding to functional groups ─CH_3 and ─CH_2. The peaks are located at 3052, 2965, 2919 and 2853 cm^{-1} wavenumbers associated with vibration produced from ─C═CH stretching, ─CH_3 asymmetric stretching, ─CH_2 asymmetric stretching and ─CH_2 symmetric stretching (Fu *et al.*, 2013). The analytically important bands related to squalene occurred at 1442, 1380, 1330, 1152, 1105, 1034, 833 and 450 cm^{-1}, representing various skeletal bending and stretching modes. However, the most distinguished band of squalene was found at wavenumber of 1667 cm^{-1}, representing symmetric stretching of six polarizable double bonds in the compound (Chun *et al.*, 2013). This could be used to differentiate double bond stretches from squalene with that of fatty acids, occurring at 1640-1660 cm^{-1} (Hall *et al.*, 2016). Thus, the absence of peaks in this region confirmed that no fatty acids were present in the purified sample. Additionally, the band at wavenumber of 833 cm^{-1} is for typical trisubstituted double bonds (Chun *et al.*, 2013). In the present work, both the vibrational bands at 1667 and 833 cm^{-1} did not show any change, compared to standard squalene, regardless of extraction process used.

A new peak was observed in fingerprint region located at 1744 cm^{-1} in squalene extracted using both conventional and U-DS processes. The intensity of band from conventional process was 3.2 fold higher than that of U-DS process. Spectral band for squalene within the frequency range of 1700-1750 cm^{-1} was mainly due to a spectral shift of double bond, possibly associated with the cis double bonds when squalene was exposed to a higher temperature (Ortega *et al.*, 2012). U-DS process could provide more suitable condition, deprived of chemical solvents, high temperature and longer time of extraction. Moreover, no additional peaks at wavenumbers of 3600-3200 and 1149-1033 cm^{-1} related to the formation of squalene primary oxidation and scission products were observed (Fu *et al.*, 2013). Additionally, squalene is an unsaponifiable lipid and is not chemically altered by alkali (He *et al.*, 2002). The results indicated that ultrasonication did not have any significant negative impact on squalene, which is a functional lipid applied in the food and pharmaceutical sectors.

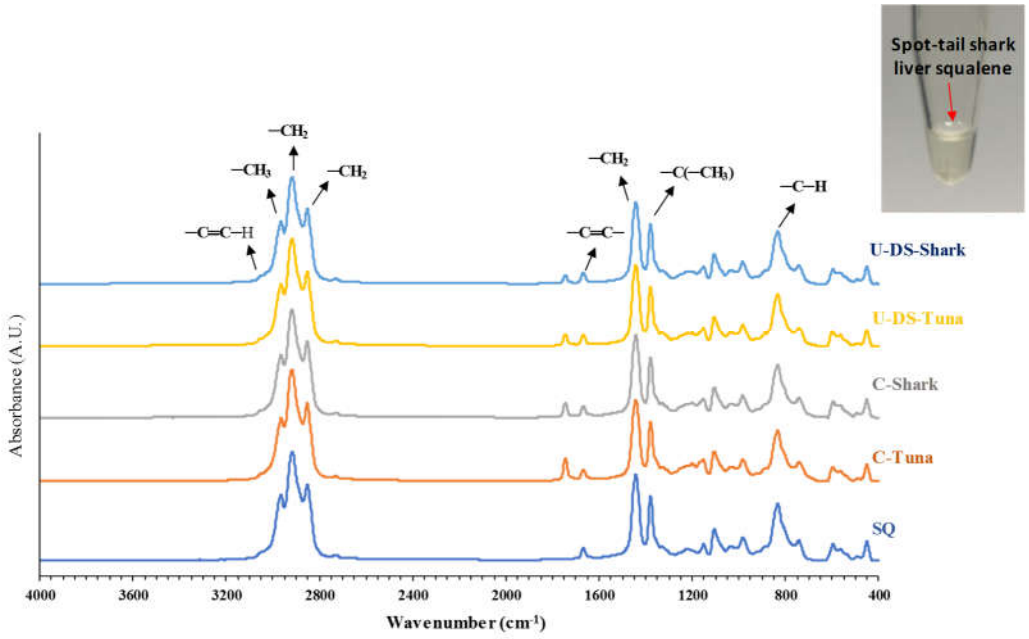

Figure 33. Fourier transform infrared (FTIR) spectra of purified squalenes extracted using conventional (C) and ultrasound assisted direct in-situ saponification (U-DS) from skipjack tuna and spot-tail shark liver. SQ represent the standard squalene (purity, ≥98%).

6.6. Conclusion

Application of ultrasound to extract squalene directly from fish liver was more effective, compared to the conventional extraction process. The optimal conditions for extraction/saponification of spot-tail shark liver were volume of 50% KOH (6.5 ml), ratio of biomass/methanol (1:6, w/v) and the sonication time (15 min), which increased the yield of unsaponifiable up to 35%. Overall, the use of sonication increased the yield and reduced the extraction time with lower consumption of chemical solvents. Fractional crystallization was found to be a crucial step to eliminate contaminants, while silica gel column effectively purified squalene. Moreover, U-DS process did not show any adverse effect on structure and property of squalene. Thus, U-DS had substantial advantages and was considered as an alternative process for production of squalene directly from fish processing by-products.

6.7. References

Achouri, N., Smichi, N., Kharrat, N., Rmili, F., Gargouri, Y., Miled, N. and Fendri, A. 2018. Characterization of liver oils from three species of sharks collected in Tunisian coasts: In vitro digestibility by pancreatic lipase. Journal of Food Biochemistry. https://doi.org/10.1111/jfbc.12453.

Adeoti, I. A. and Hawboldt, K. 2014. A review of lipid extraction from fish processing by-product for use as a biofuel. Biomass and Bioenergy. 63: 330-340.

Ali, A. M. M., Benjakul, S., Prodpran, T. and Kishimura, H. 2018a. Extraction and characterisation of collagen from the skin of golden carp (*Probarbus Jullieni*), a processing by-product. Waste and Biomass Valorization. 9: 783-791.

Ali, A. M. M., Kishimura, H. and Benjakul, S. 2018b. Extraction efficiency and characteristics of acid and pepsin soluble collagens from the skin of golden carp (*Probarbus Jullieni*) as affected by ultrasonication. Process Biochemistry. 66: 237-244.

Bakes, M. J. and Nichols, P. D. 1995. Lipid, fatty acid and squalene composition of liver oil from six species of deep-sea sharks collected in southern australian

waters. Comparative Biochemistry and Physiology Part B: Biochemistry and Molecular Biology. 110: 267-275.

Bavisetty, S. C. B. and Narayan, B. 2015. An improved RP-HPLC method for simultaneous analyses of squalene and cholesterol especially in aquatic foods. Journal of Food Science and Technology. 52: 6083-6089.

Bindu, B. S. C., Mishra, D. P. and Narayan, B. 2015. Inhibition of virulence of *Staphylococcus aureus*–a food borne pathogen–by squalene, a functional lipid. Journal of Functional Foods. 18: 224-234.

Bligh, E. G. and Dyer, W. J. 1959. A rapid method of total lipid extraction and purification. Canadian journal of biochemistry and physiology. 37: 911-917.

Blondin, G. A., Scott, J. L., Hummer, J. K., Kulkarni, B. D. and Nes, W. R. 1966. The biosynthesis of squalene and sterols in fish. Comparative Biochemistry and Physiology. 17: 391-407.

Cavonius, L. R., Carlsson, N.-G. and Undeland, I. 2014. Quantification of total fatty acids in microalgae: comparison of extraction and transesterification methods. Analytical and Bioanalytical Chemistry. 406: 7313-7322.

Chemat, F., Rombaut, N., Sicaire, A.-G., Meullemiestre, A., Fabiano-Tixier, A.-S. and Abert-Vian, M. 2017. Ultrasound assisted extraction of food and natural products. Mechanisms, techniques, combinations, protocols and applications. A review. Ultrasonics Sonochemistry. 34: 540-560.

Chen, D., Song, J., Yang, H., Xiong, S., Liu, Y. and Liu, R. 2016. Effects of acid and alkali treatment on the properties of proteins recovered from whole gutted grass carp (*Ctenopharyngodon idellus*) using isoelectric solubilization/precipitation. Journal of Food Quality. 39: 707-713.

Chun, H. J., Weiss, T. L., Devarenne, T. P. and Laane, J. 2013. Vibrational spectra and DFT calculations of squalene. Journal of Molecular Structure. 1032: 203-206.

Cristóbal, J., Caldeira, C., Corrado, S. and Sala, S. 2018. Techno-economic and profitability analysis of food waste biorefineries at European level. Bioresource Technology. 259: 244-252.

Czaplicki, S., Ogrodowska, D., Derewiaka, D., Tańska, M. and Zadernowski, R. 2011. Bioactive compounds in unsaponifiable fraction of oils from unconventional sources. European Journal of Lipid Science and Technology. 113: 1456-1464.

Fu, D., Leng, C., Kelley, J., Zeng, G., Zhang, Y. and Liu, Y. 2013. ATR-IR study of ozone initiated heterogeneous oxidation of squalene in an indoor environment. Environmental Science and Technology. 47: 10611-10618.

Ghimire, G. P., Thuan, N. H., Koirala, N. and Sohng, J. K. 2016. Advances in biochemistry and microbial production of squalene and its derivatives. Journal of Microbiology and Biotechnology. 26: 441-451.

Hall, D. W., Marshall, S. N., Gordon, K. C. and Killeen, D. P. 2016. Rapid quantitative determination of squalene in shark liver oils by Raman and IR spectroscopy. Lipids. 51: 139-147.

He, H. P., Cai, Y., Sun, M. and Corke, H. 2002. Extraction and purification of squalene from amaranthus grain. Journal of Agricultural and Food Chemistry. 50: 368-372.

Ivanovs, K. and Blumberga, D. 2017. Extraction of fish oil using green extraction methods: a short review. Energy Procedia. 128: 477-483.

KopiCoVá, Z. and VaVreiNoVá, S. 2007. Occurrence of squalene and cholesterol in various species of Czech freshwater fish. Czech Journal of Food Sciences. 25: 195-201.

Kuo, C.-H., Liao, H.-Z., Wang, Y.-H., Wang, H.-M. D., Shieh, C.-J. and Tseng, C.-Y. 2017. Highly efficient extraction of EPA/DHA-enriched oil from cobia liver using homogenization plus sonication. European Journal of Lipid Science and Technology. 119: 1600466.

Li, H., Li, C., Liu, W. and Zou, S. 2012. Optimized alkaline pretreatment of sludge before anaerobic digestion. Bioresource Technology. 123: 189-194.

Li, Y., Chen, Y. and Li, H. 2017. Recovery and purification of cholesterol from cholesterol-β-cyclodextrin inclusion complex using ultrasound-assisted extraction. Ultrasonics Sonochemistry. 34: 281-288.

Lopez, S., Bermudez, B., Montserrat-de la Paz, S., Jaramillo, S., Varela, L. M., Ortega-Gomez, A., Abia, R. and Muriana, F. J. G. 2014. Membrane composition and dynamics: A target of bioactive virgin olive oil constituents. Biochimica et Biophysica Acta (BBA) - Biomembranes. 1838: 1638-1656.

Lozano-Grande, M. A., Gorinstein, S., Espitia-Rangel, E., Dávila-Ortiz, G. and Martínez-Ayala, A. L. 2018. Plant sources, extraction methods, and uses of squalene. International Journal of Agronomy. https://doi.org/10.1155/2018/1829160.

Lu, H.-T., Jiang, Y. and Chen, F. 2003. Preparative separation and purification of squalene from the microalga *Thraustochytrium* ATCC 26185 by high-speed counter-current chromatography. Journal of Chromatography A. 994: 37-43.

Muhammed, M., Domendra, D., Muthukumar, S., Sakhare, P. and Bhaskar, N. 2015. Effects of fermentatively recovered fish waste lipids on the growth and composition of broiler meat. British Poultry Science. 56: 79-87.

Nagappan, S., Rajendra Kumar, R., Rupesh Balaji, J., Singh, S. and Verma, S. K. 2018. Direct saponification of wet microalgae by methanolic potassium hydroxide using acetone as co-solvent. Bioresource Technology Reports. 5: 351-354.

Nakamura, K. and Handa, S. 1984. Coomassie brilliant blue staining of lipids on thin-layer plates. Analytical Biochemistry. 142: 406-410.

Nenadis, N. and Tsimidou, M. 2002. Determination of squalene in olive oil using fractional crystallization for sample preparation. Journal of the American Oil Chemists' Society. 79: 257-259.

Ortega, J., Zavala, A. M., Hernández, M. and Reyes, J. D. 2012. Analysis of trans fatty acids production and squalene variation during amaranth oil extraction. Open Chemistry. 10: 1773-1778.

Peshkovsky, A. S., Peshkovsky, S. L. and Bystryak, S. 2013. Scalable high-power ultrasonic technology for the production of translucent nanoemulsions. Chemical Engineering and Processing: Process Intensification. 69: 77-82.

Popa, O., Băbeanu, N. E., Popa, I., Niță, S. and Dinu-Pârvu, C. E. 2015. Methods for obtaining and determination of squalene from natural sources. BioMed Research International. 2015: 1-16.

Ramalho, H. M. M., Casal, S. and Oliveira, M. B. P. P. 2011. Total cholesterol and desmosterol contents in raw, UHT, infant formula powder and human milks determined by a new fast micro-HPLC method. Food Analytical Methods. 4: 424-430.

Rosales-García, T., Jiménez-Martínez, C., Cardador-Martínez, A., Martín-del Campo, S. T., Galicia-Luna, L. A., Téllez-Medina, D. I. and Dávila-Ortiz, G. 2017. Squalene extraction by supercritical fluids from traditionally puffed amaranthus hypochondriacus seeds. Journal of Food Quality. https://doi.org/10.1155/2017/6879712.

Sae-leaw, T. and Benjakul, S. 2017. Lipids from visceral depot fat of Asian seabass (*Lates calcarifer*): Compositions and storage stability as affected by extraction methods. European Journal of Lipid Science and Technology. 119: 1-10.

Spanova, M. and Daum, G. 2011. Squalene–biochemistry, molecular biology, process biotechnology, and applications. European Journal of Lipid Science and Technology. 113: 1299-1320.

Upadhyay, R., Nachiappan, G. and Mishra, H. N. 2015. Ultrasound-assisted extraction of flavonoids and phenolic compounds from *Ocimum tenuiflorum* leaves. Food Science and Biotechnology. 24: 1951-1958.

Van Tamelen, E. 1968. Bioorganic chemistry: sterols and acrylic terpene terminal expoxides. Accounts of Chemical Research. 1: 111-120.

Vilkhu, K., Mawson, R., Simons, L. and Bates, D. 2008. Applications and opportunities for ultrasound assisted extraction in the food industry — A review. Innovative Food Science and Emerging Technologies. 9: 161-169.

Vlieg, P. and Murray, T. 1988. Proximate composition of albacore tuna, Thunnus alalunga, from the temperate South Pacific and Tasman Sea. New Zealand Journal of Marine and Freshwater Research. 22: 491-496.

Wiesenberg, G., Schwark, L. and Schmidt, M. 2004. Improved automated extraction and separation procedure for soil lipid analyses. European Journal of Soil Science. 55: 349-356.

Xiao, L., Ji, Y., Zhaoshuo, Y., Wenjiao, Xing, Z. and Chengjin, M. 2017. Ultrasound-assisted extraction of bighead carp viscera oil and its physiochemical properties. Journal of Jishou University (Natural Sciences Edition). 38: 49-55.

Xu, L., Brilman, D. W. W., Withag, J. A., Brem, G. and Kersten, S. 2011. Assessment of a dry and a wet route for the production of biofuels from microalgae: energy balance analysis. Bioresource Technology. 102: 5113-5122.

Yuan, C., Xie, Y., Jin, R., Ren, L., Zhou, L., Zhu, M. and Ju, Y. 2017. Simultaneous analysis of tocopherols,phytosterols, and squalene in vegetable oils by high-performance liquid chromatography. Food Analytical Methods. 10: 3716-3722.

CHAPTER 7

EFFECT OF SQUALENE RICH FRACTION FROM SPOT-TAILSHARK LIVER ON MECHANICAL, BARRIER AND THERMAL PROPERTIES OF GOLDEN CARP (*PROBARBUS JULLIENI*) SKIN GELATIN FILM

7.1. Abstract

Golden carp skin gelatin films incorporated with squalene rich fraction from shark liver (SRF) at various levels (5, 10, 15, 20 and 25%, w/w) were characterized in comparison with palm oil (PO) incorporated film and control film (CON) (without oil addition). PO films exhibited lower tensile strength (TS) but higher elongation at break (EAB) as compared to that of CON film. SRF films added with 25% SRF showed higher EAB as well as TS, compared to both CON and PO films ($p < 0.05$). SRF films showed significantly lower water vapor permeability (WVP) and lower lightness (L^*) value than CON and PO films ($p < 0.05$). Moreover, SRF films with negligible fishy odor had lower transparency and yellowness than CON and PO films. SEM images showed that CON and SRF films exhibited relatively smoother surface, compared to PO film. Additionally, SRF films had lower oil at the surface of the films than PO film. Moreover, DSC and FTIR spectra results revealed that incorporation of PO and SRF lowered interaction between gelatin molecules with coincidentally disordered structure. Besides, both SRF and PO films demonstrated lower degradation (T_d), glass transition (T_g) and melting transition (T_{max}) temperatures than CON film. Thus, incorporation of SRF could render stronger films with higher TS and enhanced flexibility and also moisture barrier property of gelatin films.

7.2. Introduction

Edible or biodegradable packaging has gained immense attention as an alternative to petrochemical-based commercial packaging, which is associated with severe ecological problem and environmental pollution (Tongnuanchan *et al.*, 2012). In the past few decades, gelatin mainly from bovine hide has been widely employed for

biodegradable coating and films in food applications. Gelatin still holds the attention for the production of biodegradable film owing to its desirable mechanical properties and excellent oxygen barrier property. However, gelatin film still encounters significant disadvantage, in which gelatin films possess poor moisture barrier property, thus restricting their uses as potential packaging (Hoque *et al.*, 2011b). This drawback is primarily associated with the hydrophilic nature of gelatin molecule as well as the plasticizer used (Carvalho *et al.*, 2008). Incorporation of hydrophobic substance such as waxes, oil, and fatty acids has been known to limit the transfer of water vapors across the film (Theerawitayaart *et al.*, 2019; Zhang *et al.*, 2018). Nevertheless, oils and fatty acids with high hydrophobicity can migrate from the film network to the surface particularly when the emulsification is not done properly (Prodpran *et al.*, 2007). Recently, Theerawitayaart *et al.* (2019) reported that increasing hydrophobicity of gelatin by oxidized fatty acid could enhance the stability of prepared gelatin film. Naturally, oils from marine sources consist of several hydrophobic compounds such as squalene, tocopherols, sterols, etc. Those compounds might contribute to the enhancement of moisture barrier property of gelatin-based film.

In addition, few components from lipid, especially squalene, exert health benefits. It has various health-promoting properties, such as, antioxidant and quenching property toward singlet oxygen in UV associated skin damage (Popa *et al.*, 2015). It also shows preventive effect against various types of cancers, cardioprotective effect, reduces serum cholesterol, and enhances immune response to various associated antigens, etc. (Czaplicki *et al.*, 2011; Reddy and Couvreur, 2009). Squalene also exerts antimicrobial activity against deadly foodborne bacterial pathogens and fungi (Bindu *et al.*, 2015; Elewski, 1993). Fish processing by-products mostly fish liver is known to have a substantial amount of squalene (Bavisetty and Narayan, 2015; KopiCoVá and VaVreiNoVá, 2007). Recently, it can be efficiently recovered using ultrasound-assisted direct in-situ saponification process (green extraction process) (Ali *et al.*, 2019).

Nowadays, gelatin from fish origin is receiving more significant interest as an alternative source primarily due to religious restrictions and health risk of mammalian counterpart (Benjakul *et al.*, 2012). Environmental management and economic valorization of fish processing waste via manufacturing of gelatin is another

aspect, promoting the production and utilization of fish gelatin (Ali *et al.*, 2018b). Fish gelatin is known to exert lower rheological and network forming properties (Benjakul *et al.*, 2012). Recently, Ali *et al.* (2018b) found that gelatin from golden carp skin demonstrated higher thermal and network forming property, attributing to their higher proportion of higher molecular weight components and imino acid content. Similar to other gelatin films, film from golden carp skin also showed poor water vapor barrier property. Incorporation of hydrophobic hydrocarbon, especially squalene, might increase hydrophobicity and amend the properties of resulting film, in which the desirable characteristic could be achieved.

7.3. Objective

To investigate the influence of squalene rich fraction from shark liver (SRF) at different levels on properties of golden carp skin gelatin film, as a prospective of developing a bioactive functional packaging.

7.4. Materials and methods

7.4.1. Chemicals

Analytical grade acetic acid, glycerol, potassium hydroxide and sodium hydroxide were obtained from Merck (Darmstadt, Germany). Tween 20 was obtained from Fisher BioReagents™ (Waltham, MA, USA). Methanol, *n*-hexane and chloroform were purchased from RCL Lab-Scan (Bangkok, Thailand). Protein molecular weight marker, squalene (≥98%) and cholesterol (≥99%) were procured from Sigma Chemicals (St. Louis, MO, USA). Palm oil was purchased from OLEEN Co. Ltd. (Bangkok, Thailand)

7.4.2. Collection of raw materials

Golden carp skin was collected and processed as describe in the section *2.4.2.1.* Spot-tail shark liver were collected and processed as described in the section 6.4.2.

7.4.3. Gelatin extraction

Removal of non-collagenous proteins and acid pretreatment were performed as describe in the sections *5.4.2.1* and *5.4.2.2*, respectively. Gelatin extraction was conducted as mentioned in the section *5.4.2.4.*

7.4.4. Preparation of squalene rich fraction from shark liver

7.4.4.1. Recovery of unsaponifiable matter

The unsaponifiable matter from spot-tail shark liver was extracted using ultrasound-assisted direct *in-situ* saponification. The optimal conditions used were adopted from the method of Ali *et al.* (2019). Ground spot-tail shark liver (100 g) was added with 95% methanol at biomass/solvent ratio of 1:6 (w/v). Subsequently, 6.5 ml of 50% aqueous KOH (0.032g of KOH g^{-1} of wet liver biomass) and 30 ml of *n*-hexane (to extract the unsaponifiables) were added. The mixture was subjected to sonication for 15 min using sonication processor (Vibra–Cell, Sonics & Material, Inc, Newtown, CT, USA) with 13 mm probe generating static output frequency of 20 kHz and power of 750 W. Ultrasound was operated at an amplitude of 80% in a pulse mode with 10 s on and 5 s off. The temperature of the sample was maintained at 40 °C using a water bath (EYELA, Tokyo Rikakikai, Co., Ltd., Tokyo, Japan). *n*-hexane phase from the extract was separated and washed using warm demineralized water till the wash water reached faintly basic pH. Drying and filtering of collected phase were performed using anhydrous sodium sulfate and Whatman filter paper No. 42, respectively. The unsaponifiable matter was concentrated using a rotary evaporator (EYELA N-1000, Tokyo Rikakikai, Co., Ltd., Tokyo, Japan), at 37 °C. Residual solvent was flushed using nitrogen gas. The resulting unsaponifiable matter was collected for fractionl crystalization.

7.4.4.2. Fractional crystallization (*section 6.4.5.1*)

7.4.4.3. Quantification of squalene using reversed-phase high-performance liquid chromatography (RP-HPLC) (*section 6.4.6.2*)

7.4.5. Preparation of gelatin film

7.4.5.1. Preparation of film forming solution and emulsion

Film forming solution (FFS) or emulsion (FFE) were prepared according to the method of Nilsuwan *et al.* (2017) with a slight modification. Gelatin was mixed in distilled water at a concentration of 3.5% (w/v) and was solubilized at 60 °C for 40 min. Glycerol (a plasticizing agent) at 30% (w/w) of protein was supplemented into the gelatin solution. The prepared solution was termed as a film-forming solution (FFS). To prepare film forming emulsion, SRF was mixed with Tween-20 at 25% (w/w), based on SRF. Subsequently, the prepared SRF was added into FFS at the levels of 5, 10, 15, 20 and 25% (w/w, based on protein). In a similar manner, PO containing Tween-20 at 25% (w/w, based on PO) was also prepared (positive control). All the suspensions were homogenized by sonication at an amplitude of 80% for 2 min and 30 s at 25 °C under the condition as mentioned previously. All film forming emulsions (FFE) were used for film casting.

7.4.5.2. Film casting and drying

FFS or FFE (4 g) was casted using silicone plate (50 × 50 mm^2) and air was blown for 24 h at 25 ± 2 °C. Subsequently, dried films were further equilibrated in an environmental chamber (WTB Binder, Tuttlingen, Germany) at relative humidity (RH) of 50 ± 5% and 25 °C for 24 h. The resulting films were peeled off manually and subjected to analyses.

7.4.6. Determination of film properties

Before testing of thickness, water vapor permeability, mechanical properties, light transmission and color, all the films were conditioned at RH of 50 ± 5% and temperature 25 ± 0.5 °C for 48 h.

7.4.6.1. Film thickness

Thickness was determined using a micrometer (ID-C112PM, Mitutoyo Corp., Kawasaki-shi, Japan). Five random positions from each film were measured and a number of ten films were used for determining the average thickness.

7.4.6.2. Mechanical properties

Mechanical properties including tensile strength (TS), Young's modulus (YM) and elongation at break (EAB) of the films were tested as described by Iwata *et al.* (2000). Ten films (20×50 mm^2) were examined using Universal Testing Machine (Lloyd Instrument, Hampshire, UK) at an initial grip length of 30 mm with a cross-head speed of 30 mm min^{-1}, equipped with a tensile load cell of 100 N.

7.4.6.3. Water vapor permeability (WVP)

WVP was determined following the ASTM method (ASTM, 2003) with a minor change as described by Nagarajan *et al.* (2014). The films (40×40 mm^2) were sealed between the rubber gasket of permeation (gas) aluminum cups containing gel beads (0% RH). Silicone vacuum grease was applied to ensure that no air leakage occurred. The cups were kept in the environmental chamber (50 ± 5% RH and 25 ± 0.5 °C) and were weighed for every 1 h over a period of 10 h. WVP was calculated using the below equation:

$$\text{WVP}\ (\text{g}\ \text{m}^{-1}\text{s}^{-1}\text{Pa}^{-1}) = \text{wl}\ \text{A}^{-1}\text{t}^{-1}\ (\text{P}_2 - \text{P}_1)^{-1} \qquad (1)$$

where w is increase in weight of aluminum cup, l is the thickness of the film (m), A is the exposed film area (m^2), t is the time of weight gain (s), P_2-P_1 is the vapor pressure difference across the film (1583.7 Pa at 25 °C).

7.4.6.4. Color and transparency

Color and transparency of the films were determined as described by Nilsuwan *et al.* (2017). Color (L^*, a^* and b^*) and color difference (ΔE^*) were analyzed using a CIE colorimeter (Hunter associates laboratory, Inc., Reston, VA, USA). White standard had $L^* = 92.82$, $a^* = -1.24$ and $b^* = 0.50$. The transparency of films was monitored at 600 nm using a UV-vis spectrophotometer (UV-1800, Shimadzu, Kyoto, Japan), and was calculated with the following equation:

$$Transparency\ value = -logT_{600}\ x^{-1} \qquad (2)$$

where T_{600} is the fractional transmission at 600 nm and x is the thickness of film (mm). Higher the transparency value signifies lower transparency of the film.

7.4.7. Characterization of FFE and selected films

Films added with SRF (10% and 25%) so called 'SRF-10' and 'SRF-25', respectively, control gelatin film (CON) (without SRF and PO), and film containing 25% with PO (positive control, PO) were selected. Before characterization, all the films were desiccated in P_2O_5 for one week at ambient temperature (25 ± 1 °C) to obtain the most dehydrated films.

7.4.7.1. Microstructure of FFE

The distributions of SRF and palm oil in FFE was determined as per the method of Tongnuanchan et al. (2015) using a confocal scanning laser microscopy (CSLM) (Fluoview FV300, Olympus, Tokyo, Japan). FFEs were mixed with Nile blue A (0.01% w/v) at a ratio of 1:1 (v/v) and with helium neon-green laser at the wavelength of 543 nm. The lase emitting single excitation wavelength (590 nm) with 10% of maximum power was set to red fluorescence mode. The emitted light was detected through a PMT detector (dichroic mirror DM570) set at confocal aperture number 2. Each sample was placed on a coverslip (20 × 50 mm^2) and the images were captured at 200× magnification.

7.4.7.2. Particle size distribution

The SRF droplet size distribution was determined using a laser particle size analyzer model LS-230 (Beckman Coulter®, Fullerton, CA, USA). The mean value of surface-weighted particle diameter (d_{32}) and volume-weighted particle diameter (d_{43}) were determined as described by Tongnuanchan *et al.* (2015).

7.4.7.3. Protein patterns of films

The film samples were mixed in 5% SDS (25 mg ml^{-1}) and solubilized at 85 °C for 1 h. The mixture was subjected to centrifugation at 4000 ×g for 10 min. Sodium decyl sulfate-polyacrylamide gel electrophoresis (SDS–PAGE) analysis was carried out as described in the section *2.4.3.2*.

7.4.7.4. Attenuated total reflectance-Fourier transform infrared (ATR-FTIR) spectroscopy of films (*section 2.4.3.4*)

7.4.7.5. Differential scanning calorimetry (DSC) of films

Thermal properties were determined according to the method of Ali *et al.* (2018a) using a differential scanning calorimeter Model DSC-7 (Perkin Elmer, Norwalk, CT, USA). Films (3–5 mg) were hermetically sealed into aluminum pans and were scanned over the temperature range of −20 to 150 °C at a heating rate of 5 °C min^{-1}. Transition temperature of the films was determined from the endothermic peak and the enthalpy change was estimated from the peak area.

7.4.7.6. Thermo-gravimetric analysis (TGA) of films

Films were subjected to thermo-gravimetric analyzer model TGA7 (PerkinElmer, Norwalk, CT, USA) and scanned from 25 to 1000 °C at a rate of 10 °C min^{-1} (Nagarajan *et al.*, 2017). During analysis, nitrogen gas was purged at a flow rate of 20 ml min^{-1}.

7.4.7.7. Scanning electron microscopy (SEM) of films

Microstructures of the gelatin films were visualized using a SEM mode JEOL JSM-5800 LV (Tokyo, Japan) at a voltage of 15 kV. Photographs of an upper surface of the films were taken at 2000× magnifications and those of cryo-fractured cross-sections were taken at 1000× magnification.

7.4.8. Statistical analysis

The experiments were conducted in triplicates with completely randomized design (CRD). The differences between means were tested by the Duncan's multiple range test and the data were shown as means ± standard deviation. Statistical analysis of experimental data was performed using the SPSS 11.0 software (SPSS Inc., Chicago, IL, USA).

7.5. Results and discussion

7.5.1. Extraction of SRF and quantification

Ultrasound-assisted direct *in-situ* saponification and fractional crystallization were used to extract and concentrate squalene from the raw liver of spot-tail shark. The SRF obtained was pale yellow in color (L^* = 76.35, a^* = -1.92 and b^* = 7.79). It contained ≥ 60% of squalene as determined by RP-HPLC analysis (Figure 1). The squalene content of spot-tail shark was up to 6.53 g 100 g^{-1} of liver tissue, in which the recovery by 95.6% was gained using the above-mentioned method.

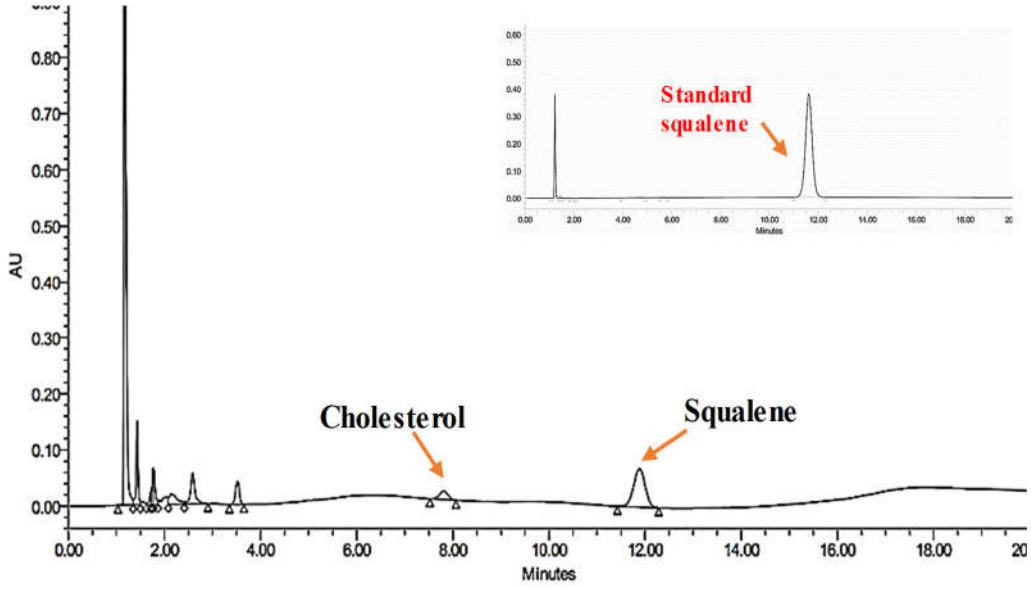

Figure 34. Reversed-phase high-performance liquid chromatograms (RP-HPLC) of squalene rich fraction from spot-tail shark liver obtained from ultrasound assisted direct in-situ saponification and fractional crystallization.

7.5.2. Properties of gelatin films incorporated with SRF from shark liver

7.5.2.1. Characteristics and thickness of gelatin film

The gelatin films without and with SRF (5, 10, 15, 20 and 25% w/w, based on protein), or with PO (25% w/w, based on protein) were all flexible and were easy to handle. Films demonstrated an increase in extensibility and flexibility but a slight reduction in transparency when incorporated with higher levels of SRF. It was noted that films incorporated with PO displayed a higher rate of transudation of oil on the surface, while the films added with SRF at different levels had no transudation. There was no fishy or off-odor in SRF films, regardless of level used. Saponification and fractional crystallization of spot-tail shark liver mostly diminished the fishy odor. As a result, the gelatin films containing SRF had a negligible fishy odor.

The thickness of films without and with SRF and PO addition are presented in Table 1. Thickness of all the films was in the range of 0.052-0.083 mm. The films incorporated with SRF showed a gradual increase in thickness when its levels increased ($p < 0.05$). The thickness of film with PO (25% w/w, based on protein) was also higher when compared to that of CON (without SRF or PO). This could be due to the dispersion of droplets of both SRF and PO in the film matrix, in which a compact structure failed to develop, and a protruded structure was formed as seen by the increased thickness. The thickness of films with SRF and PO at the same level (25% w/w, based on protein) exhibited similar thicknesses ($p \geq 0.05$). The result indicated that types of hydrophobic substances did not have the marked impact on thickens of the resulting gelatin film.

Table 15: Thickness, color and transparency value of golden carp skin gelatin film incorporated without and with squalene rich fraction from spot-tail shark liver or palm oil.

Samples	Levels (%, based on protein content)	Thickness (mm)	Color				Transparency value
			L^*	a^*	b^*	ΔE^*	
Gelatin films							
Control	0	0.052 ± 0.002^{f}	89.94 ± 0.12^{a}	-1.55 ± 0.12^{a}	2.61 ± 0.12^{f}	3.96 ± 0.12^{f}	1.72 ± 0.06^{g}
Squalene rich fraction	5	0.053 ± 0.002^{f}	89.9 ± 0.12^{a}	-1.57 ± 0.03^{b}	2.6 ± 0.08^{f}	3.99 ± 0.09^{f}	2.00 ± 0.08^{f}
	10	0.059 ± 0.003^{e}	89.76 ± 0.04^{b}	-1.61 ± 0.01^{c}	3.16 ± 0.04^{e}	4.32 ± 0.06^{e}	2.56 ± 0.21^{e}
	15	0.065 ± 0.001^{d}	89.64 ± 0.04^{b}	-1.74 ± 0.02^{d}	3.68 ± 0.02^{d}	4.96 ± 0.05^{d}	3.17 ± 0.02^{d}
	20	0.074 ± 0.003^{c}	89.56 ± 0.06^{c}	-2.02 ± 0.01^{e}	3.79 ± 0.03^{c}	5.15 ± 0.07^{c}	3.39 ± 0.13^{c}
	25	0.083 ± 0.005^{b}	88.34 ± 0.11^{d}	-2.25 ± 0.01^{f}	3.87 ± 0.05^{b}	5.26 ± 0.12^{b}	3.88 ± 0.08^{a}
Palm oil	25	0.084 ± 0.004^{a}	89.68 ± 0.12^{b}	-2.35 ± 0.12^{f}	4.78 ± 0.05^{a}	5.52 ± 0.05^{a}	3.58 ± 0.06^{b}

Mean ± SD from triplicate determination.

Different superscript letters in the same column indicate significant difference ($p < 0.05$).

7.5.2.2. Mechanical properties

TS, YM and EAB of golden carp skin gelatin (CON) film were 31.52 MPa, 61.71 MPa and 58.04%, respectively (Table 2). TS of CON film was higher when compared to gelatin films from other aquatic sources such as tilapia skin (25.79 MPa) (Nilsuwan *et al.*, 2019) and splendid squid skin (29.30) (Nagarajan *et al.*, 2012). However, it was comparable to that of cuttlefish gelatin film (32.78 MPa) (Hoque *et al.*, 2011b) when the same protein concentration of FFS was used. Nevertheless, EAB of golden carp skin gelatin film was more superior to those of aforementioned films (5-14%) (Hoque *et al.*, 2011b; Nagarajan *et al.*, 2014; Nilsuwan *et al.*, 2017). From our previous study, gelatin from golden carp skin consisted of higher MW protein chains and also contained higher residues of imino acids (204 residues (1000 residues)$^{-1}$). This more likely resulted in superior properties of film from golden carp skin gelatin to those from other sources (Ali *et al.*, 2018b). Greater number of long-chain components of golden carp skin gelatin could have facilitated the extensive aggregation and formation of a greater number of inter-junction zones, resulting in the stronger film.

Incorporation of SRF and PO at the same level (25%) affected the mechanical properties of gelatin films in different ways. Film added with PO showed lower TS but higher EAB ($p < 0.05$), compared to CON. Generally, addition of hydrophobic substance such as lipids, edible oils, essential oils, fatty acids, etc., particularly at critical concentrations, is known to reduce film strength, as the dispersed oil droplets could hinder the gelatin-gelatin interactions in film matrix, leading to discontinuity of the film network (Ma *et al.*, 2012; Prodpran *et al.*, 2007; Xiao *et al.*, 2016). Increased EAB reflected the increased flexibility, indicating that the PO droplets distributed in film network exhibited plasticizing effect, which facilitated the free mobility of gelatin molecule, thereby enhancing the extensibility of resulting film.

Conversely, films incorporated with SRF exhibited increased TS as well as EAB when levels of SRF increased ($p < 0.05$). Moreover, SRF incorporated film (at 25%) showed higher EAB (129.91%) ($p < 0.05$), compared to the film with PO (at 25%) (106%). The lowest EAB (58.04%) was found in CON film ($p < 0.05$). The enhanced EAB of gelatin films could be associated with the droplet dispersion of SRF, leading to

the discontinuity of SRF-containing films. Higher EAB indicated that SRF functioned as a plasticizer of film. In addition, Tween 20 to some extent contributed to the discontinuity of the gelatin film network and more likely contributed to higher EAB (Tongnuanchan *et al.*, 2013). Hoque *et al.* (2011b) documented that gelatin film networks were mainly stabilized by hydrophobic interactions and hydrogen bonds. The results indicated that the addition of SRF resulted in the higher strengthening effect on the gelatin film, particularly with increasing levels. This reflected that the longer chain length of squalene (C_{30}) in nature (Bindu *et al.*, 2015) could provide the strengthening impact of film network. Addition of SRF (25%) increased TS by 38.8%, compared to CON and by 93.3%, compared to PO (25%) film ($p < 0.05$). Thus, the SRF could serve as biopolymer from marine source, which could have undergone entanglement at interface or interaction in the film matrix effectively, as shown by increased film strength (TS) (Table 2). The entangled molecules of squalene might allow the molecule slippage in some extent between rupture of sample upon tensile loading. This molecular slippage prior to fracture could play a role in strengthening and toughening mechanism in which the squalene phase acted as load bearing in the film matrix. In addition, this could allow more orientation of molecules during extension prior to film rupture. This phenomenon could result in strengthening and toughening effect in squalene added gelatin film.

For YM value, CON film had a YM value of 61.71 MPa. Incorporation PO reduced YM of gelatin film ($p < 0.05$), which was reflected by the reduced interactions between gelatin molecules in the film matrix. This result was in accordance with Tongnuanchan *et al.* (2016) who reported the decreased value of YM when basil essential oil and PO were incorporated in the gelatin films, irrespective of types of plasticizers used. YM value generally increased with increasing levels of SRF incorporated. SRF (25%) film exerted the highest YM (608.44 MPa), when compared to CON and PO (25%) films ($p < 0.05$). The increase in YM value of SRF incorporated films was analogous with the increases in TS ($p < 0.05$). Squalene with long chain might undergo entanglement and interaction with gelatin via hydrophobic-hydrophobic. This could have increased YM of SRF added films.

Table 16: Tensile strength (TS), Young's modulus (YM), elongation at break (EAB), water vapor permeability (WVP) of golden carp skin gelatin film incorporated without and with squalene rich fraction from spot-tail shark liver or palm oil.

Gelatin film samples	Levels (%, based on protein content)	TS (MPa)	YM (MPa)	EAB (%)	WVP ($\times 10^{-10}$ g s^{-1} m^{-1} Pa^{-1})
Control	0	31.52 ± 2.12^{f}	61.75 ± 5.30^{f}	58.04 ± 3.09^{g}	2.56 ± 0.21^{a}
Squalene rich fraction	5	31.86 ± 2.43^{e}	101.26 ± 14.91^{e}	66.58 ± 2.61^{f}	2.04 ± 0.02^{b}
	10	34.05 ± 1.59^{d}	156.84 ± 22.03^{d}	69.16 ± 2.34^{e}	1.86 ± 0.03^{c}
	15	37.11 ± 2.60^{c}	284.11 ± 39.03^{c}	94.83 ± 4.63^{d}	1.62 ± 0.01^{e}
	20	39.72 ± 1.89^{b}	421.25 ± 38.85^{b}	115.87 ± 3.18^{b}	1.46 ± 0.02^{f}
	25	43.77 ± 2.04^{a}	608.44 ± 44.20^{a}	129.91 ± 4.12^{a}	1.4 ± 0.01^{g}
Palm oil	25	22.64 ± 0.81^{g}	50.19 ± 5.33^{g}	106 ± 3.22^{c}	1.78 ± 0.04^{d}

Mean ± SD from triplicate determination.

Different superscript letters in the same column indicate significant difference ($p < 0.05$).

7.5.2.3. WVP

Non-emulsified gelatin films (without hydrophobic substances) exerted higher WVP (2.56×10^{-10} g s^{-1} m^{-1} Pa^{-1}) mainly linked to hygroscopic nature of gelatin film (Nagarajan *et al.*, 2014). It was found that WVP decreased when SRF was added into the gelatin film in a dose dependent manner ($p < 0.05$). Films with SRF demonstrated higher water vapor barrier property (1.4×10^{-10} g s^{-1} m^{-1} Pa^{-1}) ($p < 0.05$), compared to PO (1.78×10^{-10} g s^{-1} m^{-1} Pa^{-1}) film at the same level used (25%). It was noted that the addition of SRF at level >15% yielded the film with superior water vapor barrier property to 25% PO ($p < 0.05$). Water vapor barrier property of films added with SRF, which is hydrophobic nature, was improved, probably due to homogeneous distribution of squalene in the film matrix. Generally, the intensity of water vapor barrier property of films increased significantly with higher levels of SRF ($p < 0.05$), suggesting that squalene could serve as barrier towards water migration through the gelatin film.

7.5.2.4. Color and transparency

Colors of films without and with SRF and PO expressed as L^*, a^*, b^* and ΔE^*, are shown in Table 1. Films prepared using golden carp skin gelatin showed L^* value of 89.94. Emulsified films exhibited a minor decrease in L^* value, depending on the level of SRF used. Addition of SRF more than 5% led to the decrease in L^* value ($p < 0.05$). The results were in agreement with Tongnuanchan *et al.* (2013), who documented that increasing amounts of essential oil markedly decreased the whiteness of resulting gelatin films. For films containing 25% PO or SRF, the latter presented a greater reduction in L^* value ($p > 0.05$). This could be more likely due to the difference in oil color or the degree of droplet distribution between PO and SRF in the films. Addition of both SRF and PO could result in the decrease in a^* value ($p < 0.05$). Hoque *et al.* (2011b); Tongnuanchan *et al.* (2015) reported the decrease in a^* value with addition of vegetable oil or essential oil. The higher content of oil could have attributed to the high crystallinity of oil in the film matrix, which reflected more red light and caused decreased a^* value (Gul *et al.*, 2018). Among all the gelatin films, those incorporated with PO showed higher b^* as well as ΔE^* values ($p < 0.05$). PO had yellow

color (L^*=74.61, a^*= -4.37 and b^*=20.43) due to its high content of beta-carotene than others (Tongnuanchan *et al.*, 2015). As noticed from the higher b^* values of PO (20.43) than that of SRF (7.79). Moreover, increased ΔE^* values were linked to the higher b^* values, particularly with the increasing amount of SRF. SRF was pale yellow in color, and the films demonstrated lower b^* values ($p < 0.05$) than the films with PO when the same level (25%) was used. However, films incorporated with wax did not demonstrate any significant difference in a^* and b^* values (Zhang *et al.*, 2018). Therefore, the coloring components in oil directly influenced the color of the resulting gelatin film.

Based on the transparency values (Table 1), CON film showed the least transparency value, compared to those incorporated with SRF or PO ($p < 0.05$). The lower transparency value represented films, which were more transparent. Films incorporated with SRF or PO exerted higher transparency value. Ma *et al.* (2012) documented that the addition of olive oil elevated the opacity of gelatin film. A transparency value of films containing SRF increased as the level of SRF increased ($p < 0.05$). At 25% addition, film incorporated with SRF showed the higher transparency value than that containing PO ($p > 0.05$). This could have been caused by difference in particle distribution and also structure of the film containing different substances. Solid fat/wax was reported to increase the opacity of film, compared to liquid lipids (Theerawitayaart *et al.*, 2019; Zhang *et al.*, 2018). Additionally, the higher transparency values of gelatin films with oils were in agreement with lower L^* values. Therefore, incorporation of SRF and PO influenced the transparency of resulting films.

7.5.3. Characterization of selected films

7.5.3.1. CSLM

CSLM images of FFS as well as FFE consisting of SRF at the levels 10 and 25%, (w/w, based on protein) or PO at 25% (w/w, based on protein), are illustrated in Figure 2. The images were recorded instantly after emulsions were prepared. The distribution of oil droplets was visualized in red color against the unstained protein continuous phase which was observed as a dark background.

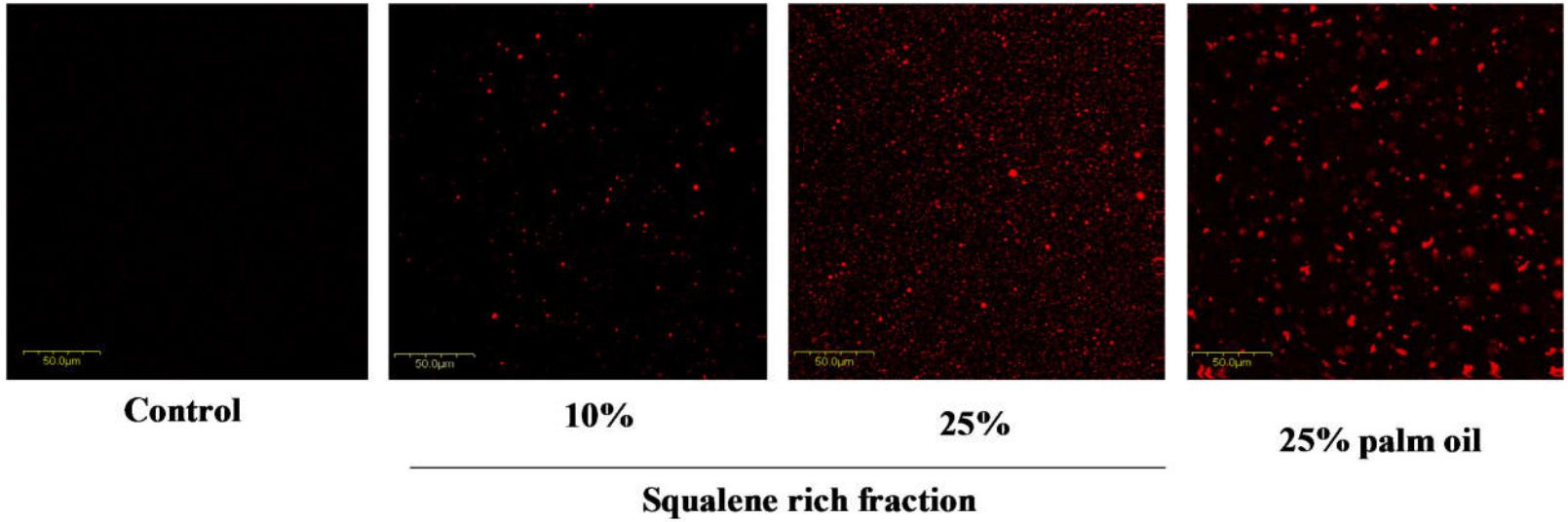

Figure 35. Confocal scanning laser microscopic (CSLM) images of film forming solution containing squalene rich fraction (SRF) from spot-tail shark liver at 10% and 25% or PO at 25%.

Both SRF and PO were homogeneously dispersed in the continuous protein phase. With increasing levels of SRF, a greater number of droplets dispersed in aqueous phase was noticeable. With the aid of ultrasound, FFE prepared using SRF, in which Tween 20 was used as a surfactant, demonstrated more stable emulsion with smaller particle size when compared to that of FFE added with PO. No coalescence was observed for FFE containing SRF. On the other hand, coalescence was clearly noticed in FFE with PO, as indicated by larger droplets with irregular shapes. The results suggested that SRF could form more stable FFE than PO when Tween-20 was used as a surfactant. Tween-20 provided suitable hydrophobic-lipophilic balance (HLB) to SRF for stabilizing FFE. Based on the hydrophobic nature of SRF, a surfactant with high HLB value (more hydrophilic) could facilitate tight molecular packing at the water/oil interphase (Fox, 2009). Tween-20 is a nonionic monolaurate ester with high HLB index (16.7), which is known to interact extensively with water than oil phase and is most commonly preferred for squalene emulsion for vaccine formulation (Chung *et al.*, 2001). Besides, squalene is reported to form the most stable emulsion with small particle size and narrow distribution at any given emulsifier concentrations (Chung *et al.*, 2001).

7.5.3.2. Particle size distribution

Particle size distribution of FFEs containing SRF at the levels of 10 and 25%, (w/w, based on protein) or PO at 25% (w/w, based on protein) is illustrated in Figure 3. All the FFEs showed trimodal particle size distribution system. PO containing FEE showed greater proportion of higher particle size. FFEs prepared using SRF displayed a higher proportion of lower particle size distribution with one distinct peak (close to 0.058 μm), irrespective of the level of SRF used. This was indicated by the similar distribution pattern between FFEs containing SRF at both levels. The results suggested that, SRF and PO had the impacts on droplet size of emulsion. During emulsification, Tween-20 with high HLB could quickly migrate and adsorb at the interface of newly formed SRF droplets than PO droplets. As a result, a reduced surface tension and larger surface of SRF droplets could be formed. This phenomenon more likely generated steric or electrostatic repulsions, which could retard the coalescence or flocculation of droplets in FFEs (Tongnuanchan *et al.*, 2015). Emulsion prepared with

SRF-10% exhibited smaller values of d_{32} and d_{43} (0.091 and 0.143 µm, respectively). The values were slightly increased with higher level of SRF-25% used (0.101 and 0.163 µm, respectively). However, PO-25% demonstrated the larger values of d_{32} and d_{43} (0.356 and 0.406 µm, respectively). Based on the estimated values of d_{32} and d_{43}, ultrasonication was highly efficient in reducing the droplets size, which ranged from nanometer to micrometer (Gul *et al.*, 2018). Thus, the higher d_{32} and d_{43} values of PO-25% FFE reflected the assembly of individual droplets into larger flocs, as evidenced by CSLM images (Figure 2). Thus, it was noticed that the particle size distribution was dependent on the type of hydrophobic compounds used for preparation of FFE.

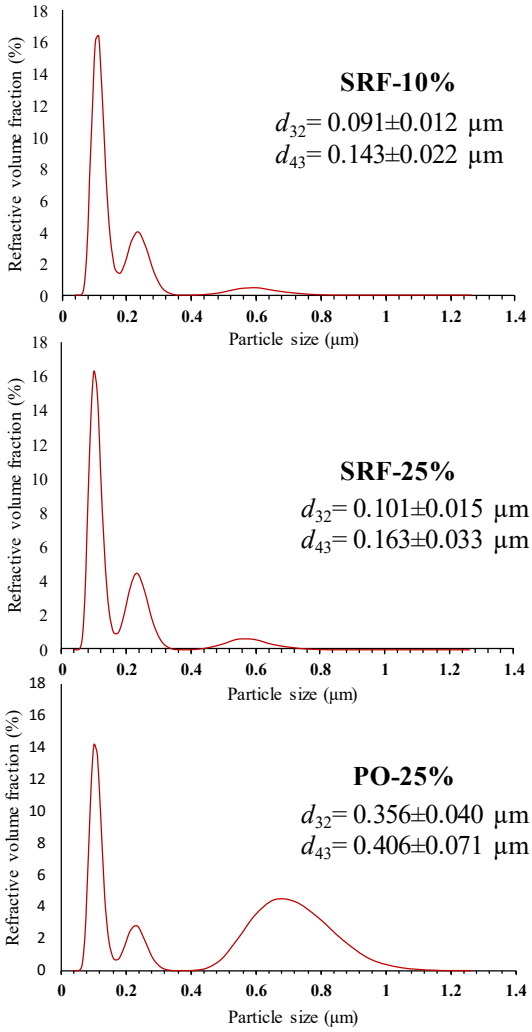

Figure 36. Particle size distribution of film forming emulsion containing squalene rich fraction (SRF) from spot-tail shark liver (10% and 25%) or PO (25%).

7.5.3.3. Protein patterns

Electrophoretic patterns of film from golden carp skin gelatin without and with SRF (10% and 25%) or PO (25%) are shown in Figure 4. All the gelatin films confirmed the presence of α_1-, α_2- (monomers) and β-chains (dimer) as the main components. Generally, α_1- and α_2-chains are the dominant components in gelatin from fish skin (Benjakul *et al.*, 2012). Usually, gelatin with higher monomeric chain component (α_1- and α_2-chains) is known to contribute to improving EAB than TS (Carvalho *et al.*, 2008; Hoque *et al.*, 2011a). The band intensities of these major chains in all the films were similar. This was mainly due to the fact that all the gelatin film matrixes were stabilized by means of weak interaction/bonds, which were easily destabilized by the denaturing agents used for electrophoresis.

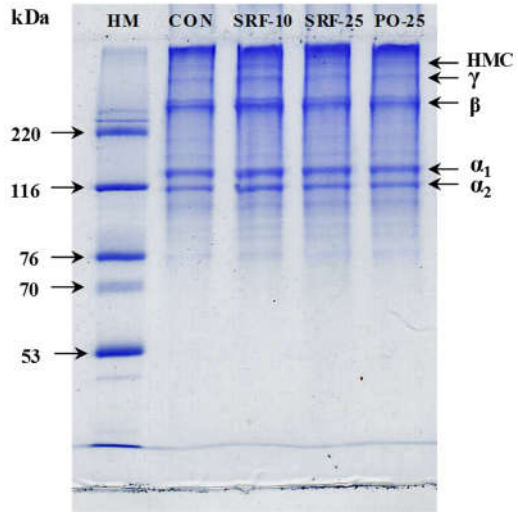

Figure 37. Protein patterns of films from golden carp skin gelatin (CON) incorporated with squalene rich fraction (SRF) from spot-tail shark liver at 10% (SRF-10) and 25% (SRF-25) or PO at 25% (PO-25). HM: high molecular weight marker. HMC: high molecular weight component.

Moreover, γ-chains (trimer) and high molecular weight component (HMC) were also present in all the gelatin films. Carvalho *et al.* (2008) studied the properties of gelatin film from Atlantic halibut skin with and without HMC. The film with HMC could form a stronger film with higher TS (11.1 MPa) than films without HMC (3.8 MPa). Additionally, oil rarely interacted with gelatin through covalent linkages (Hoque *et al.*, 2011b). It was hypothesized that oils could form hydrophobic

interaction with hydrophobic domains of gelatin molecules to some degree (Prodpran *et al.*, 2007). Nevertheless, hydrophobic-hydrophobic interaction could be destroyed by denaturants used for electrophoresis. Therefore, SRF as well as PO had no influence on protein patterns of gelatin film.

7.5.3.4. ATR-FTIR

All the films generally displayed similar spectral profile, in which major peaks including amide-A, B, I, II and III band were observed (Figure 5). However, there were some subtle changes in spectra with different film samples. It is well established that bands occurring within the range of 1600 to 1700 cm^{-1} correspond to amide-I, signifying C═O stretching vibration associated with NH bending and CN stretch, or COO group associated hydrogen bonding (Ali *et al.*, 2018b; Hoque *et al.*, 2011a). Amide-I band of CON film was situated at the wavenumber of 1631 cm^{-1}. When SRF (10 and 25%) or PO (25%) were incorporated, the wavenumber shifted to higher frequency (1633, 1634 and 1635 cm^{-1}, respectively), indicating lower interaction of C═O group with adjacent gelatin chain molecules when both SRF or PO was present, resulting in lower compactness of the film matrix. The existence of oil droplets in the film matrix restricted the interactions between gelatin molecules, thus resulting in the formation of less compact film as seen by increased film thickness. This result was in line with the previous study of Tongnuanchan *et al.* (2015) for gelatin/PO films. Also, SRF incorporated films exerted the increase in wavenumber, depending on the level of SRF added. Furthermore, at the same level (25%), films containing PO demonstrated higher wavenumber when compared to that having SRF. This could be more likely due to the difference in oil droplet size and distribution (Gul *et al.*, 2018). SRF (10 and 25%) and PO (25%) films presented a marginal increase in wavenumber of amide-II band (1548, 1548 and 1550 cm^{-1}, respectively), compared to CON film (1547 cm^{-1}). Amide-II vibration (1500-1600 cm^{-1}) generally arises from in-plane bending of NH of peptide group and stretching vibration of CN groups (Benjakul *et al.*, 2012). This indicated that the addition of SRF and PO could also hinder CN and NH groups to undergo interaction to some extent. The marginal shift was also observed in the amide-III (in-plane vibration of NH and CN stretching or waging vibrations of CH_2 groups of proline side chains and glycine backbone) bands of emulsified films (1239 cm^{-1}),

compared to that of CON film (1238 cm^{-1}) (Ali *et al.*, 2018b; Tongnuanchan *et al.*, 2016). Therefore, the amide-I band is primarily employed for infrared analysis of gelatin (Ma *et al.*, 2012). Additionally, a peak positioned at wavenumber of 1036-1037 cm^{-1} was detected in all the film samples which might correspond to the OH group, mainly from glycerol which was added as a plasticizer (Zhang *et al.*, 2018).

An amide-A band was detected at 3286 cm^{-1}, presenting NH stretching associated with hydrogen bonding (Benjakul *et al.*, 2012). When SRF (10 and 25%) or PO (25%) were added, the wavenumber of amide-A band shifted to higher wavenumbers (3290, 3291 and 3298 cm^{-1}, respectively). Typically, the shift wavenumber of amide-A band is mainly governed by the differences in hydrogen bonding among the protein molecules (Xie *et al.*, 2006). Tongnuanchan *et al.* (2014) documented that few essential oils such as basil essential oil could lower the amide-A wavenumber, which was mainly linked to the interaction of functional groups of essential oil with the reactive groups of protein than gelatin-gelatin interaction. Therefore, the higher wavenumber indicated that both SRF and PO were unable to form interactions with gelatin molecules. Amide-B band of all the films was observed within the wavenumber range of 3083-3088 cm^{-1}. The amide-B band of cuttlefish skin gelatin film at 3083 cm^{-1} was mainly due to the vibration of asymmetric stretching of CH group on double bond associated with stretching vibration of NH group (Hoque *et al.*, 2011b).

In addition, peaks situated at a wavenumber of 2878-2885 cm^{-1} and 2925-2936 cm^{-1} were also observed in all the films, representing a methylene asymmetrical stretching vibration of CH in CH_2 and CH_3 groups, respectively (Ma *et al.*, 2012). Commonly, most of the hydrophobic lipids show both methylene asymmetrical stretching vibration bands (Tongnuanchan *et al.*, 2016). Both the methylene asymmetric stretching band demonstrated an increase in amplitude for both SRF and PO incorporated films. Amplitude was continuously increased as SRF amount added increased. Furthermore, a peak arising at wavenumber 1743 cm^{-1} was distinctly observed in films added with PO. However, no peak was detected in CON film. A small peak with insignificant amplitude was noticed in SRF incorporated films. The band at 1746 cm^{-1} presents the C═O stretching vibration of ester carbonyl or aldehyde groups, which are the main chemical components in most of oils, including PO (Setiowaty *et*

al., 2000). Based on the FTIR spectra, the addition of both SRF or PO reduced protein-protein interaction. This coincided with the increased EAB and lower TS as shown in PO incorporated films. For films incorporated with SRF, which exerted higher TS, longer chain of squalene more likely underwent entanglement among themselves thus strengthening the main network of gelatin in films. Squalene with six nonconjugated double bonds have highly hydrophobic nature (Van Tamelen, 1968). SRF might have stabilized the gelatin film with hydrophobic-hydrophobic interaction and longer chain of squalene could have helped in increasing TS of resulting gelatin films.

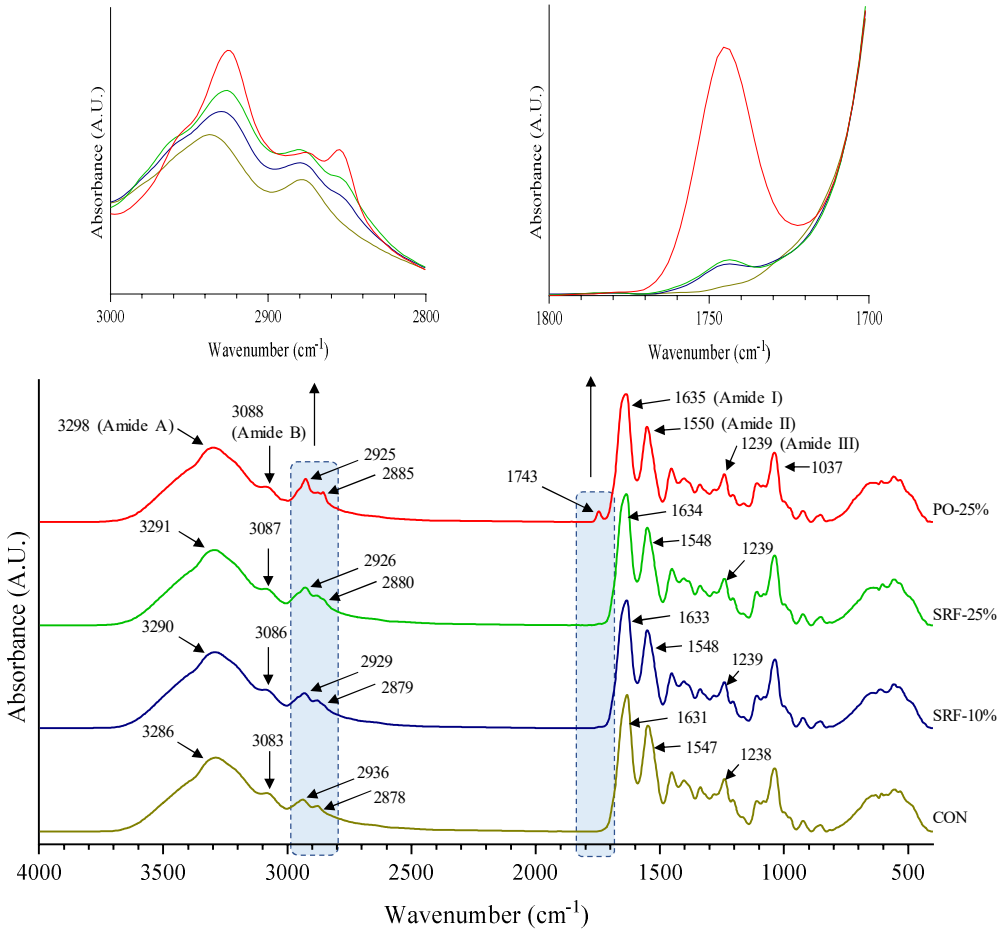

Figure 38. Attenuated total reflectance-Fourier transform infrared (ATR-FTIR) spectra of films from golden carp skin gelatin (CON) incorporated with squalene rich fraction (SRF) from spot-tail shark liver at 10% (SRF-10) and 25% (SRF-25) or PO at 25% (PO-25).

7.5.3.5. Thermal transition

Table 3 summarizes the endothermic melting transition (T_{max}), enthalpy (ΔH) and glass transition temperature (T_g) of the selected films. A heat scan (-20 to 150 °C) of all the films displayed a step-like transition curve, representing the T_g and followed by T_{max} peak. Generally, T_g of a protein-based film is related to the molecular mobility of protein chains at amorphous regions (disordered structure), in which a brittle glassy state is transformed to rubbery state. Melting transition refers to the temperature, at which disruption of ordered structure and denaturation of native protein state stabilized by means of various protein-protein interaction occurs (Nilsuwan *et al.*, 2017). CON film exhibited T_g at 46.07 °C, which was mostly associated with the transition of the plasticized phase of gelatin film. A comparable T_g (41.4 °C) was reported from porcine skin gelatin film plasticized with glycerol. Different T_g values were reported for the films plasticized with diethylene glycol and propylene glycol (13.4 and 61.9 °C, respectively) (Vanin *et al.*, 2005). Different T_g of gelatin film has been observed from various sources including cod skin (99 °C) (Staroszczyk *et al.*, 2012), Atlantic halibut skin (53 °C) (Carvalho *et al.*, 2008), tilapia skin (48.4 °C) (Theerawitayaart *et al.*, 2019) and cuttlefish skin 45.65 °C (Hoque *et al.*, 2011b). Difference might depend on the source and properties of gelatin as well as the type of plasticizer used. Furthermore, films incorporated with SRF or PO exhibited lower T_g than CON film (Table 3). Prodpran *et al.* (2007) reported that hydrophobic substances including fats and oils served as plasticizer in protein films, which could disrupt inter- and intra-molecular interactions and thereby increased the chain mobility. As a result, the lower T_g of SRF or PO films could be associated with the increased chain mobility associated with the plasticizing effect. Highly flexible films as evidenced by increased EAB were formed (Table 2). Furthermore, it was found that the T_g of PO incorporated films was lower (42.85 °C) than that added with SRF (44.26 °C) at the same level used (25%). This was more likely attributed to the larger droplet size of PO in FFE as observed from CSLM (Figure 2), where the larger particle size could cause higher obstruction to gelatin-gelatin interaction in the resulting film incorporated with PO. Consequently, different orientation and arrangement of gelatin chains could be varied in the presence of SRF and PO.

For melting transition, CON film showed an endothermic peak with T_{max2} of 124.45 °C. Generally, the peak was related to the distraction of ordered molecular structure (Staroszczyk *et al.*, 2012). Similar results were reported by Staroszczyk *et al.* (2012), Nagarajan *et al.* (2017) and Theerawitayaart *et al.* (2019). Moreover, this melting transition could also occur due to the helical coil transition of the gelatin film. Xiao *et al.* (2016) documented that gelatin molecules could experience partial renaturation during the preparation of FFS and rearrange themselves in a more ordered structure during drying process. The films incorporated with SRF or PO demonstrated lower T_{max2}, suggesting that oils which acted as plasticizers might also obstruct the renaturation of gelatin molecules in emulsified films. Additionally, CON film displayed the highest ΔH value (29.16 J g^{-1}), compared to those containing SRF (10 and 25%; 17.86 and 10.89, respectively) and PO (25%, 9.02). This result reconfirmed that ordered structure of films became lowered with the addition of SRF or PO, which were hydrophobic in nature. As a result, a discontinuity in the macromolecular network in the film matrix was formed, which possibly required lower disruption energy.

Furthermore, an additional endothermic transition peak was observed in the films incorporated with SRF or PO. The peaks were located at T_{max1} of 13.37 and 16.07 °C for the films with 25% SRF and 25% PO, respectively. The existence of endothermic at two different positions suggested the divergent ordered structures in the film matrixes. An endothermic transition occurred before glass transition could be due to the dispersed oil droplet phase present throughout the film. The obtained results were in accordance with Xiao *et al.* (2016) who documented that fish gelatin film added with different levels of PO exhibited addition endothermic peak at 17 °C. Presumably, no endothermic peak was observed within this range in the CON film. It was noted that SRF incorporated film exhibited lower ΔH (3.48 J g^{-1}) compared to that of film incorporated with PO (18.97 J g^{-1}) at the level of 25%. Moreover, film incorporated with 10% SRF did not show any endothermic transition. The lower value of ΔH in SRF film reflected that saponification and fractional crystallization process might have eliminated most of the components yielding endothermic transition.

Table 17. Melting phase transition (T_{max}), enthalpy change (ΔH) and glass transition temperature (T_g) of golden carp skin gelatin film incorporated without and with squalene rich fraction from spot-tail shark liver or palm oil.

Gelatin film samples	Levels (% based on protein content)	Oil phase				Protein phase				Glass transition
		T_{onset} (°C)	T_{max1} (°C)	T_{end} (°C)	ΔH (J g^{-1})	T_{onset} (°C)	T_{max2} (°C)	T_{end} (°C)	ΔH (J g^{-1})	T_g (°C)
Control	0	-	-	-	-	118.75	124.45	128.35	29.16	46.07
Squalene rich fraction	10	-	-	-	-	119.65	123.79	125.81	17.86	45.12
	25	11.46	13.37	20.11	3.48	108.76	110.08	111.93	10.89	44.26
Palm oil	25	12.17	16.07	28.21	18.97	100.03	107.60	112.17	9.02	42.85

7.5.3.6. Thermal stability

TGA thermograms of gelatin films without and with SRF (10 and 25%) or PO (25%) presenting thermal degradation behavior are shown in Figure 6 as expressed as thermal degradation temperatures (T_d) and weight loss (Δ_w) (Table 4). TGA curve of CON film normally demonstrated four phases of weight loss. Films added with SRF or PO showed five phases of Δ_w, regardless of SRF levels used. All the films exerted the first phase of weight loss (Δ_{w1} = 9.45-11.08%) at a temperature (T_{d1}) range of 36.79-42.59 °C, which might be due to the loss of free as well as bound water from film matrix. Similarly, Tongnuanchan *et al.* (2015) observed that films prepared from tilapia skin gelatin without and with PO at varying levels had T_{d1} ranging from 26.4 to 34.7 °C. It was observed that films added with SRF or PO demonstrated lower weight loss at T_{d1}. This was probably linked to the lower water content in the film matrix, which was mostly due to the higher hydrophobicity of substance added. Additionally, the decrease in weight loss was proportional with an increased degree of hydrophobicity (Table 4).

The second weight loss phase (Δ_{w2} = 9.45-11.08%) was distinctly observed at the temperature (T_{d2}) of 180.12-203 °C. This transition temperature is linked to the loss of glycerol (plasticizer), lower MW protein fractions and to some extent structurally bound water (Hoque *et al.*, 2011b). The third phase of weight loss (Δ_{W3}, 31.37-46.18%) was observed at Td_3 of 295.55-301.65 °C. Additionally, films containing SRF or PO showed almost similar lower weight loss values, compared to that of CON film. Nagarajan *et al.* (2017) reported that weight loss at the temperature range of 258-348 °C was related to the degradation of major constituents in the films. Thus, it is clear that higher degradation temperature (T_{d3}) was typically caused by higher interaction between the gelatin molecules, as observed from CON film, which formed more stronger and denser film matrix due to the lack of hydrophobic substances. Films incorporated with SRF or PO with a plasticizing effect could decrease gelatin-gelatin interaction and thus displayed lower heat resistance, compared to the CON film (Table 3). Additionally, films with same level of SRF and PO (25%) had comparable values of Δ_{W3} and T_{d3}. Thus, the results indicated that analogous to PO, SRF exhibited plasticizing effect and did not undergo any strong molecular linkages with gelatin to

stabilize the film network, as evidenced by increased EAB. Moreover, due to the complex structure and highly hydrophobic nature, squalene is known to undergo structural transition when exposed to the solvents with different polarity. Squalene in a hydrophobic or low polar system is known to be in a straight or extended state. On the other hand, in a polar or hydrophilic system (specially in emulsion system) squalene appears to be in a highly coiled state, which is known to be sterically shielded and chemically less reactive (Van Tamelen, 1968). Thus, coils of squalene molecule might strengthen the gelatin film network and thereby exerted the superior mechanical property, especially TS (Table 2). Additionally, at this transition phase, the loss of volatile compound and free fatty acids also occurred mainly from compounds in SRF or PO in films, especially the PO incorporated film.

The fourth phase of weight loss (Δ_{w4} = 14-23%) at T_{d4} of 367-372 °C was observed for films incorporated with SRF or PO. No weight loss was detected for CON film. Moreover, increase in Δw_4 resulted from the increasing amount of SRF added. PO (25%) incorporated film had the highest weight loss up to 23% when compared to films containing 25% SRF (18%). The Δ_{w4} indicated the loss of compounds with high-temperature stability. Nevertheless, the transition temperature phase (T_{d4}) was noted to be higher than the boiling point of PO (~221-344) (Guzman *et al.*, 2010) and squalene (~285) (Popa *et al.*, 2015). For the fifth phase, the weight loss (5.05-2.76) was observed with T_{d5} of 554.11-632.44 °C. This transition at high temperature could be associated with the degradation of highly cross-linked or interacted gelatins. All the films demonstrated smaller value of Δ_{w5}, demonstrating the existence of a small portion of these highly cross-linked domains.

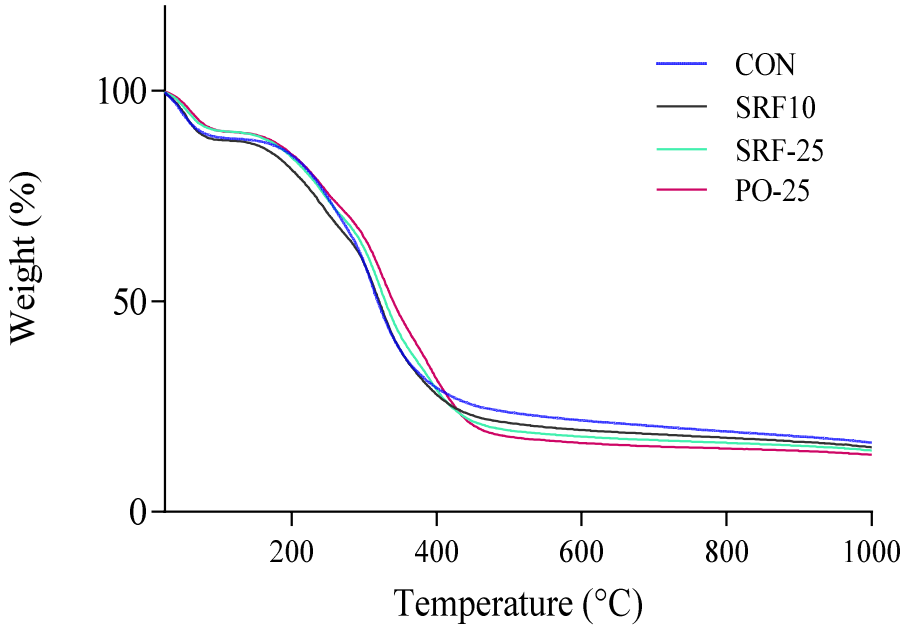

Figure 39. Thermo-gravimetric curves of films from golden carp skin gelatin (CON) incorporated with squalene rich fraction (SRF) from spot-tail shark liver at 10% (SRF-10) and 25% (SRF-25) or PO at 25% (PO-25).

Table 18. Thermal degradation temperature (T_d, °C) and weight loss (Δ_w, %) of golden carp skin gelatin film incorporated without and with squalene rich fraction from spot-tail shark liver or palm oil.

Gelatin film samples	Oil levels (% based on protein content)	Δ_1		Δ_2		Δ_3		Δ_4		Δ_5	
		$T_{d1,\ onset}$	Δ_{w1}	$T_{d2,\ onset}$	Δ_{w2}	$T_{d3,\ onset}$	Δ_{w3}	$T_{d4,\ onset}$	Δ_{w4}	$T_{d5,\ onset}$	Δ_{w5}
Control	0	36.79	11.08	203	22.27	309.65	46.18	-	-	632.44	5.05
Squalene rich fraction	10	42.59	10.49	180.12	21	302	32.98	367.26	14.00	554.11	4.85
	25	41.19	9.45	185.27	18.702	298.35	31.68	372.03	18.23	557.72	3.58
Palm oil	25	38.47	9.68	185.06	20.91	292.25	31.37	372.92	23.795	612.29	2.769

Δ_1, Δ_2, Δ_3, Δ_4 and Δ_5 denotes the first, second, third, fourth and fifth stage of weight loss, respectively, of films

7.5.3.7. Microstructure

The micrographs of a surface (2000 x) and cross-section (1000 x) of selected gelatin films prepared without and with SRF or PO are illustrated in Figure 7. The surface of CON film was homogenous and smoother than films incorporated with SRF or PO. Films incorporated with PO (25%) had apparently rougher surface than those with SRF. This could be more likely due to the smaller particle size with even distribution of SRF at all the concentration used as evidenced from CSLM (Figure 2). Conversly PO rendered relatively larger particle size with heterogeneous structures, which might be due to the aggregation of smaller droplets. Nonetheless, emulsions prepared via ultrasonication are usually known to have nano-sized droplets, irrespective of oil types and the surfactant used (Gul *et al.*, 2018). Cross-section of CON film was extremely compact when compared to that of other films, indicating higher rigidity of CON film. Relatively, the cross-section of SRF incorporated films was more compact when compared with that of film with PO. SRF containing films had clear spots of oil droplets with narrow size distributed throughout the film. On the other hand, PO incorporated film had an irregular cross-section with uneven distribution of oil droplets within the film matrix. Additionally, the surface microstructure of SRF incorporated film showed the intactness of oil droplets which remained undamaged/unbroken, but the films with PO demonstrated cavities/pockets due to the removal of oil droplets. Generally, the oil phase in emulsified gelatin films (various oils and fatty acids) are known to leach out from the film matrix (Theerawitayaart *et al.*, 2019). However, the incorporation of SRF yielded superior film morphology to that of PO. This, phenomenon could be attributed to the hydrophobic property of SRF which formed stable and uniform emulsion with narrow distribution of nanoparticle (Fox, 2009).

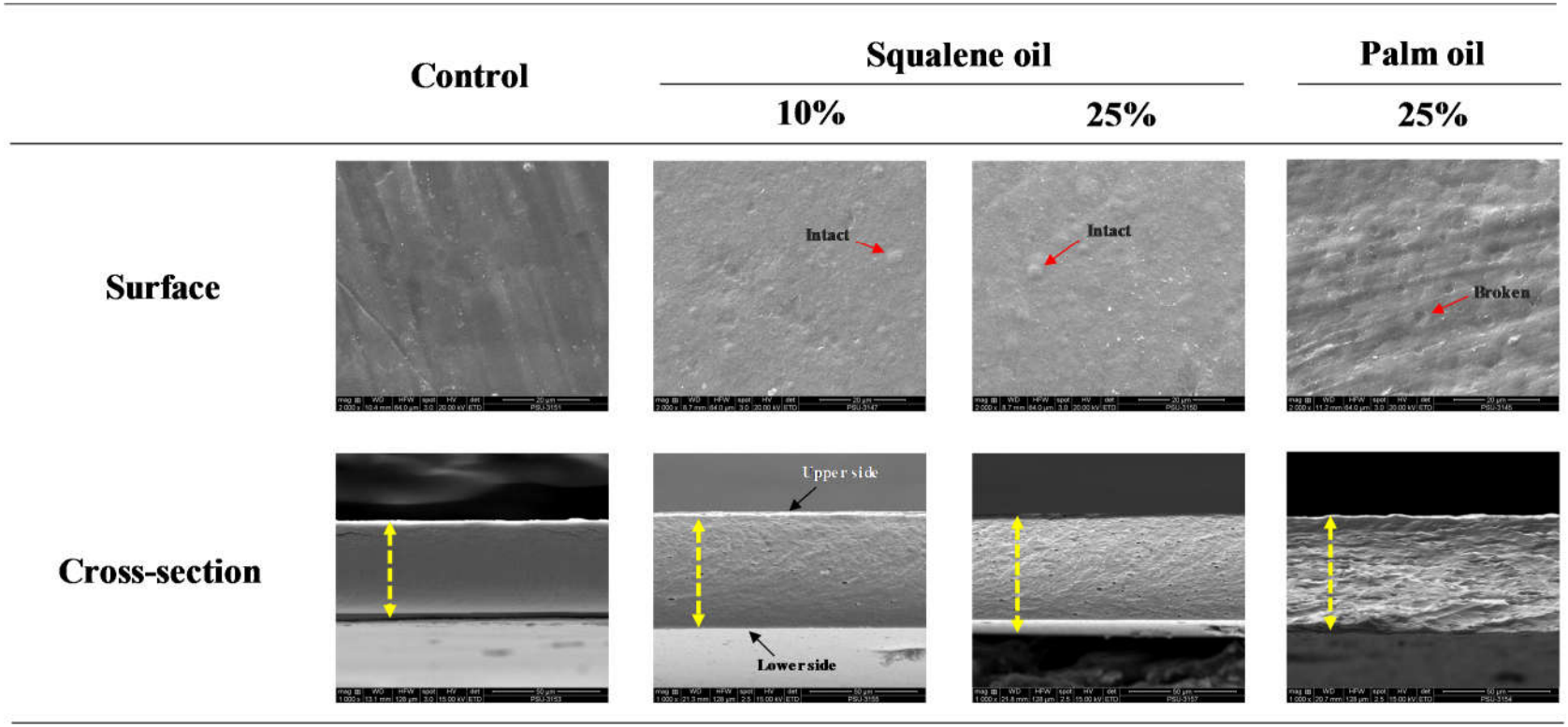

Figure 40. Scanning electron microscopy (SEM) micrographs of surface (2000 x) and cross-section (1000 x) of films from golden carp skin gelatin incorporated with squalene rich fraction (SRF) from spot-tail shark liver at 10% and 25% or PO at 25%.

7.6. Conclusions

Incorporation of highly hydrophobic SRF improved properties of gelatin film, mainly by increasing barrier properties toward moisture and light, which are crucial factor in controlling degradation, oxidation and deterioration of foods. SRF was better than PO at the same level added to enhance film properties including EAB and TS of the gelatin-based film. When compared to PO, SRF had demonstrated excellent emulsion forming properties. Additionally, films prepared with SRF generated more uniform and smoother surface that PO film. Squalene is a natural compound linked with many health benefits. Thus, squalene incorporated edible gelatin films with improved properties could be widely used in food and health applications.

7.7. References

Ali, A. M. M., Bavisetty, S. C. B., Prodpran, T. and Benjakul, S. 2019. Squalene from fish livers extracted by ultrasound assisted direct *in-situ* saponification: Purification and molecular characteristics. Journal of the American Oil Chemists' Society. DOI:10.1002/aocs.12262.

Ali, A. M. M., Kishimura, H. and Benjakul, S. 2018a. Extraction efficiency and characteristics of acid and pepsin soluble collagens from the skin of golden carp (*Probarbus Jullieni*) as affected by ultrasonication. Process Biochemistry. 66: 237-244.

Ali, A. M. M., Kishimura, H. and Benjakul, S. 2018b. Physicochemical and molecular properties of gelatin from skin of golden carp (*Probarbus Jullieni*) as influenced by acid pretreatment and prior-ultrasonication. Food Hydrocolloids. 82: 164-172.

Bavisetty, S. C. B. and Narayan, B. 2015. An improved RP-HPLC method for simultaneous analyses of squalene and cholesterol especially in aquatic foods. Journal of Food Science and Technology. 52: 6083-6089.

Benjakul, S., Kittiphattanabawon, P. and Regenstein, J. M. 2012. Fish gelatin. *In* Food Biochemistry and Food Processing, Second Edition. (Simpson, B. K., ed.). p. 388-405. Wiley-Blackwell. Iowa, USA.

Bindu, B. S. C., Mishra, D. P. and Narayan, B. 2015. Inhibition of virulence of *Staphylococcus aureus*–a food borne pathogen–by squalene, a functional lipid. Journal of Functional Foods. 18: 224-234.

Carvalho, R. A., Sobral, P. J. A., Thomazine, M., Habitante, A. M. Q. B., Giménez, B., Gómez-Guillén, M. C. and Montero, P. 2008. Development of edible films based on differently processed Atlantic halibut (*Hippoglossus hippoglossus*) skin gelatin. Food Hydrocolloids. 22: 1117-1123.

Chung, H., Kim, T. W., Kwon, M., Kwon, I. C. and Jeong, S. Y. 2001. Oil components modulate physical characteristics and function of the natural oil emulsions as drug or gene delivery system. Journal of Controlled Release. 71: 339-350.

Czaplicki, S., Ogrodowska, D., Derewiaka, D., Tańska, M. and Zadernowski, R. 2011. Bioactive compounds in unsaponifiable fraction of oils from unconventional sources. European Journal of Lipid Science and Technology. 113: 1456-1464.

Elewski, B. E. 1993. Mechanisms of action of systemic antifungal agents. Journal of the American Academy of Dermatology. 28: S28-S34.

Fox, C. 2009. Squalene emulsions for parenteral vaccine and drug delivery. Molecules. 14: 3286-3312.

Gornall, A. G., Bardawill, C. J. and David, M. M. 1949. Determination of serum proteins by means of the biuret reaction. Journal of Biological Chemistry. 177: 751-766.

Gul, O., Saricaoglu, F. T., Besir, A., Atalar, I. and Yazici, F. 2018. Effect of ultrasound treatment on the properties of nano-emulsion films obtained from hazelnut meal protein and clove essential oil. Ultrasonics Sonochemistry. 41: 466-474.

Guzman, A., Torres, J. E., Prada, L. P. and Nuñez, M. L. 2010. Hydroprocessing of crude palm oil at pilot plant scale. Catalysis Today. 156: 38-43.

Hoque, M. S., Benjakul, S. and Prodpran, T. 2011a. Effects of partial hydrolysis and plasticizer content on the properties of film from cuttlefish (*Sepia pharaonis*) skin gelatin. Food Hydrocolloids. 25: 82-90.

Hoque, M. S., Benjakul, S. and Prodpran, T. 2011b. Properties of film from cuttlefish (*Sepia pharaonis*) skin gelatin incorporated with cinnamon, clove and star anise extracts. Food Hydrocolloids. 25: 1085-1097.

Iwata, K. I., Ishizaki, S. H., Handa, A. K. and Tanaka, M. U. 2000. Preparation and characterization of edible films from fish water-soluble proteins. Fisheries Science. 66: 372-378.

KopiCoVá, Z. and VaVreiNoVá, S. 2007. Occurrence of squalene and cholesterol in various species of Czech freshwater fish. Czech Journal of Food Sciences. 25: 195-201.

Laemmli, U. K. 1970. Cleavage of structural proteins during the assembly of the head of bacteriophage T4. Nature. 227: 680-685.

Ma, W., Tang, C.-H., Yin, S.-W., Yang, X.-Q., Wang, Q., Liu, F. and Wei, Z.-H. 2012. Characterization of gelatin-based edible films incorporated with olive oil. Food Research International. 49: 572-579.

Nagarajan, M., Benjakul, S., Prodpran, T. and Songtipya, P. 2012. Properties of film from splendid squid (*Loligo formosana*) skin gelatin with various extraction temperatures. International Journal of Biological Macromolecules. 51: 489-496.

Nagarajan, M., Benjakul, S., Prodpran, T. and Songtipya, P. 2014. Properties of bio-nanocomposite films from tilapia skin gelatin as affected by different nanoclays and homogenising conditions. Food and Bioprocess Technology. 7: 3269-3281.

Nagarajan, M., Prodpran, T., Benjakul, S. and Songtipya, P. 2017. Properties and characteristics of multi-layered films from tilapia skin gelatin and poly (lactic acid). Food Biophysics. 12: 222-233.

Nilsuwan, K., Benjakul, S. and Prodpran, T. 2017. Properties, microstructure and heat seal ability of bilayer films based on fish gelatin and emulsified gelatin films. Food Biophysics. 12: 234-243.

Nilsuwan, K., Benjakul, S., Prodpran, T. and de la Caba, K. 2019. Fish gelatin monolayer and bilayer films incorporated with epigallocatechin gallate:

Properties and their use as pouches for storage of chicken skin oil. Food Hydrocolloids. 89: 783-791.

Popa, O., Băbeanu, N. E., Popa, I., Niță, S. and Dinu-Pârvu, C. E. 2015. Methods for obtaining and determination of squalene from natural sources. BioMed Research International. 2015: 1-16.

Prodpran, T., Benjakul, S. and Artharn, A. 2007. Properties and microstructure of protein-based film from round scad (*Decapterus maruadsi*) muscle as affected by palm oil and chitosan incorporation. International Journal of Biological Macromolecules. 41: 605-614.

Reddy, L. H. and Couvreur, P. 2009. Squalene: A natural triterpene for use in disease management and therapy. Advanced Drug Delivery Reviews. 61: 1412-1426.

Setiowaty, G., Che Man, Y., Jinap, S. and Moh, M. 2000. Quantitative determination of peroxide value in thermally oxidized palm olein by Fourier transform infrared spectroscopy. Phytochemical Analysis: An International Journal of Plant Chemical and Biochemical Techniques. 11: 74-78.

Staroszczyk, H., Pielichowska, J., Sztuka, K., Stangret, J. and Kołodziejska, I. 2012. Molecular and structural characteristics of cod gelatin films modified with EDC and TGase. Food Chemistry. 130: 335-343.

Theerawitayaart, W., Prodpran, T., Benjakul, S. and Sookchoo, P. 2019. Properties of films from fish gelatin prepared by molecular modification and direct addition of oxidized linoleic acid. Food Hydrocolloids. 88: 291-300.

Tongnuanchan, P., Benjakul, S. and Prodpran, T. 2012. Properties and antioxidant activity of fish skin gelatin film incorporated with citrus essential oils. Food Chemistry. 134: 1571-1579.

Tongnuanchan, P., Benjakul, S. and Prodpran, T. 2013. Characteristics and antioxidant activity of leaf essential oil–incorporated fish gelatin films as affected by surfactants. International Journal of Food Science & Technology. 48: 2143-2149.

Tongnuanchan, P., Benjakul, S. and Prodpran, T. 2014. Structural, morphological and thermal behaviour characterisations of fish gelatin film incorporated with basil and citronella essential oils as affected by surfactants. Food Hydrocolloids. 41: 33-43.

Tongnuanchan, P., Benjakul, S., Prodpran, T. and Nilsuwan, K. 2015. Emulsion film based on fish skin gelatin and palm oil: Physical, structural and thermal properties. Food Hydrocolloids. 48: 248-259.

Tongnuanchan, P., Benjakul, S., Prodpran, T., Pisuchpen, S. and Osako, K. 2016. Mechanical, thermal and heat sealing properties of fish skin gelatin film containing palm oil and basil essential oil with different surfactants. Food Hydrocolloids. 56: 93-107.

Van Tamelen, E. 1968. Bioorganic chemistry: sterols and acrylic terpene terminal expoxides. Accounts of Chemical Research. 1: 111-120.

Vanin, F., Sobral, P., Menegalli, F., Carvalho, R. and Habitante, A. 2005. Effects of plasticizers and their concentrations on thermal and functional properties of gelatin-based films. Food Hydrocolloids. 19: 899-907.

Xiao, J., Wang, W., Wang, K., Liu, Y., Liu, A., Zhang, S. and Zhao, Y. 2016. Impact of melting point of palm oil on mechanical and water barrier properties of gelatin-palm oil emulsion film. Food Hydrocolloids. 60: 243-251.

Xie, Y. L., Zhou, H. M. and Qian, H. F. 2006. Effect of addition of peach gum on physicochemical properties of gelatin-based microcapsule. Journal of Food Biochemistry. 30: 302-312.

Zhang, Y., Simpson, B. K. and Dumont, M.-J. 2018. Effect of beeswax and carnauba wax addition on properties of gelatin films: A comparative study. Food Bioscience. 26: 88-95.

CHAPTER 8

EFFECT OF SQUALENE AS A GLYCEROL SUBSTITUTE ON PHYSICO-CHEMICAL, BARRIER AND MORPHOLOGICAL PROPERTIES OF GOLDEN CARP (*PROBARBUS JULLIENI*) SKIN GELATIN FILM

8.1. Abstract

Gelatin films prepared by using glycerol (GLY) and squalene (SQ) at different ratios (10:0, 7:3, 5:5, 3:7 and 0:10; w/w) as plasticizer were characterized. Incorporation of SQ reduced the moisture content of the gelatin film ($p < 0.05$). Films plasticized with GLY/SQ at a ratio of 5:5 (w/w) had highest tensile strength (TS), which was 61.7% higher than that using GLY as plasticizer (GLY). Nevertheless, continuous decrease in elongation at break (EAB) were attained with increasing SQ ratios ($p < 0.05$). SQ films had a decrease in water vapor permeability (WVP) and oxygen permeability (OP), compared to GLY film ($p < 0.05$). Additionally, SQ films had slightly lower lightness with less transparency. Based on microstructure, cross-section of films plasticized with only SQ (without GLY) presented extremely course structure with large particle size, compared to those plasticized with GLY/SQ mixture or GLY alone. Based on FTIR and DSC spectra, SQ decreased gelatin-gelatin interactions associated with disordered structure. In addition, SQ film demonstrated lower melting transition (T_{max}), and enthalpy (ΔH), but a slightly increased glass transition temperature (T_g). Thermal degradation behavior of films showed that GLY film possessed a greater number of gelatin-gelatin interaction than that incorporated with SQ. Thus, SQ could replace GLY up to 50% to render stronger films with improved WVP as well as OP of gelatin films.

8.2. Introduction

In recent years, protein-based biodegradable and smart packagings have attracted immense attention in food and pharma industries as they partly substitute the traditional petrochemical-based counterpart. Among the different proteins, gelatin has

gained much interest due to its thermo-reversible network forming property and heat sealability (Benjakul *et al.*, 2012). Gelatin, particularly from aquatic sources showed the excellent barrier property against oxygen and UV light, which accelerate the oxidation in a food system (Nilsuwan *et al.*, 2019). Additionally, gelatin can form a colorless film with high transparency, which are characteristics required as a packaging material (Zhang *et al.*, 2018).

Generally, gelatin films are known to render relatively low mechanical property, compared to those of traditional petrochemical based films (Gómez-Guillén *et al.*, 2009). Furthermore, gelatin and most commonly used plasticizers (propylene glycol, polyethylene glycerol, glycol and sorbitol) are all hydrophilic in nature (Cao *et al.*, 2009). As a consequence, gelatin films are extremely susceptible to environmental conditions, particularly high humidity due to their poor moisture resistant property. To conquer the drawback, gelatin-based films with enhanced mechanical and moisture barrier properties with augmented bioactivity have been extensively investigated. For instance, gelatin incorporated with hydrophobic nanoclay improved moisture resistant and thermal insulation effect (Nagarajan *et al.*, 2014), and smart gelatin-EGCG film with antioxidant activity and enhanced mechanical and thermal properties was developed (Nilsuwan *et al.*, 2018). Incorporation of lipids in gelatin film is known to improve the moisture barrier property. Several edible oils (including, palm, olive, corn, and soybean oil), essential oils (including, basil, clove and citronella), fatty acids (linoleic, oleic, palmitic and stearic acids) were added to confer superior barrier properties against moisture and oxygen (Cao *et al.*, 2009; Gul *et al.*, 2018; Nilsuwan *et al.*, 2017; Theerawitayaart *et al.*, 2019; Tongnuanchan *et al.*, 2015). Incorporation of hydrophobic substances, especially different types of oils, are known to render plasticizing effect on the gelatin films (Prodpran *et al.*, 2007).

Generally, plasticizers are known to migrate between the polymers and simultaneously induce hindrance of intermolecular interactions in film matrix, thus enhancing the flexibility of films (Cao *et al.*, 2009). The concentration and type of plasticizer are critical factors which could affect the mechanical and moisture barrier properties of gelatin film. Due to the competent hydrophilicity of low MW plasticizers, the usage at lower amount could be a promising means to improve the moisture barrier

properties of gelatin film. Along with the addition of hydrophobic compounds as plasticizer, the brittleness of film could be reduced and lesser amount of hydrophilic plasticizer is needed. Theerawitayaart *et al.* (2019) documented that migration of hydrophobic compounds can be reduced by means of increasing the hydrophobicity of lipid fraction.

Squalene (SQ) ($C_{30}H_{50}$) is a linear triterpene and is known as highly hydrophobic hydrocarbon. Owing to its structural properties and health benefits, SQ has numerous applications in nutraceutical, pharmaceutical, cosmetics and food industries (Desai *et al.*, 1996; Reddy and Couvreur, 2009). Apart from this, SQ is known to possess antibacterial and antifungal activity (Bindu *et al.*, 2015; Elewski, 1993). Due to its suitability to form nano-emulsions with excellent stability and biocompatibility, SQ is widely used as vaccine deliver or drug delivery emulsions (Fox, 2009). SQ is commonly found in plants, animals and humans. In addition, fish liver, have been documented to be a significant source of SQ (Bavisetty and Narayan, 2015; KopiCoVá and VaVreiNoVá, 2007). Recently, Ali *et al.* (2019a) documented that SQ can be extracted using ultrasound-assisted direct in-situ saponification process and further purified. Thus, replacement of hydrophilic plasticizer with SQ for producing gelatin films with improved moisture barrier properties could bring about the edible films with bioactivity and enhanced water vapor barrier property.

8.3. Objective

To investigate the effect of SQ as a GLY substitute on mechanical, barrier (moisture and oxygen), morphological and thermal properties of golden carp skin gelatin film with a prospect of preparing edible film with promising health benefits.

8.4. Materials and Methods

8.4.1. Chemicals

Sodium hydroxide, acetic acid, potassium hydroxide, and glycerol were procured from Merck (Darmstadt, Germany). Methanol, chloroform and *n*-hexane were obtained from RCL Lab-Scan (Bangkok, Thailand). Tween 20 was obtained from Fisher BioReagents™ (Waltham, Massachusetts, USA). Squalene (≥98%), silica gel

(for column chromatography, 70–230 mesh) and protein molecular weight marker were purchased from Sigma Chemicals (St. Louis, MO, USA).

8.4.2. Collection of raw materials

Golden carp skin was collected and processed as describe in the section *2.4.2.1.* Spot-tail shark liver were collected and processed as described in the section 6.4.2.

8.4.3. Gelatin extraction

Removal of non-collagenous proteins and acid pretreatment were performed as describe in the sections *5.4.2.1* and *5.4.2.2*, respectively. Gelatin extraction was conducted as mentioned in the section *5.4.2.4.*

8.4.4. Extraction of squalene (SQ)

Firstly, unsaponifiable matter was extracted and subjected to concentration and purification using fractional crystallization and column purification, respectively.

8.4.4.1. Recovery of unsaponifiable matter (*section 7.4.4.1*)

8.4.4.2. Fractional crystallization (*section 6.4.5.1*)

8.4.4.3. Column purification (*section 6.4.5.2*)

8.4.4.4. Quantification of squalene using reversed-phase high-performance liquid chromatography (RP-HPLC) (*section 6.4.6.2*)

8.4.5. Preparation of gelatin film

8.4.5.1. Preparation of film forming solution and emulsion

Gelatin films were prepared as described by Nilsuwan *et al.* (2017). Gelatin from golden carp skin was solubilized in distilled water at 60 °C for 30 min to obtain a concentration of 3.5% (w/v). To study the impact of SQ as GLY substitute, GLY/SQ mixtures at different ratios (10:0, 7:3, 5:5, 3:7 and 0:10) were added at a final

concentration of 30% based on protein content (w/w). To the prepared gelatin solution, GLY was firstly added at the specified levels. Thereafter, SQ previously mixed with Tween-20 at 25% (w/w, based on crude squalene) was added. All the dispersions were sonicated (amplitude of 80%) for 3 min and 30 s at 25 °C. The resulting emulsions were referred to as film-forming emulsions (FFE). The gelatin solution containing 30% GLY was termed as film forming solution (FFS).

8.4.5.2. Characterization of FFE (*section 7.4.7.1*)

8.4.5.3. Film casting and drying (*section 7.4.5.2*)

8.4.6. Determination of film properties

Before testing of thickness, water vapor permeability, mechanical properties, light transmission and color, all the films were conditioned at RH of 50 ± 5% and temperature 25 ± 0.5 °C for 48 h.

8.4.6.1. Film thickness and moisture content

Thickness of the films was determined as described in the section *7.4.6.1.*

Moisture content of conditioned gelatin films was determined as per the AOAC (2000) method. Gelatin films were weighed (W_1) and dried in an oven at 105 ± 2 °C until a constant weight was achieved (W_2). Moisture content was calculated using the equation:

$$\text{Moisture content (\%)} = \left(\frac{W_1 - W_2}{W_1}\right) \times 100 \qquad (3)$$

8.4.6.2. Color and transparency (*section 7.4.6.4*)

8.4.6.3. Mechanical properties (*section 7.4.6.2*)

8.4.6.4. Water vapor permeability (WVP) (*section 7.4.6.3*)

8.4.6.5. Protein patterns (*section 7.4.7.3*)

8.4.7. Characterization of selected films

Gelatin film incorporated with the mixture of GLY/SQ at the ratio of 5:5 (w/w) rendering highest TS with intermediated EAB and WVP was selected for characterization. Gelatin films containing only GLY (GLY) as well as only SQ (SQ) were also characterized. Before characterization, all the films were dehydrated in a desiccator containing P_2O_5 at room temperature (25 ± 1 °C) for a period of one week.

8.4.7.1. Oxygen permeability (OP)

Oxygen transmission rate (OTR) was measured according to the ASTM method (ASTM, 2005). OTR of films were measured using an Oxygen Permeation Analyzer model 8000 (Illinois Instruments Inc., Medford, MA, USA) by placing them on a stainless-steel mask. The film loaded masks were mounted on a test cell and exposed to an atmospheric flow of oxygen on one side and with nitrogen flow on the other side. The transmission of oxygen through the film was measured at 25 ± 1 °C and 50 ± 2 % RH. The films were equilibrated for at least 10 h before analysis. OP was determined using following equation:

$$\mathrm{OP\ (mol.\,m\ m^{-2}.\,s^{-1}.\,Pa^{-1})} = \frac{\mathrm{OTR}.l}{\Delta P} \qquad (6)$$

where 'OTR' is the oxygen transmission rate (mol m^{-2} s^{-1}), 'l' is the thickness of film (m) and 'ΔP' is the partial pressure of oxygen (1.013×10^5 Pa at 25 °C).

8.4.7.2. Attenuated total reflectance-Fourier transform infrared (ATR-FTIR) spectroscopy (*section 2.4.3.4*)

8.4.7.3. Differential scanning calorimetry (DSC) of films (*section 7.4.7.5*)

8.4.7.4. Thermo-gravimetric analysis (TGA) of films (*section 7.4.7.6*)

8.4.7.5. Scanning electron microscopy (SEM) of films (*section 7.4.7.7*)

8.4.1. Statistical analysis

The experiments were conducted in triplicates with completely randomized design (CRD). The differences between means were tested by the Duncan's multiple range test and the data were shown as means ± standard deviation. Statistical analysis of experimental data was performed using the SPSS 11.0 software (SPSS Inc., Chicago, IL, USA).

8.5. Results and discussion

8.5.1. Extraction of SQ

SQ was extracted and purified from spot-tail shark liver by adopting the optimized conditions as reported by Ali *et al.* (2019a). The yield of pure SQ from spot-tail shark liver was 6.8 g 100 g^{-1} raw liver. A recovery of 95.6% was achieved as quantified by RP-HPLC and enumerated using Eq. 1. The obtained SQ had a purity of ≥ 94%, compared to the authenticated standard (calculated based on Eq. 2) (Figure1). The recovered SQ was pale yellow in color (L^* = 78.72, a^* = -1.90 and b^* = 6.43).

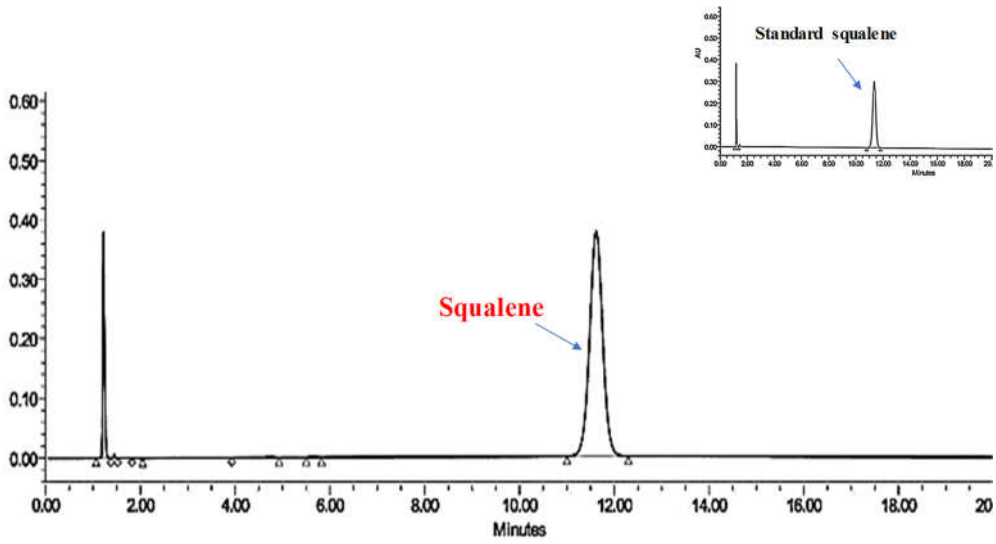

Figure 41. Reversed-phase high-performance liquid chromatograms (RP-HPLC) of spot-tail shark liver obtained from ultrasound assisted direct in-situ saponification, concentrated and purified using fractional crystallization and column purification, respectively.

8.5.2. Preparation of gelatin film with different GLY/SQ ratios

8.5.2.1. CSLM images

CSLM images of FFS and FFE containing GLY/SQ mixtures or SQ alone at various ratios are illustrated in Figure 2. The distribution of SQ droplets in FFE appeared as red color in contrast to unstained protein phase (black background). SQ was evenly distributed in the continuous protein phase, irrespective of the levels added. With the higher levels of SQ incorporated, an increased number of droplets were observed in protein phase. It was noted that at higher level of SQ in GLY/SQ mixtures (3:7) or SQ alone, the SQ droplets became denser with narrow size distribution. Additionally, ultrasonication was highly efficient to form emulsions with smaller droplet size based on CSLM scale. No coalescence was observed in FFEs, irrespective of the level of SQ used. The results implied that SQ could form highly stable FFE in presence of Tween-20. Thus, Tween-20 provided an appropriate hydrophobic-lipophilic balance (HLB) to stabilize SQ droplets in FFEs. On the basis of hydrophobic property of SQ, a surfactant with greater HLB value (more hydrophilic) was appropriate to localize at the water/oil interphase (Fox, 2009). As a result, self-association of SQ droplets through hydrophobic-hydrophobic interaction to form larger particles was prevented. This led to a consistent nano-emulsion with narrow range distribution. Tween-20 with high HLB index (16.7) is a nonionic monolaurate ester. It interacts mainly with aqueous phase and is most widely used in SQ based emulsion for developing vaccines (Fox *et al.*, 2008). Additionally, SQ is documented to form highly stable nano-emulsion when any emulsifier at sufficient concentration was used (Chung *et al.*, 2001).

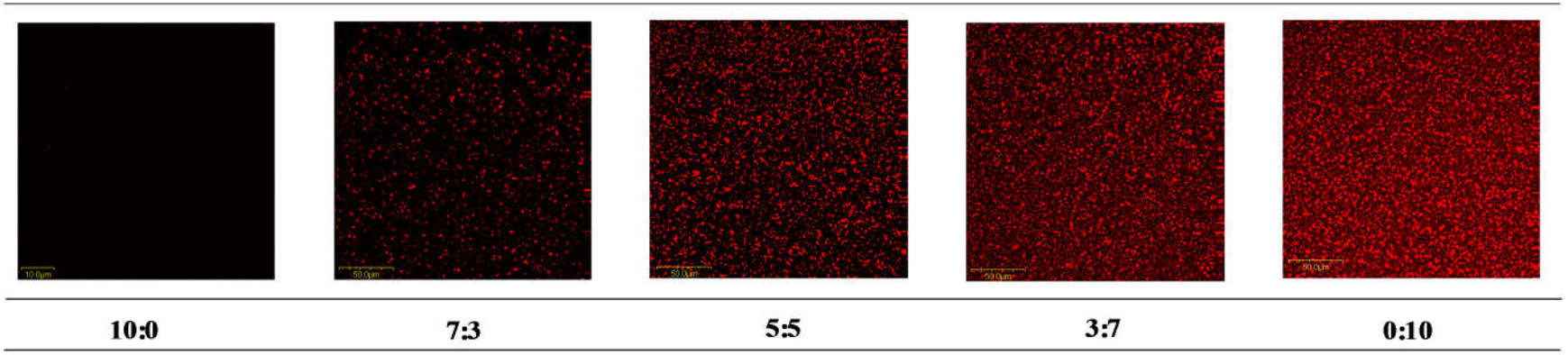

Figure 42. Confocal scanning laser microscopic (CSLM) images of film forming solution and emulsions containing different glycerol:squalene ratios (10:0, 7:3, 5:5, 3:7 and 0:10) (w/w).

8.5.2.2. Characteristics of gelatin film

Films added with GLY/SQ mixture at different ratios were easy to handle. Films had varying degree of flexibility, where the highest flexibility was achieved for film with GLY/SQ ratio of 5:5 (w/w). When GLY was replaced with SQ, films exerted a decreased extensibility and transparency, especially at higher levels of SQ. At all the levels of SQ, films were homogeneous, and no apparent transudation was observed. It was also observed that the incorporation of SQ in the GLY/SQ mixture higher than 5:5, the films had non-viscid surface. Additionally, no fishy odor or off odor was detected for all the films, irrespective of SQ level incorporated. The results suggested that extraction and purification of SQ mostly diminished the fishy odor effectively.

8.5.2.3. Thickness and moisture content of gelatin films

The thickness of all the gelatin films ranged from 0.056 to 0.080 mm (Table 1). Films showed a gradual increase in thickness with increasing levels of SQ incorporated as plasticizer. The highest thickness was obtained for the film containing only SQ, while that of film added with GLY (GLY) had the lowest thickness ($p < 0.05$). SQ with its long chain could insert between gelatin molecules, which caused a higher number of discontinuity zones and led to formation of protruded structure with higher thickness (Gul *et al.*, 2018; Prodpran *et al.*, 2007). On the other hand, GLY film showed lowest thickness value. GLY had smaller MW with hydrophilic in nature. It was efficiently dissolved and dispersed in an aqueous phase of FFS. This resulted in the formation of more dense and compact film.

Moisture content of all the gelatin films was examined after conditioning (25 °C and RH of 50 ± 5% for 48 h) ranged from 5.6 to 16.2% (based on the wet weight) (Table 1). Films prepared with different ratios of GLY/SQ mixture possessed various moisture contents ($p < 0.05$). Highest moisture or water content (16.2%) was observed for GLY film, while the lowest moisture content (5.7%) was noticed for the film plasticized with only SQ. The results indicated that the water content of gelatin films was not only associated with hydrophilicity of gelatin molecules but also was related to the type plasticizing agent used.

Table 19: Thickness, moisture content, color and transparency values of golden carp skin gelatin film incorporated with glycerol, squalene and their mixtures at different ratios.

GLY/SQ ratio (w/w)	Thickness (mm)	Moisture content (%)	Color				Transparency value
			L^*	a^*	b^*	ΔE^*	
10:0	0.056 ± 0.003^{e}	16.21 ± 0.17^{a}	89.46 ± 0.11^{a}	-1.26 ± 0.03^{a}	3.50 ± 0.02^{e}	4.50 ± 0.09^{e}	2.21 ± 0.08^{e}
7:3	0.058 ± 0.002^{d}	10.34 ± 0.08^{b}	89.19 ± 0.06^{b}	-1.32 ± 0.01^{b}	3.73 ± 0.04^{d}	4.85 ± 0.06^{d}	7.24 ± 0.21^{d}
5:5	0.069 ± 0.004^{c}	8.4 ± 0.05^{c}	89.01 ± 0.04^{c}	-1.36 ± 0.01^{c}	4.13 ± 0.03^{c}	5.26 ± 0.05^{c}	8.85 ± 0.16^{c}
3:7	0.078 ± 0.002^{b}	7.11 ± 0.06^{d}	88.96 ± 0.04^{d}	-1.39 ± 0.01^{d}	4.19 ± 0.05^{b}	5.34 ± 0.07^{b}	9.38 ± 0.13^{b}
0:10	0.080 ± 0.003^{a}	5.69 ± 0.05^{e}	88.55 ± 0.12^{e}	-1.45 ± 0.0^{e}	4.48 ± 0.02^{a}	5.83 ± 0.12^{a}	15.63 ± 0.59^{a}

Mean ± SD from triplicate determination.

Different superscript letters in the same column indicate significant difference ($p < 0.05$).

GLY: glycerol; SQ: squalene

Therefore, GLY being hydrophilic could have attracted and retained greater amount of water in the film matrix, especially via hydrogen bonding. Similarly, Cao *et al.* (2009) documented that when gelatin films plasticized with different hydrophilic plasticizing compounds such as GLY, sucrose, sorbitol, ethylene glycol, di and tri-ethylene glycol became hydrophilic. On the other hand, films substituted GLY with SQ exhibited significant reduction in moisture content ($p < 0.05$). Rivero *et al.* (2010) reported that the moisture content of gelatin film without plasticizing agent was not more than 10.3%. In this study, moisture content of films containing SQ at higher levels was significantly lower than that recommended for ideal gelatin film. This was more likely due to the hydrophobic property of SQ, which more likely repelled water molecules and resulted in less retention of water (bound as well as free) in the film matrix. Thus, the films plasticized with SQ became less hygroscopic and less susceptible to humid environmental conditions, compared to GLY film.

8.5.2.4. Color and transparency

The color of prepared gelatin films was affected when plasticized with GLY/SQ at various ratios as shown in Table 1. With increasing levels of SQ in the GLY/SQ mixture, a gradual decrease in L^* value (lightness) of the films was observed ($p \leq 0.05$). The obtained results were in line with Tongnuanchan *et al.* (2015) who reported that incorporation of palm oil notably reduced the lightness of tilapia skin gelatin film. All the films had a^*-value in the range of -1.45 to -1.26. A minor increase in a^*-value of films was noticed when GLY was replaced with SQ ($p \leq 0.05$), depending on the level of replacement. Generally, addition of SQ at higher level could have increased crystallinity in the matrix of the film, as reflected by higher green color (Ali *et al.*, 2019b). Among all the film samples, those prepared with higher levels of SQ had higher b^* values (yellowness) ($p < 0.05$), which was linked to the color of SQ ($b^* = 6.43$, pale yellow in color). However, films incorporated with colorless compounds such as different types of wax were reported to show no differences in both a^* and b^* values (Zhang *et al.*, 2018). Moreover, increased ΔE^* values were mainly related to the increased b^* values, predominantly at the higher ratios of SQ in GLY/SQ mixture. As a consequence, the color of gelatin films was affected by the color of SQ.

Transparency values of all the gelatin films are presented in Table 1. GLY film exhibited lower transparency value ($p < 0.05$), compared to others. The lower transparency value indicated that films were highly transparent. Generally, films added with SQ demonstrated greater transparency value, suggesting more opaqueness or turbidity. Tongnuanchan *et al.* (2015) reported that the incorporation of palm oil increased the opaqueness of gelatin film. Transparency value of films added with SQ was higher ($p < 0.05$) as the level of SQ in GLY/SQ mixture increased. SQ with long chain forming as solid crystals might cause the light scattering along with yellowish color. Typically, incorporation of wax/fat was documented to raise the opaqueness of resulting gelatin film (Theerawitayaart *et al.*, 2019; Zhang *et al.*, 2018). Moreover, the results for higher opacity of films with SQ was in accordance with the lower L^* values. Therefore, substitution of GLY with SQ affected the transparency of resulting gelatin films.

8.5.2.5. Mechanical properties

Mechanical properties of all the gelatin films characterized as Young's modulus (YM), elongation at break (EAB) and tensile strength (TS) are shown in Table 2. TS and EAB of GLY film were 69.6 MPa, 56.8% and 32.2 MPa and, respectively. EAB and TS of golden carp skin gelatin film were higher than to those of gelatin films reported from various fish sources (Cao *et al.*, 2009; Carvalho *et al.*, 2008; Nagarajan *et al.*, 2014). This could be mostly associated with the higher imino acid residues as well as the greater proportion of higher MW protein chains of gelatin from golden carp skin (Ali *et al.*, 2018). Moreover, films substituted GLY with SQ showed altered mechanical behavior of films ($p < 0.05$). In terms of plasticizing efficiency, GLY presented superior plasticizing efficiency to SQ as shown by higher EAB and lower value of YM of films plasticized with the former. The film incorporated with GLY presented lowest YM (69.6 MPa), whereas the SQ film had the highest value (1357.3 MPa). This indicated that GLY film was more flexible due to the plasticizing effect of GLY. When GLY was replaced with SQ, the stiffness of films gradually increased, irrespective the SQ levels used. In addition, highest EAB was noticed for GLY film (56.8%), while SQ film exhibited the lowest EAB (10.8%) ($p < 0.05$). The greater EAB of gelatin film in the presence of GLY could be linked to its water-soluble property and

smaller molecular size, thus favoring its migration and localization between the gelatin chains (Vanin *et al.*, 2005). Furthermore, the hydroxyl groups of GLY might have assisted the attraction and retention of ampule amount of water in the matrix of gelatin film, which contributed to the elasticity of film as observed from higher values of EAB. Cao *et al.* (2009) documented that water could act as a plasticizing agent in protein-based films. Enhancement of elasticity was affected by the occurrence of hydrogen bonds between gelatin-water or GLY-water (Rivero *et al.*, 2010). Those phenomena assisted the free molecular mobility of gelatin along the chain length to some extent during extension. Similarly, Jongjareonrak *et al.* (2006) documented that with increasing concentration of GLY, the EAB of gelatin film was significantly increased, while TS was comparatively decreased.

Typically, the incorporation of hydrophobic compounds like lipids, oil, fatty acids, etc., is known to enhance the elasticity and decreases the strength of gelatin film (Tongnuanchan *et al.*, 2014). This was caused by the increased number of discontinuity zones, whereas hydrophilic plasticizer such as GLY was still functioned to lower protein chain interaction (Prodpran *et al.*, 2007). When GLY was replaced with SQ, a decreased elasticity and an increased film strength were noticed. The decrease in EAB or increase in YM values of gelatin film could be associated with the reduction of GLY level as well as water content in the film. SQ film exhibited the highest value of YM and lowest EAB ($p < 0.05$). Furthermore, with addition of increased levels of SQ in GLY/SQ mixture (3:7) or SQ alone, the resulting films were more brittle. Although SQ incorporated films demonstrated discontinuity in the film matrix, the water repelling property and hydrophobic interaction between SQ-gelatin chains could have restricted the molecular mobility of gelatin chains. Furthermore, this could have also contributed to the film strengthening effect to some extent as noticed by increased TS when GLY was replaced with SQ (Table 2).

Films containing GLY substituted with SQ or film containing SQ alone exhibited the increased TS (40.1-52.2 MPa) ($p < 0.05$). The extent of increment in TS of SQ films was higher when compared to that reported for gelatin films such as films fabricated with poly lactic acid having TS up to 31.3 MPa (Nagarajan *et al.*, 2017), as well as a gelatin film crosslinked using epigallocatechin gallate possessing TS up to

31.1 MPa (Nilsuwan *et al.*, 2018). Incorporation of hydrophobic substances has been reported to reduce the film strength due to the higher the number of discontinuity zone in film matrix (Ma *et al.*, 2012; Xiao *et al.*, 2016). Nevertheless, incorporation of SQ demonstrated film strengthening effect. This could mainly be associated with the long chain length of SQ (C_{30}) (Bavisetty and Narayan, 2015), which could contribute to the strengthening effect on film network. SQ could undergo entanglement along with the gelatin chains as shown by increased TS of films ($p < 0.05$) (Table 2). In addition, the SQ solid phase homogeneously dispersed in the film matrix might act as load bearing in the film matrix. This might enable more reinforcement effect during extension before the film rupture. Thus, SQ exhibited strengthening or reinforcing effects in gelatin film.

Furthermore, the maximum TS (52.2 MPa) was achieved when GLY/SQ (5:5 w/w) was used. However, further increase in SQ levels or decrease in GLY levels slightly decreased TS of films. This could be mainly linked to the dispersion of SQ in conjunction with GLY. GLY being a smaller molecule with adequate solubility had a tendency to penetrate and locate between gelatin molecules after casting and drying process. Thus, the presence of GLY could facilitate homogeneous dispersion of hydrophobic SQ droplets in the dried film matrix. GLY/SQ at a ratio of 5:5 (w/w) was noted to be an appropriate level for maximum dispersion of SQ in the presence of GLY in the dried films to achieve the highest TS. With lower level of GLY in GLY/SQ mixture (3:7) or SQ alone, uneven dispersion of film matrix during the drying process plausibly occurred, thus resulting in minor reduction in TS (Table 2). Similarly, Cao *et al.* (2009) documented that incorporation of hydrophobic substance such as oleic acid as plasticizer diminished all the mechanical properties (TS, EAB and EM) of gelatin film due to uneven dispersion of particles in film matrix. To obtain the desired mechanical properties of gelatin film, an appropriate concentration of GLY and SQ was mandatory.

Table 20: Tensile strength (TS), Young's modulus (YM), elongation at break (EAB), water vapor permeability (WVP) and oxygen permeability (OP) of golden carp skin gelatin film incorporated with glycerol, squalene and their mixtures at different ratios.

GLY/SQ ratio (w/w)	TS (MPa)	YM (MPa)	EAB (%)	WVP ($\times 10^{-10}$ g s^{-1} m^{-1} Pa^{-1})	OP ($\times 10^{-18}$ mol m m^{-2} s^{-1} Pa^{-1})
10:0	32.21 ± 3.32^{e}	69.67 ± 5.35^{e}	56.87 ± 2.09^{a}	2.61 ± 0.11^{a}	5.72 ± 0.15^{a}
7:3	40.1 ± 1.43^{d}	219.82 ± 23.92^{d}	46.65 ± 1.86^{b}	1.44 ± 0.03^{b}	-
5:5	52.22 ± 2.4^{a}	604.25 ± 48.93^{c}	39.45 ± 2.3^{c}	0.96 ± 0.02^{c}	3.18 ± 0.03^{b}
3:7	50.4 ± 2.6^{b}	1067.5 ± 53.77^{b}	26.44 ± 1.63^{d}	0.84 ± 0.01^{d}	-
0:10	47.87 ± 0.09^{c}	1357.31 ± 56.19^{a}	10.82 ± 1.12^{e}	1.21 ± 0.09^{e}	2.12 ± 0.07^{c}

Mean ± SD from triplicate determination.

Different superscript letters in the same column indicate significant difference ($p < 0.05$).

GLY: glycerol; SQ: squalene

8.5.2.6. WVP

GLY film exerted the highest WVP (2.61×10^{-10} g s^{-1} m^{-1} Pa^{-1}) ($p < 0.05$). WVP of films prepared by substituting GLY with SQ was reduced ($p < 0.05$) with increasing levels of SQ in GLY/SQ mixture up to 3:7 (w/w) (Table 2). As compared to GLY film, that containing GLY/SQ ratio of 3:7 (w/w) exhibited the lowest WVP (0.84×10^{-10} g s^{-1} m^{-1} Pa^{-1}), in which 67.9% decrease in WVP was gained, compared with that of GLY film. However, SQ film (without GLY) demonstrated a slight increase in WVP (1.21×10^{-10} g s^{-1} m^{-1} Pa^{-1}) ($p < 0.05$). In general, the films plasticized with GLY exhibited higher WVP, depending on the levels used, suggesting that the hygroscopic nature of GLY increased the absorption of water (Zhang *et al.*, 2018). This increased the moisture content of the films and consequently increased the mobility of water molecules. On the contrary, films substituted with SQ had improved water barrier properties, which could be mainly linked to the hydrophobic nature and its distribution in the film matrix. Furthermore, the higher WVP of film plasticized with only SQ might be primarily accounted to the permeability of water vapors through less uniform film network, which was disrupted by the hydrophobic SQ.

8.5.2.7. Protein patterns

Figure 3 depicts the protein patterns of films plasticized with different GLY/SQ ratios. All the gelatin films contained α_1-, α_2- and β-chains as the major components. Generally, gelatin from fish skin contains α_1- and α_2-chains as the dominant components (Benjakul *et al.*, 2012). Usually, gelatin films containing higher proportion of monomeric chain components (α_1- and α_2-chains) are known to improve the EAB than TS (Ali *et al.*, 2019b; Carvalho *et al.*, 2008). All the major components showed similar band intensity. Additionally, γ-chains (trimer) was also present in all the gelatin films. No difference in protein patterns was observed in all the gelatin films. The results indicated that all the film networks were stabilized by means of weak bonding, which were destabilized with the denaturing agents used for electrophoresis (Gómez-Guillén *et al.*, 2009). Moreover, oils could rarely interact with gelatin by strong linkages (Tongnuanchan *et al.*, 2016). Thus, it was presumed that SQ might interact

with hydrophobic domains of gelatin mainly through weak hydrophobic-hydrophobic interactions. Therefore, SQ had no effect on protein patterns of resulting gelatin film.

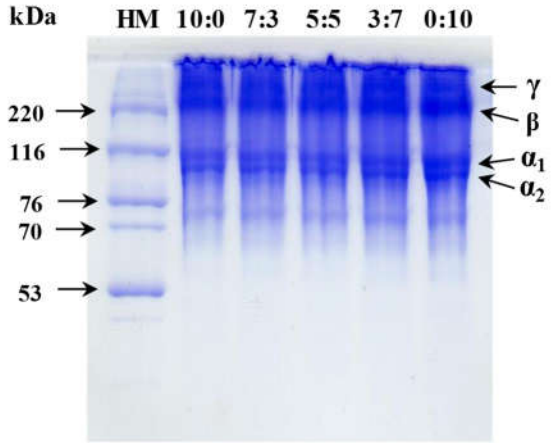

Figure 43. Protein patterns of golden carp skin gelatin film incorporated with glycerol, squalene and their mixtures at different ratios. HM: high molecular weight marker. Ratio (10:0, 7:3, 5:5, 3:7 and 0:10) represent glycerol:squalene ratio (w/w).

8.5.3. Characteristics of the selected gelatin film plasticized with GLY, SQ and GLY/SQ mixture

8.5.3.1. OP

OP of GLY film was 5.72×10^{-18} mol m m^{-2} s^{-1} Pa^{-1} (Table 2). The OP value was comparable to that reported for gelatin film from tilapia skin (4.6×10^{-18} mol m m^{-2} s^{-1} Pa^{-1}). Generally, OP of gelatin film was lower than those of synthetic nylon or linear low-density polyethylene packaging materials (Nilsuwan *et al.*, 2017). Among all the films, the lowest OP value (2.12×10^{-18} mol m m^{-2} s^{-1} Pa^{-1}) was noted for the film containing only SQ, which was found to be 63% lower, compared to that of GLY film ($p < 0.05$). Generally, addition of hydrophobic substances such as oils or poly (lactic acid) is known to increase the oxygen permeability of gelatin films, which was mainly linked to the discontinuity in the film matrix (Hosseini *et al.*, 2016; Nilsuwan *et al.*, 2017). However, incorporation of hydrophobic SQ decreased the transmission of oxygen across the film ($p < 0.05$). Furthermore, the rate of reduction was dependent on the level of SQ incorporated. This indicated that the dispersed SQ crystal phase might

act as a barrier to oxygen transportation through the film matrix. Uniform distribution of SQ crystal phase might increase the tortuosity of diffusion path of oxygen molecule, resulting in decreased diffusion coefficient and lowered permeability. SQ is also known as a potential antioxidant, which quenches the singlet oxygen, particularly in *in-vivo* process (Reddy and Couvreur, 2009). Thus, the addition of SQ as hydrophobic plasticizer could enhance the oxygen barrier property of gelatin film.

8.5.3.2. ATR-FTIR

FTIR spectra of films plasticized with GLY/SQ mixture at different ratios are presented in Figure 4. IR spectra presented the characteristic major peaks of amide- I, II, III, A and B, of gelatin (Gómez-Guillén *et al.*, 2009). Amide-I band of all the gelatin film was situated in the wavenumber 1600 to 1700 cm^{-1} (correspond to C═O stretching vibration related to CN stretch and NH bend, or COO group related hydrogen bending) (Benjakul *et al.*, 2012). Typically, Amide-I infrared analysis is employed for predicting the secondary structure of proteins, mainly used for determination of gelatin structure (Ma *et al.*, 2012). GLY film showed amide-I band at the wavenumber 1630 cm^{-1}. With GLY/SQ ratio of 5:5 (w/w) and only SQ, a slight shift in wavenumber (1633 cm^{-1}) was noticed, indicating that the replacement of GLY with SQ had affected the interaction between the gelatin chains corresponding to C═O group. When GLY was replaced completely with SQ, amide-I band was slightly shifted to the higher wavenumber (1633 cm^{-1}). This might be due to the reduced interaction between gelatin-gelatin chain to some degree.

Similarly, Tongnuanchan *et al.* (2015) documented the shift in amide-I band to higher wavenumber when palm oil was incorporated in tilapia gelatin film. The amide-II band of GLY film was situated at 1544 cm^{-1} corresponding to stretching vibration of CN groups and in-plane bending of NH of peptide group (Ali *et al.*, 2018). A marginal increase wavenumber of amide-II band was noticed for the films containing GLY/SQ (5:5) or SQ alone (1546 and 1548 cm^{-1}, respectively). SQ plausibly underwent interaction with CN and NH groups of gelatin to some extent. However, amide amide-III band of all the films was observed at same wavenumber of 1238 cm^{-1}, which was related to the waging or stretching vibrations of CH_2 of proline side chains and glycine

backbone as well as the in-plane vibration of NH and CN groups (Gómez-Guillén *et al.*, 2009). Additionally, a distinct peak at wavenumber 1037 cm^{-1} was observed for GLY film and films with GLY/SQ ratio of 5:5 (w/w). The peak at this wavenumber (1037 cm^{-1}) was due to the vibration of OH group, which was primarily from the glycerol used as a plasticizer (Zhang *et al.*, 2018). It was noted that no peak at 1037 cm^{-1} was detected for the film added with SQ alone.

Amide-A band exhibited similar wavenumber shift pattern compared to amide-I, where the band of GLY film was situated at 3288 and 3291 cm^{-1}. For the films with GLY/SQ at a ratio of 5:5 (w/w) and SQ alone, the band was shifted to higher wavenumber (3291 cm^{-1}). Amide-A band representing NH stretching associated with hydrogen bonding, where the shift in wavenumber is primarily due to the differences in hydrogen bonding of the gelatin molecules (Ali *et al.*, 2017). Gelatin-gelatin interaction might be enhanced via hydrogen bond when SQ was absent. Additionally, Tongnuanchan *et al.* (2014) reported that lower wavenumber of amide-A band was noticed with the addition of few essential oils such as basil essential oil, etc. This was mainly due to the higher interaction between functional groups of essential oil with reactive groups of proteins than protein-protein interaction. However, SQ does not contain any reactive functional groups except methyl group. Thus, SQ was more likely unable to interact with gelatin molecules, except hydrophobic-hydrophobic interactions. The amide-B band of all the gelatin films was situated in the wavenumber range of 3079-3081 cm^{-1}, which was mainly associated with the stretching vibration of NH group, resulting from asymmetric stretching of CH group on double bond (Fontaine-Vive *et al.*, 2009). In addition, the major bands at 3400-3600 cm^{-1} with a broad shoulder, represents OH and NH stretching associated with hydrogen bonding (Theerawitayaart *et al.*, 2019). It was noticed that the absorption band of GLY film was broader than those of other gelatin films. The broadening of this band suggested that presence of hydrogen bond between OH group of GLY and NH group of gelatin chains. This result was in accordance with EAB, which could explain the increased mobility of gelatin chain plasticized with GLY, and the films were highly flexible.

Additionally, the peaks corresponding to the asymmetrical stretching vibration of methylene groups (CH , CH_2 and CH_3) were also detected at wavenumbers

of 2878 cm^{-1} and 2922-2925 cm^{-1} (Ma *et al.*, 2012). Moreover, no additional peaks at wavenumbers of 3600-3200 and 1149-1033 cm^{-1} related to the formation of primary oxidation and scission products of SQ were observed (Fu *et al.*, 2013). Based on the FTIR spectra, the replacement of GLY with SQ in the range tested did not have a major impact on gelatin-gelatin interaction. This confirmed that SQ might stabilize the gelatin film network by means of hydrophobic-hydrophobic interaction and long chain length of SQ might help increase TS of resulting gelatin films. In addition, the long chain length of SQ could have undergone entanglement with each other and strengthened the network of gelatin film.

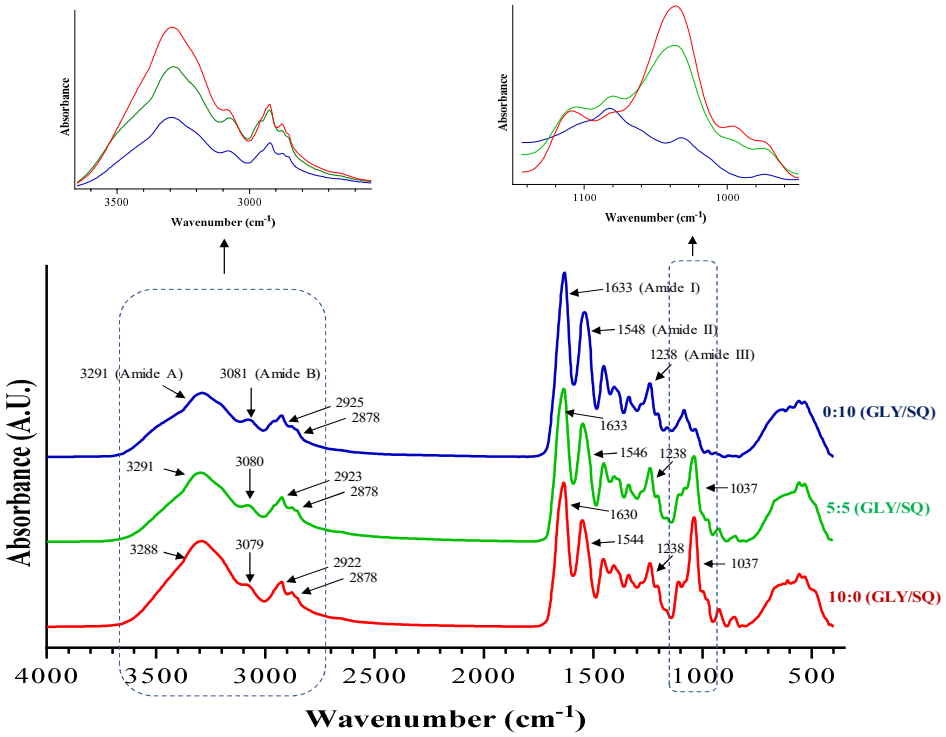

Figure 44. Attenuated total reflectance-Fourier transform infrared (ATR-FTIR) spectra of golden carp skin gelatin film incorporated with glycerol, squalene and their mixture (5:5).

8.5.3.3. Thermal transition

Thermal properties of the films expressed as glass transition temperature (T_g), melting transition (T_{max}) and enthalpy (ΔH) are summarized in Table 3. A heat

scan of all the gelatin films exhibited a partly step-like transition curve (T_g) with subsequent T_{max} peak. GLY film exhibited T_g at 43.26 °C, which was characteristically related with the transition of the plasticized disorder phase of gelatin film. Furthermore, films with GLY/SQ (5:5) and SQ alone had the higher T_g values (45.6 and 50.15 °C, respectively). Vanin *et al.* (2005) documented that gelatin films plasticized with propylene and diethylene glycol exerted different T_g values (61.9 and 13.4 °C, respectively). Difference in T_g might depend on the type of plasticizer used, where addition of rigid SQ crystal phase as a modifier increased the intra- and inter-molecular interactions at the SQ-gelatin interface to some extent, thereby reducing the chain mobility. As a result, higher T_g of SQ films could be related with the decreased chain mobility linked with its lower plasticizing effect. In the presence of SQ alone, film was stiffer and more brittle when compared to the GLY film and films with GLY/SQ (5:5). This was more likely attributed to the different chain mobility of gelatin molecules in the presence of GLY and SQ. The high T_g value of SQ added films was in relation with the increased value of YM and enhanced TS of these films, compared to GLY film.

Melting transition of GLY film was observed at the T_{max} of 109.14 °C, which was associated with the distraction of ordered molecular structure (Staroszczyk *et al.*, 2012). Additionally, this melting transition could occur as a result of helical-coil transition of the gelatin molecule in the film. Normally, during the film casting and drying process, the gelatin molecules could rearrange themselves to form a more ordered structure or could undergo partial renaturation (Xiao *et al.*, 2016). The films added with SQ exhibited lower T_{max}, indicating that SQ added might impede renaturation of gelatin in the film network, particularly via hydrophobic-hydrophobic interactions. Besides, GLY film presented the highest ΔH value (35.21 J g^{-1}), compared to those with GLY/SQ mixture or SQ alone (13.37 and 28.93 J g^{-1}, respectively). No endothermic transition peak was detected for SQ. This could mostly due to the low melting and high boiling temperature of SQ (-70 °C and ~285 °C, respectively) (Bavisetty and Narayan, 2015; Reddy and Couvreur, 2009).

Table 21. Melting phase transition (T_{max}), enthalpy change (ΔH) and glass transition temperature (T_g) of golden carp skin gelatin film incorporated with glycerol, squalene and their mixture (5:5).

GLY/SQ ratio (w/w)	Endothermic peak transition (Protein phase)				Glass transition
	T_{onset} (°C)	T_{max} (°C)	T_{end} (°C)	ΔH (J g^{-1})	T_g (°C)
10:0	99.7	105.3	109.14	35.21	43.26
5:5	70.3	71.26	76.17	13.37	45.6
0:10	87.35	92.64	102.97	28.93	50.15

GLY: glycerol; SQ: squalene

8.5.3.4. Thermal stability

Thermal stability of selected gelatin films expressed in terms of weight loss (Δ_w) and thermal degradation temperatures (T_d) is presented in Table 4, and the thermogram representing the thermal degradation behavior is illustrated in Figure 5. TGA curve of GLY film as well as film incorporated with SQ alone demonstrated four phases of Δ_w. Nevertheless, the film with GLY/SQ (5:5) showed five phases of Δ_W. The first phase of weight loss (Δ_{w1} = 6.39-10.64%) of all the films was observed at a temperature (T_{d1}) range of 42.01-47.6 °C, which could be related to the loss of bound and free water from the film matrix (Ali *et al.*, 2019b). It was noticed that the films plasticized with GLY/SQ mixture exerted lower weight loss and T_{d1}. This was more related with the higher SQ, hydrophobic substance added. Likewise, Tongnuanchan *et al.* (2015) documented that gelatin films added without and with different levels of palm exerted varying T_{d1} ranging from 26.4 to 34.7 °C. Reduction in Δ_{w1} was generally proportional to an increased hydrophobic substance in the resulting film. The obtained results were in agreement with moisture content of the gelatin films, where the lowest moisture content was found in the film containing only SQ. The second phase of weight loss (Δ_{w2} = 24.25% and 13.11%) was markedly observed for the films with GLY film and film with GLY/SQ mixture at the temperatures (T_{d2}) of 195.14 and 217.65 °C, respectively. Films with SQ alone did not exhibit any transition at the aforementioned temperature range. This transition temperature was mostly related to the degradation of glycerol (plasticizer) (Nagarajan *et al.*, 2017).

The third phase of weight loss (Δ_{w3}, 45.88-42.82%) was observed at T_{d3} of 287.52 to 296.69 °C. Zhang *et al.* (2018) documented that at the temperature range of 292 to 320 °C, weight loss was related with the loss of major constituents in films. Moreover, Δ_{w3} and T_{d3} of GLY film was higher when compared to those of other films. At high temperature (T_{d3}), degradation of higher cross-links between gelatin molecules could occur, as observed for GLY film, in which denser and stronger film matrix was possibly formed as a result of absence of hydrophobic substance (SQ). In presence of SQ, gelatin-gelatin interaction could be decreased and film with lower heat resistance was formed, compared to GLY film (Table 3). The results suggested that the SQ did not stabilize the gelatin film network with strong molecular linkages. Due to its highly hydrophobic nature and complex structure, SQ in presence of solvents with different polarity is known to undergo structural transition. SQ in a hydrophobic system is known to be in its straight or extended form. Nontheless, in the polar or hydrophilic system, SQ is more likely in a coiled conformation, in which SQ is chemically less reactive and sterically shielded (Van Tamelen, 1968). Thus, SQ in coil conformation more likely strengthened the gelatin film network, leading to increased TS (Table 2).

Fourth phase of weight loss (Δ_{w4} = 16.23 and 29.43%) was detected from the films added with GLY/SQ mixture or SQ alone at the transition temperature (T_{d4}) of 362.65 and 367.22 °C, respectively. However, GLY film did not demonstrate weight loss at this transition temperature. Moreover, T_{d4} was higher, compared to the boiling point of SQ (~ 285 °C) (Reddy and Couvreur, 2009). Thus, the result clearly indicated that weight loss (Δ_{W4}) at Td_4 could be associated with the degradation of compounds with high thermal stability. The fifth phase of weight loss (Δ_{w5} = 1.98-4.76%) was observed with T_{d5} of 513.67-565.32 °C. Δ_{W5} and T_{d5} were higher for GLY film and were correspondingly lower with the addition of higher proportion of SQ. Thus, the thermal transition at such a high temperature could be related to the degradation of interacted gelatin molecules or highly-cross-linked from. This could also be associated with the higher protein content in the GLY film, compared with that of SQ films. However, all the films demonstrated a small portion of these highly cross-linked protein domains, particularly via covalent bond.

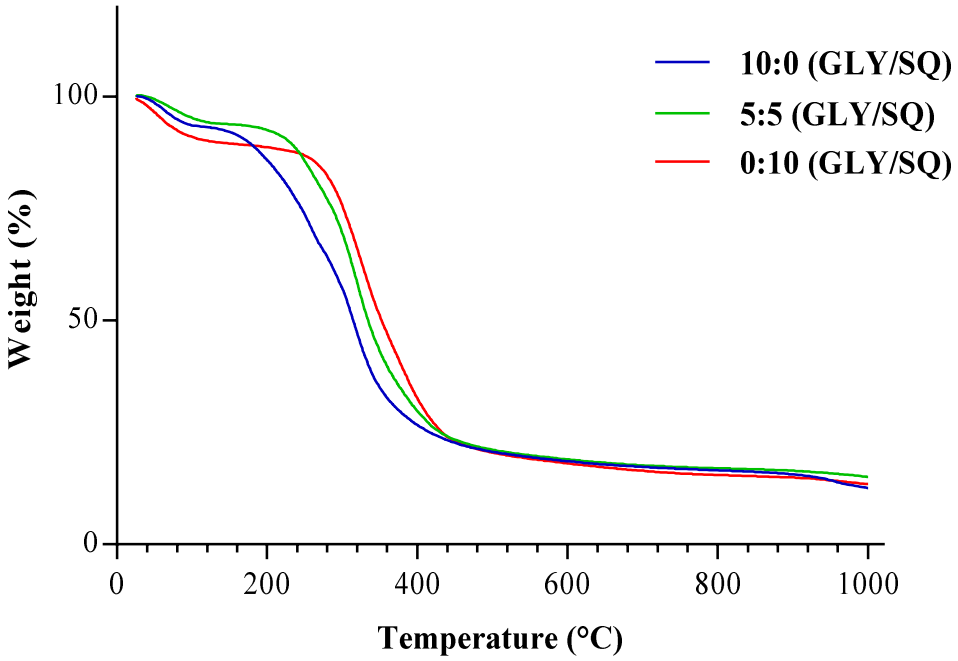

Figure 45. Thermo-gravimetric curves of golden carp skin gelatin film incorporated with glycerol, squalene and their mixture (5:5).

Table 22. Thermal degradation temperature (T_d, °C) and weight loss (Δ_w, %) of golden carp skin gelatin film incorporated with glycerol, squalene and their mixture (5:5).

GLY/SQ ratio (w/w)	Δ_1		Δ_2		Δ_3		Δ_4		Δ_5	
	$T_{d1,\ onset}$	Δ_{w1}	$T_{d2,\ onset}$	Δ_{w2}	$T_{d3,\ onset}$	Δ_{w3}	$T_{d4,\ onset}$	Δ_{w4}	$T_{d5,\ onset}$	Δ_{w5}
10:0	47.6	10.64	195.14	24.25	296.69	45.88	-	-	565.32	4.76
5:5	44.96	8.12	207.65	13.11	295.38	43.73	362.65	16.23	549.27	3.29
0:10	42.01	6.39	-	-	287.52	42.82	367.22	29.43	513.67	1.98

GLY: glycerol; SQ: squalene

8.5.3.5. Microstructure

Figure 6 depicts the SEM images of surface and cross-section of selected gelatin films. The surface of film plasticized with GLY was smoother and more uniform than the films added with GLY/SQ mixture or SQ alone. The rough surface of SQ incorporated films were possibly due to the larger particle size with homogenous dispersion of SQ droplets as evidenced from CSLM (Figure 2). Nevertheless, sonication is generally known to reduce the particle size of emulsion to have nano-sized droplets, irrespective of surfactant type and oils used (Gul *et al.*, 2018).

Based on the cross-section, GLY film displayed highly compact structure, compared to the films containing SQ. Relatively, cross-section of film with GLY/SQ mixture (5:5) was highly compact, compared to the film containing SQ alone. Additionally, the cross-section of film incorporated with SQ alone showed uneven and irregular distribution of SQ droplets within the film matrix, compared to those containing both GLY and SQ (5:5). The results suggested that existence of GLY possibly facilitated the retention of SQ droplets in their place during the process of drying. On the other hand, the films with only SQ showed larger droplets, owing to its hydrophobicity. Nano-droplets could have fused together to form the bigger particle. As a result, film network with courser structure was formed. This more likely resulted in the small decrease in TS and the increase in WVP of film added with SQ alone.

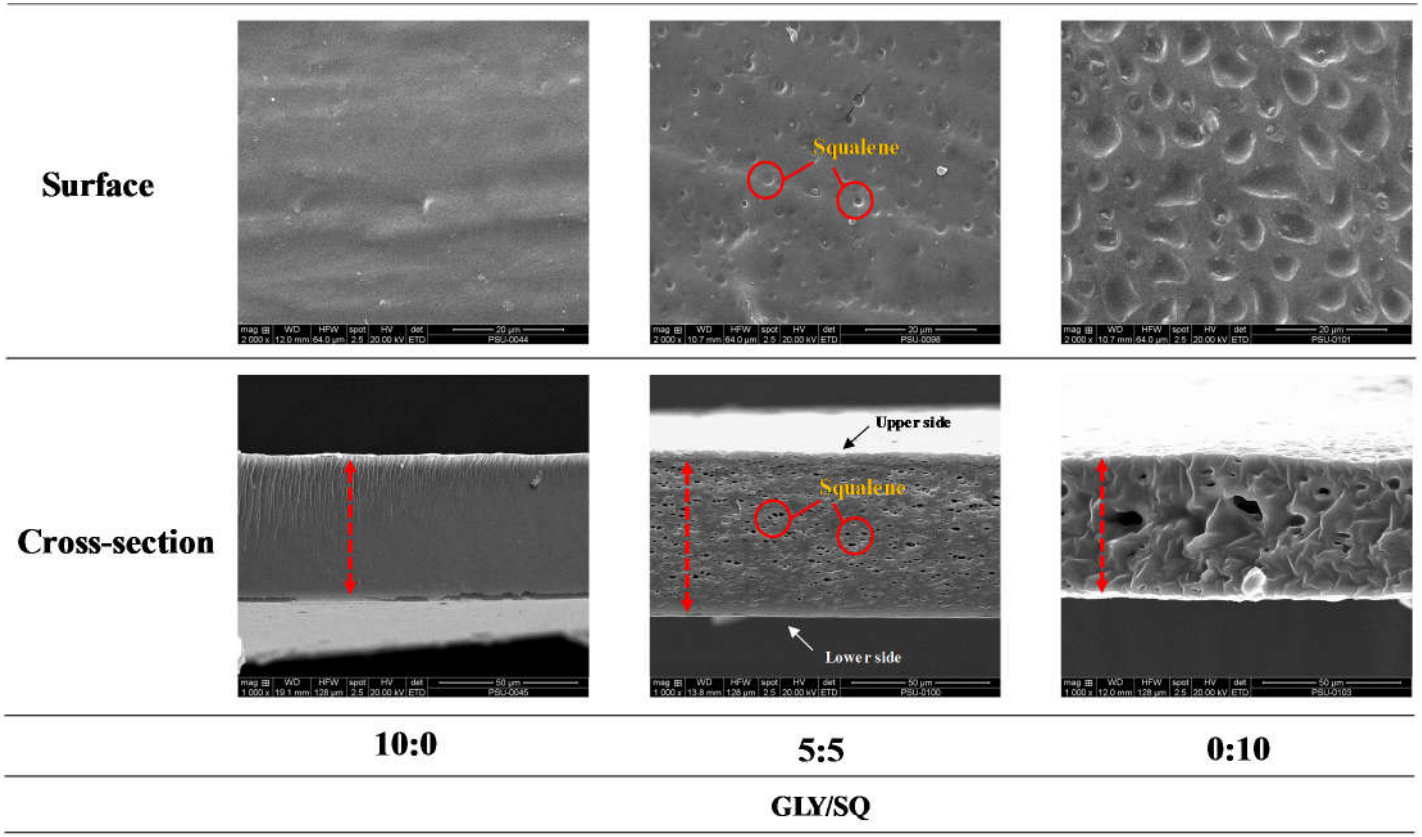

Figure 46. Scanning electron microscopic (SEM) micrographs of surface (2000 x) and cross-section (1000 x) of golden carp skin gelatin film incorporated with glycerol, squalene and their mixture (5:5).

8.6. Conclusions

Incorporation of SQ as GLY substitute could enhance the properties of gelatin film. The dispersed SQ crystal phase could serve as a moisture and oxygen barrier, which are the key factors to control oxidation, deterioration and degradation of food components. To achieve the desirable gelatin film properties, GLY could be replaced by SQ up to 50%. Unlike other oils used for improvement of the barrier properties, SQ demonstrated the superior barrier properties. Based on the hydrophobic nature and complex structure, SQ could also improve the mechanical strength of the gelatin film, which could be a greater advantage as a packaging material. Additionally, films containing both GLY and SQ were more uniform with non-viscid surface. They were sufficiently flexible and easy to handle. Thus, gelatin films prepared with GLY/SQ mixture at appropriate ratio had improved properties and could be extensively used in food possessing health promoting properties.

8.7. References

Ali, A. M. M., Bavisetty, S. C. B., Prodpran, T. and Benjakul, S. 2019a. Squalene from fish livers extracted by ultrasound assisted direct *in-situ* saponification: Purification and molecular characteristics. Journal of the American Oil Chemists' Society. DOI:10.1002/aocs.12262.

Ali, A. M. M., Benjakul, S. and Kishimura, H. 2017. Molecular characteristics of acid and pepsin soluble collagens from the scales of golden carp (*Probarbus jullieni*). Emirits Journal of Food and Agriculture. 29: 450-457.

Ali, A. M. M., Kishimura, H. and Benjakul, S. 2018. Physicochemical and molecular properties of gelatin from skin of golden carp (*Probarbus Jullieni*) as influenced by acid pretreatment and prior-ultrasonication. Food Hydrocolloids. 82: 164-172.

Ali, A. M. M., Prodpran, T. and Benjakul, S. 2019b. Effect of squalene rich fraction from shark liver on mechanical, barrier and thermal properties of fish (*Probarbus Jullieni*) skin gelatin film. Food Hydrocolloids. https://doi.org/10.1016/j.foodhyd.2019.105201

Bavisetty, S. C. B. and Narayan, B. 2015. An improved RP-HPLC method for simultaneous analyses of squalene and cholesterol especially in aquatic foods. Journal of Food Science and Technology. 52: 6083-6089.

Benjakul, S., Kittiphattanabawon, P. and Regenstein, J. M. 2012. Fish gelatin. *In* Food Biochemistry and Food Processing, Second Edition. (Simpson, B. K., ed.). p. 388-405. Wiley-Blackwell. Iowa, USA.

Bindu, B. S. C., Mishra, D. P. and Narayan, B. 2015. Inhibition of virulence of *Staphylococcus aureus*–a food borne pathogen–by squalene, a functional lipid. Journal of Functional Foods. 18: 224-234.

Cao, N., Yang, X. and Fu, Y. 2009. Effects of various plasticizers on mechanical and water vapor barrier properties of gelatin films. Food hydrocolloids. 23: 729-735.

Carvalho, R. A., Sobral, P. J. A., Thomazine, M., Habitante, A. M. Q. B., Giménez, B., Gómez-Guillén, M. C. and Montero, P. 2008. Development of edible films based on differently processed Atlantic halibut (*Hippoglossus hippoglossus*) skin gelatin. Food Hydrocolloids. 22: 1117-1123.

Chung, H., Kim, T. W., Kwon, M., Kwon, I. C. and Jeong, S. Y. 2001. Oil components modulate physical characteristics and function of the natural oil emulsions as drug or gene delivery system. Journal of Controlled Release. 71: 339-350.

Desai, K., Wei, H. and Lamartiniere, C. 1996. The preventive and therapeutic potential of the squalene-containing compound, Roidex, on tumor promotion and regression. Cancer Letters. 101: 93-96.

Elewski, B. E. 1993. Mechanisms of action of systemic antifungal agents. Journal of the American Academy of Dermatology. 28: S28-S34.

Fontaine-Vive, F., Merzel, F., Johnson, M. and Kearley, G. 2009. Collagen and component polypeptides: Low frequency and amide vibrations. Chemical Physics. 355: 141-148.

Fox, C. B. 2009. Squalene emulsions for parenteral vaccine and drug delivery. Molecules. 14: 3286-3312.

Fox, C. B., Anderson, R. C., Dutill, T. S., Goto, Y., Reed, S. G. and Vedvick, T. S. 2008. Monitoring the effects of component structure and source on formulation stability and adjuvant activity of oil-in-water emulsions. Colloids and Surfaces B: Biointerfaces. 65: 98-105.

Fu, D., Leng, C., Kelley, J., Zeng, G., Zhang, Y. and Liu, Y. 2013. ATR-IR study of ozone initiated heterogeneous oxidation of squalene in an indoor environment. Environmental Science and Technology. 47: 10611-10618.

Gómez-Guillén, M. C., Pérez-Mateos, M., Gómez-Estaca, J., López-Caballero, E., Giménez, B. and Montero, P. 2009. Fish gelatin: a renewable material for developing active biodegradable films. Trends in Food Science and Technology. 20: 3-16.

Gul, O., Saricaoglu, F. T., Besir, A., Atalar, I. and Yazici, F. 2018. Effect of ultrasound treatment on the properties of nano-emulsion films obtained from hazelnut meal protein and clove essential oil. Ultrasonics Sonochemistry. 41: 466-474.

Hosseini, S. F., Javidi, Z. and Rezaei, M. 2016. Efficient gas barrier properties of multi-layer films based on poly(lactic acid) and fish gelatin. International Journal of Biological Macromolecules. 92: 1205-1214.

Jongjareonrak, A., Benjakul, S., Visessanguan, W. and Tanaka, M. 2006. Effects of plasticizers on the properties of edible films from skin gelatin of bigeye snapper and brownstripe red snapper. European Food Research and Technology. 222: 229-235.

KopiCoVá, Z. and VaVreiNoVá, S. 2007. Occurrence of squalene and cholesterol in various species of Czech freshwater fish. Czech Journal of Food Sciences. 25: 195-201.

Ma, W., Tang, C.-H., Yin, S.-W., Yang, X.-Q., Wang, Q., Liu, F. and Wei, Z.-H. 2012. Characterization of gelatin-based edible films incorporated with olive oil. Food Research International. 49: 572-579.

Nagarajan, M., Benjakul, S., Prodpran, T. and Songtipya, P. 2014. Properties of bio-nanocomposite films from tilapia skin gelatin as affected by different nanoclays and homogenising conditions. Food and Bioprocess Technology. 7: 3269-3281.

Nagarajan, M., Prodpran, T., Benjakul, S. and Songtipya, P. 2017. Properties and characteristics of multi-layered films from tilapia skin gelatin and poly (lactic acid). Food Biophysics. 12: 222-233.

Nilsuwan, K., Benjakul, S. and Prodpran, T. 2017. Properties, microstructure and heat seal ability of bilayer films based on fish gelatin and emulsified gelatin films. Food Biophysics. 12: 234-243.

Nilsuwan, K., Benjakul, S. and Prodpran, T. 2018. Properties and antioxidative activity of fish gelatin-based film incorporated with epigallocatechin gallate. Food Hydrocolloids. 80: 212-221.

Nilsuwan, K., Benjakul, S., Prodpran, T. and de la Caba, K. 2019. Fish gelatin monolayer and bilayer films incorporated with epigallocatechin gallate: Properties and their use as pouches for storage of chicken skin oil. Food Hydrocolloids. 89: 783-791.

Prodpran, T., Benjakul, S. and Artharn, A. 2007. Properties and microstructure of protein-based film from round scad (*Decapterus maruadsi*) muscle as affected by palm oil and chitosan incorporation. International Journal of Biological Macromolecules. 41: 605-614.

Reddy, L. H. and Couvreur, P. 2009. Squalene: A natural triterpene for use in disease management and therapy. Advanced Drug Delivery Reviews. 61: 1412-1426.

Rivero, S., García, M. and Pinotti, A. 2010. Correlations between structural, barrier, thermal and mechanical properties of plasticized gelatin films. Innovative Food Science and Emerging Technologies. 11: 369-375.

Staroszczyk, H., Pielichowska, J., Sztuka, K., Stangret, J. and Kołodziejska, I. 2012. Molecular and structural characteristics of cod gelatin films modified with EDC and TGase. Food Chemistry. 130: 335-343.

Theerawitayaart, W., Prodpran, T., Benjakul, S. and Sookchoo, P. 2019. Properties of films from fish gelatin prepared by molecular modification and direct addition of oxidized linoleic acid. Food Hydrocolloids. 88: 291-300.

Tongnuanchan, P., Benjakul, S. and Prodpran, T. 2014. Structural, morphological and thermal behaviour characterisations of fish gelatin film incorporated with basil and citronella essential oils as affected by surfactants. Food Hydrocolloids. 41: 33-43.

Tongnuanchan, P., Benjakul, S., Prodpran, T. and Nilsuwan, K. 2015. Emulsion film based on fish skin gelatin and palm oil: physical, structural and thermal properties. Food Hydrocolloids. 48: 248-259.

Tongnuanchan, P., Benjakul, S., Prodpran, T., Pisuchpen, S. and Osako, K. 2016. Mechanical, thermal and heat sealing properties of fish skin gelatin film containing palm oil and basil essential oil with different surfactants. Food Hydrocolloids. 56: 93-107.

Van Tamelen, E. 1968. Bioorganic chemistry: sterols and acrylic terpene terminal expoxides. Accounts of Chemical Research. 1: 111-120.

Vanin, F., Sobral, P., Menegalli, F., Carvalho, R. and Habitante, A. 2005. Effects of plasticizers and their concentrations on thermal and functional properties of gelatin-based films. Food Hydrocolloids. 19: 899-907.

Xiao, J., Wang, W., Wang, K., Liu, Y., Liu, A., Zhang, S. and Zhao, Y. 2016. Impact of melting point of palm oil on mechanical and water barrier properties of gelatin-palm oil emulsion film. Food Hydrocolloids. 60: 243-251.

Zhang, Y., Simpson, B. K. and Dumont, M.-J. 2018. Effect of beeswax and carnauba wax addition on properties of gelatin films: A comparative study. Food Bioscience. 26: 88-95.

CHAPTER 9

QUALITY CHARACTERISTICS OF FISH CRACKERS STORED IN GELATIN BAGS AS INFLUENCED BY GLYCEROL SUBSTITUTED WITH SQUALENE AS A PLASTICIZER

9.1. Abstract

The influence of bags from fish skin gelatin film prepared by substituting glycerol (GLY) with squalene (SQ) at 50% (GLY/SQ) was evaluated on the quality characteristics of fried fish crackers (FFC) stored for 30 days at 28 ± 0.5 °C and 70 ± 5 % RH, in comparison with bags from control (CON) gelatin film and nylon/LLDPE film. The prepared GLY/SQ film had improved moisture vapor barrier and oxygen barrier properties ($p < 0.05$). FFC stored in GLY/SQ bag had lower moisture content and water activity, compared to those stored in CON bag and without packing (WOP) ($p < 0.05$). After 30 days, GLY/SQ and nylon/LLDPE stored FFC had lower values of PV and TBARS than others. In addition, GLY/SQ and nylon/LLDPE stored FFC had less volatile compounds, especially those formed from autoxidation and non-enzymatic browning reaction. GLY/SQ bag lowered the oxidation and loss of polyunsaturated fatty acids, mainly n-3 and n-6 when compared to other bags. Moreover, FFC stored in nylon/LLDPE and GLY/SQ bags exhibited negligible changes in color and texture. GLY/SQ bag had an excellent oxygen barrier property and could lower water vapor permeability (WVP), thus lowering migration of reactants and oxidizing radicals. The prepared GLY/SQ bag could therefore improve oxidative stability of FFC

9.2. Introduction

Mass transfer between external atmosphere and packaging material is a crucial factor governing shelf-life and rate of deterioration of packed food products. Oxygen and water vapors have been known to cause the loss of food quality and might create a favorable environment for the growth of microorganisms (Buege and Aust,

1978; Maqsood and Benjakul, 2011; Nilsuwan *et al.*, 2016). Over the last decade, films or packaging made from biodegradable polymers have gained immense attention to replace those from synthetic polymer. Among the different biopolymers, gelatin has gained widespread interest due to its thermo-reversible network forming property and heat sealability (Tongnuanchan *et al.*, 2016). Moreover, gelatin films possess the exceptional barrier property against aroma and UV light. They also have superior oxygen and carbon dioxide barrier property (Gómez-Guillén *et al.*, 2009).

Nevertheless, the application of gelatin-based film has been limited, mainly owing to its poorer moisture vapor barrier property and lower mechanical properties, compared to the traditional petrochemical-based packaging material (Benjakul *et al.*, 2012). Therefore, gelatin films are highly vulnerable to environment, particularly at high humidity. Improvement of moisture vapor barrier property as well as mechanical properties of gelatin film has been intensively studied. For instance, addition of lipids and lipid fractions such as essential oils, edible oils, wax and fatty acids can augment the hydrophobicity of gelatin film (Tongnuanchan *et al.*, 2016; Zhang *et al.*, 2018b). Incorporation of nanoparticles such as nanoclay was documented to influence moisture barrier and thermal insulation properties (Nagarajan *et al.*, 2014). Addition of antioxidant compounds such as phenolic compounds could reinforce the mechanical property and antioxidant activity of gelatin film (Nilsuwan *et al.*, 2018). Recently, Ali *et al.* (2019) documented that substituting glycerol (hydrophilic plasticizer) with squalene up to 50% had substantially increased moisture vapor and oxygen barrier properties as well as tensile strength. This was mainly linked to hydrophobicity, singlet oxygen quenching property and the long chain length of squalene. Nevertheless, gelatin film containing squalene, a marine bio-functional compound, could render health-promoting properties (Reddy and Couvreur, 2009). Squalene is also known to exert antifungal and antibacterial properties (Bindu *et al.*, 2015; Elewski, 1993), which could be one of the essential requirements for active packaging.

In a food system, oxidation of lipids is one of the most detrimental factors inducing quality deterioration during the storage. Generally, oxidation of lipid in foods can be initiated by enzymatic and non-enzymatic reactions (Lu *et al.*, 2013).

The reaction between oxidized lipids with proteins, amino acids and amines could cause undesirable changes in food properties including loss of functional properties, texture, color, flavor, and nutritive value (Thanonkaew *et al.*, 2007). The degree and extent of deterioration depend on the storage time, temperature, relative humidity, degree of fatty acid saturation, presence of prooxidants and availability of oxygen (Han *et al.*, 2018). The highly unsaturated fatty acids are sensitive and more readily undergo oxidation during storage, especially seafood rich in poly-unsaturated fatty acids (Muhammed *et al.*, 2015). Packaging, have been employed to protect and retard the oxidation of lipid in seafoods and their products. Due to the improved barrier properties of gelatin film incorporated with squalene as glycerol substitute, bag based on the aforementioned film could be used to extend the shelf-life of snack, especially deep-fried product such as fish cracker.

9.3. Objective

To study physical, textural and lipid oxidation of fish cracker packed in different bags during the extended storage.

9.4. Material and methods

9.4.1. Chemicals

Glycerol, acetic acid, trichloroacetic acid sodium hydroxide, potassium hydroxide and ferrous chloride were purchased from Merck (Darmstadt, Germany). Solvents including acetonitrile, methanol, *n*-hexane and ethanol were obtained from Lab-Scan (Bangkok, Thailand). Supelco® 37 component FAME mix, 1,1,3,3-tetramethoxypropane (MDA) and ammonium thiocyanate were procured from Sigma-Aldrich (St. Louis, MO, USA). Cumene hydroperoxide and 2-thiobarbituric acid were obtained from Fluka Co. (Buchs, St. Gallen, Switzerland). Rest of other chemicals were obtained from Lab-Scan Ltd. (Bangkok, Thailand). All the chemicals used were of analytical grade.

9.4.2. Materials

Palm oil was purchased from OLEEN Co. Ltd. (Bangkok, Thailand). Dried fish chips (5 cm diameter and 1.5 mm thickness) were procured from MANORA® (Bangkok, Thailand). Nylon/linear low-density polyethylene bags were obtained from the local market at Hat Yai, Thailand.

9.4.2.1. Collection of raw materials

Golden carp skin was collected and processed as describe in the section *2.4.2.1.* Spot-tail shark liver were collected and processed as described in the section 6.4.2.

9.4.3. Gelatin extraction

Removal of non-collagenous proteins and acid pretreatment were performed as describe in the sections *5.4.2.1* and *5.4.2.2*, respectively. Gelatin extraction was conducted as mentioned in the section *5.4.2.4.*

9.4.4. Extraction of squalene (SQ)

Firstly, unsaponifiable matter was extracted and subjected to concentration and purification using fractional crystallization and column purification, respectively.

9.4.4.1. Recovery of unsaponifiable matter (*section 7.4.4.1*)

9.4.4.2. Fractional crystallization (*section 6.4.5.1*)

9.4.4.3. Column purification (*section 6.4.5.2*)

Quantification of squalene using reversed-phase high-performance liquid chromatography (RP-HPLC) (*section 6.4.6.2*)

9.4.5. Preparation of film using glycerol or glycerol/squalene mixture as plasticizer

Film forming solution (FFS) containing glycerol (GLY) 30% (w/w, based on protein content) and film forming emulsion (FFE) containing GLY and squalene (SQ) at the ratio of 1:1 at a final concentration of 30% based on protein content (w/w) were prepared as describe in the section *8.4.5.1*.

9.4.6. Characterization and storage stability of films

Before testing the properties, all the films were conditioned at 25 ± 0.5 °C and 50 ± 5% RH for 48 h. Control gelatin films containing only GLY was termed 'CON', while gelatin film added with the mixture of GLY/SQ at the ratio of 1:1 at a final concentration of 30% based on protein content (w/w) was named as 'GLY/SQ'.

CON and GLY/SQ films were subjected to determination in comparison with nylon/linear low-density polyethylene (nylon/LLDPE) film.

9.4.6.1. Characterization

9.4.6.1.1. Film thickness and moisture content (*section 8.4.6.1*)

9.4.6.1.2. Mechanical properties (*section 7.4.6.2*)

9.4.6.1.3. Water vapor permeability (WVP) (*section 7.4.6.3*)

9.4.6.1.4. Color and transparency (*section 7.4.6.4*)

9.4.6.1.5. Oxygen permeability (OP) (*section 8.4.7.1*)

9.4.6.1.6. Heat sealing ability

Seal efficiency and seal strength of the films (CON and GLY/SQ) were analyzed as detailed by Tongnuanchan *et al.* (2016). Film samples (40 × 20 mm^2) were placed facing together and sealed using an impulse heat-sealer with a magnet Model (ME-300HIM, S.N.MARK Ltd., Nonthaburi, Thailand). CON films were sealed at 120 ± 0.5 °C for 1 min 30 s and GLY/SQ films were sealed 160 ± 0.5 °C for 1 min 75 s, subsequently cooling for 60 s. The width of seal area was 2 mm. The heat-seal strength

was assessed using a peel test. The seal efficiency and seal strength and were analyzed according to the standard method ASTM F-88 (ASTM, 2001) with small amendments using Universal Testing Machine, and were calculated using the equations shown below:

$$Seal\ efficiency\ (\%) = \frac{Peak\ force}{Tensile\ force} \times 100 \quad (1)$$

$$Seal\ strength\ (\mathrm{N/m}) = \frac{Peak\ force}{Film\ width} \quad (2)$$

where peak force (N) is the maximum force obtained from seal testing and tensile force is the force (N) obtained from tensile strength testing.

9.4.6.2. Storage stability of film during extended storage

The prepared CON and GLY/SQ films were monitored for their characteristic changes with respect to their mechanical properties, color and transparency when stored at 28 ± 0.5 °C and 70 ± 5 % RH for 30 days. The analyses were done at day 0, 15 and 30 in comparison with nylon/LLDPE films.

9.4.7. Studies on quality changes of fried fish crackers (FFC) packaged in different bags during storage

To prepare the gelatin bags, FFS and FFE were firstly casted on silicon resin plate of size 16 × 16 cm^2 cm, and were dried and conditioned as aforementioned. The conditioned gelatin films (CON and GLY/SQ) along with nylon/LLDPE films were cut into the size of 8 × 8 cm^2. The bags were prepared by heat sealing of two films for three sides, while the fourth side was remained unsealed. CON films were sealed at 120 ± 0.5 °C for 1 min 30 s, GLY/SQ and nylon/LLDPE films were sealed 160 ± 0.5 °C for 1 min 75 s. After being sealed, all the films were cooled for 1 min 50 s. The obtained bags were used for packaging FFC.

9.4.7.1. Preparation and packing of FFC

Raw dried fish chips were fried employing an electric deep fryer comprising 2 l of palm oil. The fryer was set at 180 ºC. The chips were kept in frying basked and were dipped in oil for 30 s. The obtained fried fish crackers (FFC) were

drained on a screen for 6 min and blotted using a paper towel to eliminate the excessive oil. Then all FFC were allowed to cool at ambient temperature (28 ± 2 ºC) for 15 min and were broken into pieces. The FFC (~5 g) were placed into different bags prepared from CON, GLY/SQ and nylon/LLDPE films and heat sealed.

9.4.7.2. Storage study of packed FFC in different bags

All the samples with FFC were stored at 28 ± 0.5 °C and 70 ± 5 % RH for 30 days and were analyzed every 5 days. Prior to analysis, the FFC were coarsely ground using mixer blender (model MX-898N, Panasonic, Selangor, Malaysia).

9.4.7.2.1. Moisture content, water activity and color

Moisture content and color of ground FFC were determined as describe in the section *8.4.6.1* and *7.4.6.4*, respectively. Water activity (a_w) of ground FFC was measured using a water activity meter (4TEV, Aqualab, Pullman, WA, USA).

9.4.7.2.2. Peroxide value (PV)

PV was measured as per the method of Nilsuwan *et al.* (2016), using 1 g of ground FFC. A standard curve was plotted using cumene hydroperoxide at the concentration range of 0.5–50 ppm. PV of samples was expressed as mg cumene hydroperoxide kg^{-1} sample.

9.4.7.2.3. Thiobarbituric acid-reactive substances (TBARS)

TBARS was measured as described by Buege and Aust (1978), using 0.2 g of ground FFC. A standard curve was plotted using 1,1,3,3-tetramethoxypropane (MDA) at the concentration ranging from 0 to 10 ppm. TBARS value of samples was expressed as mg MDA equivalent kg^{-1} sample.

9.4.7.2.4. Textural properties

FFC having a uniform size (2 × 2 cm^2) were used for analysis. The textural property was determined using a texture analyzer model TA-XT Plus (Stable Micro Systems Guildford, UK). Miniature Ottawa and Kramer shear cell with a flat square probe was employed to measure the crispiness and toughness via compression test. Crispiness was measured as the maximum force in grams required to fracture the

cracker into small pieces. Toughness was enumerated by the total area under the positive peak from each compression test and was expressed in terms of g force. The condition used for measurement included pre-test speed of 1.0 mm s^{-1}, test speed of 2.0 mm s^{-1}, distance of 4.0 mm and a load cell of 50 kg.

9.4.7.2.5. Fatty acid composition (FAC)

Extraction of total lipids and preparation of fatty acid methyl esters (FAMEs) using alkali catalyzed transmethylation was determined as described by Muhammed *et al.* (2015). The derivatized FAMEs (1 µl) were subjected to gas chromatography system 7890B Series (Agilent Technologies, Santa Clara, CA, USA) equipped with flame ionization detector (FID) and CP-Sil 88 capillary column (J & W Scientific Column from Agilent Technologies) of 100 m length with 0.25 mm (ID) and 0.20 µm (film thickness). The GC inlet temperature and FID detector temperature was maintained at 240˚C, and the initial column temperature was set at 140 ºC. The column temperature was increased at the rate of 4 ºC min^{-1} up to 240 ºC. Helium was used as the mobile phase at 1 ml min^{-1}. Peak identification was done based on the retention time of external standard from Supelco (37 Component FAME Mix). Standard (FAME mix). The identified peaks were integrated and calibrated against the standard curve using the software Open LAB CDS (Chem Station edition, Agilent Technologies, Santa Clara, CA, USA).

9.4.7.2.6. Volatile compounds

Volatile compounds in the fish crackers were determined as detailed by Nilsuwan *et al.* (2016). To extract volatile compound, 1 g of ground cracker was added in 4 ml of Millipore water in a headspace vial (Agilent Technologies, Santa Clara, CA, USA) and extracted at 60 °C for 10 h. The SPME fiber (50/30 µm) (Supelco, Bellefonte, PA, USA) was exposed to headspace at 270 °C for 15 min followed by 60 °C for 1 h. The volatile compounds were determined using gas chromatography-mass spectrometer (GC-MS) HP 5890 series II (Hewlett Packard, Atlanta, GA, USA) equipped with HP 5972 quadrupole mass detector.

For GC, the inlet temperature was set to 270 °C in a splitless mode. A column HP-Innowax capillary column (30 m × 0.25 mm ID) (Hewlett Packard, Atlanta,

GA, USA) was used. The initial column temperature was set at 35 °C with a hold time of 3 min and the temperature was raised to 70 °C at the rate of 3 °C min^{-1}. Thereafter the temperature was increased up to 200 °C at the rate of 10 °C min^{-1} with a holding time of 10 min. The final temperature was raised to 250 °C for 10 min. Helium gas was used as a carrier at a constant flow of 1 ml min^{-1}.

MS was operated in electron ionization (EI) mode at the temperature 250 °C. Spectra were obtained at ionization energy of 70 eV. The acquisition was monitored at 25–500 amu with a scanning rate of 0.220 s $scan^{-1}$. Identification of volatile compounds was performed using ChemStation Library (Wiley 275.L). The identified volatile compounds were expressed in terms of abundance, based on the peak area.

9.4.8. Statistical analysis

The experiments were performed in triplicates and data was determined by analysis of variance (ANOVA). The Duncan's multiple range test was used to enumerate the difference between mean values and the data were represented as means ± standard deviation. Statistical software SPSS 11.0 software (SPSS Inc., Chicago, IL, USA) was used to determine the experimental data.

9.5. Results and discussion

9.5.1. Characteristics of different films

9.5.1.1. Thickness and mechanical properties

Thickness of all the films. CON and GLY/SQ films had lower thickness (0.056 and 0.069 mm, respectively), compared to that of multilayer nylon/LLDPE film (0.079 mm) ($p < 0.05$) (Table 1).

Mechanical properties of gelatin films and nylon/LLDPE film expressed as tensile strength (TS) and elongation at break (EB) are presented in Table 1. CON film had the lowest TS and YM ($p < 0.05$). Replacement of GLY with SQ increased TS of gelatin film ($p < 0.05$). The increment was 61.7% higher when compared to that of CON film. This was probably associated with hydrophobic-hydrophobic interaction

between SQ and hydrophobic domain of gelatin molecules. Apart from this, SQ with the long chain length could undergo entanglement along with the gelatin chains and established strengthening effect on the gelatin film network (Ali *et al.*, 2019). It was suggested that the uniform dispersion of SQ solid phase in the film matrix could act as a load bearing in the film matrix and enable higher reinforcement during extension before rupture of film. Thus, SQ exhibited the reinforcing and strengthening effects on gelatin film. TS of GLY/SQ film was higher than the TS of nylon/LLDPE film ($p < 0.05$). For EAB, nylon/LLDPE film had the highest value ($p < 0.05$). The film incorporated with SQ presented the lowest EAB, compared to others ($p < 0.05$). This was mostly owing to the reduced plasticizing effect when GLY was substituted with SQ. As a result, GLY/SQ film was stiffer and less flexible than CON film. This could be mostly linked to the hydrophobic nature of SQ, which resisted the migration and retention of water molecules in the film matrix. Thus, the substitution of GLY with SQ reduced elasticity but increased the strength of resulting film.

9.5.1.2. Color and moisture content

All the films had varying color and transparency values as shown in Table 1. Among all the films, CON film had higher L^* value (lightness) ($p < 0.05$). The L^*value of gelatin film was reduced with incorporation of SQ as a partial GLY substitute ($p < 0.05$). Additionally, GLY/SQ and nylon/LLDPE films had comparable lightness values. For a^* and b^* values (redness and yellowness), nylon/LLDPE film presented the lowest values, while CON film displayed higher a^* and b^* values ($p < 0.05$). Furthermore, A slight increase in both the values was noticed with addition of SQ in the film. This was more likely linked to the crystallinity and color of SQ, which was yellowish in color. Transparency value of nylon/LLDPE was lesser than CON and GLY/SQ film; the highest value was noticed for GLY/SQ film ($p < 0.05$). The lower transparency value suggested that films were more transparent.

Table 23. Change in thickness, tensile strength (TS), elongation at break (EAB), color and transparency values of the golden carp skin gelatin film incorporated with glycerol (GLY) or glycerol/squalene (GLY/SQ) at 1:1 ratio and nylon/linear low density polyethylene (nylon/LLDPE) film during the storage of 30 days.

Films	Storage time (Days)	Thickness	TS (MPa)	YM (MPa)	EAB (%)	Moisture content	Color				Transparency value
							L^*	a^*	b^*	ΔE^*	
CON	0	0.056 ± 0.03^{f}	32.21 ± 3.32^{e}	70.36 ± 3.23^{a}	56.87 ± 2.09^{b}	16.21 ± 0.17^{c}	89.46 ± 0.11^{b}	-1.26 ± 0.03^{c}	3.50 ± 0.02^{b}	4.50 ± 0.09^{c}	2.21 ± 0.08^{d}
	15	0.058 ± 0.02^{f}	31.57 ± 2.37^{f}	67.51 ± 2.17^{a}	57.03 ± 2.81^{c}	16.92 ± 0.06^{b}	89.51 ± 0.06^{a}	-1.26 ± 0.02^{c}	3.51 ± 0.04^{b}	4.46 ± 0.12^{c}	2.22 ± 0.12^{d}
	30	0.060 ± 0.04^{e}	30.14 ± 2.86^{g}	63.77 ± 4.08^{a}	57.22 ± 1.72^{c}	17.35 ± 0.11^{a}	89.53 ± 0.12^{a}	-1.25 ± 0.05^{d}	3.50 ± 0.03^{b}	4.52 ± 0.06^{c}	2.19 ± 0.07^{d}
GLY/SQ	0	0.072 ± 0.04^{b}	52.22 ± 2.4^{c}	610.84 ± 36.22^{a}	39.45 ± 2.3^{d}	8.4 ± 0.05^{d}	89.01 ± 0.04^{c}	-1.36 ± 0.01^{a}	4.13 ± 0.03^{a}	5.26 ± 0.05^{b}	8.85 ± 0.16^{c}
	15	0.068 ± 0.02^{c}	52.73 ± 2.19^{b}	638.3 ± 40.56^{a}	38.79 ± 1.87^{e}	7.8 ± 0. 03^{e}	88.98 ± 0.02^{d}	-1.36 ± 0.01^{a}	4.12 ± 0.03^{a}	5.27 ± 0.07^{b}	9.26 ± 0.13^{b}
	30	0.066 ± 0.04^{d}	53.24 ± 1.53^{a}	645.72 ± 28.41^{a}	37.66 ± 2.09^{f}	7.2 ± 0.08^{f}	88.82 ± 0.0^{e}	-1.35 ± 0.03^{b}	4.14 ± 0.06^{a}	5.40 ± 0.09^{a}	10.32 ± 0.21^{a}
Nylon/ LLDPE	0	0.079 ± 0.02^{a}	45.64 ± 2.08^{d}	710.87 ± 22.49^{a}	121.42 ± 3.65^{a}	1.04 ± 0.07^{g}	88.71 ± 0.06^{f}	-1.18 ± 0.03^{e}	1.9 ± 0.09^{c}	4.34 ± 0.13^{d}	1.70 ± 0.04^{e}
	15	0.078 ± 0.03^{a}	45.53 ± 2.42^{d}	706.04 ± 14.17^{a}	121.48 ± 3.45^{a}	0.98 ± 0.03^{g}	88.60 ± 0.09^{f}	-1.18 ± 0.05^{e}	2.0 ± 0.05^{c}	4.46 ± 0.09^{d}	1.68 ± 0.07^{e}
	30	0.079 ± 0.02^{a}	45.71 ± 2.18^{d}	713.91 ± 20.63^{a}	121.37 ± 3.22^{a}	1.02 ± 0.05^{g}	88.55 ± 0.015^{f}	-1.17 ± 0.08^{e}	2.0 ± 0.03^{c}	4.42 ± 0.04^{d}	1.70 ± 0.02^{e}

Mean ± SD from triplicate determination.

Different lowercase superscripts in the same column indicate significant difference ($P < 0.05$).

9.5.1.3. WVP, OP and heat sealability

CON and GLY/SQ as well as nylon/LLDPE films demonstrated different barrier properties against water vapor and oxygen as given in Table 2. Among all the films, WVP of CON film was highest. WVP of GLY/SQ film prepared by replacing GLY with 50% SQ was significantly decreased up to 63.21 % ($p < 0.05$), but was moderately higher (22.9%) than that of nylon/LLDPE film. The lowered WVP of GLY/SQ film, compared to that of CON film, was more likely due to the droplet distribution of hydrophobic SQ, which acted as a barrier for moisture vapor migration (Ali *et al.*, 2019). Among all the films, the lowest WVP was noticed for nylon/LLDPE film. Films made from synthetic polymers possess an excellent barrier property against water vapors when compared to those prepared from natural biodegradable polymers (Gómez-Guillén *et al.*, 2009).

However, the OP of nylon/LLDPE film was higher than that of CON and GLY/SQ films ($p < 0.05$). Generally, protein-based films are known to own higher barrier property against oxygen when compared to those of synthetic films including high-density polyethylene (HDPE), low-density polyethylene (LDPE) and nylon/metallocene catalyzed linear low-density polyethylene (nylon/mLLDPE) (Ansorena *et al.*, 2018). Additionally, Nilsuwan *et al.* (2016) documented that gelatin film possessed an excellent oxygen barrier property. Furthermore, it was noticed that OP of gelatin film was decreased with the replacement of GLY by SQ. Homogeneous dispersion of SQ crystal phase could increase the tortuosity to diffusion path of oxygen molecule, leading to lower diffusion coefficient and decreased permeability.

Table 24. Water vapor permeability (WVP), oxygen permeability (OP), seal strength and seal efficiency of golden carp skin gelatin film incorporated with glycerol (GLY or glycerol/squalene (GLY/SQ) at 1:1 ratio and nylon/linear low-density polyethylene (nylon/LLDPE).

Films	**Thickness (mm)**	**WVP ($\times 10^{-10}$ g s^{-1} m^{-1} Pa^{-1})**	**OP ($\times 10^{-18}$ mol m m^{-2} s^{-1} Pa^{-1})**	**Seal strength (N/m)**	**Seal efficiency (%)**
CON	0.056 ± 0.03^{c}	2.61 ± 0.11^{a}	5.72 ± 0.15^{b}	332.53 ± 21.40^{c}	34.10 ± 3.17^{c}
GLY/SQ	0.069 ± 0.04^{b}	0.96 ± 0.02^{b}	3.18 ± 0.03^{c}	863.68 ± 49.55^{b}	63.16 ± 2.89^{b}
Nylon/LLDPE	0.079 ± 0.02^{a}	0.73 ± 0.26^{c}	7.31 ± 0.09^{a}	1326.04 ± 25.72^{a}	68.44 ± 1.24^{a}

Mean ± SD from triplicate determination.

Different lowercase superscripts in the same column indicate significant difference ($P < 0.05$).

Seal strength and seal efficiency of all the films analyzed by peal test are shown in Table 2. CON film showed lower seal strength and efficiency ($p < 0.05$). The addition of SQ in the gelatin film resulted in higher seal strength and efficiency. This indicated the stronger sealing ability of GLY/SQ film. However, the values were lower when compared to multilayer nylon/LLDPE film. To achieve the optimal heat-sealing property, CON film required lower temperature (120 ± 0.5 °C) and sealing time (1 min 30 s), while GLY/SQ and nylon/LLDPE films acquired higher temperature and longer sealing time (160 ± 0.5 °C and 1 min 75 s, respectively). The difference in sealing temperature could be mainly due to the varying melting transition temperature of different films (Tongnuanchan *et al.*, 2016). All the films were sealed at temperature close to or higher than melting transition temperature. Moreover, very high heat or longer time than optimal values caused the burning of sealing area, whereas lower temperature and shorter time did not provide sufficient melting to cause fusion in the sealing area.

9.5.2. Property changes of different films during storage

Films stored at 28 ± 0.5 °C and 70 ± 5 % RH were tested for their properties during the storage of 30 days. CON and GLY/SQ films demonstrated minor changes with respect to their properties (Table 1). On the other hand, nylon/LLDPE film did not undergo any change throughout the storage. During storage, CON film presented a slight increase in thickness and moisture content, while those of GLY/SQ and nylon/LLDP films remained unchanged. This could be due to the hygroscopic nature of gelatin and GLY, which attracted water molecules to some extent. The water could be retained in the film matrix via hydrogen bond (Rivero *et al.*, 2010). When GLY was substituted with SQ up to 50%, an increased hydrophobicity of gelatin film was obtained, which served as a barrier to water molecules. As a result, lesser water was retained in the film matrix after extended storage. Similarly, Ali *et al.* (2019) documented that increase in hydrophobic substance in the gelatin film resulted in a gradual reduction in moisture content. For CON film, a minor increase in water content led to swelling of film with coincidentally slight increase in thickness. Upon extended storage, the mechanical properties of both the gelatin films were affected differently. CON film showed small decrease in TS and YM but the augmented EAB ($p < 0.05$),

suggesting that increase in water content in the gelatin film could have favored higher molecular mobility of gelatin chains, thereby increasing the plasticizing effect. On the contrary, GLY/SQ film showed increased TS, YM but decreased EAB ($p < 0.05$). This was mostly owing to the dehydration of gelatin film, which could have favored the increased gelatin-gelatin, as well as gelatin-SQ interactions. As a consequence, stiffness of GLY/SQ film was increased during the storage. For color, both gelatin films did not show any notable difference in a^* and b^* values. However, a subtle change in L^* and transparency values were noticed in both films ($p < 0.05$). CON film showed increased L^* with the decreased transparency value, but GLY/SQ films had little reduction in L^* value with increased transparency value. Thus, CON film was more transparent and GLY/SQ film became slightly opaque during the storage ($p < 0.05$).

9.5.3. Quality changes of FFC packaged in different bags during storage

9.5.3.1. Moisture content and water activity

Moisture contents of FFC packed and stored in CON, GLY/SQ, nylon/LLDPE bags in comparison with sample without packaging (WOP) at 28 ± 0.5 °C and 70 ± 5 % RH for 30 days are presented in Figure 1(a). Freshly FFC had moisture content of 3.19%. A shape increase in moisture content was observed for WOP samples as well as those kept in CON bag within the first 5 days ($p < 0.05$), followed by a slow increase up to the end of storage. For those stored in GLY/SQ and nylon/LLDPE bags, a sluggish increase in moisture content was obtained throughout the storage up to 30 days. At day 30, WOP sample and those kept in CON, GLY/SQ and nylon/LLDPE bags showed higher moisture content by 3.39, 3.06, 2.09 and 1.44 folds, respectively. The obtained results were in line with the WVP of all the film samples (Table 2). Due to higher WVP of CON than GLY/SQ films (Table 2), the FFC packed in in bag of the former absorbed higher water ($p < 0.05$). Thus, the results reconfirmed that the addition of SQ to partially replace GLY in the gelatin film might reduce the migration of water vapors across the film, as shown by the lower moisture content of FFC packed in GLY/SQ bag.

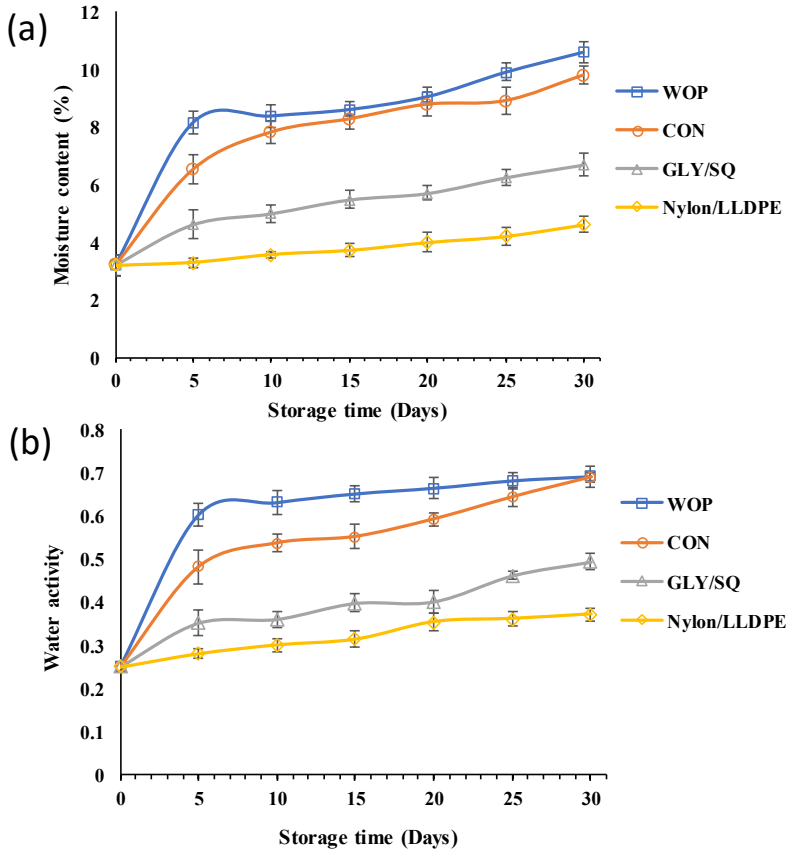

Figure 47. Moisture content (a) and water activity (b) of fried fish crackers stored in CON, GLY/SQ and nylon/LLDPE bags as well as sample without packing (WOP) at 28 ± 0.5 °C and 70 ± 5 % RH for 30 days. Bars represent the standard deviation (n = 3). CON and GLY/SQ are the gelatin films plasticized with glycerol and glycerol:squalene (1:1), respectively. Nylon/LLDPE is nylon/linear low-density polyethylene multilayer film. WOP: without packaging.

Water activity of the FFC stored in different bags and that without packaging is illustrated in Figure 1(b). The pattern of water activity curves of all stored FFC was mostly identical to that observed in moisture content with some minor variations. Initial water activity of FFC at day 0 was 0.24. At the fifth day of storage, the highest water activity was observed from FFC without packing (WOP), followed by those kept in CON bag ($p < 0.05$). The results showed that CON films resisted the migration of moisture vapors to some level. Moreover, at day 30, the water activity of sample stored in CON bag reached the apex. Thus, CON bag had low impact in preventing water migration, especially after the prolonged storage. Nevertheless, the

sample stored in GLY/SQ bag demonstrated lower water activity even after extended storage time. The water activity of sample in GLY/SQ bag was 71.34% lower, compared to that of GLY bag samples. Lowest water activity was found in the FFC stored in nylon/LLDP bags. The results were in accordance with that of moisture content and the WVP of respective films used for bag making (Table 1 and 2). Thus, increased hydrophobicity of gelatin film could reduce the diffusion of water vapor from the surrounding atmosphere (Theerawitayaart *et al.*, 2019). Therefore, replacement of GLY with SQ, hydrophobic substance, was able to serve as a barrier against water vapor transmission. As a result, changes in quality of FFC could be retarded during the extended storage.

9.5.3.2. Color

Table 3 presents the color of FFC stored in CON, GLY/SQ and nylon/LLDPE bags in comparison with WOP samples at day 0 and day 30. At day 0, FFC had higher L^* value and lower a^* and b^* values, compared to those stored for 30 days ($p < 0.05$). After 30 days of storage, the lightness values of FFC stored in CON bag and WOP samples were decreased to high extent ($p < 0.05$). The lightness values of FFC stored in GLY/SQ and nylon/LLDPE bags were slightly reduced. A substantial increase in a^* and b^* values of FFC were detected from samples kept in CON bag and WOP sample. Only slight increases in both values were found in those stored in GLY/SQ and nylon/LLDPE bags. The results indicated that increased yellowness could due to the yellow discoloration of FFC as influenced by lipid oxidation (Thanonkaew *et al.*, 2007). Increased redness of FFC stored in CON bag and WOP sample was mostly caused by interaction between oxidized lipid compounds with amino groups of amino acids, peptides and proteins known as Maillard reaction (Lu *et al.*, 2013). Moreover, the higher water content (Figure 1) in FFC stored in CON bag and WOP sample could have facilitated the migration of reactants, which led to the drastic changes in color of samples. The visual difference in terms of color change can be seen from the images shown in Table 3. Overall, FFC stored in GLY/SQ and nylon/LLDPE bags had less changes in color, compared to those observed at day 0. On the other hand, the FFC stored in CON bags and WOP sample had the drastic change in color, especially increased browning.

Table 25. Images and color of freshly fried fish crackers (day 0) and the crackers stored in CON, GLY/SQ and nylon/LLDPE bags as well as sample without packing (WOP) stored at 28 ± 0.5 °C and 70 ± 5 % RH for 30 days.

Storage time (days)	Packaging conditions	Color			
		L^*	a^*	b^*	ΔE^*
0	-	71.03 ± 0.08^{a}	5.74 ± 0.05^{e}	20.69 ± 0.03^{e}	30.51 ± 0.08^{e}
30	WOP	60.13 ± 0.15^{e}	9.65 ± 0.06^{b}	29.91 ± 0.09^{b}	45.3 ± 0.12^{a}
	CON	60.71 ± 0.06^{d}	10.23 ± 0.11^{a}	30.04 ± 0.05^{a}	45.11 ± 0.07^{b}
	GLY/SQ	67.41 ± 0.07^{c}	6.74 ± 0.04^{c}	21.53 ± 0.04^{c}	35.45 ± 0.05^{c}
	Nylon/LLDPE	68.5 ± 0.02^{b}	6.12 ± 0.07^{d}	21.38 ±0.03^{d}	32.88 ± 0.06^{d}

Mean ± SD from triplicate determination.
Different lowercase superscripts in the same column indicate significant difference ($P < 0.05$).
CON and GLY/SQ are the bags prepared from gelatin films plasticized with glycerol and glycerol:squalene (1:1), respectively. nylon/LLDPE is nylon/linear low-density polyethylene multilayer film. WOP: without packaging.

9.5.3.3. PV and TBARS

Lipid oxidation of FFC as affected by different bags in comparison with sample without packing during the storage of 30 days are illustrated in Figure 2 (a and b). All the samples exhibited different rates of oxidation ($p < 0.05$). Freshly FFC had PV of 2.1 mg cumene hydroperoxide kg^{-1}, suggesting that oxidation of lipids probably occurred during frying to some level. An increase in PV was observed in all the samples during the storage ($p < 0.05$). It was noted that the drastic increases in PV were found in WOP sample and sample packed in CON bag in comparison with those stored in GLY/SQ or nylon/LLDPE bags. This suggested that lipid oxidation occurred in FFC in the existence of atmospheric oxygen to form primary oxidation products including hydroperoxides and carbonyl compounds (Muhammed *et al.*, 2015; Nilsuwan *et al.*, 2016). This was evidenced by highest PV in WOP sample without any packaging. The higher value could be due to the rapid rate of oxidation of unsaturated fatty acids, mainly from fish used as ingredient in the fish chips. In addition, Maqsood and Benjakul (2011) reported that oxidation of lipid could take place in the presence of pro-oxidants from meat such as heme iron, which more likely accelerates the oxidation of unsaturated fatty acids. Samples kept in CON bag and WOP sample exerted a gradual increase in PV up to 20 days ($p < 0.05$). Subsequently a small decline in PV was noticed in WOP sample until the end of storage time. The rise in PV indicated that lipid oxidation was in propagation stage through the continuous chain reaction. The reduction in PV could be possibly due to the decomposition of hydroperoxides to generate other compounds (Buege and Aust, 1978). The FFC stored in GLY/SQ and nylon/LLDPE bags demonstrated slight increases in PV throughout the storage of 30 days ($p < 0.05$). Nevertheless, the oxidation rate of sample kept in GLY/SQ bag was higher, compared to that of the sample stored in nylon/LLDPE bag ($p < 0.05$). Owing to higher oxygen barrier properties of CON or GLY/SQ films, the oxidation rate of FFC was expected to be lower when packed in CON or GLY/SQ bags. Nonetheless, WVP of both the films was higher than that of nylon/LLDPE film. As a result, water content of the FFC was increased when stored in both bags based on gelatin (Figure 1). The increased water content could facilitate the migration of reactants, particularly prooxidants and reactants in crackers. Therefore, PV of samples stored in CON or

GLY/SQ bags were increased though the oxygen was for oxidation depleted. Overall, the lower permeability of water vapor and oxygen of GLY/SQ bags was effective for retardation of lipid oxidation of FFC during extended storage.

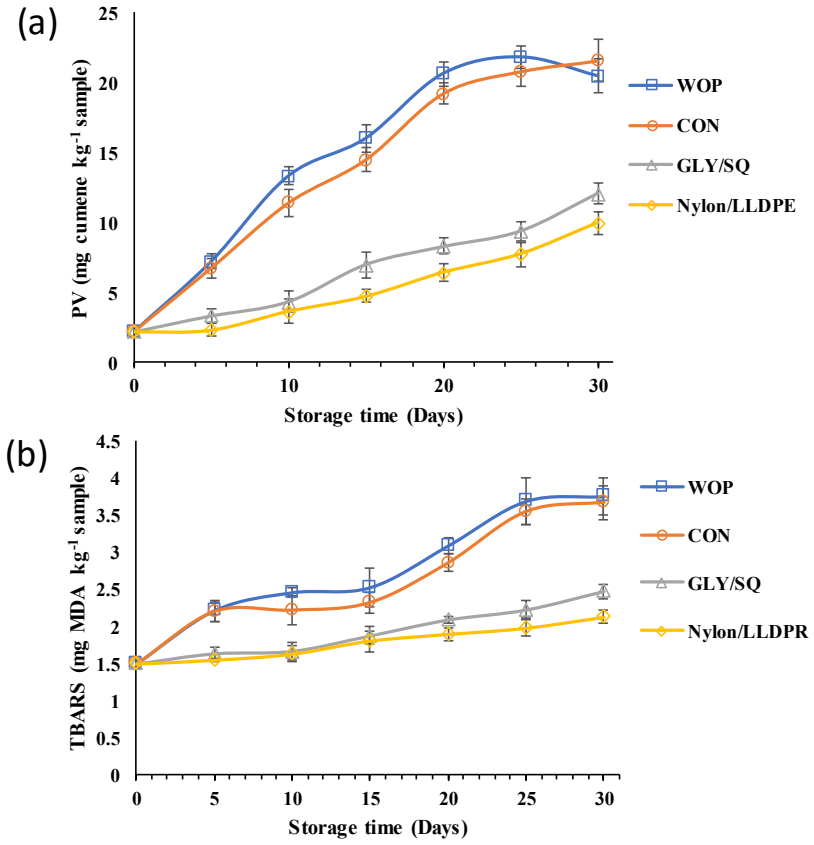

Figure 48. Peroxide value (a) and TBARS (b) of fried fish crackers stored in CON, GLY/SQ and nylon/LLDPE bags as well as sample without packing (WOP) at 28 ± 0.5 °C and 70 ± 5 % RH for 30 days. Bars represent the standard deviation (n = 3). CON and GLY/SQ are the gelatin films plasticized with glycerol and glycerol:squalene (1:1), respectively. Nylon/LLDPE is nylon/linear low-density polyethylene multilayer film. WOP: without packaging.

TBARS values of all the FFC stored for 30 days in different bags and sample without packing are shown in Figure 2 (b). No change in TBARS values of sample kept in nylon/LLDPE and GLY/SQ bags were noticed until 10-12 days of storage. Subsequently, a slight increase in TBARS value was observed in both the samples until the end of storage time ($p < 0.05$). However, the FFC stored in CON bag and WOP sample showed a sharp increase in TBARS value from day 1 to day 5 ($p <$

0.05) and remained constant till day 14. Thereafter the marked increase was found up to 25 days ($p < 0.05$) and then the TBARS value remained unchanged up to day 30. When comparing with samples stored in CON bag and WOP samples, that kept in GLY/SQ bag presented much lower TBARS values ($p < 0.05$). Thus, addition of SQ in gelatin film as GLY replacer could efficiently limit the formation of volatile compound associated with lipid oxidation. The obtained results were in agreement with PV, indicating that WVP and OP were the critical factors influencing the oxidative stability of FFC during the extended storage.

9.5.3.4. Textural properties

Change in textural properties of stored FFC was monitored in terms of crispiness and toughness as illustrated in Figure 3 (a and b). Crispiness is one of the crucial factors of sensory attribute. Crispiness is associated with the fracture and deformation of subsequent layers in the structure of food products (Agarwal *et al.*, 2018). Oil and moisture content are the most influential parameters affecting the crispness of fried crackers (Mohamed *et al.*, 1998). Crispiness of FFC stored in CON bag and WOP sample drastically decreased ($p < 0.05$) within the first 5 days of storage. Those kept in nylon/LLDPE and GLY/SQ bags showed the lower degree of decrease in crispiness. During day 5 to 30, there was a steady reduction in crispiness of all the samples. Compared to all the samples, those stored in nylon/LLDPE bag showed higher crispiness throughout the storage ($p < 0.05$). For the FFC stored in GLY/SQ bags, samples were still crispy till 15-18 days of storage with crunchy fracture behavior. Nevertheless, sample in CON bag and WOP sample, crispness was lost within the first two days of storage ($p < 0.05$). Moreover, FFC packed in CON bag had similar crispness profile to that of WOP sample. Similarly, toughness of FFC stored in CON bags and WOP sample was increased within the first 2 days of storage ($p < 0.05$). No remarkable changes in toughness of FFC packed in nylon/LLDPE bag were noticed during the first 15 days of storage ($p > 0.05$). Greater increase in toughness was observed for FFC stored in GLY/SQ bags during extended storage. The results were in agreement with higher WVP during storage of respective films (CON, GLY/SQ and nylon/LLDPE films) (Table 1 and 2). Similarly, Nilsuwan *et al.* (2016) documented that change in textural properties of shrimp crackers stored by covering with gelatin

and emulsified gelatin film was caused by the migration of water vapors through the film matrix. This might have fluidized the cracker networks, which altered the textural properties of FFC as indicated by the increased toughness and reduced crispiness. Although the incorporation of SQ could improve WVP of GLY/SQ film, the textual properties of FFC were affected to some level when compared to that of sample kept in synthetic nylon/LLDPE bag.

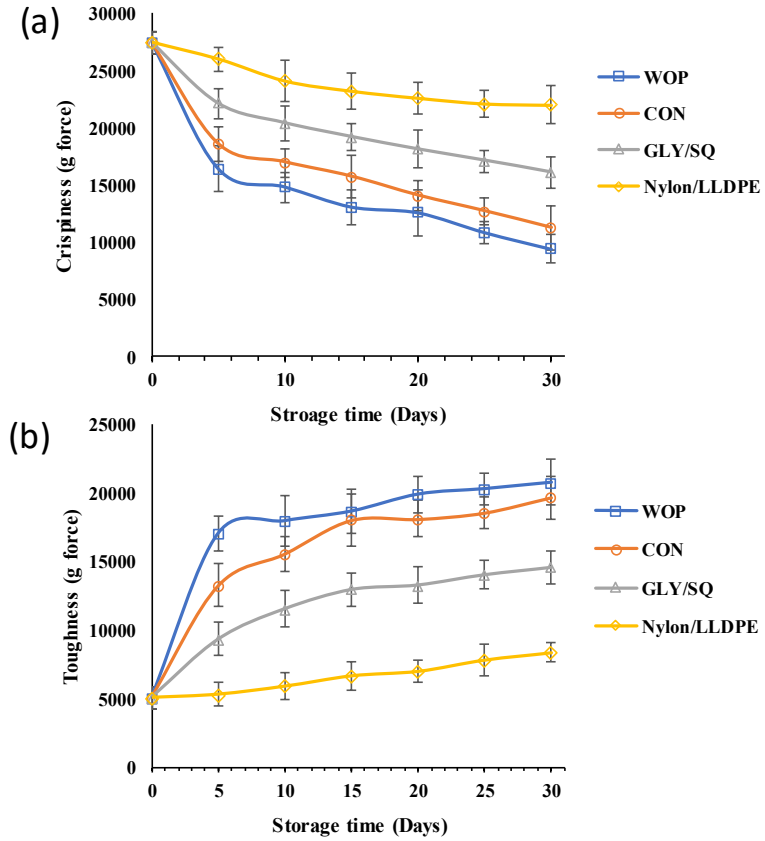

Figure 49. Crispiness (a) and toughness (b) of fried fish crackers stored in CON, GLY/SQ and nylon/LLDPE bags as well as sample without packing (WOP) at 28 ± 0.5 °C and 70 ± 5 % RH for 30 days. Error bars represent the standard deviation (n = 3). CON and GLY/SQ are the gelatin films plasticized with glycerol and glycerol:squalene (1:1), respectively. Nylon/LLDPE is nylon/linear low-density polyethylene multilayer film. WOP: without packaging.

9.5.3.5. Fatty acid compositions (FACs)

FACs of FFC at day 0 and day 30 of storage as affected by different bags including CON, GLY/SQ and nylon/LLDPE bags as well as WOP sample stored at 28 ± 0.5 °C and 70 ± 5 % RH, are presented in Table 4. For the fresh FFC (day 0), the most predominant fatty acids (FAs) were palmitic acid (2126.2 µg g^{-1}), oleic acid (1601.2 µg g^{-1}) and arachidic acid (351.9 µg g^{-1}). Freshly prepared FFC had a substantial amount of monounsaturated fatty acids (MUFAs) (1633.7 µg g^{-1}) and small amount of polyunsaturated fatty acids (63.5 µg g^{-1}). Moreover, eicosapentaenoic acid (EPA) (6.4 µg g^{-1}) and docosahexaenoic acid (DHA) (10.4 µg g^{-1}) were also detected, which were mainly from fish meat incorporated as an ingredient in the crackers. The different packagings or bags used demonstrated a huge variation in the FACs of all the FFC ($p < 0.05$). After 30 days of storage, unsaturated fatty acids including MUFAs and PUFAs were not detected and a significant loss of saturated fatty acids (SFAs) were found in WOP sample ($p < 0.05$). This could be due to the severe oxidation and hydrolysis of FAs, more likely accelerated by the highest availability of oxygen and water (Maqsood and Benjakul, 2011; Muhammed *et al.*, 2015). The FFC stored in CON bag exerted the controlled rate of oxidation and degradation to some extent. As observed from the FAC, a greater quantity of fatty acids (1309.6 µg g^{-1}) was detected in sample stored in CON bag at the end of 30 days of storage, compared with that of WOP sample. FFC stored in CON bag had retained lesser quantity of MUFAs (272.5 µg g^{-1}) and PUFAs (2.6 µg g^{-1}) but greater proportion of SFAs. However, the n-3 and n-6 FAs were completely degraded ($p < 0.05$). This indicated that CON bag could reduce oxidation of fatty acid to some extent, because of its lowered OP (Table 2). During storage, the breakdown of ester bond and release of free fatty acid favors various reactions, especially oxidation (Sae-leaw and Benjakul, 2017). Furthermore, sample stored in GLY/SQ bag showed the greater quantity of FAs, particularly PUFAs (47.5 µg g^{-1}) and MUFAs (1158.7 µg g^{-1}). On the other hand, FFC packed in nylon/LLDPE bag demonstrated comparatively lower concentration of PUFAs and MUFAs (40.9 and 984.4 µg g^{-1}, respectively), than those of sample kept in GLY/SQ bag.

Table 26. Fatty acid composition of freshly fried fish crackers (day 0) and the crackers stored in CON, GLY/SQ and nylon/LLDPE bags as well as sample without packing (WOP) stored at 28 ± 0.5 °C and 70 ± 5 % RH for 30 days.

Fatty acids (μg g^{-1})	Day-0	Day-30			
		WOP bag	CON bag	GLY/SQ bag	Nylon/LLDPE bag
C4:0 (butyric acid)	12.60	ND	25.77	10.58	11.23
C8:0 (caprylic acid)	12.22	ND	ND	10.28	11.81
C10:0 (capric acid)	10.31	ND	ND	10.03	10.51
C12:0 (lauric acid)	24.44	2.73	15.09	16.30	19.83
C14:0 (myristic acid)	46.98	3.201	29.10	33.29	60.71
C15:0 (pentadecanoic acid)	6.65	ND	1.428	5.63	6.93
C16:0 (palmitic acid)	2126.23	53.02	836.99	1006.53	1458.93
C16:1 (palmitoleic acid)	14.17	ND	ND	5.35	5.17
C17:1 (heptadecanoic acid)	20.37	ND	5.58	10.73	11.99
C17:1 (cis-10-heptadecanoic acid)	5.92	ND	ND	5.058	5.98
C18:0 (stearic acid)	171.73	ND	73.64	119.17	150.38
C18:1 (oleic acid)	1601.18	ND	268.16	1138.33	962.22
C18:2 (linoelaidic acid)	10.74	ND	2.58	7.41	9.24
C18:2 (linoleic acid)	8.44	ND	ND	5.134	ND
C18:3 (alpha-linolenic acid)	15.11	ND	ND	12.43	9.07
C20:0 (arachidic acid)	351.92	ND	28.32	242.95	274.64
C20:0 (docosanoic acid)	12.11	5.44	8.39	10.26	11.83
C20:1 (cis-11-eicosenoic acid)	12.50	ND	4.38	10.08	11.06
C20:0 (eicosadienoic acid)	6.43	ND	ND	5.34	6.27
C20:3 (eicosatrienoic acid)	5.90	ND	ND	5.32	5.67
C20:5 (eicosapentaenoic acid)	6.44	ND	ND	5.15	5.05
C22:6 (docosahexaenoic acid)	10.38	ND	ND	6.72	5.67
C23:0 (tricosanoic acid)	5.27	ND	ND	4.81	5.12
C23:0 (lignoceric acid)	12.47	4.12	10.09	10.44	11.82
Saturated fatty acids	2813.34	68.53	1034.44	1491.04	2045.79
Monounsaturated fatty acids	1633.77	0	272.54	1158.72	984.44
Polyunsaturated fatty acids	63.47	0	2.58	47.53	40.98
Omega-3	37.849	0	0	29.64	25.47
Omega-6	14.886	0	0	10.47	6.27
Total fatty acids	4510.6	68.53	1309.56	2697.31	3071.22

Fatty acid analysis was performed in duplicate.

CON and GLY/SQ are the bags prepared from gelatin films plasticized with glycerol and glycerol:squalene (1:1), respectively. nylon/LLDPE is nylon/linear low-density polyethylene multilayer film. WOP: without packaging.

Most importantly, GLY/SQ bag could reduce the oxidation of n-3 and n-6 FAs more efficiently than nylon/LLDPE film, which could correlate to the lower OP of the GLY/SQ film than that of nylon/LLDPE film as shown from Table 2. However, some difference in total FAs content was found between GLY/SQ (2697.3 μg g^{-1}) and nylon/LLDPE (3071.2 μg g^{-1}) bags. This could be most likely due to the difference in WVP of both the bags (Table 2), which led to the different rate of degradation and loss of FAs. The obtained results were in agreement with the lower degree of PV and TBARS of samples stored in GLY/SQ and nylon/LLDPE bags (Figure 2). This indicated that the incorporation of SQ in gelatin film as the GLY substitute could reduce oxidation and degradation of FAs in FFC to some extent.

9.5.3.6. Volatile compounds

Selected volatile compounds from FFC stored without packing and packed in different bags, analyzed at day 30 in comparison with freshly FFC (day 0) are presented in Table 5. PUFAs, especially alpha-linolenic acid (C18:3), linoelaidic acid (C18:2) and docosahexaenoic acid (C22:6) were the major PUFAs in FFC (Table 4). PUFAs can readily undergo oxidation in the existence of atmospheric oxygen to procedure secondary oxidation products namely ketones, aldehydes, and alcohols (Maqsood and Benjakul, 2011). The predominant compounds found in FFC were related to hydrocarbons and aldehydes. Among aldehydes, hexanal was produced at higher levels. Hexanal was also found at day 0, which could have been generated during the frying process with the further increase during the extended storage. Among all the samples, hexanal was found at the highest level in the WOP sample, followed by the samples packed in nylon/LLDPE and CON bags. The lower level was found in the sample kept in GLY/SQ bag. This was in relation with the lower amount of oxygen available during extended storage. Moreover, the obtained results were in line with Koelsch *et al.* (1991) who documented that the formation of hexanal via lipid oxidation is the function of oxygen concentration. Other aldehydes detected after 30 days of storage were octanal, nonanal and 2-decenal. Among all the samples, the WOP sample had the highest abundance of aldehydes, followed by samples kept in CON and nylon/LLDPE bags, respectively. The lowest level of aldehydes was found in the samples packed in GLY/SQ bags. Nevertheless, some minor difference among the

samples was noticed. This reconfirmed the higher barrier oxygen property GLY/SQ films (Table 2). Generation of aldehydes has been used as an indicator of lipid oxidation from various food products as they are the main contributors for off-flavor and off-odor (Ross and Smith, 2006). The results suggested that all the samples underwent lipid oxidation during the storage process and at different degrees. Similarly, Nilsuwan *et al.* (2016) reported the generation of some groups of aldehydes during the storage of fried shrimp crackers covered with gelatin as well as emulsified gelatin film containing palm oil.

Ketones are other class of secondary products of lipid oxidation, which are produced by the degradation of hydroperoxides (Thanonkaew *et al.*, 2007). 2,3-butanedione, 2-propanone, 2-cyclohexene-1-one and 3,5-cycloheptadien-1-one were noticed in all the samples after 30 days of storage time, while 2,3-butanedione and 2-propanone were detected only in fresh FFC (day 0). Alcoholic volatile compounds including aliphatic alcohols such as 1-pentanol, 1-hexanol, and 1-nonanol were also found. Furthermore, new aromatic alcohols including 10,10-dimethyl-2,6-dimethylenebicyclo [7.2.0] undecane, cyclohexanol, 1-methyl-4-(1-methylethenyl), and isospathulenol were also detected, which more likely contributed to aroma. Generally, alcohols are the secondary products originated by the breakdown of hydroperoxides (Ross and Smith, 2006). The unsaturated aliphatic alcohol, 2,6-Octadien-1-ol, is generated by the autoxidation of *n*-6 fatty acid, especially linoleic acid (Lee and Min, 2010). It was observed that, 2,6-octadien-1-ol was not found in the fresh FFC and was detected at a lower level for sample stored in GLY/SQ bag. Conversely, it was found predominantly in WOP sample, samples kept in nylon/LLDPE and CON bags, indicating higher oxidation and decomposition of linoleic acid. This reconfirmed the results obtained for fatty acid composition for linoleic acid (Table 3). Aliphatic alcohols, mainly the unsaturated ones, are also involved in rancidity and off-flavor, owing to the low threshold value than those of the saturated counterpart (Zhang *et al.*, 2018a). The abundance of these volatile lipid oxidation secondary products found in all stored samples was in relation with the higher TBARS values, especially the WOP samples and that stored in CON bags.

Table 27. Selected volatile compounds from freshly fried fish crackers (day 0) and the crackers stored in CON, GLY/SQ and nylon/LLDPE bags as well as sample without packing (WOP) stored at 28 ± 0.5 °C and 70 ± 5 % RH for 30 days.

Volatile compounds	Day-0*	Day 30*				MF
		WOP bag	CON bag	GLY/SQ bag	Nylon/LLDPE bag	
Aldehydes						
Hexanal	15.5	135.76	130.06	54.57	78.22	88.76
Octanal	ND	4.53	3.20	2.52	1.68	82
Heptanal	ND	3.69	ND	ND	1.72	97.2
Nonanal	ND	10.19	8.23	ND	ND	89.5
2-Decenal	ND	12.71	6.71	4.8	1.5	88.2
Ketones						
2,3-Butanedione	0.89	ND	ND	ND	ND	86.7
2-Propanone	2.77	ND	ND	ND	ND	93.9
2-Cyclohexen-1-one, 3-methyl-6-(1-methylethyl)-	ND	11.81	9.79	4.57	7.49	88.9
3,5-Cycloheptadien-1-one, 3,6-dimethyl-	ND	7.2	6.35	5.88	3.14	74.6
Alcohol						
1-Pentanol	2.1	11.75	11.02	9.46	11.76	77.2
1-Hexanol	0.64	11.14	3.31	1.99	2.51	80.07

Table 5. (continued)

Volatile compounds	Day-0*	Day 30*				MF
		WOP bag	CON bag	GLY/SQ bag	Nylon/LLDPE bag	
1-nonanol	ND	1.55	1.45	ND	ND	76.5
Isospathulenol	ND	6.41	ND	ND	5.77	86.8
10,10-Dimethyl-2,6-dimethylenebicyclo[7.2.0]undecane	0.43	4.72	1.56	1.21	1.85	95.2
Cyclohexanol, 1-methyl-4-(1-methylethenyl)-	ND	2.16	2.07	1.84	ND	77.3
2,6-Octadien-1-ol, 3,7-dimethyl-, propanoate, (E)-	ND	52.89	48.32	7.41	14.60	74.2
Nitrogen containing compounds						
Pyrazine	3.31	24.56	45.40	6.71	5.28	94.7
Methyl-Pyrazine	ND	7.6	ND	ND	ND	70.8
2,3-Dimethyl-Pyrazine	ND	3.65	2.13	2.05	ND	94.8
2,5-Dimethyl-Pyrazine	ND	3.96	2.41	ND	ND	93
Ethyl-Pyrazine	ND	6.7	7.1	3.5	ND	94.8
2-Ethyl-3,5-dimethyl-Pyrazine	5.43	56.72	47.69	8.07	5.93	93.8
2-Ethyl-6-methyl-Pyrazine	ND	2.5	1.73	ND	ND	82.4
2-Ethyl-5-methyl-Pyrazine	2.10	24.16	22.04	4.3	4.16	94

Table 5. (continued)

Volatile compounds	Day-0*	Day 30*				MF
		WOP bag	CON bag	GLY/SQ bag	Nylon/LLDPE bag	
2-Ethyl-3-methyl-Pyrazine	ND	8.4	5.21	ND	ND	68.3
2,6-Diethyl-Pyrazine	ND	2.8	ND	ND	ND	88.8
2,3,5-Trimethyl-6-ethylpyrazine	ND	4.0	5.4	ND	ND	85.4
2-Isoamyl-6-methylpyrazine	ND	1.8	1.78	ND	ND	77.6
Hydrocarbons						
Decane	ND	48.9	28.56	7.63	5.16	95.4
Dodecane	ND	37.03	15.23	10.25	7.22	90.4
5-Ethyldecane	ND	6.72	4.57	ND	ND	86.9
Bicyclo[5.2.0]nonane, 2-methylene-4,8,8-trimethyl-4-vinyl-	0.72	12.53	9.72	3.58	1.46	89.7
Cyclohexene, 4-ethenyl-4-methyl-3-(1-methylethenyl)-1-(1-methylethyl)-, (3R-trans)-	ND	4.09	4.26	2.1	ND	92.6

*: The values are expressed as abundance value of volatile compound based on the peak area (× 10^9), ND: not-detected, MF: is the match factor. CON and GLY/SQ are the bags prepared from gelatin films plasticized with glycerol and glycerol:squalene (1:1), respectively. nylon/LLDPE is nylon/linear low-density polyethylene multilayer film. WOP: without packaging.

Moreover, nitrogen-containing secondary compounds, particularly the pyrazines derivatives were detected in FFC. Pyrazine compound is known to be formed through the Maillard reaction caused by the degraded nitrogenous compounds such as amino acid and peptides (Scalone *et al.*, 2019). Freshly prepared FFC along with that packed in nylon/LLDPE bag had of the low abundance of pyrazine, 2-ethyl-3,5-dimethly-pyrazine and, 2-ethyl-5-methyl-pyrazine, indicating that FFC packed in nylon/LLDPE bags had negligible amount of products related to non-enzymatic browning. The highest number of pyrazine derived products could be detected in the WOP samples (12 different derivatives) and sample kept in CON bag (9 derivatives), in which most of the derivatives were newly formed. Sample kept in GLY/SQ bag showed of few pyrazine derivatives, where two derivatives including 2,3-dimethyl-pyrazine and ethyl-pyrazine were newly generated during the storage. The results were in agreement with Agarwal *et al.* (2018); Nilsuwan *et al.* (2016) who reported that new pyrazine derivatives were formed as a result of Maillard reaction during the extended storage of fried shrimp crackers and potato chips. Thus, the occurrence and formation or new pyrazine derivatives suggested that non-enzymatic browning reaction associated with Maillard reaction occurred during the storage. It was noticed that the rate of reaction was higher in the samples with elevated moisture content. This could be mainly owing to the higher degree of hydrolysis and migration of reactants to a greater extent. The results were in line with the change in moisture content and color of the FFC during the extended storage (Figure 1 and Table 3).

Furthermore, few hydrocarbons including noncyclic (decane, dodecane and 5-ethyldecane) and cyclic compounds (2,6,6-trimethylbicyclo[3.1.1]hept-2-ene, bicyclo[5.2.0]nonane, 2-methylene-4,8,8-trimethyl-4-vinyl- and Cyclohexene, 4-ethenyl-4-methyl-3-(1-methylethenyl)-1-(1-methylethyl)-, (3R-trans)- were generated during 30 days of storage. Decane and its derivatives are mainly formed from the autoxidation of phospholipids due to the presence of oxidizing radicals (Feng *et al.*, 2019). The formed hydroperoxides could undergo β-cleavage to generate conjugated diene radicals, which further reacted with oxygen to form vinyl hydroperoxides. The breakdown of these vinyl hydroperoxides could form alkoxyl radicals which undergo cyclization to form cyclic compounds (Maqsood and Benjakul, 2011). The presence of

cyclic and noncyclic hydrocarbons indicated that the autoxidation of lipids occurred during the storage, caused by occurrence and migration of various oxidizing radicals. The higher formation of hydrocarbons through the decomposition of hydroperoxides was noticed in the WOP sample and the sample stored in CON bag, followed by the samples kept in GLY/SQ and nylon/LLDPE bags, respectively.

9.6. Conclusion

Fish gelatin film prepared by substituting GLY with SQ as plasticizer had the effect on properties of films. Addition of SQ reduced WVP and OP of gelatin film significantly. Furthermore, SQ improved TS, thus improving the mechanical resistance of the gelatin film, which was comparable to that of nylon/LLDPE film. GLY/SQ bag effectively enhanced the oxidative stability of MUFA and PUFA of FFC, compared to nylon/LLDPE bag. GLY/SQ bag could maintain the textural property of FFC. The improvement of barrier properties of GLY/SQ bag reduced PV and TBARS of FFC. Moreover, GLY/SQ bag retarded the formation of volatile compounds effectively, especially those generated via Maillard reaction. Therefore, the bags based on gelation prepared by replacing GLY with SQ at a ratio of 1:1 can be applied for improving the shelf-life extension of nutritional food products, particularly those highly susceptible to oxidation.

9.7. References

Agarwal, D., Mui, L., Aldridge, E., Mottram, R., McKinney, J. and Fisk, I. D. 2018. The impact of nitrogen gas flushing on the stability of seasonings: volatile compounds and sensory perception of cheese and onion seasoned potato crisps. Food and Function. 9: 4730-4741.

Ali, A. M. M., Prodpran, T. and Benjakul, S. 2019. Effect of squalene as a glycerol substitute on morphological and barrier properties of golden carp (*Probarbus Jullieni*) skin gelatin film. Food Hydrocolloids. https://doi.org/10.1016/j.foodhyd.2019.105201.

Ansorena, M. R., Pereda, M. and Marcovich, N. E. 2018. Edible films. *In* Polymers for food applications. (Gutiérrez, T. J., ed.). p. 5-24. Springer International Publishing. Cham, Switzerland.

Benjakul, S., Kittiphattanabawon, P. and Regenstein, J. M. 2012. Fish gelatin. *In* Food Biochemistry and Food Processing, Second Edition. (Simpson, B. K., ed.). p. 388-405. Wiley-Blackwell. Iowa, USA.

Bindu, B. S. C., Mishra, D. P. and Narayan, B. 2015. Inhibition of virulence of *Staphylococcus aureus*–a food borne pathogen–by squalene, a functional lipid. Journal of Functional Foods. 18: 224-234.

Buege, J. A. and Aust, S. D. 1978. [30] Microsomal lipid peroxidation. *In* Methods in Enzymology. Vol. 52. (Abelson, J. *et al.*, eds.). p. 302-310. Elsevier. Amsterdam, Netherlands.

Elewski, B. E. 1993. Mechanisms of action of systemic antifungal agents. Journal of the American Academy of Dermatology. 28: S28-S34.

Feng, X., Jo, C., Nam, K. C. and Ahn, D. U. 2019. Impact of electron-beam irradiation on the quality characteristics of raw ground beef. Innovative Food Science and Emerging Technologies. 54: 87-92.

Gómez-Guillén, M. C., Pérez-Mateos, M., Gómez-Estaca, J., López-Caballero, E., Giménez, B. and Montero, P. 2009. Fish gelatin: a renewable material for developing active biodegradable films. Trends in Food Science and Technology. 20: 3-16.

Han, J.-W., Ruiz-Garcia, L., Qian, J.-P. and Yang, X.-T. 2018. Food Packaging: A Comprehensive Review and Future Trends. Comprehensive Reviews in Food Science and Food Safety. 17: 860-877.

Koelsch, C., Downes, T. and Labuza, T. P. 1991. Hexanal formation via lipid oxidation as a function of oxygen concentration: measurement and kinetics. Journal of Food Science. 56: 816-820.

Lee, J. and Min, D. B. 2010. Analysis of volatile compounds from chlorophyll photosensitized linoleic acid by headspace solid-phase microextraction (HS-SPME). Food Science and Biotechnology. 19: 611-616.

Lu, F. S. H., Nielsen, N. S., Baron, C. P., Diehl, B. W. K. and Jacobsen, C. 2013. Impact of primary amine group from aminophospholipids and amino acids on marine phospholipids stability: Non-enzymatic browning and lipid oxidation. Food Chemistry. 141: 879-888.

Maqsood, S. and Benjakul, S. 2011. Retardation of haemoglobin-mediated lipid oxidation of Asian sea bass muscle by tannic acid during iced storage. Food Chemistry. 124: 1056-1062.

Mohamed, S., Hamid, N. A. and Hamid, M. A. 1998. Food components affecting the oil absorption and crispness of fried batter. Journal of the Science of Food and Agriculture. 78: 39-45.

Muhammed, M., Domendra, D., Muthukumar, S., Sakhare, P. and Bhaskar, N. 2015. Effects of fermentatively recovered fish waste lipids on the growth and composition of broiler meat. British Poultry Science. 56: 79-87.

Nagarajan, M., Benjakul, S., Prodpran, T. and Songtipya, P. 2014. Properties of bio-nanocomposite films from tilapia skin gelatin as affected by different nanoclays and homogenising conditions. Food and Bioprocess Technology. 7: 3269-3281.

Nilsuwan, K., Benjakul, S. and Prodpran, T. 2016. Quality changes of shrimp cracker covered with fish gelatin film without and with palm oil incorporated during storage. International Aquatic Research. 8: 227-238.

Nilsuwan, K., Benjakul, S. and Prodpran, T. 2018. Properties and antioxidative activity of fish gelatin-based film incorporated with epigallocatechin gallate. Food Hydrocolloids. 80: 212-221.

Reddy, L. H. and Couvreur, P. 2009. Squalene: A natural triterpene for use in disease management and therapy. Advanced Drug Delivery Reviews. 61: 1412-1426.

Rivero, S., García, M. and Pinotti, A. 2010. Correlations between structural, barrier, thermal and mechanical properties of plasticized gelatin films. Innovative Food Science and Emerging Technologies. 11: 369-375.

Ross, C. F. and Smith, D. M. 2006. Use of volatiles as indicators of lipid oxidation in muscle foods. Comprehensive Reviews in Food Science and Food Safety. 5: 18-25.

Sae-leaw, T. and Benjakul, S. 2017. Lipids from visceral depot fat of Asian seabass (*Lates calcarifer*): Compositions and storage stability as affected by extraction methods. European Journal of Lipid Science and Technology. 119: 1-10.

Scalone, G. L. L., Lamichhane, P., Cucu, T., De Kimpe, N. and De Meulenaer, B. 2019. Impact of different enzymatic hydrolysates of whey protein on the formation of pyrazines in Maillard model systems. Food Chemistry. 278: 533-544.

Thanonkaew, A., Benjakul, S., Visessanguan, W. and Decker, E. A. 2007. Yellow discoloration of the liposome system of cuttlefish (*Sepia pharaonis*) as influenced by lipid oxidation. Food Chemistry. 102: 219-224.

Theerawitayaart, W., Prodpran, T., Benjakul, S. and Sookchoo, P. 2019. Properties of films from fish gelatin prepared by molecular modification and direct addition of oxidized linoleic acid. Food Hydrocolloids. 88: 291-300.

Tongnuanchan, P., Benjakul, S., Prodpran, T., Pisuchpen, S. and Osako, K. 2016. Mechanical, thermal and heat sealing properties of fish skin gelatin film containing palm oil and basil essential oil with different surfactants. Food Hydrocolloids. 56: 93-107.

Zhang, M., Chen, X., Hayat, K., Duhoranimana, E., Zhang, X., Xia, S., Yu, J. and Xing, F. 2018a. Characterization of odor-active compounds of chicken broth and improved flavor by thermal modulation in electrical stewpots. Food Research International. 109: 72-81.

Zhang, Y., Simpson, B. K. and Dumont, M.-J. 2018b. Effect of beeswax and carnauba wax addition on properties of gelatin films: A comparative study. Food Bioscience. 26: 88-95.

CHAPTER 10

CONCLUSION AND SUGGESTION

10.1. Conclusions

1. ASC and PSC extracted from golden carp skin were and scale as type I collagen. Cleavage of telopeptides increased the yield of collagen. PSC had higher structural integrity than ASC. PSC had higher T_{max} than ASC. Both ASC and PSC showed high imino acid content and had high solubility in acidic pH (1-3). ASC and PSC were in triple helical structure. Nevertheless, lower yield was obtained when ASC or PSC were extracted from scales, compared to skin.
2. The use of ultrasonication (20 kHz, amplitude 80% for 30 min) could increase the yield of ASC from skin than that extracted using conventional method. Ultrasonication in combination with pepsin (1%) could increase the yield up to 180% and 120% higher than ASC and PSC. Protein pattern, FTIR and CD spectra confirmed that all the collagens had the native triple helical conformation.
3. Acid pretreatment in combination with prior-ultrasonication improved the extraction efficiency of gelatin from golden carp skin, compared to the conventional method. Prior-ultrasonication of both acid pretreated types (A-U-6 and SA-U-6) contained higher amounts of glycine and imino acid residues. Gelling and melting temperatures of gelatins were greater than that of commercial fish gelatin.
4. Application of ultrasound to extract squalene directly from fish liver was more effective, compared to the conventional extraction process. The volume of

50% KOH (6.5 ml), ratio of mass/methanol (1:6, w/v) and the sonication time (15 min) increased the yield of unsaponifiable up to 35%. Moreover, U-DS process did not show any adverse effect on structure and property of squalene.

5. Incorporation of highly hydrophobic SRF improved properties of gelatin film, mainly by increasing barrier properties. SRF demonstrated excellent emulsifying property than PO. SRF was better than PO at the same level added in enhancing film properties including EAB and TS of the gelatin-based film. Additionally, films prepared with SRF had more uniform and smoother surface that PO film.
6. Incorporation of SQ as GLY substitute could enhance the properties of gelatin film. Dispersed SQ crystal phase could serve as a moisture and oxygen barrier. To achieve the desirable gelatin film properties, GLY could be replaced by SQ up to 50%. The hydrophobic nature and long chain length of SQ improved the mechanical strength of gelatin film.
7. GLY/SQ film effectively enhanced the oxidative stability of MUFA and PUFA of the stored sample compared those of GLY or nylon/LLDPE film during extended storage. GLY/SQ film with improved oxygen barrier and moisture vapor barrier properties of gelatin film had reduced PV and TBARS. Moreover, GLY/SQ film retarded the formation of volatile compounds effectively, especially those participated in Maillard reaction.

10.2. Suggestions

1. Rheological and gelling properties of golden carp fish skin gelatin with high imino acid content and T_{max} values should be further investigated.
2. The effect of phosphoric acid pretreatment on prior-ultrasonication in conjunction with subsequent addition of divalent cation should be studied to improve the gelling property of resulting gelatin.
3. For the ultrasound assisted direct *in-situ* process, the residue after squalene extraction should be used for recovery of pigment and fatty acids.
4. Antioxidant, antimicrobial and health benefits of developed GLY/SQ film should be tested and further improved.

VITAE

Name Mr. Ali Muhammed Moula Ali

Student ID 6011030014

Education Attainment

Degree	Name of Institution	Year of Graduation
Master of Science	Punjab Technical University, Punjab	2009
Bachelor of Science	Gulbarga University, Karnataka	2007

Scholarship Awards during Enrolment

- Thailand's Education Hub for Southern Region of ASEAN Countries (TEH-AC) Scholarship 2014.
- Graduate School Research Support Funding for Thesis.

List of Publication and Proceedings

Publications

1. Ali Muhammed Moula Ali, Soottawat Benjakul and Hideki Kishimura (2017). Molecular characteristics of acid and pepsin soluble collagens from the scales of golden carp (*Probarbus jullieni*). Emirates Journal of Food and Agriculture. 29(6): 450-457.
2. Ali Muhammed Moula Ali, Soottawat Benjakul, Thaummanoon Prodpran and Hideki Kishimura (2017). Extraction and Characterisation of Collagen from the Skin of Golden Carp (*Probarbus jullieni*), a Processing By-Product. Waste and Biomass Valorization. 9(5): 783-791.
3. Ali Muhammed Moula Ali, Hideki Kishimura and Soottawat Benjakul (2018). Extraction efficiency and characteristics of acid and pepsin soluble collagens from the skin of golden carp (*Probarbus jullieni*) as affected by ultrasonication. Process Biochemistry. 66: 237-244.

4. Ali Muhammed Moula Ali, Hideki Kishimura and Soottawat Benjakul (2018). Physicochemical and molecular properties of gelatin from skin of golden carp (*Probarbus Jullieni*) as influenced by acid pretreatment and prior-ultrasonication. Food Hydrocolloids. 82: 164-172.
5. Ali Muhammed Moula Ali, Thaummanoon Prodpran and Soottawat Benjakul (2019). Effect of squalene rich fraction from shark liver on mechanical, barrier and thermal properties of fish (*Probarbus Jullieni*) skin gelatin film. Food Hydrocolloids. 96: 123-133.
6. Ali Muhammed Moula Ali, Sri Charan Bindu Bavisetty, Thummanoon Prodpran and Soottawat Benjakul (2019). Squalene from fish livers extracted by ultrasound assisted direct in-situ saponification: Purification and molecular characteristics. Journal of the American Oil and Chemists' Society. DOI:10.1002/aocs.12262.
7. Ali Muhammed Moula Ali, Thaummanoon Prodpran and Soottawat Benjakul (2019). Effect of squalene as glycerol substitute on morphological and barrier properties of edible gelatin film. Food Hydrocolloids. https://doi.org/10.1016/j.foodhyd.2019.105201.
8. Ali Muhammed Moula Ali, Koro de la Caba, Thaummanoon Prodpran and Soottawat Benjakul (2019). Quality characteristics of fish crackers stored in gelatin bags as influenced by glycerol substituted with squalene as a plasticizer. Food Hydrocolloids. (in review)

Book chapters

1. Soottawat Benjakul, Ali Muhammed Moula Ali and Avtar Singh. (2019). Application of ultrasonication in seafood processing. In: Innovative technologies in seafood processing 1st Ed. (Yesim Ozogul). CRC Press, Baco Raton, FL, USA. (in press)
2. Sri Charan Bindu Bavisetty, Soottawat Benjakul, Oladipupo Olatunde and Ali Muhammed Moula Ali. (2019). Bioactive in fermented fish and meat products: health aspects. In: Bioactive compounds in fermented foods: health aspects. 1st Ed. (Rai A.K. and Anu Appaiah K.A.) CRC Press, Baco Raton, FL, USA. (in press)

Proceedings

1 Ali Muhammed Moula Ali, Thaummanoon Prodpran and Soottawat Benjakul. Extraction efficiency and molecular properties of gelatin from skin of golden carp as affected by acid pretreatment and prior-ultrasonication. International Conference on Animal Production for Food Sustainability. 10-12 Oct, 2018, Indonesia.